

Electronic Thesis and Dissertation Repository

---

8-22-2011 12:00 AM

## Purine Transport and Metabolism in Microvascular Endothelial Cells

Derek B J Bone, *University of Western Ontario*

Supervisor: Dr. James Hammond, *The University of Western Ontario*

A thesis submitted in partial fulfillment of the requirements for the Doctor of Philosophy degree in Pharmacology and Toxicology

© Derek B J Bone 2011

Follow this and additional works at: <https://ir.lib.uwo.ca/etd>



Part of the [Cellular and Molecular Physiology Commons](#), and the [Pharmacology Commons](#)

---

### Recommended Citation

Bone, Derek B J, "Purine Transport and Metabolism in Microvascular Endothelial Cells" (2011). *Electronic Thesis and Dissertation Repository*. 241.

<https://ir.lib.uwo.ca/etd/241>

This Dissertation/Thesis is brought to you for free and open access by Scholarship@Western. It has been accepted for inclusion in Electronic Thesis and Dissertation Repository by an authorized administrator of Scholarship@Western. For more information, please contact [wlsadmin@uwo.ca](mailto:wlsadmin@uwo.ca).

**PURINE TRANSPORT AND METABOLISM IN MICROVASCULAR  
ENDOTHELIAL CELLS**

(Spine Title: Purine Transport and Metabolism)

(Thesis format: Integrated-Article)

By

Derek B. J. Bone

Department of Physiology and Pharmacology

Graduate Program in  
Pharmacology and Toxicology

A thesis submitted in partial fulfillment  
of the requirements for the degree of  
Doctor of Philosophy

The School of Graduate and Postdoctoral Studies  
The University of Western Ontario  
London, Ontario, Canada

© Derek B. J. Bone, 2011

THE UNIVERSITY OF WESTERN ONTARIO  
SCHOOL OF GRADUATE AND POSTDOCTORAL STUDIES

**CERTIFICATE OF EXAMINATION**

Supervisor

\_\_\_\_\_  
Dr. James Hammond

Supervisory Committee

\_\_\_\_\_  
Dr. Qingping Feng

\_\_\_\_\_  
Dr. Timothy Regnault

Examiners

\_\_\_\_\_  
Dr. Ross Feldman

\_\_\_\_\_  
Dr. Brad Urquhart

\_\_\_\_\_  
Dr. Zia A. Khan

\_\_\_\_\_  
Dr. Fiona Parkinson

The thesis by

**Derek Benjamin James Bone**

entitled:

**Purine Transport and Metabolism in Microvascular Endothelial Cells**

is accepted in partial fulfillment of the  
requirements for the degree of  
Doctor of Philosophy

Date \_\_\_\_\_

\_\_\_\_\_  
Chair of the Thesis Examination Board

## ABSTRACT

The microvascular endothelium serves as the barrier between the blood and perfused tissues. Proper function of the endothelium is dependent on the ability of the endothelial cells to produce nitric oxide and form tight junctions between themselves. Dysfunction occurs when stresses overwhelm the endothelial cell, with oxidative stress being a leading cause. Intracellular metabolism of purine nucleosides and nucleobases has been implicated in the production of oxidative stress. Nucleosides (e.g. adenosine) and nucleobases (e.g. hypoxanthine) are moved across cell membranes by a specialized family of proteins called equilibrative nucleoside transporters (ENTs).

We characterized primary human cardiac microvascular endothelial cells (MVECs) for expression, function, and regulation of nucleoside and nucleobase transporters. It was discovered that nucleobase transport in these MVECs was mediated by a novel, purine selective transporter that was insensitive to inhibitors of ENTs, which we named equilibrative nucleobase transporter 1 (ENBT1). ENBT1 and the nucleoside selective transporter ENT1 were differentially regulated by a number of intracellular protein kinases, vascular endothelial growth factor, and oxidative stress.

The role of nucleoside and nucleobase transport in the physiology of MVECs was also studied, using primary MVECs isolated from wild-type (WT) and ENT1<sup>-/-</sup> mice. Altered gene expression of adenosine metabolizing enzymes and adenosine signaling was identified and confirmed at the protein level, however, there was no compensatory changes in other nucleoside or nucleobase transporters. Coinciding with the loss of



adenosine transport capabilities, ENT1<sup>-/-</sup> mice had elevated adenosine plasma concentrations compared to WT and lowered blood pressure.

Unexpectedly, the ENT1<sup>-/-</sup> began to develop hind limb paralysis at about 12 months old. Post-mortem analysis revealed abnormal mineralization on the spine leading to spinal cord compression. MicroCT analysis was used to determine a time course of development, with mineralization being apparent as early as 2 months old. The pattern of mineralization resembled the human condition known as diffuse idiopathic skeletal hyperostosis (DISH).

Nucleoside and nucleobase transporters are important in the regulation of cardiovascular effects of purines, with special consideration to oxidative stress and blood pressure. We may have also discovered a novel role for ENT1 in the development of DISH.

Keywords: adenosine, hypoxanthine, microvascular endothelium, transporters, metabolism, reactive oxygen species, regulation, ischemia-reperfusion injury, hypotension, diffuse idiopathic skeletal hyperostosis

## CO-AUTHORSHIP

Chapters of this thesis that have been previously published in peer reviewed journals have been marked as so on the title page of that chapter. All experimental work and manuscript preparation was performed by Derek B. J. Bone. However, some of the research presented herein was performed by someone else, under the guidance and supervision of the author. These contributions are recognized here as follows:

### **Chapter Three.**

Experiments involving the OCT inhibitor decynium-22, [<sup>3</sup>H]adenine uptake, and inhibition of [<sup>3</sup>H]hypoxanthine uptake by OCT substrates were performed by 4<sup>th</sup> year honors student Lance Frieburger. Some characterization of the HMEC-1 cell line was performed by 4<sup>th</sup> year honors student Samantha Li.

### **Chapter Four.**

Concentration-dependent and time course experiments of the effects of VEGF on [<sup>3</sup>H]NBMMPR binding in HMEC-1 cells were performed by withdrawn M.Sc. candidate Samer Serhan. They were performed in close collaboration with Derek B J Bone as part of the laboratory technique training required to be self sufficient.

### **Chapter Five.**

Experiments on WT mouse MVECs involving CoCl<sub>2</sub>, mineral-oil ischemia, and hypoxia were performed by 4<sup>th</sup> year honors student Mallory Troup.

Doo-Sup Choi, listed as an author on the published manuscript provided the ENT1<sup>-/-</sup> mouse. Imogen R Coe, listed as an author on the published manuscript was recognized

for ongoing collaboration and facility usage. Both authors contributed to the writing of the published manuscript.

### **Chapter Six.**

Quantitative real-time PCR experiments performed on WT and ENT1<sup>-/-</sup> organs was performed by 4<sup>th</sup> year honors student Jeffery Bruce. Haemodynamic measurements were performed with the assistance of Dr. Rob Gros. HPLC analysis of mouse plasma was performed with the assistance of Dr. Murray Cutler.  $\mu$ CT scans of ENT1<sup>-/-</sup> mice were performed by Drs. Joseph Umoh and David Holdsworth. Some histological interpretation of ENT1<sup>-/-</sup> spines was done with the aid of Dr. Ian Welch.

In all cases, Dr. James Hammond assisted in experimental design and manuscript preparation.

*To*  
*Mom and Dad*

## ACKNOWLEDGEMENTS

Thank you to all past and present members of the Hammond Lab for providing an excellent work environment and assistance when needed. The last six years would have been much more difficult without you.

Mike Knauer, thank you for showing me that young people can be passionate about research and teaching and not feel alone.

To Jake Witucki, thank you for being there to discuss family, relationships, and life in general. You're my connection to the 'real world'.

My advisors, Drs. Chidiac, Feng, and Regnault, your guidance and support has been greatly appreciated. Please continue to support the development of graduate students, we need dedicated professor like yourselves to keep the challenges of our education enjoyable.

Justin Cutler, thanks 'roomie' for giving me a great place to call home during the last few months of my schooling. I don't think I could have made it without your gross dangles and your domination over me in NHL'11.

Thank you, Julia Visentin, for your constant support. You showed me I can be myself and balance school and life and have a great time doing it. You were the calm during the storm that was the preparation of this thesis.

Murray Cutler, colleague and best friend. Grad school, and therefore my life, would not have been the same without you. Here is to many more years of hard work, funny t-shirts, and hosting lectures when we need a break from the lab. I wish you and Cindy all the best.

To my Mom and Dad for your un-ending support. You have always been there to make sure I would reach the end of the track. Thank you for being interested in what I do, even if you had to pretend that you understood what I was talking about. I couldn't have asked for anything more.

None of this would have been possible without Dr. James Hammond. I still remember meeting you for the first time in undergrad and learning that nucleoside transporters existed. Now, seven years later, it's impossible to think about life without them. Your passion for research and teaching is an inspiration and your dedication to your students is unmatched. You've allowed me to see the world. You've pushed for the recognition of my work. You've shown me that research is the career path for me. You've done more for me than this thank you can say.

TABLE OF CONTENTS

CERTIFICATE OF EXAMINATION.....ii

ABSTRACT.....iii

KEYWORDS.....iv

CO-AUTHORSHIP.....v

DEDICATION.....vii

ACKNOWLEDGEMENTS.....viii

TABLE OF CONTENTS.....x

LIST OF TABLES.....xx

LIST OF FIGURES.....xxi

LIST OF APPENDICES.....xxiv

LIST OF ABBREVIATIONS.....xxv

CHAPTER ONE: INTRODUCTION.....1

    1.1 The Endothelium.....2

        1.1.1 Classifications of Endothelia.....3

        1.1.2 The Endothelial Cell.....4

            1.1.2.1 Identification and Function.....4

            1.1.2.2 Endothelial Dysfunction.....5

    1.2 Ischemia and Reperfusion.....5

        1.2.1 Cardiovascular Ischemia.....6

        1.2.2 Reperfusion and the Microvasculature.....6

            1.2.2.1 Reperfusion-Induced Inflammation.....6

1.2.2.2 Reperfusion and ROS.....	7
1.2.3 Purines and Cardiovascular Ischemia.....	7
1.3 Nucleobases, Nucleosides, and Nucleotides.....	8
1.4 Adenosine.....	10
1.4.1 Adenosine Bioactivity.....	10
1.4.2 Adenosine in Ischemia-Reperfusion.....	10
1.4.2.1 Adenosine and Cardioprotection.....	11
1.4.2.2 Endothelial Adenosine Metabolism.....	11
1.5 Nucleoside Transporters.....	14
1.5.1 Concentrative Nucleoside Transporters.....	14
1.5.2 Equilibrative Nucleoside Transporters.....	15
1.5.2.1 ENT1.....	15
1.5.2.2 ENT2.....	16
1.5.2.3 ENT3.....	17
1.5.2.4 ENT4.....	17
1.6 Nucleobase Transporters.....	19
1.6.1 ENT2.....	19
1.6.2 SLC23a4/Sodium-dependent Nucleobase Transporter 1 (SNBT1).....	20
1.6.3 SVCT/Nucleobase-ascorbate Transporter (NAT).....	21
1.7 References.....	22



CHAPTER TWO: RESEARCH QUESTIONS, HYPOTHESES, AND GENERAL METHODOLOGIES.....	30
2.1 Research Questions.....	31
2.2 Hypotheses.....	32
2.2.1 Chapter 3 – Human Primary MVEC Characterization.....	32
2.2.2 Chapter 4 – Regulation of purine transporters in human primary MVECs.....	33
2.2.3 Chapter 5 – MVECs from ENT1 <sup>-/-</sup> Mice.....	33
2.2.4 Chapter 6 – Additional Phenotypes of ENT1 <sup>-/-</sup> Mice.....	34
2.3 Common Methodologies.....	35
2.3.1 Mammalian Cell Culture.....	35
2.3.1.1 Cell Harvesting.....	35
2.3.2 [ <sup>3</sup> H]NBMPR Binding Assay.....	36
2.3.3 Oil-Stop Transport Assay.....	37
2.3.3.1 [ <sup>3</sup> H]Substrate Preparation.....	37
2.3.3.2 Transport Assay Setup – Nucleoside Substrate.....	38
2.3.3.3 Transport Assay Setup – Nucleobase Substrate.....	41
2.3.3.4 Intracellular Volume.....	42
2.3.3.5 Transport Data Analysis.....	42
2.4 References.....	43

CHAPTER THREE: NUCLEOSIDE AND NUCLEOBASE TRANSPORTERS OF PRIMARY HUMAN  
CARDIAC MICROVASCULAR ENDOTHELIAL CELLS: CHARACTERIZATION OF A NOVEL  
TRANSPORTER.....48

    3.1 Introduction.....49

    3.2 Materials and Methods.....50

        3.2.1 Materials.....50

        3.2.2 Cell Culture.....51

        3.2.3 Substrate Efflux Assay.....52

        3.2.4 Data Analysis and Statistics.....53

    3.3 Results.....53

        3.3.1 [<sup>3</sup>H]NBMPR Binding.....53

        3.3.2 2-[<sup>3</sup>H]Chloroadenosine Uptake.....53

        3.3.3 [<sup>3</sup>H]Hypoxanthine Uptake.....54

        3.3.4 Nucleobase Transport in Other Cell Types.....65

        3.3.5 Characterization of HMEC-1 Cells.....70

        3.3.6 Decynium-22 and [<sup>3</sup>H]Adenine  $K_m/V_{max}$ .....71

        3.3.7 [<sup>3</sup>H]Hypoxanthine Efflux.....71

        3.3.8 Candidates for the Identity of ENBT1.....71

            3.3.8.1 The Unnamed Human Protein Product hUPP1.....72

            3.3.8.2 Organic Cation Transporter as a Possible Candidate for  
                    ENBT1.....72

    3.4 Discussion.....83

3.4.1	Characterization of Nucleoside Transport in Human Cardiac Microvascular Endothelial Cells.....	83
3.4.2	Identification of a Novel Nucleobase Transporter in Human Cardiac Microvascular Endothelial Cells.....	84
3.4.3	Physiological Importance of Nucleobase Transport.....	85
3.5	References.....	90
CHAPTER FOUR: REGULATION OF HUMAN MICROVASCULAR ENDOTHELIAL CELL PURINE TRANSPORTERS.....		94
4.1	Introduction.....	95
4.2	Materials and Methods.....	97
4.2.1	Materials.....	97
4.2.2	Vascular Endothelial Growth Factor Treatment.....	98
4.2.3	Protein Kinase Modulation.....	101
4.2.4	Adenosine Receptor Agonists.....	101
4.2.5	Treatment with a Reactive Oxygen Species Generator.....	101
4.2.6	Simulated Hypoxia and Ischemia.....	102
4.2.6.1	Cobalt Chloride Treatment.....	102
4.2.6.2	Simulated Ischemia.....	102
4.3	Results.....	103
4.3.1	Regulation of transport by VEGF.....	103

4.3.1.1 VEGF protects against serum starvation cell death in primary but not immortalized microvascular endothelial cells.....	103
4.3.1.2 VEGF reduces [ <sup>3</sup> H]NBMPR binding sites in microvascular endothelial cells.....	103
4.3.1.3 The reduction in [ <sup>3</sup> H]NBMPR binding is temporally different between MVEC and HMEC-1 cells.....	103
4.3.1.4 VEGF reduction in [ <sup>3</sup> H]NBMPR binding sites in MVECs may be mediated by VEGFR2.....	104
4.3.1.5 Nucleobase transport, but not nucleoside transport is increased by VEGF.....	104
4.3.2 Regulation by PKC.....	105
4.3.3 Regulation by CKII.....	105
4.3.4 Regulation by PKA.....	119
4.3.5 Effect of ROS on nucleoside and nucleobase transporter function.....	119
4.3.6 Simulated Ischemia.....	125
4.4 Discussion.....	128
4.4.1 Regulation of Transport by VEGF.....	128
4.4.2 Regulation by Protein Kinase C.....	131
4.4.3 Regulation by CKII.....	132
4.4.4 Regulation by Protein Kinase A.....	133

4.4.5	Effects of ROS on Purine Transporters.....	134
4.4.6	Effects of Simulated Hypoxia and Ischemia on Purine Transporters.....	135
4.4.7	Conclusions.....	136
4.5	References.....	137
CHAPTER FIVE: MICROVASCULAR ENDOTHELIAL CELLS ISOLATED FROM MICE: TRANSPORTER CHARACTERIZATION AND REGULATION, SUBSTRATE METABOLISM, AND CONSEQUENCES OF ENT1 KNOCKOUT.....		
5.1	Introduction.....	144
5.2	Materials and Methods.....	145
5.2.1	Materials.....	145
5.2.2	ENT1 <sup>-/-</sup> mouse model.....	146
5.2.3	MVEC isolation/culture.....	147
5.2.4	Analysis of [ <sup>3</sup> H]hypoxanthine metabolites in MVECs.....	148
5.2.5	Reverse-transcriptase polymerase chain reaction.....	150
5.2.6	Immunoblots.....	151
5.2.7	Treatment with Reactive Oxygen Species Generators.....	152
5.2.8	Simulated Ischemia and Hypoxia.....	153
5.2.8.1	Cobalt Chloride Treatment.....	153
5.2.8.2	Simulated Ischemia.....	153
5.2.8.3	Hypoxia.....	154
5.3	Results.....	154

5.3.1	MVECs from ENT1 <sup>-/-</sup> Lack [ <sup>3</sup> H]NBMPR Binding.....	154
5.3.2	Compensatory Changes in Purinergic Genes in ENT1 <sup>-/-</sup> MVECs...	154
5.3.3	Nucleoside and Nucleobase Transport Function in WT and ENT1 <sup>-/-</sup> MVECs.....	155
5.3.4	Purine Metabolism in ENT1 <sup>-/-</sup> MVECs.....	172
5.3.5	Effects of Free Radical Generators on Purine Transport in Mouse MVECs.....	172
5.3.6	Effects of Ischemia and Hypoxia on Purine Transporters.....	175
5.4	Discussion.....	182
5.4.1	Compensatory Changes in ENT1 <sup>-/-</sup> MVECs.....	182
5.4.2	Alterations in Purine Transport Capacity.....	183
5.4.3	Impact of Ischemia and Hypoxia on Purine Transport in WT MVECs.....	185
5.4.4	Conclusions.....	188
5.5	References.....	190
 CHAPTER SIX: ADDITIONAL PHENOTYPES OF THE ENT1 <sup>-/-</sup> MOUSE: FROM HYPOTENSION TO SPINAL HYPEROSTOSIS.....		
6.1	Introduction.....	195
6.2	Materials and Methods.....	196
6.2.1	Animals.....	196
6.2.2	Quantitative Real-Time PCR.....	196
6.2.3	Haemodynamics.....	197

6.2.4	High Performance Liquid Chromatography.....	197
6.2.5	Micro Computed Tomography ( $\mu$ CT) Imaging.....	197
6.2.6	Histology.....	198
6.2.7	Scanning Electron Microscopy.....	198
6.3	Results.....	199
6.3.1	Changes in Purinergic Genes in Organs.....	199
6.3.2	Haemodynamics.....	199
6.3.3	Plasma Purines.....	200
6.3.4	Unexpected Paresis and Paralysis.....	200
6.3.5	Histology.....	206
6.3.6	6 $\mu$ CT Scanning.....	206
6.3.7	Scanning Electron Microscopy.....	211
6.4	Discussion.....	218
6.4.1	Altered gene expression.....	218
6.4.2	Altered cardiovascular function.....	219
6.4.3	Abnormal mineral deposits in the spine.....	220
6.4.4	Conclusions.....	222
6.5	References.....	224
CHAPTER SEVEN: GENERAL DISCUSSION.....		228
7.1	Review of Research Questions.....	229
7.2	Picking an Appropriate Model: Differences in species and cell type.....	229

7.2.1	Differences in expression of nucleoside and nucleobase between species.....	230
7.2.2	Impact of cell type.....	230
7.2.3	Species differences and cell types: conclusions.....	231
7.3	Physiological Relevance.....	233
7.3.1	Discovery of a novel purine nucleobase transporter: A change in dogma.....	233
7.3.1.1	Future Directions: The Genetic Identity of ENBT1.....	233
7.3.2	ENBT1 and Ischemia-Reperfusion Injury of MVECs.....	234
7.3.2.1	Future Directions: ENT1, ENBT1, and ROS production.....	239
7.3.3	New roles of ENT1 in disease.....	240
7.3.3.1	Future Directions: The Role of ENT1 in Disease.....	240
7.4	Closing Remarks.....	242
7.5	References.....	243
	APPENDICES.....	246
	CURRICULUM VITAE.....	251



## LIST OF TABLES

Table		Page
3.1	$K_i$ values for inhibition of uptake by hMVECs 2-chloroadenosine and hypoxanthine	64
5.1	RT-PCR primers	159
5.2	Kinetic parameters for the transporter-mediated uptake of 2-chloroadenosine and hypoxanthine by MVECs isolated from WT and ENT1 <sup>-/-</sup> mice	173
7.1	Relative expression of nucleoside and nucleobase transporters in primary MVECs from different species	232

## LIST OF FIGURES

Figure		Page
1.1	Nucleobases, nucleosides, and nucleotides.	9
1.2	Endothelial purine metabolism during ischemia-reperfusion.	13
1.3	Predicted 2-dimensional structure of ENT proteins.	18
2.1	Schematic of the Oil-Stop Method.	40
3.1	<sup>3</sup> H-labeled nitrobenzylmercaptapurine riboside (NBMPR) binding to human cardiac microvascular endothelial cells (MVECs).	56
3.2	2-[ <sup>3</sup> H]chloroadenosine uptake characteristics of human cardiac MVECs.	58
3.3	Inhibition of 2-[ <sup>3</sup> H]chloroadenosine uptake.	59
3.4	[ <sup>3</sup> H]hypoxanthine uptake characteristics of human cardiac MVECs	61
3.5	Inhibition of [ <sup>3</sup> H]hypoxanthine uptake.	63
3.6	Dipyridamole-insensitive [ <sup>3</sup> H]hypoxanthine uptake in various cell types.	67
3.7	PK15NTD cells as a model for nucleobase transport.	69
3.8	Complex effects of nucleoside and nucleobase transporter coexpression and inhibition.	74
3.9	Characterization of HMEC-1 cells.	76
3.10	Decynium-22 and [ <sup>3</sup> H]adenine $K_m/V_{max}$ .	78
3.11	[ <sup>3</sup> H]hypoxanthine efflux.	79
3.12	GFP-hUPP1 does not increase hypoxanthine uptake in HEK cells.	81
3.13	OCT substrate acyclovir but not metformin can inhibit hypoxanthine uptake.	82
4.1	Putative intracellular phosphorylation sites on human ENT1.	100

4.2	VEGF enhances cell concentration in primary MVECs but not immortalized HMEC-1 cells.	106
4.3	VEGF decreased [ <sup>3</sup> H]NBMPR binding B <sub>max</sub> in both hMVECs and HMEC-1 cells.	108
4.4	The reduction in [ <sup>3</sup> H]NBMPR binding was temporally different between MVEC and HMEC-1 cells.	110
4.5	VEGF reduction in [ <sup>3</sup> H]NBMPR B <sub>max</sub> was mediated by VEGF receptor VEGFR2.	112
4.6	Sunitinib inhibition of [ <sup>3</sup> H]NBMPR binding does not correspond to B <sub>max</sub> decreases.	113
4.7	Nucleobase transport, but not nucleoside transport, is increased by VEGF.	115
4.8	Nucleoside and nucleobase transport are differentially regulated by PKC.	117
4.9	Inhibition of CKII decreases nucleoside and nucleobase uptake.	118
4.10	Effect of cAMP on nucleoside and nucleobase transporter function.	121
4.11	Adenosine A <sub>2</sub> receptor agonism does not alter ENT1 function.	122
4.12	Intracellular superoxide production by menadione reduced ENBT1 but not ENT1 function.	124
4.13	Effects of hypoxia and ischemia on nucleoside and nucleobase transport.	127
5.1	MVECs from ENT1 <sup>-/-</sup> lack [ <sup>3</sup> H]NBMPR binding.	158
5.2	Analysis of purine transporter/metabolic enzyme gene expression in MVECs.	161
5.3	ADA and A <sub>2A</sub> are upregulated at the protein level.	163
5.4	Formycin B uptake by ENT2 is unchanged in MVECs from ENT1 <sup>-/-</sup> mice.	165
5.5	Uptake of 2-[ <sup>3</sup> H]chloroadenosine by ENT2 is reduced in MVECS from ENT1 <sup>-/-</sup> mice.	167

5.6	Uptake of [ <sup>3</sup> H]hypoxanthine was mediated by a dipyridamole-insensitive transporter.	169
5.7	Dipyridamole enhances [ <sup>3</sup> H]hypoxanthine uptake in WT, but not ENT1 <sup>-/-</sup> MVECS.	171
5.8	[ <sup>3</sup> H]Metabolite profile in WT and ENT1 <sup>-/-</sup> MVECS.	174
5.9	TBHP had no effect on purine transport.	177
5.10	Menadione reduced the Vmax of ENT1 mediated 2-chloroadenosine uptake.	179
5.11	Hypoxanthine uptake can be altered by both ischemia and hypoxia in mouse MVECS.	181
6.1	Purinergic gene changes in other organs.	202
6.2	ENT1 <sup>-/-</sup> mice have lower blood pressure than WT mice.	204
6.3	Circulating plasma adenosine is elevated in ENT1 <sup>-/-</sup> mice.	205
6.4	ENT1 <sup>-/-</sup> mice develop mineralized lesions on the spine.	208
6.5	Histology of ENT1 <sup>-/-</sup> spines reveals spinal cord impingement.	210
6.6	Micro computed tomography of ENT1 <sup>-/-</sup> spines.	213
6.7	Time course of lesion development in ENT1 <sup>-/-</sup> mice.	215
6.8	Scanning electron microscopy (SEM) images of mineral deposits in ENT1 <sup>-/-</sup> intervertebral spaces.	217
6.9	Alterations in Boxer dog ENT1 protein.	223
7.1	Changes in nucleoside and nucleobase transporter dogma.	236
7.2	ENBT1 and ischemia-reperfusion injury.	238

## LIST OF APPENDICES

1	Copyright permission for Chapter 3	247
2	Copyright permission for Chapter 5	248
3	Ethics approval for the usage of animals	249
4	Lack of mineralization in other joints	250

## LIST OF ABBREVIATIONS

5-FU, 5-fluorouracil

6-MP, 6-mercaptopurine

6-TG, 6-thioguanine

8-CPT-2Me-cAMP, 8-(4-Chlorophenylthio)-2'-*O*-methyladenosine-3',5'-cyclic  
monophosphate sodium salt

ADA, adenosine deaminase

ANOVA, analysis of variance

ATP, adenosine triphosphate

BGS, bovine growth serum

$B_{max}$ , maximum number of ligand binding sites

BPM, beats per minute

BSA, bovine serum albumin

cAMP, cyclic adenosine monophosphate

cDNA, complementary deoxyribonucleic acid

cGMP, cyclic guanosine monophosphate

CGS21680, 4-[2-[[6-Amino-9-(*N*-ethyl- $\beta$ -D-ribofuranuronamidosyl)-9*H*-purin-2-yl]amino]ethyl]benzene propanoic acid hydrochloride

CKII, casein kinase II

CNT, concentrative nucleoside transporter

CO<sub>2</sub>, carbon dioxide

CoCl<sub>2</sub>, cobalt (II) chloride

D-22, decynium-22, 1,1'-diethyl-2,2'-cyanine iodide

ddH<sub>2</sub>O, deionized distilled water

Dilazep, (N,N'-bis[3-(3,4,5-trimethoxybenzyloxy)propyl]-homo-piperazine)

Dipyridamole, [2,6-bis (diethanolamino)-4,8-dipiperidinopyrimido-[5,4-d]pyrimidine]

DISH, diffuse idiopathic spinal hyperostosis

DMEM-F12, Dulbecco's Modified Eagle Medium: Nutrient Mixture F-12

DMSO, dimethylsulfoxide

dpm, disintegrations per minute

Draflazine, [2-(aminocarbonyl)-4-amino-2,6-dichlorophenyl]-4-[5,5-bis(4-fluorophenyl)pentyl]-1-piperazine acetamide 2HCl]

EBM-2, endothelial basal medium-2

ECGS, endothelial cell growth supplement

EDTA, Ethylenediaminetetraacetic acid

EGF, epithelial growth factor

EGM-2MV, endothelial growth medium-2, microvascular

EGTA, ethylene glycol tetraacetic acid

ENBT, equilibrative nucleobase transporter

ENT, equilibrative nucleoside transporter

*es*, equilibrative nucleoside transport sensitive to inhibition by NBMPR

*ei*, equilibrative nucleoside transport insensitive to inhibition by NBMPR

FBS, fetal bovine serum

G418, Geneticin

GAPDH, Glyceraldehyde 3-phosphate dehydrogenase

GFP, green fluorescent protein

Gö6976, 5,6,7,13-Tetrahydro-13-methyl-5-oxo-12*H*-indolo[2,3-*a*]pyrrolo[3,4-  
c]carbazole-12-propanenitrile

Gö6983, 3-[1-[3-(Dimethylamino)propyl]-5-methoxy-1*H*-indol-3-yl]-4-(1*H*-indol-3-yl)-1*H*-  
pyrrole-2,5-dione

h, human

HBSS, Hank's buffered salt solution

HCl, hydrochloric acid

HEK-293, human embryonic kidney 293 cell line

HEPES, 4-(2-hydroxyethyl)-1-piperazineethanesulfonic acid

HIF-1 $\alpha$ , hypoxia inducible factor, 1 alpha

HMEC-1, human microvascular endothelial cell line 1

HPLC, high performance liquid chromatography

hUPP1, human unnamed protein product 1

HUVEC, human umbilical vein endothelial cell

IC<sub>50</sub>, the concentration of inhibitor needed to inhibit 50% of ligand binding

kDa, kilodalton

K<sub>d</sub>, equilibrium dissociation constant, affinity of ligand binding

K<sub>i</sub>, equilibrium dissociation constant for an inhibitor

K<sub>m</sub>, the concentration of substrate that gives half the maximal rate of uptake

KO, knock-out



KT5270, (9*R*,10*S*,12*S*)-2,3,9,10,11,12-Hexahydro-10-hydroxy-9-methyl-1-oxo-9,12-epoxy-1*H*-diindolo[1,2,3-*fg*:3',2',1'-*kl*]pyrrolo[3,4-][1,6]benzodiazocine-10-carboxylic acid, hexyl ester

m, mouse

menadione, 2-Methylnaphthalene-1,4-dione

MEM, modified Eagle medium

MDCK, Madin-Darby canine kidney cell line

μCT, micro computed tomography

MnTMPyP, manganese(III) tetrakis(1-methyl-4-pyridyl)porphyrin

mRNA, messenger ribonucleic acid

MVEC, microvascular endothelial cell

NAT, nucleobase-ascorbate transporter

Na<sub>3</sub>VO<sub>4</sub>, sodium ortho-vanadate

NBMPR, nitrobenzylemercaptapurine ribonucleoside

NBTGR, nitrobenzylthioguanosine

NECA, 1-(6-Amino-9*H*-purin-9-yl)-1-deoxy-*N*-ethyl-β-D-ribofuranuronamide

nH, Hill coefficient

NMG, N-methyl-d-glucamine

NO, nitric oxide

NTD, nucleoside transport deficient

O<sub>2</sub>, oxygen gas

OCT, organic cation transporter

PBS, phosphate buffered saline

PCR, polymerase chain reaction

PK15, porcine kidney epithelial cell line

PKA, protein kinase A

PKC, protein kinase C

PMA, phorbol-12-myristate13-acetate

PNP, purine nucleoside phosphorylase

r, rat

RNS, reactive nitrogen species

ROS, reactive oxygen species

RT, reverse transcriptase

RTK, receptor tyrosine kinase

SDS-PAGE, sodium dodecyl sulfate polyacrylamide gel electrophoresis

SEM, standard error of the mean

SIN-1, 3-Morpholinosydnonimine hydrochloride

SLC, solute carrier

Sunitinib, *N*-[2-(Diethylamino)ethyl]-5-[(*Z*)-(5-fluoro-1,2-dihydro-2-oxo-3*H*-indol-3-ylidene)methyl]-2,4-dimethyl-1*H*-pyrrole-3-carboxamide (2*S*)-2-hydroxybutanedioate salt

SVCT, sodium-dependent vitamin C transporter

TBB, 4,5,6,7-Tetrabromobenzotriazole

TBHP, tert-butyl hydroperoxide

TLC, thin-layer chromatography

Tris, 2-Amino-2-hydroxymethyl-propane-1,3-diol

U2OS, human osteosarcoma cell line

UMR-108, Sprague-Dawley rat osteosarcoma cell line

VEGF, vascular endothelial growth factor

VEGFR, vascular endothelial growth factor receptor

$V_i$ , initial rate of substrate uptake

$V_{max}$ , maximum velocity

WT, wild-type

XO, xanthine oxidase

ZM323881, 5-((7-Benzyloxyquinazolin-4-yl)amino)-4-fluoro-2-methylphenol

hydrochloride

CHAPTER ONE

INTRODUCTION

The work presented in this thesis was focused on understanding the function, regulation, and physiological roles of nucleoside and nucleobase transporters expressed in microvascular endothelial cells (MVECs). Following a brief introduction and information on the hypotheses addressed in this thesis, research will be presented in two main sections. The first section, which includes Chapters Three and Four, discuss the expression, function, and regulation of nucleoside and nucleobase transporters in primary human MVECs. The second section, which includes Chapters Five and Six, focus on mouse models for nucleoside and nucleobase transport and with the aid of a nucleoside transporter deficient mouse, it aims to help further the understanding of the physiological importance of nucleoside and nucleobase transporters. The thesis will conclude with a concise chapter pulling together all the information discussed and provide clear concepts that can be derived from the work as a whole.

### **1.1 The Endothelium**

The bulk of the research presented in this thesis was conducted with endothelial cells. The following section will highlight the importance of this cell type and the unique properties of the endothelium as a tissue. The endothelium is the specialized lining of both the cardiovascular and lymphatic systems. It is estimated to cover 350 m<sup>2</sup> in the average person and is the barrier between the blood and tissues (44). The endothelium is also an important regulator of vascular tone and other important biological processes including angiogenesis (the formation of new blood vessels), fluid and solute transport, and inflammation (44). The endothelium can perform these multiple functions because

rather than being one single identical sheet, there is a great deal of heterogeneity across organs and even within continuous vascular beds(44).

### *1.1.1 Classifications of Endothelia*

The simplest distinction of endothelia is based on the size of the vasculature where they are found. There are two classifications: macrovasculature and microvasculature. Macrovasculature includes any vessel 500  $\mu\text{m}$  or greater in diameter. This includes major arteries like the aorta, and major veins, like the superior vena cava. Everything else is thus considered microvasculature, the major component of which is the capillaries, which have a diameter of 10  $\mu\text{m}$  or less. The microvasculature can also include smaller arterioles and venuoles (55).

The other important classification of endothelia is based on the cellular morphology, which also determines permeability. There are three types of morphologies: continuous, fenestrated, and discontinuous (44). Continuous endothelium is the least permeable, with cells forming tight junctions between themselves. Continuous endothelium exists where controlling exchange between the blood and tissue is most important, for example at the blood-brain barrier. Fenestrated endothelia have very fine pores (fenestrae) less than 100 nm in diameter that are sealed with a semi-permeable diaphragm. This design allows for increased permeability of hydrophilic, low-molecular weight molecules and water. Fenestrated endothelium is found in locations where absorption and secretion are important, for example in the kidney glomerulus or in endocrine glands. Finally, discontinuous endothelium is the most permeable, with larger fenestrae (up to 1  $\mu\text{m}$  in diameter). However these fenestrae lack the diaphragm seen in

fenestrated endothelium, and are also either lacking a basement membrane or the basement membrane is also porous. Discontinuous endothelium is commonly found in organs like the liver and spleen where they act as less selective filters for macromolecules or aid in filtering the blood, respectively (44).

### *1.1.2 The Endothelial Cell*

#### *1.1.2.1 Identification and Function*

Endothelial cells, the specialized cell type that makes up the endothelium tissue, can be identified by several unique characteristics. These characteristics contribute to the normal functioning of the endothelial cell, and therefore the endothelium tissue as a whole.

The endothelial cell is most well known for the expression of endothelial nitric oxide synthase (eNOS). eNOS produces nitric oxide (NO) from the amino acid L-arginine, which can then alter transcription of genes in the endothelial cell and reduce vascular tone by promoting the relaxation of smooth muscle cells through the activation of soluble guanylate cyclase.

An important feature of the endothelial cell is the endothelial glycocalyx, a layer of glycoproteins and proteoglycans about 100 nm thick on the surface of the endothelial cell. Of the proteoglycans in the glycocalyx, up to 90% are heparin sulphate proteoglycans. These heparin sulphate proteoglycans bind antithrombin III, and this combination is what gives the endothelial surface its anti coagulation properties (44). The endothelial surface layer also limits mechanical stress both on the circulating red blood cells and the endothelial cell itself. The loss of the endothelial surface layer can

alter blood clotting, red blood cell life-span, blood flow dynamics through capillaries, and mechanical damage to endothelial cells (44).

Endothelial cells can also be identified by the presence of specific proteins they express. These proteins include eNOS, vascular endothelial growth factor receptor 2, von Willebrand factor, vascular endothelial cadherin, and E-selectin (28).

#### 1.1.2.2 Endothelial Dysfunction

Endothelial dysfunction is a blanket term that covers any change that prevents the endothelial cell from functioning normally. However, in practice, endothelial dysfunction is most commonly used to describe the decreased ability of the endothelial cell to produce NO, leading to increased smooth muscle tone and hypertension. Additionally, endothelial dysfunction may refer to a loss of the barrier function, resulting in vascular leakage. The inability to prevent coagulation, leading to the formation of clots is also a type of endothelial dysfunction. Ultimately, dysfunction may lead to the loss of endothelial cells through cellular death.

Endothelial dysfunction can be caused a number of different factors including inflammation (43) and reactive oxygen species (ROS) (59; 63), or conditions that promote inflammation or ROS production such as hypertension (9) and diabetes (18).

### **1.2 Ischemia and Reperfusion**

Ischemia is the lack of blood flow to a tissue. The area affected by ischemia is characterized by reduced oxygen concentrations, known as hypoxia, and nutrient supply. There is also an accumulation of metabolic products that cannot be removed



due to the lack of blood flow. It is important to know that hypoxia can occur without ischemia. Reperfusion is the return of oxygenated blood flow to the tissue that was previously ischemic.

### *1.2.1 Cardiovascular Ischemia*

Ischemia in the cardiovascular system is a life threatening condition. Cardiac ischemia can cause a myocardial infarction, or heart attack. The length and severity of the ischemic attack can influence the extent of cardiomyocyte death (30).

### *1.2.2 Reperfusion and the Microvasculature*

The return of oxygenated blood flow to an ischemic tissue, especially in the heart, is mandatory for survival of the cardiomyocytes. However, reperfusion is the start of a second wave of damage, one that affects the microvascular endothelium. Perhaps the best evidence that the microvasculature can be damaged as a result of ischemia is the 'no-reflow' phenomenon seen in cardiac angiograms 24 hours after reperfusion. No-reflow is the lack of the return of blood flow to the microvasculature in a previously ischemic area of the heart, usually in correlation to the infarct zone (7; 47).

#### *1.2.2.1 Reperfusion-Induced Inflammation*

During ischemia the lowered oxygen concentrations lead to the release of P-selectin and the activation of the transcription factor NF- $\kappa$ B, which in turn increases the expression of adhesion molecules on the endothelial cell surface (7). With reperfusion, the returning blood brings white blood cells, including leukocytes. The leukocytes are attracted to the adhesion molecules expressed on the endothelial cell and are slowed down, a process called leukocyte rolling. Once the leukocytes have slowed enough, they

will adhere to the endothelial cell and then migrate through inter-endothelial spaces into the surrounding tissue. At this time the leukocytes are activated and release ROS damaging the endothelial cells ultimately leading to endothelial dysfunction and the no-reflow phenomenon (7; 23).

#### 1.2.2.2. Reperfusion and ROS

In addition to the ROS produced by recruited leukocytes, intracellular processes contribute to the production of ROS and endothelial damage. The return of oxygen allows mitochondria and intracellular oxidation proteins to function again. However, mitochondrial electron transport processes are uncoupled, leading to more ROS production and the opening of the mitochondria permeability transition pore, which leads to cellular apoptosis (12). Increased ROS formation through NADPH oxidase and xanthine oxidase interfere with the proper functioning of eNOS and directly react with NO, effectively reducing NO bioavailability and thus contributing to endothelial dysfunction (12; 23; 30).

#### 1.2.3 Purines and Cardiovascular Ischemia

As mentioned above, the purine metabolizing enzyme xanthine oxidase, is capable of producing ROS during reperfusion. This thesis will focus on the role of purine transporters and metabolism in the microvascular endothelium in the context of ischemia-reperfusion. The following sections of this chapter will introduce the necessary concepts of purines, purine metabolism, and purine transport required to appreciate the work presented in subsequent chapters.

### **1.3 Nucleobases, Nucleosides, and Nucleotides**

Nucleobases (also known as nitrogenous bases) are the building blocks of some of the most important molecules in life. The bases are classified in two types, purine or pyrimidine. Purine bases have a double ring structure compared to the pyrimidine single ring structure. In fact, purine bases are pyrimidine rings fused to an imidazole ring.

Nucleosides are nucleobases bound to a ribose or deoxyribose sugar through an N-glycosidic bond. Nucleosides, especially the purine adenosine, have important biological roles. Nucleosides can also have phosphate groups added to them to become nucleotides. Nucleotides are the monomers of DNA and RNA. Nucleotides are also used as cellular energy molecules and in intracellular signalling cascades. Figure 1.1 outlines the relationship between these molecules.

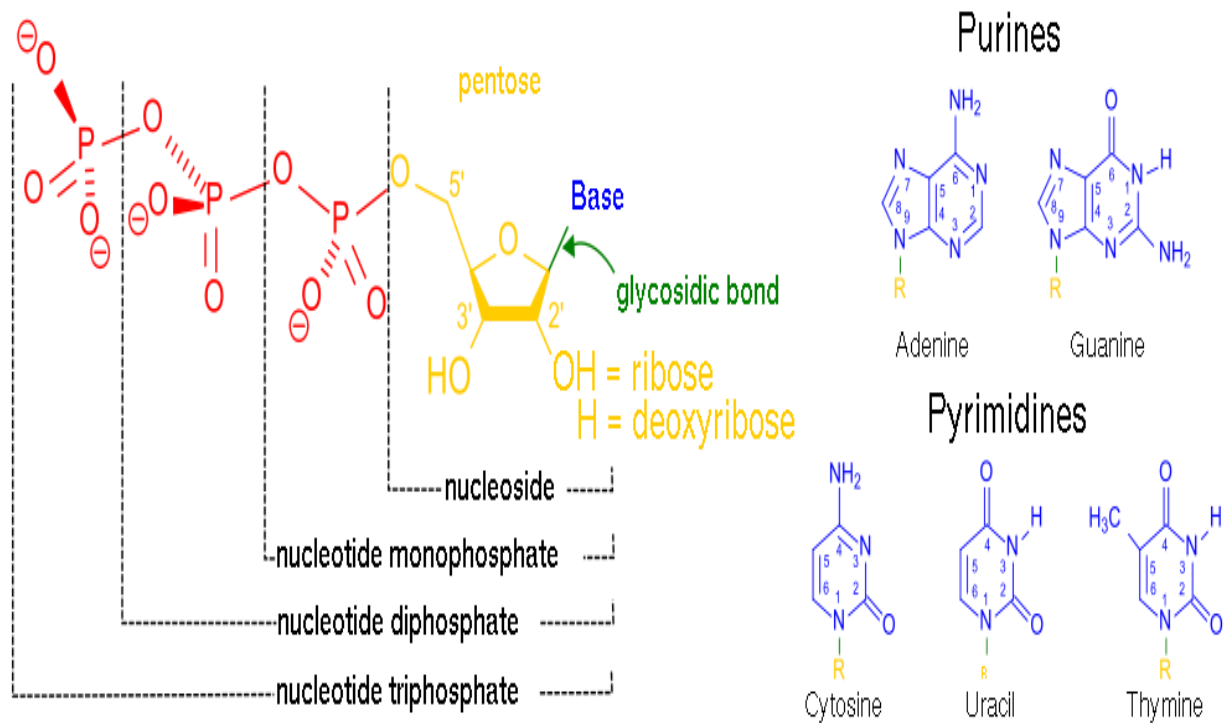


Figure 1.1. Nucleobase, nucleosides, and nucleotides.

A schematic showing the relationship between nucleobases, nucleosides, and nucleotides. Purine and pyrimidine nucleobases are shown in blue on the right hand side of the figure. On the bases, R represents the location of where the base is attached to the sugar moiety by the glycosidic bond. The yellow sugar in the middle of the figure can vary at the 2' position, where the presence of an OH group defines a ribose, whereas if there is only an H, the sugar is a deoxyribose, and thus a nucleoside or deoxynucleoside respectively. When phosphate groups, shown in red, are bound to a nucleoside, a nucleotide is formed. The number of phosphate groups determines the type of nucleotide.

## **1.4 Adenosine**

The purine nucleoside adenosine is one of the most important molecules in biology. In addition to well known roles as the starting point of the cellular energy molecule adenosine triphosphate (ATP), free adenosine can regulate the physiology of a variety of different systems including the CNS (sleep, anxiety, addiction), cardiovascular, renal, and immune system (4; 11; 27; 56). Adenosine is also important in pathophysiology, acting as a protector of cardiac and neuronal tissue during ischemic insult (33; 36; 40; 46). To accomplish these feats, adenosine must be present in the extracellular space to interact with specific adenosine receptors.

### *1.4.1 Adenosine Bioactivity*

Adenosine mediates cellular effects through the family of P1 purinergic G protein coupled receptors, more commonly referred to as adenosine receptors. To date, 4 adenosine receptor subtypes have been identified and cloned: A<sub>1</sub>, A<sub>2A</sub>, A<sub>2B</sub>, and A<sub>3</sub> (20). A<sub>1</sub> and A<sub>3</sub> receptors have been shown to signal through G<sub>i</sub>, inhibiting cAMP production by adenylate cyclase, where as the A<sub>2</sub> subtypes signal through G<sub>s</sub>, stimulating cAMP production (20).

### *1.4.2 Adenosine in Ischemia-Reperfusion*

During ischemia adenosine is released from cardiomyocytes and local extracellular concentrations can rise from nanomolar to micromolar levels (26). Adenosine is formed in cardiomyocytes during ischemia from two major sources: breakdown of ATP and s-adenosylhomocystine catabolism (26; 32).

#### 1.4.2.1 Adenosine and Cardioprotection

The release of adenosine during ischemia is a defensive mechanism to reduce cardiac infarct size.

The A<sub>1</sub> receptor subtype has been the most extensively studied and is the key player in the ability of adenosine to protect cardiac myocytes from infarction following an ischemic insult (10; 40; 66; 69). In fact, A<sub>1</sub> receptor agonism with pharmacological ligands can also confer cardioprotection (29; 60; 65). However, vascular endothelial cells, which are also susceptible to damage from ischemia/reperfusion, do not express A<sub>1</sub> receptors; the A<sub>2</sub> subtypes are the predominant receptors (16; 19; 51).

#### 1.4.2.2 Endothelial Adenosine Metabolism

While adenosine is initially cardioprotective – reducing infarct size – this excess adenosine will eventually accumulate in the microvasculature. The surrounding cardiac microvascular endothelium acts as a 'sink' removing approximately 65% of released adenosine from the interstitium (8).

Adenosine is metabolized intracellularly by two distinct pathways: a high affinity pathway via adenosine kinase, producing adenosine-5'-monophosphate, and a low affinity pathway via adenosine deaminase, producing the nucleoside inosine (32). Under normal conditions, adenosine kinase works below its K<sub>m</sub> value due to low intracellular free adenosine concentrations. However, during ischemia, the excess adenosine leads to adenosine kinase saturation and inactivation, thus shifting metabolism to adenosine deaminase, increasing intracellular inosine concentrations. Inosine is metabolized by purine nucleoside phosphorylase to form the purine

nucleobase hypoxanthine. Xanthine oxidase then catalyzes the conversion of hypoxanthine to xanthine and xanthine to uric acid (Figure 1.2) (38). These reactions result in the production of superoxide anion which is converted to hydrogen peroxide by superoxide dismutase. Hydrogen peroxide can either be detoxified to water and oxygen through the enzymes catalase and glutathione peroxidase or can be used to form strong oxidizing chemicals such as hypochlorous acid by myeloperoxidase (5). In addition to enzymatic reactions, hydrogen peroxide can spontaneously form hydroxyl radicals in the presence of ferrous iron by the Fenton reaction. Hydroxyl radicals are extremely reactive and will oxidize almost any cellular target. In endothelial cells, nitric oxide produced by endothelial nitric oxide synthase can also react with hydrogen peroxide to form the reactive peroxynitrite anion radical. Xanthine oxidase mediated superoxide production is thought to contribute to cellular damage upon reperfusion, when the return of oxygen allows the enzyme to metabolize the hypoxanthine that accumulated during ischemia. In fact ROS generated by xanthine oxidase have been implicated in microvascular endothelial dysfunction (5; 48).

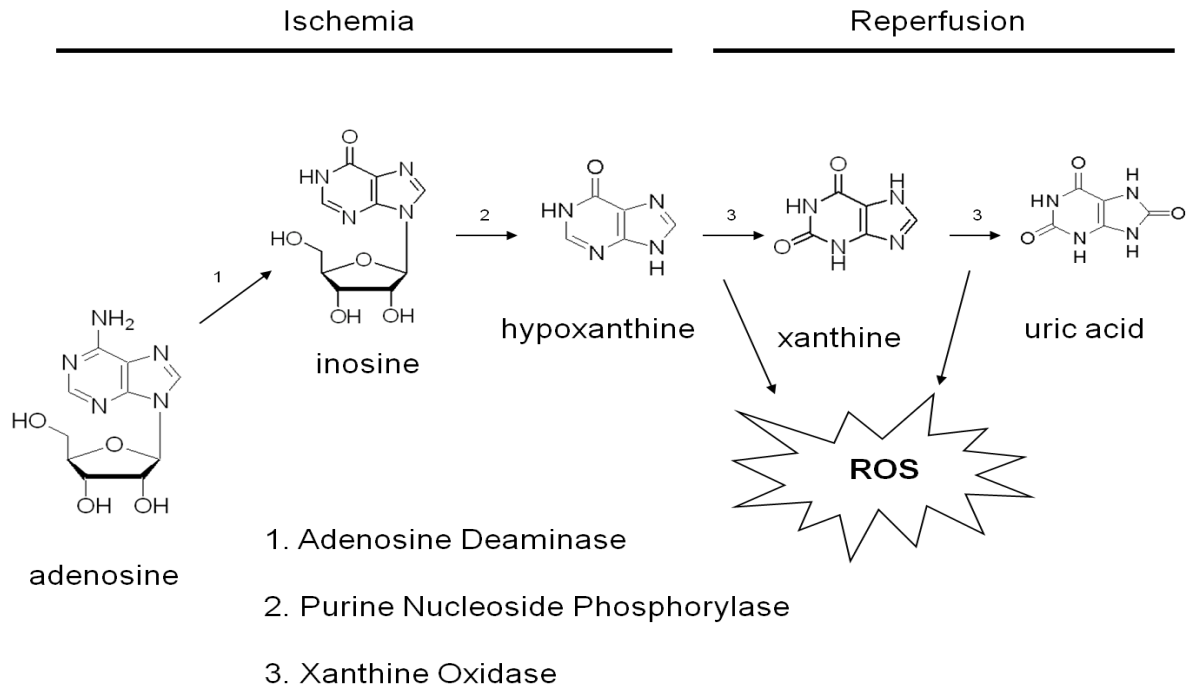


Figure 1.2. Endothelial purine metabolism during ischemia-reperfusion.

During cardiac ischemia, adenosine is released from cardiomyocytes and accumulates within the surrounding endothelial cells. This schematic highlights the deamination pathway of adenosine metabolism that is enhanced when the adenosine kinase enzyme becomes saturated. Adenosine is metabolized to inosine by enzyme 1, adenosine deaminase. Enzyme 2, purine nucleoside phosphorylase, catalyzes the formation of the nucleobase hypoxanthine from inosine. This pathway will not progress until reperfusion and the return of oxygen. During reperfusion, enzyme 3, xanthine oxidase, is capable of metabolizing hypoxanthine to xanthine, and xanthine to uric acid. Xanthine oxidase mediated oxidation of hypoxanthine and xanthine produces ROS, specifically superoxide anion, which contributes to endothelial damage and dysfunction.



## 1.5 Nucleoside Transporters

Regulation of extra- and intracellular nucleoside concentrations is important in controlling energy balance as well as cellular signalling in response to physiological stimuli. However, nucleosides are hydrophilic and therefore are incapable of crossing the plasma membrane. Two families of the solute carrier (SLC) superfamily of membrane transporters specialize in the transmembrane flux of nucleosides; the concentrative nucleoside transporters (SLC28A) and the equilibrative nucleoside transporters (SLC29A).

### *1.5.1 Concentrative Nucleoside Transporters*

Concentrative nucleoside transporters (CNTs) are a family of sodium-dependent transporters. CNTs move substrates against their concentration gradients into a cell, while co-transporting sodium ions. CNTs require energy from ATP to function, however the energy is used indirectly as CNTs do not catalyze ATP hydrolysis. Since CNTs require sodium as a co-transported ion, they depend on larger extracellular sodium concentrations compared to intracellular. This gradient is achieved by the sodium-potassium ATPase (24).

To date, three CNTs have been cloned: CNT1-3. CNT1 transports pyrimidines, CNT2 purines, and CNT3 is broadly selective (24). CNTs have very specialized expression, with CNT1 being localized to the kidney and liver and CNT2 having highest expression in the intestine (41).

### 1.5.2 Equilibrative Nucleoside Transporters

Equilibrative nucleoside transporters (ENTs) are sodium-independent, facilitative diffusion transporters. As such, ENTs mediate the transmembrane flux of nucleoside down their concentration gradient, either in to or out of the cell. Currently four members of the family have been identified and cloned; ENT1-4. All members share a common 11 membrane spanning domain topology with an intracellular N-terminus, and extracellular C-terminus, a large glycosylated extracellular loop between TMD1 and TMD2, and a large intracellular loop between TMD6 and TMD7. The orientation of the termini and loops was confirmed by the work of Sundaram and colleagues in 2001 (57). (Figure 1.3).

#### 1.5.2.1 ENT1

ENT1 is the most widely distributed and most studied of the ENTs. Before the gene was cloned, ENT1 was defined pharmacologically as the nucleoside transport system that was sensitive to nanomolar concentrations of the nucleoside analogue nitrobenzylmercaptapurine riboside (NBMPR). Consequently, this transporter was referred to as *es*, or equilibrative sensitive (1; 68). ENT1 is also inhibited by vasoactive drugs dipyridamole, drafazine, and dilazep (62). Inhibition of ENT1 by these drugs promotes local increases in adenosine concentrations, leading to enhanced adenosine receptor signalling and a vasodilation response (34). ENT1 is also exploited in chemotherapy to mediate the uptake of nucleoside analogue drugs in to tumour cells (13; 25; 61), or cells infected with parasites (e.g. malaria) (61; 68) or viruses (e.g. HIV)

(21; 35; 45). The level of expression of ENT1 in various cancers has been linked to chemotherapy resistance and survival rates (17; 42).

The human ENT1 transporter was first cloned in 1997 (25), followed by the mouse in 2000 (31). Interestingly, the mouse ENT1 differed from human in respect to a variety of splice variants that produced three different proteins, mENT1a, mENT1b, and mENT1 $\Delta$ 11(31). The mENT1a and 1b variants differed in the number of protein kinase CKII consensus sites, which resulted in a sensitive (1b) or insensitive (1a) transporter to the effects of inhibiting CKII with the compound TBB(6). The human ENT1 is more like the mENT1b variant (6). The mENT1 $\Delta$ 11 variant lacked the last three transmembrane domains. Interestingly, the protein was still made and fully functional, but lacked the ability to be irreversibly linked to NBMPR via photoaffinity labelling (50).

#### 1.5.2.2 ENT2

ENT2 varies from ENT1 in several key ways. First, ENT2 is insensitive to NBMPR, leading to the early identifier of *ei*, equilibrative insensitive. Chimeric proteins of rat ENT1 and ENT2 identified transmembrane regions 3-6 as the site of NBMPR sensitivity (58). In studies using human transporters, two glycine residues, G154 and G179, in transmembrane domains 4 and 5 respectively, were identified as conferring NBMPR sensitivity to ENT1 (53; 54). In fact, in ENT2, the residue at position 154 is a serine, which may contribute to the lack of NBMPR sensitivity (54). Second, ENT2 is capable of transporting nucleobases, in addition to nucleosides. This feature of ENT2 will be discussed in Section 1.6.

ENT2 also has a more discrete expression profile compared to ENT1, with the highest level of expression in skeletal muscle (41). Other tissues that express ENT2 at notable levels are kidney, small intestine, stomach, and pituitary gland (41).

#### 1.5.2.3 ENT3

Unlike ENT1 and ENT2, ENT3 is not found on the plasma membrane (68). Instead, ENT3 is localized to lysosomes due to a endosomal/lysosomal targeting motif in the N-terminal of the protein (2). ENT3 is broadly selective for nucleosides and is capable of transporting the nucleobase adenine, but not hypoxanthine (2). Additionally, ENT3 differs from ENT1 and ENT2 by requiring an acidic pH of 5.5 to operate optimally (2).

#### 1.5.2.4 ENT4

ENT4 was originally identified as a monoamine transporter in the brain and named plasma membrane monoamine transporter (PMAT) (15; 70). Substrates were neurotransmitters such as serotonin and dopamine, and the neurotoxin MPP<sup>+</sup> (14). However, it was subsequently found that ENT4 was expressed in the heart and gained the ability to transport adenosine at acidic pH, whereas serotonin transport was insensitive to pH (3). To date, no other nucleoside (or nucleobase) substrates of ENT4 have been identified (68).

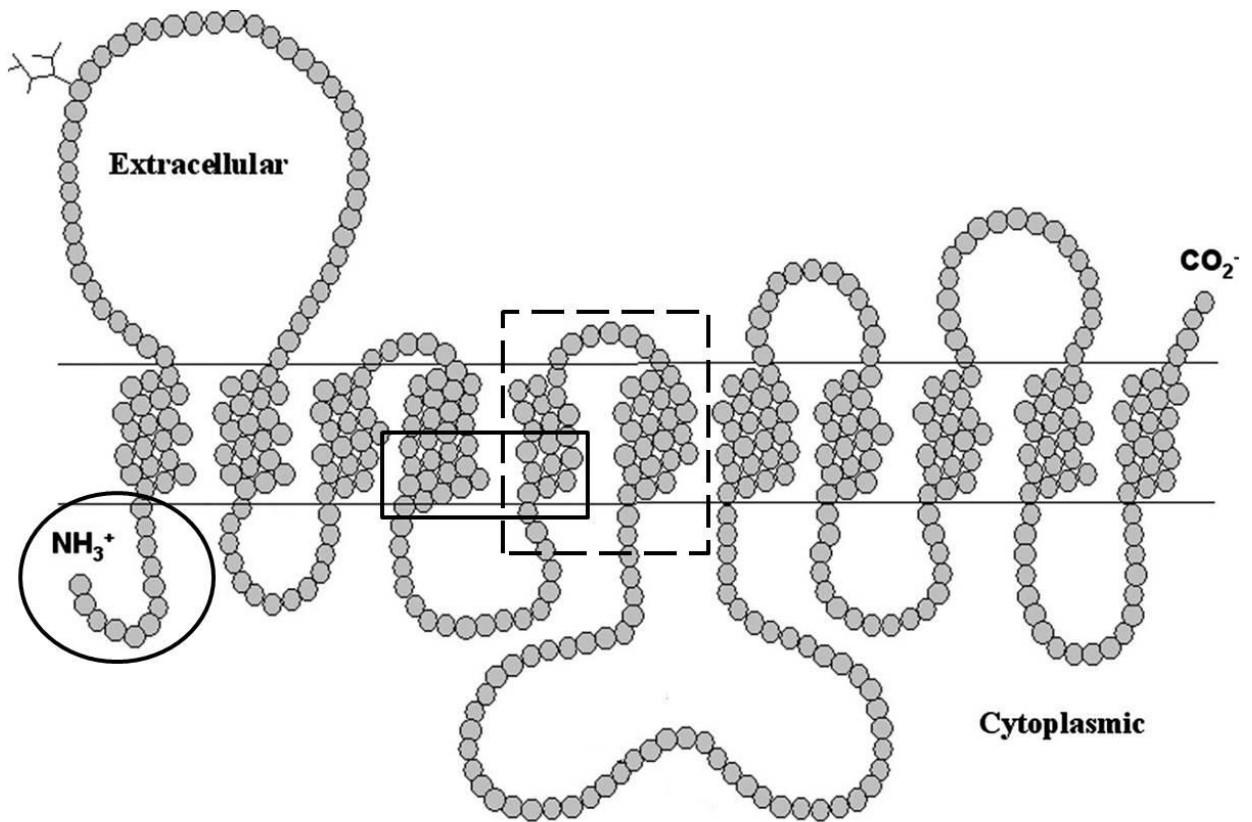


Figure 1.3. Predicted 2-dimensional structure of ENT proteins.

The predicted 2-dimensional structure of ENT proteins with the intracellular N-terminal, extracellular C-terminal, and 11 transmembrane domains. A large glycosolated extracellular loop can be found between transmembrane domains 1 and 2. Between transmembrane domains 6 and 7 there is a large intracellular loop. The circle represents the location of the endosomal/lysosomal targeting motif found in ENT3. The solid square highlights the regions of transmembrane domains 4 and 5 where G154 and G179 are found that confer NBMPR sensitivity to ENT1. The dashed line box around transmembrane domains 5 and 6 represent the part of ENT2 that is responsible for conferring the ability to transport nucleobases.

## 1.6 Nucleobase Transporters

As with nucleosides, nucleobases are unable to cross the plasma membrane without specialized transport proteins to facilitate the process. However, unlike nucleoside transport, nucleobase transport in mammalian cells not been highly studied.

### 1.6.1 ENT2

As mentioned in Section 1.3.2.2, the nucleoside transporter ENT2 is also capable of transporting nucleobases. Substrates recognized include the purine nucleobase hypoxanthine (39; 49), the pyrimidine nucleobase uracil (67), and the chemotherapeutic nucleobase analogues 6-mercaptopurine and 6-thioguanine (37). Uptake of nucleobases by ENT2 is sodium-independent and can be inhibited by excess nucleobases and nucleosides (67). Additionally, the nucleoside transport inhibitors NBMPR and dipyridamole prevent hypoxanthine uptake through ENT2 at concentrations of 10  $\mu\text{M}$  (49; 67).

The affinity of ENT2 for nucleobases varies in the literature. Recombinant human ENT2 and rat ENT2 expressed in *Xenopus* oocytes have reported  $K_m$  values for hypoxanthine of  $700 \pm 100 \mu\text{M}$  and  $1000 \pm 100 \mu\text{M}$  respectively (67). In primary rat microvascular endothelial cells (MVECs), the reported  $K_m$  value for hypoxanthine was  $300 \pm 100 \mu\text{M}$  (49).

In addition to uptake, ENT2 is capable of releasing nucleobases from cells. In primary rat MVECs, hypoxanthine was released from cells with a  $K_m$  of  $189 \pm 67 \mu\text{M}$ , very similar to the reported uptake affinity in the same cells (49). The efflux of hypoxanthine was inhibited by dipyridamole (49).

Using chimeras of rat ENT1 and ENT2 proteins, it was found that ENT1 gained the ability to transport hypoxanthine when transmembrane regions 5 and 6 were replaced with the corresponding regions from ENT2 (Figure 1.3) (67).

#### 1.6.2 SLC23a4/Sodium-dependent nucleobase transporter 1 (SNBT1)

Recently, a novel nucleobase transporter was cloned from rat small intestine (64). This transporter belonged to the SLC23 family, the sodium-dependent ascorbic acid transporter (SVCT) family, and was predicted to have 12 transmembrane domains. Recombinant SNBT1 expressed in HEK293 cells was able to transport guanine, hypoxanthine, xanthine, thymine, and uracil. Notably, SNBT1 was unable to transport adenine or ascorbic acid. Transport of xanthine and uracil was sodium-dependent and of high affinity, with  $K_m$  values of approximately 80  $\mu\text{M}$  and 20  $\mu\text{M}$  respectively (64). Uptake could be inhibited by nucleobase analogues 5-fluorouracil and 6-mercaptopurine, as well as the ENT inhibitor dipyridamole. Nucleosides had no effect on SNBT1-mediated transport of nucleobases, nor did another ENT inhibitor, NBMPR (64). A human ortholog was found by *in silico* analysis; however the human gene for SNBT1 contained seven exons instead of the twelve exons found in the rat gene. The exons missing corresponded to highly conserved, transmembrane domain encoding regions in the rat gene (64). Reverse-transcriptase polymerase chain reaction (RT-PCR) was performed and it was determined that the human SNBT1 gene is in reality a pseudogene, and thus does not produce a functional protein (64).

### 1.6.3 SVCT/Nucleobase-ascorbate Transporter (NAT)

It seems strange to discuss ascorbic acid transporters in a section on nucleobase transporters, as the chemical structure of ascorbic acid resembles a sugar more so than a nucleobase (52). Moreover, there is no evidence that SVCTs can transport nucleobases at all.

As mentioned in the previous section, SVCTs belong to the SLC23 family of transport proteins. In humans, the SLC23 members are SVCT1 and SVCT2 (52). However, in lower organisms like bacteria, fungi, and plants, NATs are common and actually transport nucleobases (although they may not necessarily transport ascorbic acid) (22). The most well known transporters, UrpA, UrpC, and UraA are fungal uric acid-xanthine transporters found in *Aspergillus nidulan*, and bacterial uracil transporter of *Escherichia coli* respectively.

In fungi, NATs are thought to be scavengers of uric acid and xanthine as a source of nitrogen. Bacteria, on the other hand, use NATs to scavenge uracil for nucleoside synthesis, which can then be used for nucleotide and DNA/RNA production.

It is not understood how or why the evolutionary progression of NATs in lower organisms resulted in the SVCT proteins in humans that are incapable of transporting nucleobases.



## 1.7 References

1. **Baldwin SA, Beal PR, Yao SY, King AE, Cass CE and Young JD.** The equilibrative nucleoside transporter family, SLC29. *Pflugers Arch* 447: 735-743, 2004.
2. **Baldwin SA, Yao SY, Hyde RJ, Ng AM, Foppolo S, Barnes K, Ritzel MW, Cass CE and Young JD.** Functional characterization of novel human and mouse equilibrative nucleoside transporters (hENT3 and mENT3) located in intracellular membranes. *J Biol Chem* 280: 15880-15887, 2005.
3. **Barnes K, Dobrzynski H, Foppolo S, Beal PR, Ismat F, Scullion ER, Sun L, Tellez J, Ritzel MW, Claycomb WC, Cass CE, Young JD, Billeter-Clark R, Boyett MR and Baldwin SA.** Distribution and functional characterization of equilibrative nucleoside transporter-4, a novel cardiac adenosine transporter activated at acidic pH. *Circ Res* 99: 510-519, 2006.
4. **Belardinelli L, Shryock JC, Snowdy S, Zhang Y, Monopoli A, Lozza G, Ongini E, Olsson RA and Dennis DM.** The A2A adenosine receptor mediates coronary vasodilation. *J Pharmacol Exp Ther* 284: 1066-1073, 1998.
5. **Berry CE and Hare JM.** Xanthine oxidoreductase and cardiovascular disease: molecular mechanisms and pathophysiological implications. *J Physiol* 555: 589-606, 2004.
6. **Bone DB, Robillard KR, Stolk M and Hammond JR.** Differential regulation of mouse equilibrative nucleoside transporter 1 (mENT1) splice variants by protein kinase CK2. *Mol Membr Biol* 24: 294-303, 2007.
7. **Boyle EM, Jr., Pohlman TH, Cornejo CJ and Verrier ED.** Endothelial cell injury in cardiovascular surgery: ischemia-reperfusion. *Ann Thorac Surg* 62: 1868-1875, 1996.
8. **Deussen A, Stappert M, Schafer S and Kelm M.** Quantification of extracellular and intracellular adenosine production: understanding the transmembranous concentration gradient. *Circulation* 99: 2041-2047, 1999.

9. **Dharmashankar K and Widlansky ME.** Vascular endothelial function and hypertension: insights and directions. *Curr Hypertens Rep* 12: 448-455, 2010.
10. **Dougherty C, Barucha J, Schofield PR, Jacobson KA and Liang BT.** Cardiac myocytes rendered ischemia resistant by expressing the human adenosine A1 or A3 receptor. *FASEB J* 12: 1785-1792, 1998.
11. **Dunwiddie TV and Masino SA.** The role and regulation of adenosine in the central nervous system. *Annu Rev Neurosci* 24:31-55.: 31-55, 2001.
12. **Elahi MM, Kong YX and Matata BM.** Oxidative stress as a mediator of cardiovascular disease. *Oxid Med Cell Longev* 2: 259-269, 2009.
13. **Endo Y, Obata T, Murata D, Ito M, Sakamoto K, Fukushima M, Yamasaki Y, Yamada Y, Natsume N and Sasaki T.** Cellular localization and functional characterization of the equilibrative nucleoside transporters of antitumor nucleosides. *Cancer Sci* 98: 1633-1637, 2007.
14. **Engel K and Wang J.** Interaction of organic cations with a newly identified plasma membrane monoamine transporter. *Mol Pharmacol* 68: 1397-1407, 2005.
15. **Engel K, Zhou M and Wang J.** Identification and characterization of a novel monoamine transporter in the human brain. *J Biol Chem* 279: 50042-50049, 2004.
16. **Escudero C, Casanello P and Sobrevia L.** Human equilibrative nucleoside transporters 1 and 2 may be differentially modulated by A2B adenosine receptors in placenta microvascular endothelial cells from pre-eclampsia. *Placenta* 29: 816-825, 2008.
17. **Farrell JJ, Elsaleh H, Garcia M, Lai R, Ammar A, Regine WF, Abrams R, Benson AB, Macdonald J, Cass CE, Dicker AP and Mackey JR.** Human equilibrative nucleoside transporter 1 levels predict response to gemcitabine in patients with pancreatic cancer. *Gastroenterology* 136: 187-195, 2009.
18. **Fatehi-Hassanabad Z, Chan CB and Furman BL.** Reactive oxygen species and endothelial function in diabetes. *Eur J Pharmacol* 636: 8-17, 2010.

19. **Feoktistov I, Goldstein AE, Ryzhov S, Zeng D, Belardinelli L, Voyno-Yasenetskaya T and Biaggioni I.** Differential expression of adenosine receptors in human endothelial cells: role of A2B receptors in angiogenic factor regulation. *Circ Res* 90: 531-538, 2002.
20. **Fredholm BB, IJzerman AP, Jacobson KA, Klotz KN and Linden J.** International Union of Pharmacology. XXV. Nomenclature and classification of adenosine receptors. *Pharmacol Rev* 53: 527-552, 2001.
21. **Gibbs JE, Jayabalan P and Thomas SA.** Mechanisms by which 2',3'-dideoxyinosine (ddI) crosses the guinea-pig CNS barriers; relevance to HIV therapy. *J Neurochem* 84: 725-734, 2003.
22. **Gournas C, Papageorgiou I and Diallinas G.** The nucleobase-ascorbate transporter (NAT) family: genomics, evolution, structure-function relationships and physiological role. *Mol Biosyst* 4: 404-416, 2008.
23. **Granger DN.** Ischemia-reperfusion: mechanisms of microvascular dysfunction and the influence of risk factors for cardiovascular disease. *Microcirculation* 6: 167-178, 1999.
24. **Gray JH, Owen RP and Giacomini KM.** The concentrative nucleoside transporter family, SLC28. *Pflugers Arch* 447: 728-734, 2004.
25. **Griffiths M, Beaumont N, Yao SY, Sundaram M, Boumah CE, Davies A, Kwong FY, Coe I, Cass CE, Young JD and Baldwin SA.** Cloning of a human nucleoside transporter implicated in the cellular uptake of adenosine and chemotherapeutic drugs. *Nat Med* 3: 89-93, 1997.
26. **Hagberg H, Andersson P, Lacarewicz J, Jacobson I, Butcher S and Sandberg M.** Extracellular adenosine, inosine, hypoxanthine, and xanthine in relation to tissue nucleotides and purines in rat striatum during transient ischemia. *J Neurochem* 49: 227-231, 1987.
27. **Hasko G and Pacher P.** A2A receptors in inflammation and injury: lessons learned from transgenic animals. *J Leukoc Biol* 83: 447-455, 2008.

28. **Hristov M and Weber C.** Endothelial progenitor cells: characterization, pathophysiology, and possible clinical relevance. *J Cell Mol Med* 8: 498-508, 2004.
29. **Jacobson KA, Xie R, Young L, Chang L and Liang BT.** A novel pharmacological approach to treating cardiac ischemia. Binary conjugates of A1 and A3 adenosine receptor agonists. *J Biol Chem* 275: 30272-30279, 2000.
30. **Kharbanda RK.** Cardiac conditioning: a review of evolving strategies to reduce ischaemia-reperfusion injury. *Heart* 96: 1179-1186, 2010.
31. **Kiss A, Farah K, Kim J, Garriock RJ, Drysdale TA and Hammond JR.** Molecular cloning and functional characterization of inhibitor-sensitive (mENT1) and inhibitor-resistant (mENT2) equilibrative nucleoside transporters from mouse brain. *Biochem J* 352 Pt 2:363-72.: 363-372, 2000.
32. **Kroll K, Deussen A and Sweet IR.** Comprehensive model of transport and metabolism of adenosine and S-adenosylhomocysteine in the guinea pig heart. *Circ Res* 71: 590-604, 1992.
33. **Linden J.** Adenosine in tissue protection and tissue regeneration. *Mol Pharmacol* 67: 1385-1387, 2005.
34. **Loffler M, Morote-Garcia JC, Eltzschig SA, Coe IR and Eltzschig HK.** Physiological roles of vascular nucleoside transporters. *Arterioscler Thromb Vasc Biol* 27: 1004-1013, 2007.
35. **Minuesa G, Purcet S, Erkizia I, Molina-Arcas M, Bofill M, Izquierdo-Useros N, Casado FJ, Clotet B, Pastor-Anglada M and Martinez-Picado J.** Expression and functionality of anti-human immunodeficiency virus and anticancer drug uptake transporters in immune cells. *J Pharmacol Exp Ther* 324: 558-567, 2008.
36. **Mubagwa K and Flameng W.** Adenosine, adenosine receptors and myocardial protection: an updated overview. *Cardiovasc Res* 52: 25-39, 2001.
37. **Nagai K, Nagasawa K, Kihara Y, Okuda H and Fujimoto S.** Anticancer nucleobase analogues 6-mercaptopurine and 6-thioguanine are novel substrates for equilibrative nucleoside transporter 2. *Int J Pharm* 333: 56-61, 2007.

38. **Nemeth I, Talosi G, Papp A and Boda D.** Xanthine oxidase activation in mild gestational hypertension. *Hypertens Pregnancy* 21: 1-11, 2002.
39. **Osses N, Pearson JD, Yudilevich DL and Jarvis SM.** Hypoxanthine enters human vascular endothelial cells (ECV 304) via the nitrobenzylthioinosine-insensitive equilibrative nucleoside transporter. *Biochem J* 317: 843-848, 1996.
40. **Peart J, Flood A, Linden J, Matherne GP and Headrick JP.** Adenosine-mediated cardioprotection in ischemic-reperfused mouse heart. *J Cardiovasc Pharmacol* 39: 117-129, 2002.
41. **Pennycooke M, Chaudary N, Shuralyova I, Zhang Y and Coe IR.** Differential expression of human nucleoside transporters in normal and tumor tissue. *Biochem Biophys Res Commun* 280: 951-959, 2001.
42. **Perez-Torras S, Garcia-Manteiga J, Mercade E, Casado FJ, Carbo N, Pastor-Anglada M and Mazo A.** Adenoviral-mediated overexpression of human equilibrative nucleoside transporter 1 (hENT1) enhances gemcitabine response in human pancreatic cancer. *Biochem Pharmacol* 76: 322-329, 2008.
43. **Pober JS and Min W.** Endothelial cell dysfunction, injury and death. *Handb Exp Pharmacol* 135-156, 2006.
44. **Pries AR and Kuebler WM.** Normal endothelium. *Handb Exp Pharmacol* 1-40, 2006.
45. **Purcet S, Minuesa G, Molina-Arcas M, Erkizia I, Casado FJ, Clotet B, Martinez-Picado J and Pastor-Anglada M.** 3'-Azido-2',3'-dideoxythymidine (zidovudine) uptake mechanisms in T lymphocytes. *Antivir Ther* 11: 803-811, 2006.
46. **Ran R, Xu H, Lu A, Bernaudin M and Sharp FR.** Hypoxia preconditioning in the brain. *Dev Neurosci* 27: 87-92, 2005.
47. **Rezkalla SH and Kloner RA.** No-reflow phenomenon. *Circulation* 105: 656-662, 2002.

48. **Rieger JM, Shah AR and Gidday JM.** Ischemia-reperfusion injury of retinal endothelium by cyclooxygenase- and xanthine oxidase-derived superoxide. *Exp Eye Res* 74: 493-501, 2002.
49. **Robillard KR, Bone DB and Hammond JR.** Hypoxanthine uptake and release by equilibrative nucleoside transporter 2 (ENT2) of rat microvascular endothelial cells. *Microvasc Res* 75: 351-357, 2008.
50. **Robillard KR, Bone DB, Park JS and Hammond JR.** Characterization of mENT1Delta11, a novel alternative splice variant of the mouse equilibrative nucleoside transporter 1. *Mol Pharmacol* 74: 264-273, 2008.
51. **Ryzhov S, Solenkova NV, Goldstein AE, Lamparter M, Fleenor T, Young PP, Greelish JP, Byrne JG, Vaughan DE, Biaggioni I, Hatzopoulos AK and Feoktistov I.** Adenosine receptor-mediated adhesion of endothelial progenitors to cardiac microvascular endothelial cells. *Circ Res* 102: 356-363, 2008.
52. **Savini I, Rossi A, Pierro C, Avigliano L and Catani MV.** SVCT1 and SVCT2: key proteins for vitamin C uptake. *Amino Acids* 34: 347-355, 2008.
53. **SenGupta DJ, Lum PY, Lai Y, Shubochkina E, Bakken AH, Schneider G and Unadkat JD.** A single glycine mutation in the equilibrative nucleoside transporter gene, hENT1, alters nucleoside transport activity and sensitivity to nitrobenzylthioinosine. *Biochemistry* 41: 1512-1519, 2002.
54. **SenGupta DJ and Unadkat JD.** Glycine 154 of the equilibrative nucleoside transporter, hENT1, is important for nucleoside transport and for conferring sensitivity to the inhibitors nitrobenzylthioinosine, dipyridamole, and dilazep. *Biochem Pharmacol* 67: 453-458, 2004.
55. **Shimokawa H and Yasuda S.** Myocardial ischemia: current concepts and future perspectives. *J Cardiol* 52: 67-78, 2008.
56. **Shryock JC and Belardinelli L.** Adenosine and adenosine receptors in the cardiovascular system: biochemistry, physiology, and pharmacology. *Am J Cardiol* 79: 2-10, 1997.

57. **Sundaram M, Yao SY, Ingram JC, Berry ZA, Abidi F, Cass CE, Baldwin SA and Young JD.** Topology of a human equilibrative, nitrobenzylthioinosine (NBMPR)-sensitive nucleoside transporter (hENT1) implicated in the cellular uptake of adenosine and anti-cancer drugs. *J Biol Chem* 276: 45270-45275, 2001.
58. **Sundaram M, Yao SY, Ng AM, Cass CE, Baldwin SA and Young JD.** Equilibrative nucleoside transporters: mapping regions of interaction for the substrate analogue nitrobenzylthioinosine (NBMPR) using rat chimeric proteins. *Biochemistry* 40: 8146-8151, 2001.
59. **Szocs K.** Endothelial dysfunction and reactive oxygen species production in ischemia/reperfusion and nitrate tolerance. *Gen Physiol Biophys* 23: 265-295, 2004.
60. **Tracey WR, Magee WP, Oleynek JJ, Hill RJ, Smith AH, Flynn DM and Knight DR.** Novel N6-substituted adenosine 5'-N-methyluronamides with high selectivity for human adenosine A3 receptors reduce ischemic myocardial injury. *Am J Physiol Heart Circ Physiol* 285: H2780-H2787, 2003.
61. **Veltkamp SA, Pluim D, van Eijndhoven MA, Bolijn MJ, Ong FH, Govindarajan R, Unadkat JD, Beijnen JH and Schellens JH.** New insights into the pharmacology and cytotoxicity of gemcitabine and 2',2'-difluorodeoxyuridine. *Mol Cancer Ther* 7: 2415-2425, 2008.
62. **Ward JL, Serali A, Mo ZP and Tse CM.** Kinetic and pharmacological properties of cloned human equilibrative nucleoside transporters, ENT1 and ENT2, stably expressed in nucleoside transporter-deficient PK15 cells. Ent2 exhibits a low affinity for guanosine and cytidine but a high affinity for inosine. *J Biol Chem* 275: 8375-8381, 2000.
63. **Weseler AR and Bast A.** Oxidative stress and vascular function: implications for pharmacologic treatments. *Curr Hypertens Rep* 12: 154-161, 2010.
64. **Yamamoto S, Inoue K, Murata T, Kamigaso S, Yasujima T, Maeda JY, Yoshida Y, Ohta KY and Yuasa H.** Identification and functional characterization of the first nucleobase transporter in mammals: implication in the species difference in the intestinal absorption mechanism of nucleobases and their analogs between higher primates and other mammals. *J Biol Chem* 285: 6522-6531, 2010.

65. **Yang XM, Krieg T, Cui L, Downey JM and Cohen MV.** NECA and bradykinin at reperfusion reduce infarction in rabbit hearts by signaling through PI3K, ERK, and NO. *J Mol Cell Cardiol* 36: 411-421, 2004.
66. **Yang Z, Cerniway RJ, Byford AM, Berr SS, French BA and Matherne GP.** Cardiac overexpression of A1-adenosine receptor protects intact mice against myocardial infarction. *Am J Physiol Heart Circ Physiol* 282: H949-H955, 2002.
67. **Yao SY, Ng AM, Vickers MF, Sundaram M, Cass CE, Baldwin SA and Young JD.** Functional and molecular characterization of nucleobase transport by recombinant human and rat equilibrative nucleoside transporters 1 and 2. Chimeric constructs reveal a role for the ENT2 helix 5-6 region in nucleobase translocation. *J Biol Chem* 277: 24938-24948, 2002.
68. **Young JD, Yao SY, Sun L, Cass CE and Baldwin SA.** Human equilibrative nucleoside transporter (ENT) family of nucleoside and nucleobase transporter proteins. *Xenobiotica* 38: 995-1021, 2008.
69. **Zhao ZQ, Nakanishi K, McGee DS, Tan P and Vinten-Johansen J.** A1 receptor mediated myocardial infarct size reduction by endogenous adenosine is exerted primarily during ischaemia. *Cardiovasc Res* 28: 270-279, 1994.
70. **Zhou M, Engel K and Wang J.** Evidence for significant contribution of a newly identified monoamine transporter (PMAT) to serotonin uptake in the human brain. *Biochem Pharmacol* 73: 147-154, 2007.



## CHAPTER TWO

### RESEARCH QUESTIONS, GENERAL HYPOTHESES, AND COMMON METHODOLOGIES

## 2.1 Research Questions

The microvasculature has been an understudied tissue with respect to nucleoside and nucleobase transport. Human umbilical vein endothelial cells have been a popular model to study nucleoside transport, however these cells are derived from a macrovessel. Nucleobase transport in humans is even less studied and those studies that have been conducted tend to focus on infection or cancer, as there are a variety of nucleobase analogues used as chemotherapeutic agents, including 5-FU, 6-MP, and 6-TG (18; 29; 31).

Thus, to understand nucleoside and nucleobase transport and metabolism in the human microvasculature, the most direct approach is to use human primary microvascular endothelial cells. What purine transporters are expressed in MVECs? Are MVECs capable of transporting nucleobases? These are the kinds of basic questions that were addressed early on in this work.

Once those basic questions are answered, the focus turns to regulation of the transporters. ENT1 regulation is an area of extensive research, however the models used are generally cancer cells lines, artificial over-expression systems, non-human cell lines, and even non-mammalian organisms. While important for general understanding of ENT1 regulation, these data may not be readily extrapolated to normal human cells. Does ENT1 respond in the same manner to intracellular kinase activity in primary cells as compared to cancerous or artificial cell lines? How are nucleobase transporters regulated? Additionally, questions regarding how nucleoside and nucleobase

transporters are affected by reactive oxygen species and hypoxia/ischemia have not been addressed.

Finally, the role of ENT1 in the regulation of purine homeostasis is still not completely understood. By using an ENT1 null animal, questions regarding compensatory mechanisms in purine handling can be addressed. As well, given the important cardiovascular role of adenosine, questions about the cardiovascular health and functionality of animals with comprised adenosine handling can also be addressed.

## **2.2 Hypotheses**

### *2.2.1 Chapter 3 – Human Primary MVEC Characterization*

As outlined in Chapter 1, movement of nucleosides and nucleobases across the cell membrane requires specialized transport proteins. Both ENT1 and ENT2 contribute to nucleoside transport, and as in the case with primary rat MVECs from skeletal muscle, ENT2 can contribute up to 50 % of nucleoside transport capacity (3). Nucleobases, on the other hand appear to be transported only by ENT2 as other known nucleobase transporters do not exist in human cells (39; 40). Therefore it is hypothesized that:

- Uptake of nucleosides, as measured with 2-[<sup>3</sup>H]chloroadenosine, in human MVECs is mediated by ENT1 and ENT2. ENT2 will contribute up to 50 % of total uptake capacity.
- Nucleobase uptake, as measured with [<sup>3</sup>H]hypoxanthine, is facilitated by ENT2, not ENT1 in human MVECs.

### 2.2.2 Chapter 4 – Regulation of purine transporters in human primary MVECs.

Evidence has been amassed in other cell types that support the regulation of ENT1 function by a variety of molecular mechanisms, including intracellular kinases PKA (10), PKC (9; 21), CKII (4; 35), adenosine A<sub>2</sub> receptors(15; 32), and a receptor tyrosine kinase (RTK) (37). Transcriptional regulation of ENT1 has also been studied and found to be altered by hypoxia inducible factor 1 alpha (1; 13), elevated glucose (33), and nitric oxide (16; 17). ENT1 and ENT2 function has been shown to decrease in response to hypoxia in a variety of models (5; 6; 19; 27; 28). However, ENT2 may not be affected by elevated glucose (2). Additionally, adenosine uptake has been affected by peroxynitrite treatment (36). Therefore it was hypothesized that:

- Both ENT1 and ENT2 function is regulated by the activation and/or inhibition of the intracellular kinases PKA, PKC, or CKII.
- Nucleoside and nucleobase uptake is diminished after hypoxia, ischemia, or oxidative stress.
- Nucleoside and nucleobase uptake is sensitive to regulation by vascular endothelial growth factor (VEGF), a major protein produced during hypoxia that acts through a family of RTKs (41).

### 2.2.3 Chapter 5 – MVECs from ENT1<sup>-/-</sup> Mice

The ENT1<sup>-/-</sup> mouse generated by Choi and colleagues (8) has been studied at the level of the central nervous system (7; 8; 30; 38), the heart (34), kidney (22), and anti-viral pharmacokinetics (14). No studies on the vasculature have been conducted. Given the

importance of nucleosides in the vasculature, MVECs were isolated from wild-type and ENT1<sup>-/-</sup> mice and characterized.

It was hypothesized that:

- As previously found in rat MVECs, mouse primary MVECs from skeletal muscle will express ENT1 and ENT2, with ENT2 accounting for up to 50% of total nucleoside uptake capacity.
- ENT2 expression or other ENT subtypes will be up-regulated in ENT1<sup>-/-</sup> MVECs to compensate for the lack of the primary nucleoside transporter ENT1.
- Genes related to metabolism, and/or signalling would have altered expression levels to compensate for changes in cellular purine metabolite concentrations.
- Mouse ENT1 and ENT2 would respond in a similar manner to hypoxia, ischemia, and oxidative stresses compared to human ENT1 and ENT2.

#### *2.2.4 Chapter 6 – Additional Phenotypes of ENT1<sup>-/-</sup> Mice*

The ENT1<sup>-/-</sup> mouse appeared phenotypically normal, however only ethanol consumption and anxiety behaviour was examined (7; 8). No in-depth phenotype profile was generated. An independent laboratory generated their own ENT1<sup>-/-</sup> mouse and found altered gene expression with quantitative PCR that was different between tissues (20). Adenosine accumulates in extracellular spaces during times of stress, otherwise the amount of free adenosine is minimal (11).

Therefore it was hypothesized that:

- Circulating adenosine concentrations will be reduced in resting ENT1<sup>-/-</sup> mice relative to wild-type.

- Organs will have altered expression of genes related to purine transport and metabolism

## 2.3 Common Methodologies

Many of the experiments relied on a common set of techniques and methods. In the interest of clarity and readability, the basics of those techniques are described here, allowing the unique details of each experiment to stand out without being lost in repetition.

### 2.3.1 Mammalian Cell Culture

The most common cell type used was primary human cardiac microvascular endothelial cells obtained from Lonza (Walkersville, MD). These cells were used between *passage* 4-7 and cultured in EGM2-MV medium as supplied by the manufacture. Medium was changed 24 hr following seeding and then every 48 hr thereafter. Generally, MVECs were *passaged* at a ratio of 1:7 as determined by cell counting to seed 5,000 cells/cm<sup>2</sup> growth area as instructed by the supplier.

Additional cell types used when required are described in the appropriate chapter. All cultured cells were maintained in a humidified atmosphere of 95% air-5% CO<sub>2</sub> at 37°C.

#### 2.3.1.1 Cell Harvesting

All [<sup>3</sup>H]NBMPR binding assays and transport assays were conducted with cell suspensions to achieve the short incubation times required for transport kinetic analysis. All cell types were harvested in the same manner. Cells were first washed with phosphate-buffered saline (PBS: in mM: 137 NaCl, 6.3 Na<sub>2</sub>HPO<sub>4</sub>, 2.7 KCl, 1.5 KH<sub>2</sub>PO<sub>4</sub>, 0.9

CaCl<sub>2</sub>·2H<sub>2</sub>O, 0.5 MgCl<sub>2</sub>·6H<sub>2</sub>O; pH 7.4) followed by trypsinization with 0.05% trypsin-0.53 mM EDTA. Trypsinized cells were then diluted 4-fold in 500µg/ml trypsin inhibitor in PBS and collected by centrifugation at ~220 x *g* for 5 minutes. Pellets were washed in the desired assay buffer, re-centrifuged, and resuspended in the same buffer for immediate use in the assay.

### 2.3.2 [<sup>3</sup>H]NBMPR Binding Assay

To measure the amount of ENT1 protein present on the cell membrane, radioligand binding using [<sup>3</sup>H]NBMPR was employed. NBMPR is a high affinity, non-transported ligand that is selective for ENT1. Assays were conducted in 13x100 mm borosilicate glass tubes in duplicate. A working stock of [<sup>3</sup>H]NBMPR at a desired concentration (usually 1.5 or 5 nM) was made by diluting stock [<sup>3</sup>H]NBMPR PBS and adjusted to the required disintegrations per minute (DPM) as dictated by the specific activity of the stock. Volumes of [<sup>3</sup>H]NBMPR were added to give the desired concentration in a final volume of 1 ml. PBS was added to a volume of 925 µl and the reaction was started by adding 75 µl of cell suspension. To determine non-specific binding, a set of tubes included 10 µM nitrobenzylthioguanine riboside (NBTGR) or dipyridamole. Reactions were incubated at room temperature (~22°C) for 45 min to allow equilibrium to be achieved. Assays were terminated by filtration using a 24-port Brandell Cell Harvester with ice cold 10 mM Tris buffer (pH 7.4) and collected on Whatman A-937 grade filter paper strips. Perforated filter paper circles were placed in scintillation vials, mixed with 5 ml of liquid scintillation cocktail and incubated overnight (≥12 hr) before counting on a liquid scintillation analyzer.

Data were obtained as DPM and converted to pmol using the equation:

$$\text{pmol} = \text{DPM} / \text{specific activity (DPM/fmol)} / 1000.$$

Specific binding was defined as the difference between total binding (no inhibitor present) and non-specific binding (in the presence of 10  $\mu\text{M}$  inhibitor). Equilibrium free concentrations of [ $^3\text{H}$ ]NBMPR were determined for each condition (total, specific, non-specific) by subtracting pmol bound from pmol added and dividing by the assay volume of 1 ml. Since one molecule of [ $^3\text{H}$ ]NBMPR binds to one ENT1 protein (23; 24), specific bound pmol [ $^3\text{H}$ ]NBMPR were converted to ENT1 per cell using the equation  $\text{ENT1/cell} = \text{pmol/cells ml}^{-1} * 6.023 \times 10^{11} \text{ molecules pmol}^{-1}$ . Cell concentrations were obtained using a haemocytometer or a Bio-Rad TC-10 automated cell counter.

### *2.3.3 Oil-Stop Transport Assay*

To measure accurately the transport kinetics of transporters a reliable, reproducible, efficient stopping technique is required. To achieve this, the oil-stop method was employed. A schematic overview of the technique is presented in Figure 2.1.

#### *2.3.3.1 [ $^3\text{H}$ ]Substrate Preparation*

In contrast to [ $^3\text{H}$ ]NBMPR binding, much higher concentrations of substrate are required for transport assays. To reduce the amount of [ $^3\text{H}$ ]substrate required, the desired concentrations of substrate were established with non-radioactive versions of the substrate. These non-radioactive substrate concentrations were then spiked with small amounts of radioactive substrate to allow the accumulation of substrate inside the cell to be measured by liquid scintillation counting. Standards of the spiked substrate were taken to determine the specific activity of each concentration using the equation:



specific activity =  $\text{dpm}/[\text{substrate}] * \text{volume of standard}$

### *2.3.3.2 Transport Assay Setup – Nucleoside Substrate*

A mixture of Dow 550 silicone oil was mixed with light mineral oil in a 21:4 v/v ratio. This mixture had a specific gravity of 1.04, allowing aqueous solutions to be layered on top of the oil. Transport assays were performed in 1.5 ml microcentrifuge tubes, in which 200  $\mu\text{l}$  of oil was added. On top of the oil cushion, 250  $\mu\text{l}$  of 2- $^3\text{H}$ chloroadenosine (prepared as described in Section 2.3.3.1) was placed. Tubes were centrifuged briefly to establish a clean aqueous-oil interface. Cells were harvested as described in section 2.3.1.1 and divided into lots for ‘total’ uptake and ‘non-mediated’ uptake. ‘Non-mediated’ uptake cells were pretreated with 10  $\mu\text{M}$  NBMPR and 10  $\mu\text{M}$  dipyridamole for 15 min at room temperature, whereas ‘total’ uptake cells were treated with an equal volume of DMSO (vehicle control). To initiate uptake, a 250  $\mu\text{l}$  aliquot of cell suspension was added to the microcentrifuge tube and incubated at room temperature for a desired time point (range 3-180 s). 2-Chloroadenosine is an agonist at adenosine receptors and thus there is a potential that uptake may be affected by adenosine receptor signaling. Peak cyclic AMP production by 2-chloroadenosine varies on cell type and has been reported in the range of 30 s to 5 min (12; 25; 26). Since the most common time point used in uptake studies was 10 s, contribution of adenosine receptor activation was expected to be negligible. Following incubation the tube was centrifuged at  $\sim 10,000 \times g$  for 10 s to pellet the cells in the oil layer of the tube while the aqueous  $^3\text{H}$ substrate remains above the oil. This removal of the cells from the substrate stops transport. The aqueous

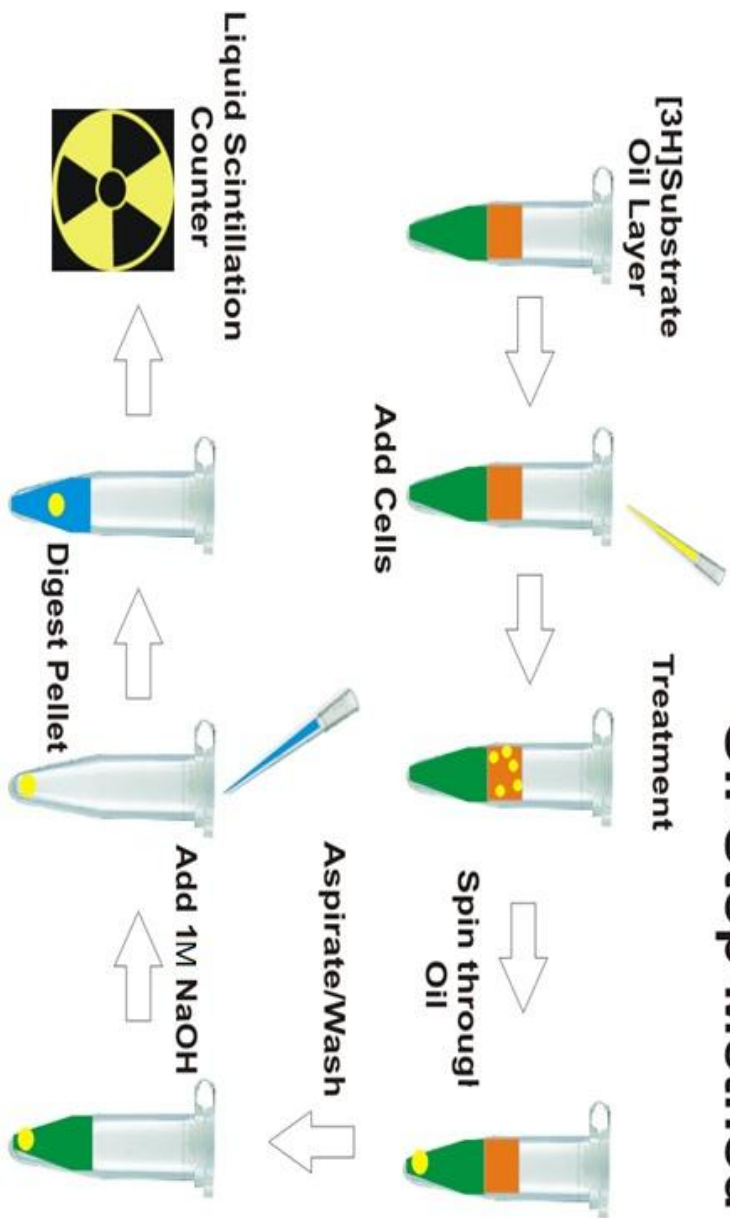


Figure 2.1. Schematic of the Oil-Stop Method.

A [<sup>3</sup>H]labelled substrate was layered on top of Dow 550 silicone oil was mixed with light mineral oil (21:4 v/v). Cells harvested by trypsinization were resuspended in buffer. An aliquot of cells was added to the tube and incubated with the [<sup>3</sup>H]substrate for the desired treatment time. Uptake was terminated by centrifugation at ~10,000 x *g* for 10 s to pellet the cells in the oil layer. The aqueous [<sup>3</sup>H]substrate was removed and the oil layer was washed with ddH<sub>2</sub>O before removal. The cell pellet was digested overnight in 1 M sodium hydroxide. The following day, the cell digest was transferred to a liquid scintillation vial and mixed with liquid scintillation fluid for determination of [<sup>3</sup>H] content by liquid scintillation counting.

(Original schematic drawn by Kevin Robillard)

## Oil-Stop Method



[<sup>3</sup>H]substrate was then removed by aspiration and the top of the oil was washed with ddH<sub>2</sub>O.

Subsequently, the water and oil were removed by aspiration to expose the cell pellet. Cells were digested overnight in 250 μl of 1 M NaOH at room temperature. A 220 μl aliquot of cell digest was then transferred to a scintillation vial, mixed with 5 ml of liquid scintillation cocktail and allowed to sit overnight before counting on a liquid scintillation analyzer.

#### 2.3.3.3 Transport Assay Setup – Nucleobase Substrate

The set up for nucleobase transport was essentially the same as nucleoside uptake except for one key difference. Most experiments were performed with a competing, non-radioactive nucleobase for the non-mediated condition. Since this competitor could also be transported and metabolized by cells, pre-incubation with the cells was not a possibility. Therefore, a high concentration of the competing nucleobase had to be included with the [<sup>3</sup>H]substrate in the microcentrifuge tube. The most common inhibitor was adenine, where 25 μl of 20 mM adenine was added to uptake tubes for non-mediated uptake; total uptake tubes received 25 μl of buffer. To maintain the a final volume of 500 μl in the uptake tube after the addition of cells, only 225 μl of cell suspension was added to the uptake tubes to initiate uptake. From the addition of cells on, nucleobase transport assays were treated identically to the nucleoside uptake tubes, with the exception of longer incubation times to account for slower transport rates.

#### 2.3.3.4 Intracellular Volume

Uptake of substrates was normalized to the amount of intracellular water volume. To determine total volume of the cell pellet, cells were incubated with  $^3\text{H}_2\text{O}$  for 3 min at room temperature and then processed as described in section 2.3.3.2. To determine extracellular volume of the pellet, non-mediated uptake was extrapolated back to zero time to estimate the dpm present on the outside of the cells. Volume was then determined with the equation:

$$\text{Extracellular volume} = \text{dpm}_{t=0} / \text{specific activity (dpm}/\mu\text{l)}$$

Intracellular volume was then defined as the difference between total volume and extracellular volume.

#### 2.3.3.5 Transport Data Analysis

Mediated uptake, that is, the uptake of substrate for which the transporter is directly responsible, was defined as total uptake (in the absence of inhibitors) minus non-mediated uptake (in the presence of inhibitors) in pmol/ $\mu\text{l}$  of intracellular water volume.

Using GraphPad Prism software the Michaelis-Menten equation:  $Y = V_{\text{max}} * X / (K_m + X)$ , where X was the concentration of substrate, was used to fit each curve and derive kinetic parameters.

## 2.4 References

1. **Abdulla P and Coe IR.** Characterization and functional analysis of the promoter for the human equilibrative nucleoside transporter gene, hENT1. *Nucleosides Nucleotides Nucleic Acids* 26: 99-110, 2007.
2. **Aguayo C, Casado J, Gonzalez M, Pearson JD, Martin RS, Casanello P, Pastor-Anglada M and Sobrevia L.** Equilibrative nucleoside transporter 2 is expressed in human umbilical vein endothelium, but is not involved in the inhibition of adenosine transport induced by hyperglycaemia. *Placenta* 26: 641-653, 2005.
3. **Archer RG, Pitelka V and Hammond JR.** Nucleoside transporter subtype expression and function in rat skeletal muscle microvascular endothelial cells. *Br J Pharmacol* 143: 202-214, 2004.
4. **Bone DB, Robillard KR, Stolk M and Hammond JR.** Differential regulation of mouse equilibrative nucleoside transporter 1 (mENT1) splice variants by protein kinase CK2. *Mol Membr Biol* 24: 294-303, 2007.
5. **Casanello P, Torres A, Sanhueza F, Gonzalez M, Farias M, Gallardo V, Pastor-Anglada M, San MR and Sobrevia L.** Equilibrative nucleoside transporter 1 expression is downregulated by hypoxia in human umbilical vein endothelium. *Circ Res* 97: 16-24, 2005.
6. **Chaudary N, Naydenova Z, Shuralyova I and Coe IR.** Hypoxia regulates the adenosine transporter, mENT1, in the murine cardiomyocyte cell line, HL-1. *Cardiovasc Res* 61: 780-788, 2004.
7. **Chen J, Rinaldo L, Lim SJ, Young H, Messing RO and Choi DS.** The type 1 equilibrative nucleoside transporter regulates anxiety-like behavior in mice. *Genes Brain Behav* 6: 776-783, 2007.
8. **Choi DS, Cascini MG, Mailliard W, Young H, Paredes P, McMahon T, Diamond I, Bonci A and Messing RO.** The type 1 equilibrative nucleoside transporter regulates ethanol intoxication and preference. *Nat Neurosci* 7: 855-861, 2004.
9. **Coe I, Zhang Y, McKenzie T and Naydenova Z.** PKC regulation of the human equilibrative nucleoside transporter, hENT1. *FEBS Lett* 517: 201-205, 2002.

10. **Coe IR, Dohrman DP, Constantinescu A, Diamond I and Gordon AS.** Activation of cyclic AMP-dependent protein kinase reverses tolerance of a nucleoside transporter to ethanol. *J Pharmacol Exp Ther* 276: 365-369, 1996.
11. **Deussen A, Stappert M, Schafer S and Kelm M.** Quantification of extracellular and intracellular adenosine production: understanding the transmembranous concentration gradient. *Circulation* %20;99: 2041-2047, 1999.
12. **Dobson JG, Jr.** Mechanism of adenosine inhibition of catecholamine-induced responses in heart. *Circ Res* 52: 151-160, 1983.
13. **Eltzschig HK, Abdulla P, Hoffman E, Hamilton KE, Daniels D, Schonfeld C, Loffler M, Reyes G, Duszenko M, Karhausen J, Robinson A, Westerman KA, Coe IR and Colgan SP.** HIF-1-dependent repression of equilibrative nucleoside transporter (ENT) in hypoxia. *J Exp Med* 202: 1493-1505, 2005.
14. **Endres CJ, Moss AM, Govindarajan R, Choi DS and Unadkat JD.** The role of nucleoside transporters in the erythrocyte disposition and oral absorption of ribavirin in the wild-type and equilibrative nucleoside transporter 1-/- mice. *J Pharmacol Exp Ther* 331: 287-296, 2009.
15. **Escudero C, Casanello P and Sobrevia L.** Human equilibrative nucleoside transporters 1 and 2 may be differentially modulated by A2B adenosine receptors in placenta microvascular endothelial cells from pre-eclampsia. *Placenta* 29: 816-825, 2008.
16. **Farias M, Puebla C, Westermeier F, Jo MJ, Pastor-Anglada M, Casanello P and Sobrevia L.** Nitric oxide reduces SLC29A1 promoter activity and adenosine transport involving transcription factor complex hCHOP-C/EBPalpha in human umbilical vein endothelial cells from gestational diabetes. *Cardiovasc Res* 86: 45-54, 2010.
17. **Farias M, San MR, Puebla C, Pearson JD, Casado JF, Pastor-Anglada M, Casanello P and Sobrevia L.** Nitric oxide reduces adenosine transporter ENT1 gene (SLC29A1) promoter activity in human fetal endothelium from gestational diabetes. *J Cell Physiol* 208: 451-460, 2006.
18. **Fotoohi AK, Lindqvist M, Peterson C and Albertioni F.** Involvement of the concentrative nucleoside transporter 3 and equilibrative nucleoside transporter



- 2 in the resistance of T-lymphoblastic cell lines to thiopurines. *Biochem Biophys Res Commun* 343: 208-215, 2006.
19. **Gorlach A.** Control of adenosine transport by hypoxia. *Circ Res* 97: 1-3, 2005.
  20. **Graham K, Yao S, Johnson L, Mowles D, Ng A, Wilkinson J, Young JD and Cass CE.** Nucleoside transporter gene expression in wild-type and mENT1 knockout mice. *Biochem Cell Biol* 89: 236-245, 2011.
  21. **Grden M, Podgorska M, Kocbuch K, Rzepko R, Szutowicz A and Pawelczyk T.** High glucose suppresses expression of equilibrative nucleoside transporter 1 (ENT1) in rat cardiac fibroblasts through a mechanism dependent on PKC-zeta and MAP kinases. *J Cell Physiol* 215: 151-160, 2008.
  22. **Guillen-Gomez E, Pinilla-Macua I, Perez-Torras S, Choi DS, Arce Y, Ballarin JA, Pastor-Anglada M and Diaz-Encarnacion MM.** New role of the human equilibrative nucleoside transporter 1 (hENT1) in epithelial-to-mesenchymal transition in renal tubular cells. *J Cell Physiol* 10, 2011.
  23. **Hammond JR.** Kinetic analysis of ligand binding to the Ehrlich cell nucleoside transporter: pharmacological characterization of allosteric interactions with the [3H]nitrobenzylthioinosine binding site. *Mol Pharmacol* 39: 771-779, 1991.
  24. **Hammond JR and Clanachan AS.** [3H]nitrobenzylthioinosine binding to the guinea pig CNS nucleoside transport system: a pharmacological characterization. *J Neurochem* 43: 1582-1592, 1984.
  25. **Husted RF, Clancy GP, Adams-Brotherton A and Stokes JB.** Inhibition of Na transport by 2-chloroadenosine: dissociation from production of cyclic nucleotides. *Can J Physiol Pharmacol* 68: 1357-1362, 1990.
  26. **Jonzon B, Nilsson J and Fredholm BB.** Adenosine receptor-mediated changes in cyclic AMP production and DNA synthesis in cultured arterial smooth muscle cells. *J Cell Physiol* 124: 451-456, 1985.
  27. **Kobayashi S, Zimmermann H and Millhorn DE.** Chronic hypoxia enhances adenosine release in rat PC12 cells by altering adenosine metabolism and membrane transport. *J Neurochem* 74: 621-632, 2000.

28. **Morote-Garcia JC, Rosenberger P, Nivillac NM, Coe IR and Eltzschig HK.** Hypoxia-inducible factor-dependent repression of equilibrative nucleoside transporter 2 attenuates mucosal inflammation during intestinal hypoxia. *Gastroenterology* 136: 607-618, 2009.
29. **Nagai K, Nagasawa K, Kihara Y, Okuda H and Fujimoto S.** Anticancer nucleobase analogues 6-mercaptopurine and 6-thioguanine are novel substrates for equilibrative nucleoside transporter 2. *Int J Pharm* 333: 56-61, 2007.
30. **Nam HW, Lee MR, Zhu Y, Wu J, Hinton DJ, Choi S, Kim T, Hammack N, Yin JC and Choi DS.** Type 1 equilibrative nucleoside transporter regulates ethanol drinking through accumbal N-methyl-D-aspartate receptor signaling. *Biol Psychiatry* 69: 1043-1051, 2011.
31. **Peng XX, Shi Z, Damaraju VL, Huang XC, Kruh GD, Wu HC, Zhou Y, Tiwari A, Fu L, Cass CE and Chen ZS.** Up-regulation of MRP4 and down-regulation of influx transporters in human leukemic cells with acquired resistance to 6-mercaptopurine. *Leuk Res* 32: 799-809, 2008.
32. **Pinto-Duarte A, Coelho JE, Cunha RA, Ribeiro JA and Sebastiao AM.** Adenosine A2A receptors control the extracellular levels of adenosine through modulation of nucleoside transporters activity in the rat hippocampus. *J Neurochem* 93: 595-604, 2005.
33. **Puebla C, Farias M, Gonzalez M, Vecchiola A, Aguayo C, Krause B, Pastor-Anglada M, Casanello P and Sobrevia L.** High D-glucose reduces SLC29A1 promoter activity and adenosine transport involving specific protein 1 in human umbilical vein endothelium. *J Cell Physiol* 215: 645-656, 2008.
34. **Rose JB, Naydenova Z, Bang A, Eguchi M, Sweeney G, Choi DS, Hammond JR and Coe IR.** Equilibrative nucleoside transporter 1 plays an essential role in cardioprotection. *Am J Physiol Heart Circ Physiol* 298: H771-H777, 2010.
35. **Stolk M, Cooper E, Vilks G, Litchfield DW and Hammond JR.** Subtype-specific regulation of equilibrative nucleoside transporters by protein kinase CK2. *Biochem J* 386: 281-289, 2005.

36. **Tanaka A, Nishida K, Okuda H, Nishiura T, Higashi Y, Fujimoto S and Nagasawa K.** Peroxynitrite treatment reduces adenosine uptake via the equilibrative nucleoside transporter in rat astrocytes. *Neurosci Lett* 498: 52-56, 2011.
37. **Vega JL, Puebla C, Vasquez R, Farias M, Alarcon J, Pastor-Anglada M, Krause B, Casanello P and Sobrevia L.** TGF-beta1 inhibits expression and activity of hENT1 in a nitric oxide-dependent manner in human umbilical vein endothelium. *Cardiovasc Res* 82: 458-467, 2009.
38. **Wu J, Lee MR, Kim T, Johng S, Rohrback S, Kang N and Choi DS.** Regulation of ethanol-sensitive EAAT2 expression through adenosine A1 receptor in astrocytes. *Biochem Biophys Res Commun* 406: 47-52, 2011.
39. **Yamamoto S, Inoue K, Murata T, Kamigaso S, Yasujima T, Maeda JY, Yoshida Y, Ohta KY and Yuasa H.** Identification and functional characterization of the first nucleobase transporter in mammals: implication in the species difference in the intestinal absorption mechanism of nucleobases and their analogs between higher primates and other mammals. *J Biol Chem* 285: 6522-6531, 2010.
40. **Yao SY, Ng AM, Vickers MF, Sundaram M, Cass CE, Baldwin SA and Young JD.** Functional and molecular characterization of nucleobase transport by recombinant human and rat equilibrative nucleoside transporters 1 and 2. Chimeric constructs reveal a role for the ENT2 helix 5-6 region in nucleobase translocation. *J Biol Chem* 277: 24938-24948, 2002.
41. **Zachary I and Glikli G.** Signaling transduction mechanisms mediating biological actions of the vascular endothelial growth factor family. *Cardiovasc Res* 49: 568-581, 2001.

## CHAPTER THREE

NUCLEOSIDE AND NUCLEOBASE TRANSPORTERS OF PRIMARY HUMAN CARDIAC  
MICROVASCULAR ENDOTHELIAL CELLS: CHARACTERIZATION OF A NOVEL TRANSPORTER<sup>1</sup>

<sup>1</sup>A version of this chapter has been published:

Bone, DBJ and Hammond JR. Nucleoside and nucleobase transporters of primary human cardiac microvascular endothelial cells: Characterization of a novel nucleobase transporter. *Am J Physiol Heart Circ Physiol*. Dec; 293(6):H3325-32. Epub: 2007 Oct 5.  
doi:10.1152/ajpheart.01006.2007

### 3.1 Introduction

The transmembrane flux of hydrophilic nucleosides and nucleobases is mediated by integral membrane proteins, including equilibrative nucleoside transporters (SLC29; ENTs) and concentrative nucleoside transporters (SLC28; CNTs) (4; 17). These nucleoside transporters (NTs) have roles in salvaging endogenous nucleosides, such as adenosine, and have been exploited for cancer chemotherapy and treatments for viral infection (21). The CNTs are Na<sup>+</sup>-dependent transporters that facilitate movement of nucleosides against their concentration gradient. Three members of the CNT family have been cloned, each with distinct substrate specificity. CNT1 transports adenosine and pyrimidine nucleosides, CNT2 transports purine nucleosides and uridine, and CNT3 is broadly selective for both purine and pyrimidine nucleosides (27). The ENTs, on the other hand, are Na<sup>+</sup>-independent facilitative diffusion transporters that rely on the concentration gradient of the substrate and thus are capable of mediating both influx and efflux of nucleosides. The two classical ENTs have been identified as being sensitive (ENT1) or insensitive (ENT2) to the nucleoside analog nitrobenzylmercaptapurine riboside (NBMPR) (36). ENT2 is also able to transport nucleobases like hypoxanthine (26). Recently, two more ENT family members have been identified: ENT3 is associated with intracellular acidic environments (19), and ENT4 was initially discovered as a monoamine transporter in the brain (15).

The purine nucleoside adenosine is an important compound in the vasculature. Acting through a variety of G-protein-coupled receptors, adenosine mediates physiological actions such as, among others, vasodilation, bradycardia, and inhibition of platelet

aggregation (33). NTs play a role in regulating adenosine levels in the vasculature by facilitating its removal from the extracellular environment (23). In fact, cardiovascular drugs like dipyridamole inhibit NTs, thereby extending the lifespan of adenosine in the vasculature (30). Analogs of NBMPR (38) and dipyridamole (22) are now being designed and tested for the potential to act as cardioprotective agents, thus highlighting the importance of vascular NTs as potential therapeutic targets.

Investigations of NTs in the vasculature have primarily utilized models derived from the macrovasculature, with a particular focus on umbilical vein endothelial cells, due to the ease of obtaining the source tissue. However, the majority of exchange between the blood and peripheral tissues occurs in the microvasculature, in which microvascular endothelial cells (MVECs) are responsible for the regulation of this exchange. It has been shown that endothelial cells in the heart are responsible for the uptake of up to 65% of free adenosine (12). Therefore, changes in the ability of MVECs to transport or metabolize adenosine can have profound effects on the cardiovascular and surrounding tissues.

Here, we describe the nucleoside and nucleobase transport capabilities of primary human cardiac MVECs.

## **3.2 MATERIALS AND METHODS**

### *3.2.1 Materials.*

2-[8-<sup>3</sup>H]chloroadenosine (4-7 Ci/mmol), [2,8-<sup>3</sup>H]hypoxanthine (24-35 Ci/mmol), [2,8-<sup>3</sup>H]adenine (50 Ci/mmol), [<sup>3</sup>H] NBMPR (5.5 Ci/mmol), and [<sup>3</sup>H]water (1 mCi/g) were

purchased from Moravек Biochemicals (Brea, CA). Nonradiolabeled 2-chloroadenosine, hypoxanthine, NBMPR, nitrobenzylthioguanine riboside, dipyridamole {2,6-bis(diethanolamino)-4,8-dipiperidinopyrimido-[5,4-d] pyrimidine}, and all other nucleosides and nucleobases were obtained from Sigma-Aldrich (St. Louis, MO). Dilazep {*N,N'*-bis[3-(3,4,5-trimethoxybenzoyloxy)propyl] homopiperazine} was from Asta Werke (Frankfurt, Germany), and draflazine {2-(aminocarbonyl)-4-amino-2,6-dichlorophenyl-4-[5,5-bis(4-fluorophenyl)-pentyl]-1-piperazineacetamide 2HCl} was provided by Janssen Research Foundation (Beerse, Belgium).

### *3.2.2 Cell culture.*

Culture of primary human cardiac MVECs is described in Chapter Two. HMEC-1 cells were obtained from the Center for Disease Control (Atlanta, GA) and cultured in MCDB-131 medium supplemented with 10 % fetal bovine serum (FBS), 100 U/ml penicillin G, 100 µg/ml streptomycin sulfate, 10 ng/ml epidermal growth factor, and 1 µg/ml hydrocortisone. HMEC-1 cells were used between passage 15-40. Some studies required the use of additional cell types, and all media and culture reagents were from Invitrogen (Burlington, ON). All cells were cultured and harvested as described in Chapter Two. Primary rat MVECs were isolated as previously described (3) and cultured in M199 medium containing 10% FBS, 100 U/ml penicillin G, 100 µg/ml streptomycin sulfate, 0.25 µg/ml amphotericin B, 2 mM L-glutamine, 0.025 U/ml heparin, and 75 µg/ml endothelial cell growth supplement. Nucleoside transporter-deficient PK15 cell line (PK15NTD) and PK15NTD-human ENT2 (hENT2) cells were a generous gift from Dr. Ming Tse (Johns Hopkins University) and were cultured in MEM containing 10% bovine growth serum

with penicillin G (100 U/ml), streptomycin sulfate (100 mg/ml), nonessential amino acids (0.1 mM), and sodium pyruvate (1 mM). G418 (300 µg/ml) was added to the culture medium of the PK15NTD-human ENT2 cells to maintain a selection pressure on the stable transfection. UMR-108 and HEK-293 cells were a gift from Dr. Peter Chidiac (Department of Physiology and Pharmacology, University of Western Ontario). UMR-108 cells were cultured in  $\alpha$ -MEM with 10% FBS, penicillin G (100 U/ml), and streptomycin sulfate (100 mg/ml). HEK-293 cells were cultured in MEM with 10% FBS and 10 µg/ml gentamicin. Madin-Darby canine kidney cells were cultured in MEM with 10% FBS and penicillin G (100 U/ml) and streptomycin sulfate (100 µg/ml). Cells were collected by centrifugation, and pellets were washed in either PBS or a Na<sup>+</sup>-free buffer [NMG (in mM): 140 N-methyl-D-glucamine, 5 KCl, 4.2 KH<sub>2</sub>PO<sub>4</sub>, 0.36 K<sub>2</sub>HPO<sub>4</sub>, 10 HEPES, 1.3 CaCl<sub>2</sub>·2H<sub>2</sub>O, and 0.5 MgCl<sub>2</sub>·6H<sub>2</sub>O; pH 7.4] and resuspended in the same buffer as required for immediate use. In some cases, cells were depleted of ATP by sequential incubation at 37°C with rotenone and 2-deoxyglucose as described previously (3).

### *3.2.3 Substrate efflux assay.*

ATP-depleted cells were loaded with 100 µM [<sup>3</sup>H]hypoxanthine for 10 min. Cells were collected by brief centrifugation and resuspended in buffer  $\pm$  1 mM adenine. One ml aliquots were taken at desired time points and centrifuged through a mixture of silicone and light mineral oil (21:4 v/v) to terminate efflux. Remaining [<sup>3</sup>H] activity in the pellet was determined and expressed as pmol/10<sup>6</sup> cells.



### 3.2.4 Data analysis and statistics.

Data are presented as means  $\pm$  SEM. Curves were fitted with the use of Graphpad Prism 4.03 software. Where appropriate, statistical analysis was performed using a two-tailed Student's *t*-test with  $P < 0.05$  considered significant.  $K_i$  values were determined with the Cheng-Prusoff relationship (10).

## 3.3 RESULTS

### 3.3.1 [ $^3\text{H}$ ]NBMPR binding.

Specific [ $^3\text{H}$ ]NBMPR binding to human cardiac MVECs revealed  $53,000 \pm 6,000$  ENT1 sites/cell with a  $K_d$  of  $0.031 \pm 0.003$  nM (Figure 3.1). A second population of low-affinity ( $K_d > 5$  nM) binding sites was also present.

### 3.3.2 2-[ $^3\text{H}$ ]Chloroadenosine uptake.

A time course profile showed that human cardiac MVECs accumulated  $10 \mu\text{M}$  2-[ $^3\text{H}$ ]chloroadenosine with an initial rate of  $1.6 \pm 0.5$  pmol/ $\mu\text{l/s}$ . Incubation of cells with  $50$  nM NBMPR to block ENT1-mediated uptake resulted in a rate of uptake that was not significantly different from that seen in the presence of  $10 \mu\text{M}$  dipyridamole and NBMPR (Figure 3.2A). Furthermore, when uptake buffer was changed from NMG ( $-\text{Na}^+$ ) to PBS ( $+\text{Na}^+$ ), there was no change in initial rate of uptake or maximal intracellular accumulation (Figure 3.2B). Uptake of increasing concentrations of 2-[ $^3\text{H}$ ]chloroadenosine demonstrated a  $K_m$  of  $42 \pm 19 \mu\text{M}$  and a  $V_{\text{max}}$  of  $3.4 \pm 1.0$  pmol/ $\mu\text{l/s}$  (Figure 3.2C). Inhibition of  $10 \mu\text{M}$  2-[ $^3\text{H}$ ]chloroadenosine was examined with the classical ENT inhibitors NBMPR, dipyridamole, drafazine, and dilazep. All four compounds (Figure

3.3) displayed high-affinity inhibition with no indication of an inhibitor-insensitive (ENT2) component to the uptake. The lack of ENT2 was especially evident from the monophasic NBMPR inhibition curve.  $K_i$  values derived from these data are listed in Table 3.1.

### 3.3.3 [ $^3\text{H}$ ]hypoxanthine uptake.

Human cardiac MVECs were able to accumulate [ $^3\text{H}$ ]hypoxanthine under  $\text{Na}^+$ -free conditions despite an apparent lack of ENT2 activity. Uptake was insensitive to dipyridamole; however, the addition of 1 mM adenine was able to block uptake (Figure 3.4A). As with 2-[ $^3\text{H}$ ]chloroadenosine,  $\text{Na}^+$  had no effect on the uptake of [ $^3\text{H}$ ]hypoxanthine (Figure 3.4B). ATP depletion of the cells before exposure to 5  $\mu\text{M}$  [ $^3\text{H}$ ]hypoxanthine reduced the extrapolated maximum intracellular accumulation from  $39 \pm 18$  to  $4.1 \pm 0.2$  pmol/ $\mu\text{l}$  (Figure 3.4C). Consequently, subsequent experiments were performed under ATP-depleted conditions to minimize the effects of intracellular metabolism. With the use of a 15-s time point to estimate initial rate, the  $V_{\text{max}}$  of [ $^3\text{H}$ ]hypoxanthine influx was determined as  $1.6 \pm 0.3$  pmol/ $\mu\text{l/s}$  with a  $K_m$  of  $96 \pm 37$   $\mu\text{M}$  (Figure 3.4D). Additional nucleobases were tested for the ability to inhibit 5  $\mu\text{M}$  [ $^3\text{H}$ ]hypoxanthine uptake. Adenine was the most effective, with a  $K_i$  of  $19 \pm 7$   $\mu\text{M}$ . Guanine produced significant inhibition of  $17 \pm 4\%$  at a concentration of 1  $\mu\text{M}$  (Figure 3.5A). Higher concentrations of guanine could not be achieved because of low solubility in assay buffers at physiological pH. Pyrimidines were much less effective, with thymine producing inhibition only at 1 mM ( $59 \pm 6\%$ ) and cytosine and uracil had no effect at 1 mM concentrations.

The chemotherapeutic thiopurine analogs 6-mercaptopurine (6-MP) and 6-thioguanine (6-TG) and the pyrimidine analog 5-fluorouracil (5-FU) were also examined. Both 6-MP and 6-TG were able to inhibit 5  $\mu\text{M}$  [ $^3\text{H}$ ]hypoxanthine uptake with an  $\text{IC}_{50}$  of  $37 \pm 11 \mu\text{M}$  and  $20 \pm 2 \mu\text{M}$ , respectively (Figure 3.5B). As with other pyrimidines, 5-FU had no effect on [ $^3\text{H}$ ]hypoxanthine uptake (data not shown).

To confirm that the dipyridamole-insensitive hypoxanthine uptake mechanism was nucleobase selective, the nucleosides adenosine and uridine were tested. Adenosine had an extrapolated  $\text{IC}_{50}$  value of  $1.3 \pm 0.9 \text{ mM}$  (Figure 3.5A), and uridine had no effect.

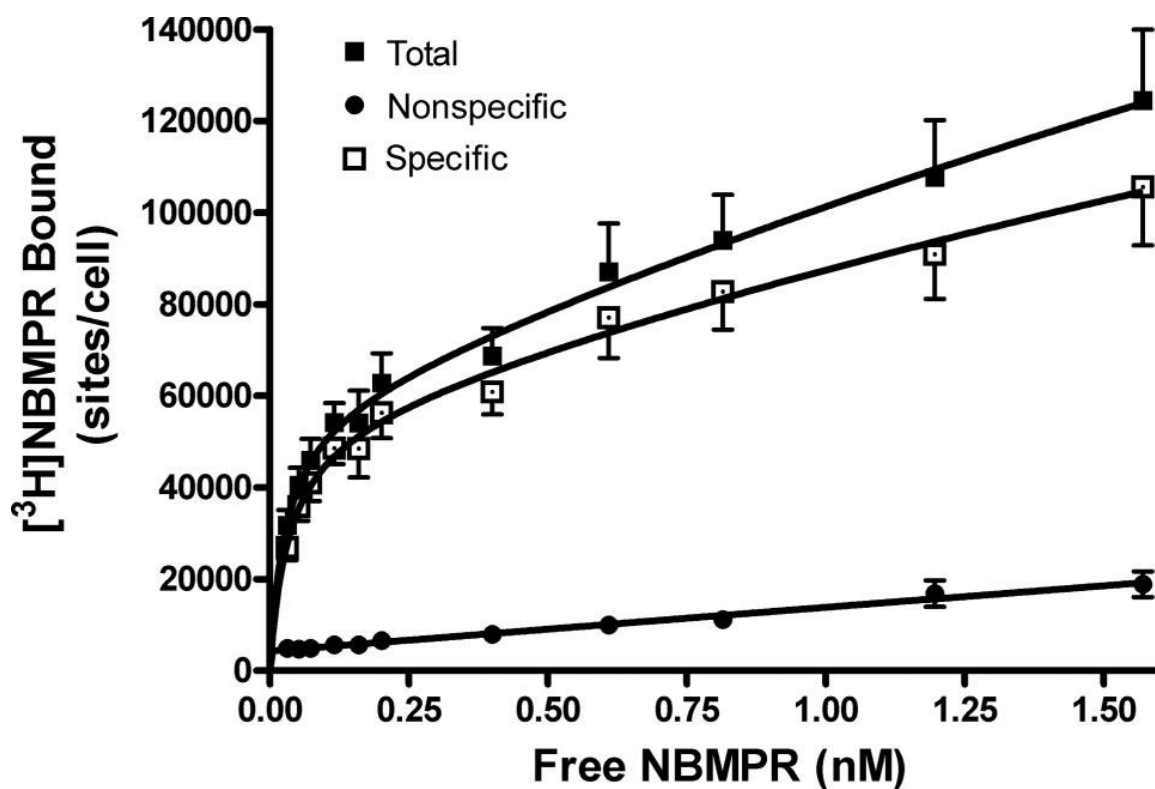


Figure 3.1. <sup>3</sup>H-labeled nitrobenzylmercaptapurine riboside (NBMPR) binding to human cardiac microvascular endothelial cells (MVECs).

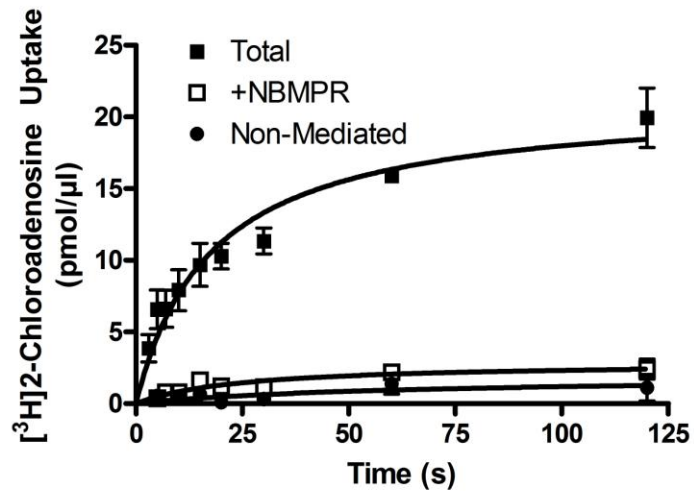
Human cardiac MVECs were incubated with increasing concentrations of [<sup>3</sup>H]NBMPR in the presence (nonspecific) or absence (total) of 10  $\mu$ M nitrobenzylthioguanine riboside (NBTGR) for 45 min. Cells were collected on glass fiber filters, and cell-associated <sup>3</sup>H content was determined. Specific binding was determined as total bound minus nonspecific bound ( $n = 5$ ).



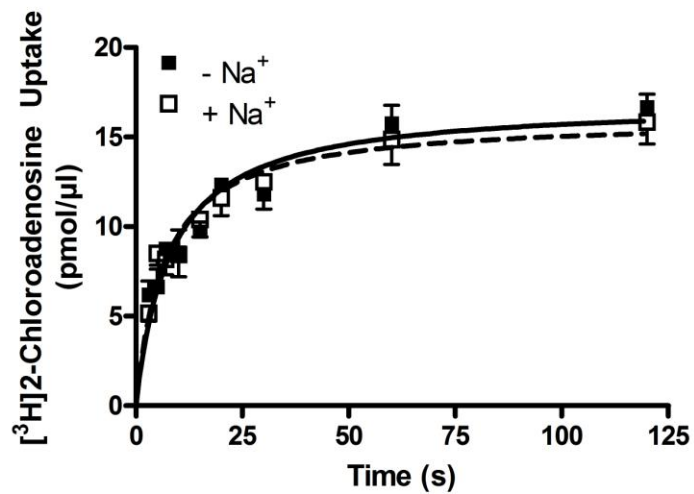
Figure 3.2. 2-[<sup>3</sup>H]chloroadenosine uptake characteristics of human cardiac MVECs.

*A*: time course of 2-[<sup>3</sup>H]chloroadenosine uptake. Human cardiac MVECs were incubated with 10 μM 2-[<sup>3</sup>H]chloroadenosine for the times indicated. Some cell lots were preincubated with 50 nM NBMPR to inhibit only equilibrative nucleoside transporter 1 (ENT1). Total uptake (no inhibitors) minus ENT1 inhibited uptake represents ENT2-mediated uptake. Nonmediated uptake was determined with cells preincubated with 10 μM NBMPR and 10 μM dipyridamole ( $n = 5$ ). *B*: Effect of sodium (Na<sup>+</sup>) on 2-[<sup>3</sup>H]chloroadenosine uptake. Uptake was performed as in *A* in either sodium free (-Na<sup>+</sup>) or sodium replete (+Na<sup>+</sup>) conditions ( $n = 5$ ). *C*: concentration-dependent uptake of 2-[<sup>3</sup>H]chloroadenosine. Cells were incubated with increasing concentrations of 2-[<sup>3</sup>H]chloroadenosine for 7 s. Transporter-mediated uptake is presented as pmol/μl/s and was defined as total uptake minus nonmediated uptake ( $n = 4$ ).

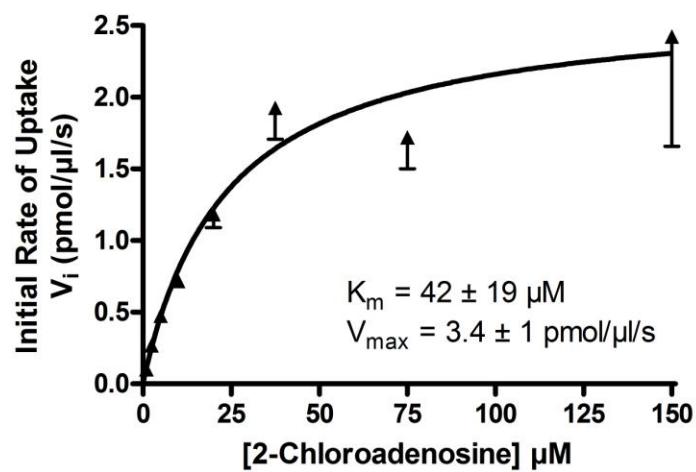
A



B



C



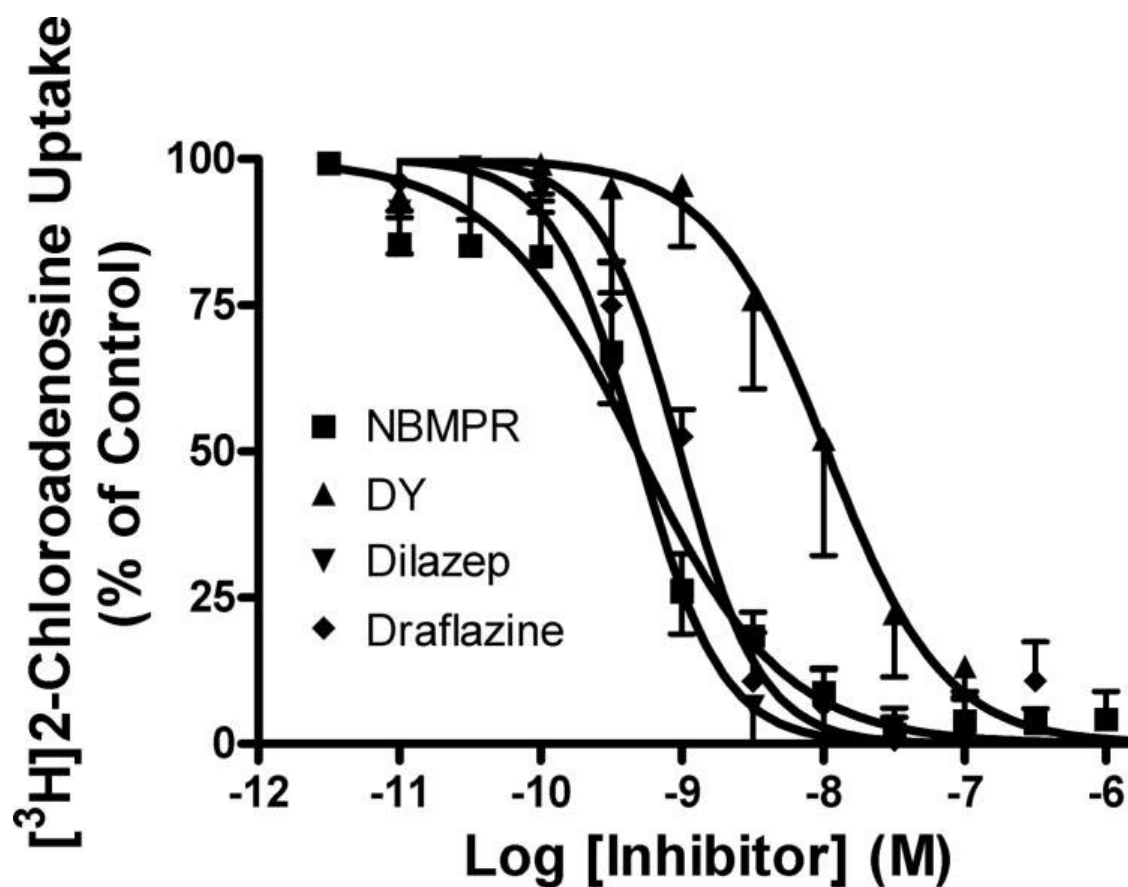


Figure 3.3. Inhibition of 2- $[^3\text{H}]$ chloroadenosine uptake.

Cells were incubated with increasing concentrations of inhibitor for 15 min before uptake of  $10\ \mu\text{M}$  2- $[^3\text{H}]$ chloroadenosine for 15 s. Uptake in the absence of any inhibitor was defined as 100%, and totally inhibited cells ( $10\ \mu\text{M}$  NBMPR +  $10\ \mu\text{M}$  dipyridamole) was defined as 0% ( $n = 4$ ).  $K_i$  values are reported in Table 1. DY, dipyridamole.





Figure 3.4. [<sup>3</sup>H]hypoxanthine uptake characteristics of human cardiac MVECs (hMVECs).

A: [<sup>3</sup>H]hypoxanthine time course. Cells were incubated with 5 μM [<sup>3</sup>H]hypoxanthine for the times indicated. Some cells were preincubated with 10 μM DY to inhibit any ENT2 that may be present in the cells. To completely block uptake, cells were coincubated with 1 mM adenine (*n* = 5). B: Effect of sodium on [<sup>3</sup>H]hypoxanthine uptake. Uptake was performed as in A) in the absence (-Na<sup>+</sup>) or presence (+Na<sup>+</sup>) of sodium (*n* = 5). C: ATP-depleted [<sup>3</sup>H]hypoxanthine time course. Uptake was performed identical to A, except that cells were depleted of ATP before assay (*n* = 6). D: concentration-dependent [<sup>3</sup>H]hypoxanthine uptake. ATP-depleted cells were incubated with increasing concentrations of [<sup>3</sup>H]hypoxanthine for 15 s. Transporter-mediated uptake is presented and was defined as uptake in the absence of any inhibitor minus uptake in the presence of 1 mM adenine (*n* = 4).

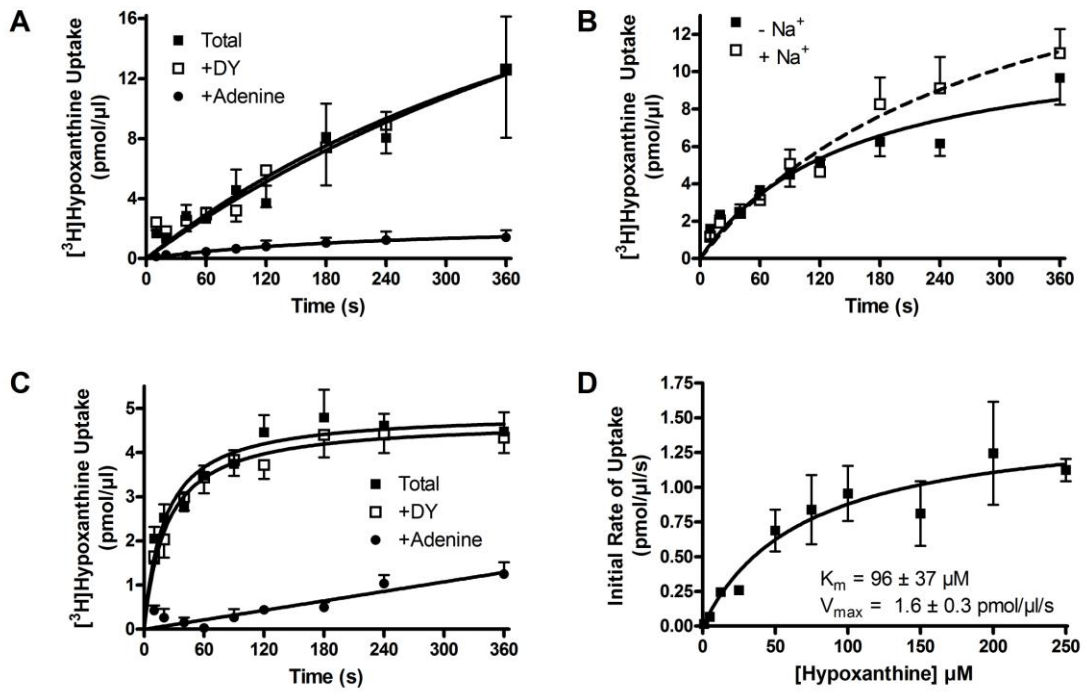




Figure 3.5. Inhibition of [<sup>3</sup>H]hypoxanthine uptake.

A: Inhibition of [<sup>3</sup>H]hypoxanthine uptake by nucleobases and nucleosides. Cells were coincubated with 5 μM [<sup>3</sup>H]hypoxanthine and indicated purine for 60 s. Uptake in the absence of inhibitor was defined as 100%, and totally inhibited uptake (1 mM adenine) was defined as 0% (*n* = 3). B: Inhibition of [<sup>3</sup>H]hypoxanthine uptake by pyrimidine nucleobases. Assays were conducted in the same manner as A (*n* = 3). C: Inhibition of [<sup>3</sup>H]hypoxanthine uptake by purine and pyrimidine nucleobase analogs. 6-MP, 6-mercaptopurine; 6-TG, 6-thioguanine; 5-FU, 5-flurouracil. Assays were conducted in the same manner as A (*n* = 3). *K<sub>i</sub>* values are reported in Table 1.

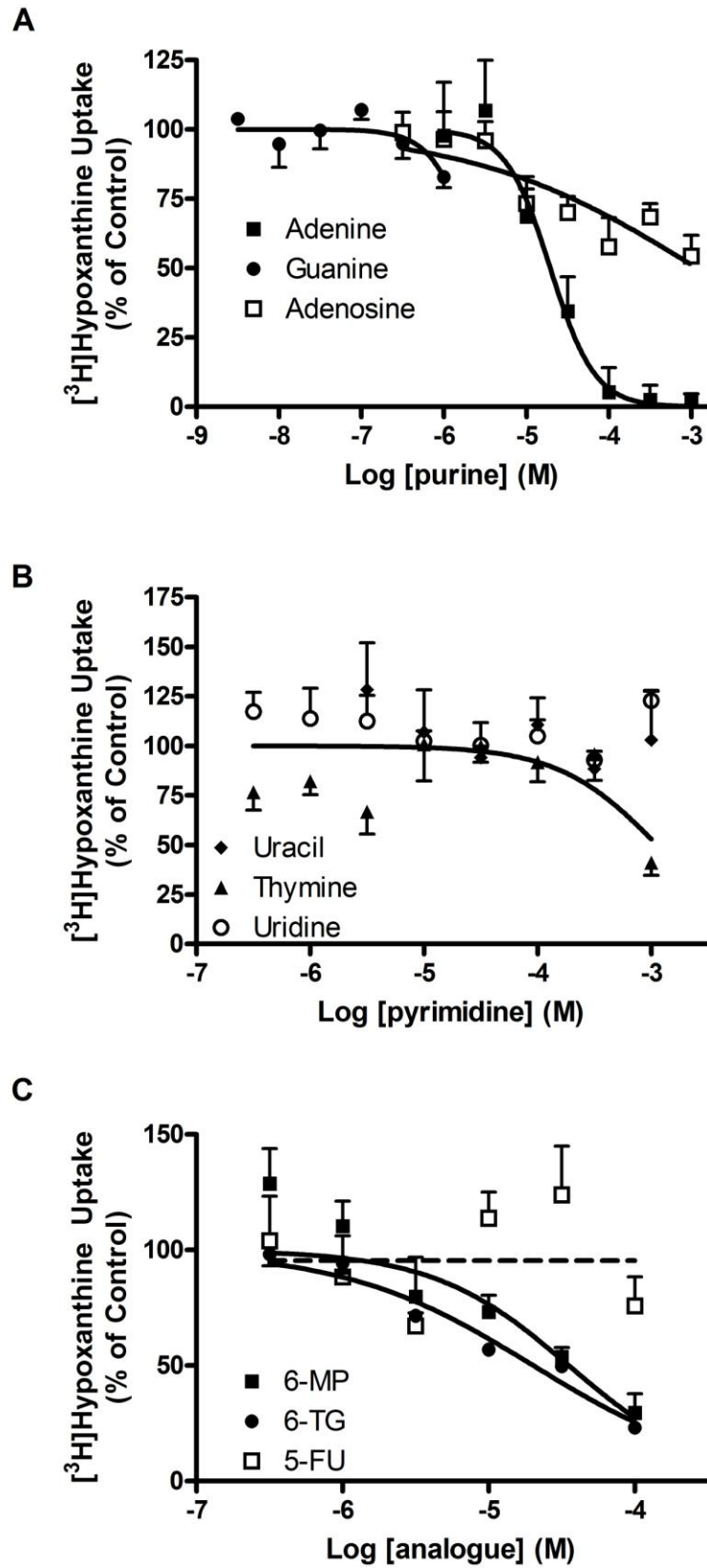


Table 3.1  $K_i$  values for inhibition of uptake by hMVECs 2-chloroadenosine and hypoxanthine

	$K_i$
2-chloroadenosine uptake	
NBMPR	$0.5 \pm 0.2$ nM
Dipyridamole	$14 \pm 8$ nM
Dilazep	$0.4 \pm 0.1$ nM
Draflazine	$0.9 \pm 0.2$ nM
Hypoxanthine uptake	
Adenine	$19 \pm 7$ $\mu$ M
Guanine	>1 $\mu$ M
Cytosine	No effect
Thymine	>1 mM
Uracil	No effect
6-MP	$37 \pm 11$ $\mu$ M
6-TG	$20 \pm 2$ $\mu$ M
5-FU	No effect
Adenosine	$1.2 \pm 0.8$ mM
Uridine	No effect

$K_i$  values were determined with the Cheng-Prusoff relationship from  $IC_{50}$  values obtained from data presented in Figs. 3 and 5. ( $n \geq 3$ ). NBMPR, nitrobenzylmercaptapurine riboside; 6-MP, 6-mercaptopurine; 6-TG, 6-thioguanine; 5-FU, 5-fluorouracil.

### 3.3.4 Nucleobase transport in other cell types.

The identification of Na<sup>+</sup>-independent [<sup>3</sup>H]hypoxanthine transport in human cardiac MVECs, by a mechanism other than ENT2, led to the examination of other cell types for evidence of a similar dipyridamole-insensitive nucleobase transport system. Established cell lines from human (U2OS and HEK-293), rat (UMR-108), pig (PK15NTD), and dog (Madin-Darby canine kidney) were examined along with primary rat skeletal muscle MVECs. Figure 3.6 shows the time course profiles for dipyridamole-insensitive hypoxanthine uptake by these cells. All cells tested displayed evidence of dipyridamole-insensitive nucleobase transport with the exception of HEK-293 cells.

PK15NTD cells were chosen for further characterization of this nucleobase transporter. These cells do not have ENT1 or ENT2 (10; 32), thereby eliminating any contribution from other nucleoside/nucleobase transporters to the results obtained. [<sup>3</sup>H]hypoxanthine uptake by PK15NTD cells was concentration dependent with a similar  $K_m$  ( $122 \pm 31$  pmol/ $\mu$ l) to the human cardiac MVEC in ATP-depleted conditions and a  $V_{max}$  of  $7.0 \pm 0.6$  pmol/ $\mu$ l/s (Figure 3.7A). There was no effect of pH on [<sup>3</sup>H]hypoxanthine uptake, and the thiopurines 6-MP and 6-TG displayed  $K_i$  values ( $21 \pm 5$  and  $19 \pm 1$   $\mu$ M, respectively) similar to those for human cardiac MVECs (data not shown). [<sup>3</sup>H]adenine was tested as a transport substrate with unlabeled hypoxanthine as the inhibitor (Figure 3.7B). Hypoxanthine at 150  $\mu$ M was able to produce ~20% inhibition of 500 nM [<sup>3</sup>H]adenine uptake under ATP-depleted conditions. The use of unlabeled 1 mM adenine was required for total inhibition.





Figure 3.6. Dipyridamole-insensitive [<sup>3</sup>H]hypoxanthine uptake in various cell types. Cells were incubated with 5 μM [<sup>3</sup>H]hypoxanthine for the times indicated. Cell lots were preincubated with 10 μM DY to inhibit any ENT2. To completely block uptake, cells were coincubated with 1 mM adenine (*n* = 2). UMR, UMR-108 cells; NTD, nucleoside transporter deficient PK15 cells (PK15NTD); MDCK, Madin-Darby canine kidney cells; rMVEC, rat skeletal muscle MVECs; HEK, HEK-293 cells.

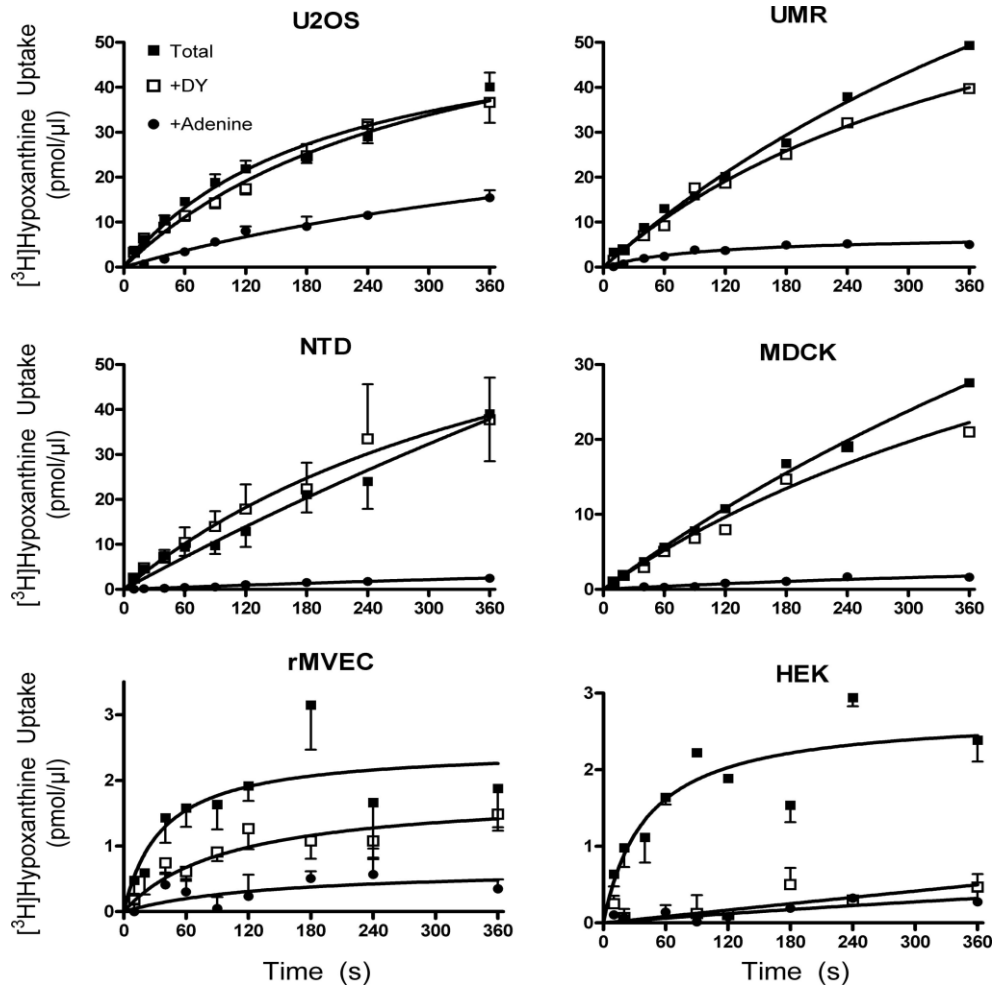
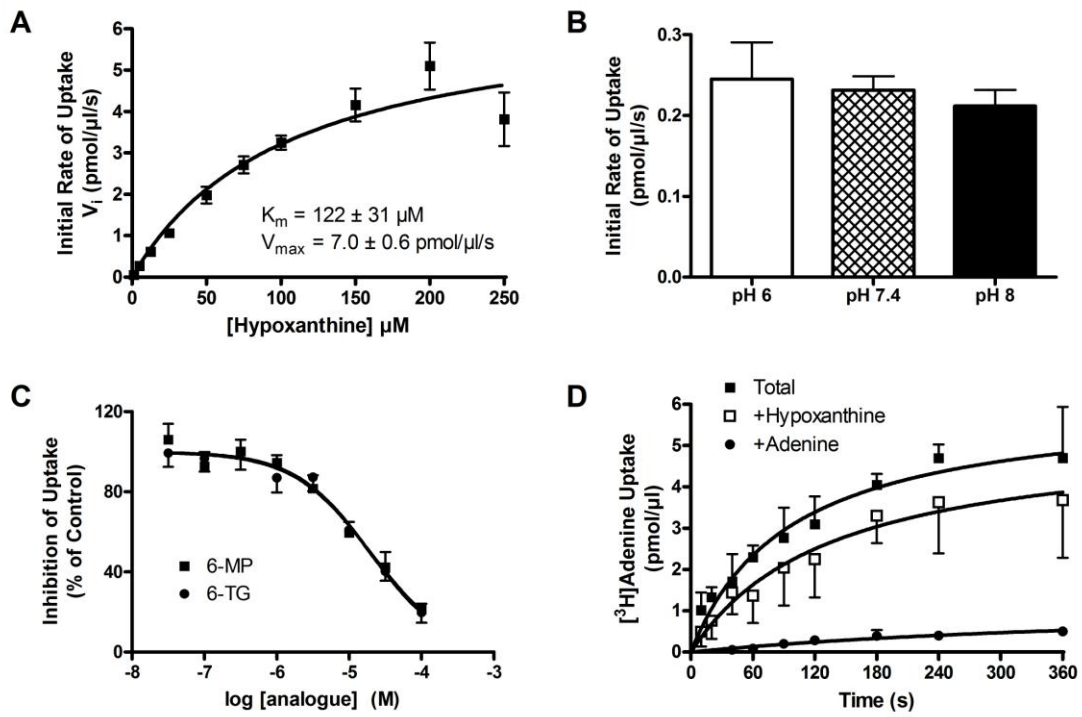




Figure 3.7. PK15NTD cells as a model for nucleobase transport.

*A*: concentration dependent uptake of [<sup>3</sup>H]hypoxanthine under ATP-depleted conditions. Cells were incubated with increasing concentrations of [<sup>3</sup>H]hypoxanthine for 15 s. Transporter-mediated uptake is presented and was defined as uptake in the absence of any inhibitor minus uptake in the presence of 1 mM unlabeled adenine (*n* = 3). *B*: Initial rate of 5 μM [<sup>3</sup>H]hypoxanthine was determined in NMG at varying pH. (*n* = 4). *C*: Inhibition of [<sup>3</sup>H]hypoxanthine uptake by 6-MP and 6-TG (*n* = 3) *D*: [<sup>3</sup>H]adenine uptake time course. ATP-depleted cells were incubated with 500 nM [<sup>3</sup>H]adenine in the presence or absence of 150 μM hypoxanthine or 1 mM adenine (*n* = 2).



[<sup>3</sup>H]hypoxanthine uptake in the presence or absence of dipyridamole was also examined in PK15NTD cells that had been previously transfected with human ENT2. Accumulation of 5 μM [<sup>3</sup>H]hypoxanthine in ATP-depleted conditions reached a maximum intracellular concentration of  $3.8 \pm 0.03$  pmol/μl; however, in the presence of dipyridamole, the amount of [<sup>3</sup>H]hypoxanthine that accumulated in the cell rose to  $18 \pm 4$  pmol/μl. Blocking ENT1 with NBMPR in the human cardiac MVECs (no ENT2) did not have an effect on [<sup>3</sup>H]hypoxanthine accumulation (Figure 3.8).

### *3.3.5 Characterization of HMEC-1 Cells*

In the interest of having a MVEC cell model that was more economical than the primary human cells, HMEC-1 cells were tested as a suitable replacement. HMEC-1 cells bound [<sup>3</sup>H]NBMPR with two apparent populations, similar to the primary human cardiac MVECs. The high affinity binding had  $76,000 \pm 14,000$  sites with a  $K_d$  of  $0.03 \pm 0.01$  nM (Figure 3.9A). The low affinity binding was not always rational, and thus was probably an artifact of the binding assay.

The time course of 10 μM 2-[<sup>3</sup>H]chloroadenosine uptake in the presence or absence of 50 nM NBMPR showed a lack of NBMPR-insensitive uptake much like the primary human cardiac MVECs (Figure 3.9B). Inhibition of 10 μM 2-[<sup>3</sup>H]chloroadenosine by NBMPR was also monophasic and had a  $K_i$  of  $0.098 \pm 0.011$  nM (Figure 3.9C)

Finally, the time course of 5 μM [<sup>3</sup>H]hypoxanthine uptake was also similar to the primary human MVECs with uptake being insensitive to dipyridamole but could be inhibited by 1 mM adenine (Figure 3.9D).

### 3.3.6 Decynium-22 and [<sup>3</sup>H]Adenine $K_m/V_{max}$

A report by Hoque and colleagues (18) suggested that the compound decynium-22 (D-22) was capable of inhibiting purine nucleobase uptake. Indeed, in PK15NTD cells, D-22 inhibited hypoxanthine uptake with a  $K_i$  of  $202 \pm 156$  nM. Similarly, D-22 inhibited 5  $\mu$ M adenine uptake with an  $IC_{50}$  of  $1.01 \pm 0.59$   $\mu$ M (Figure 3.10A). Using D-22 to define non-mediated uptake, concentration-dependent uptake of [<sup>3</sup>H]adenine was observed for concentrations of [<sup>3</sup>H]adenine up to 150  $\mu$ M. Higher concentrations of [<sup>3</sup>H]adenine appeared to actually inhibit the transport mechanism. A curve was fit to the data up to 150  $\mu$ M to generate a  $K_m$  of  $36 \pm 10$   $\mu$ M and a  $V_{max}$  of  $8.2 \pm 0.8$  pmol/ $\mu$ l/s (Figure 3.10B).

### 3.3.7 [<sup>3</sup>H]Hypoxanthine Efflux

ATP-depleted PK15NTD cells were preloaded with 100  $\mu$ M [<sup>3</sup>H]hypoxanthine for 10 minutes, then transferred to buffer with or without 1 mM adenine. [<sup>3</sup>H]hypoxanthine was released from cells by an adenine sensitive mechanism as illustrated by a significant increase in efflux half-time from  $0.9 \pm 0.3$  min in the absence of 1 mM adenine to  $4.8 \pm 0.9$  min in the presence of 1 mM adenine (Figure 3.11).

### 3.3.8 Candidates for the identity of ENBT1

The purine selective dipyridamole-insensitive nucleobase transporter ENBT1 identified in this chapter was done so through functional and pharmacological analyses only. The molecular identity of the transporter is still unresolved. Some potential candidates were identified and tested.



### 3.3.8.1 The unnamed human protein product hUPP1

Through collaboration with Dr. Imogen Coe at York University (Toronto, Canada), a gene product for a potential new transporter was identified. Known only as unnamed protein product (Genbank Accession: BAC86869), this protein was predicted to be a member of the Major Facilitator Superfamily (MFS) which contains all transporters that rely on the concentration gradient of their substrate for transport. Stable expression of GFP-hUPP1 in HEK cells was confirmed by fluorescent microscopy, however there was no gain of dipyridamole-insensitive [ $^3\text{H}$ ]hypoxanthine uptake (Figure 3.12).

### 3.3.8.2 Organic Cation Transporter as a possible candidate for ENBT1

The compound D-22 used in section 3.3.6 as an inhibitor of ENBT1 is a known organic cation transporter (OCT) inhibitor (31). OCTs have been shown to transport nucleobase analogues, therefore we tested one nucleobase analogue substrate, acyclovir, and one non-nucleobase substrate, metformin (11; 35). At a concentration of 1 mM, acyclovir inhibited the uptake of 5  $\mu\text{M}$  [ $^3\text{H}$ ]hypoxanthine by  $36 \pm 7\%$ , however 1 mM metformin had no effect (Figure 3.13).



Figure 3.8. Complex effects of nucleoside and nucleobase transporter coexpression and inhibition.

A: PK15NTD [<sup>3</sup>H]hypoxanthine uptake ± dipyridamole (DY). ATP-depleted PK15NTD cells were incubated with 5 μM [<sup>3</sup>H]hypoxanthine for the times indicated in the presence or absence of 5 μM DY (*n* = 3). B: PK15NTD-human ENT2 (hENT2) [<sup>3</sup>H]hypoxanthine uptake ± DY. ATP-depleted PK15NTD-human ENT2 cells were incubated with 5 μM [<sup>3</sup>H]hypoxanthine for the times indicated in the presence or absence of 5 μM DY (*n* = 2). C: hMVEC [<sup>3</sup>H]hypoxanthine uptake ± NBMPR. Cells were incubated in 100 μM [<sup>3</sup>H]hypoxanthine in the presence or absence of 50 nM NBMPR (*n* = 4).

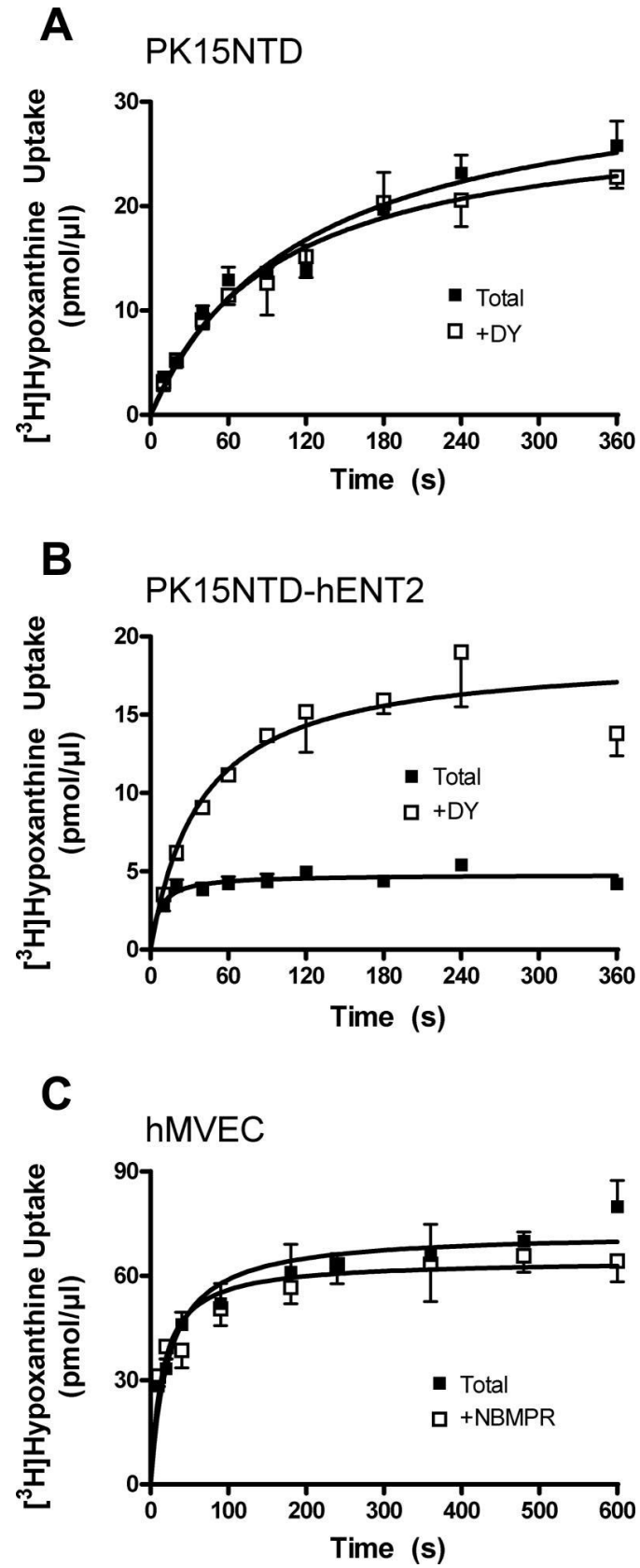




Figure 3.9. Characterization of HMEC-1 cells.

A) Cells were harvested, resuspended in PBS and subjected to [<sup>3</sup>H]NBMPR binding as described in the methods. ENT1 sites per cell was determined by subtracting [<sup>3</sup>H]NBMPR binding in the presence of NBTGR (non-specific binding) from total binding. Data are means ± SEM of four independent experiments performed in duplicate. B) Cells were harvested, resuspended in NMG buffer and subjected to 2-[<sup>3</sup>H]chloroadenosine uptake as described in the methods. Solid squares represent uptake of 10 μM 2-[<sup>3</sup>H]chloroadenosine in the absence of inhibitors (total uptake). Half-solid circles with dashed line represent uptake in the presence of 50 nM NBMPR (+NBMPR), or the contribution of NBMPR-insensitive ENT2 mediated uptake. Open circles with the dotted line represent uptake in the presence of both 5 μM NBMPR and 5 μM dipyridamole (non-mediated uptake). ENT1 mediated uptake is the difference between ENT2 mediated uptake (+NBMPR minus non-mediated) and total mediated uptake (total minus non-mediated). Only ENT1 mediated 2-chloroadenosine transport was present in these cells. Data are means ± SEM of seven independent experiments. C) Cells were incubated with increasing concentrations of NBMPR for 15 min before analysis of the uptake of 10 μM 2-[<sup>3</sup>H]chloroadenosine for 15 s. Uptake in the absence of any inhibitor was defined as 100%, and totally inhibited cells (10 μM NBMPR + 10 μM dipyridamole) was defined as 0% (*n* = 3). D) Cells were harvested, resuspended in NMG, ATP-depleted, and subjected to [<sup>3</sup>H]hypoxanthine uptake as described in the methods. Solid squares represent uptake of 5 μM [<sup>3</sup>H]hypoxanthine in the absence of any inhibitors (total uptake). Half-solid circles with dashed line represent uptake in the presence of 5 μM dipyridamole (+DY), or the contribution of the dipyridamole-insensitive nucleobase transporter. Open circles with the dotted line represent uptake in the presence of both 5 μM dipyridamole and 1 mM adenine (+DY and adenine; non-mediated uptake). Data are means ± SEM of three independent experiments.

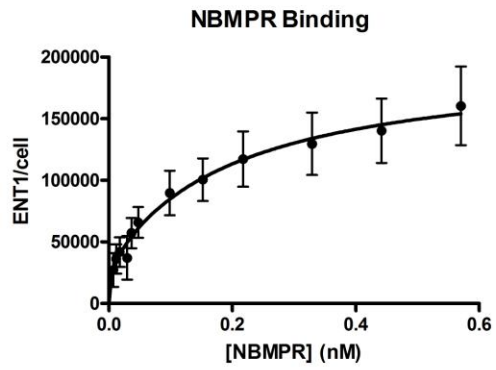
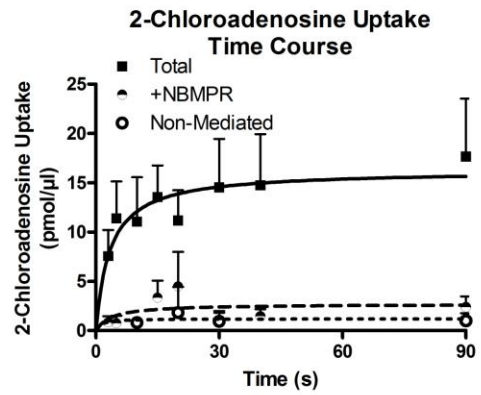
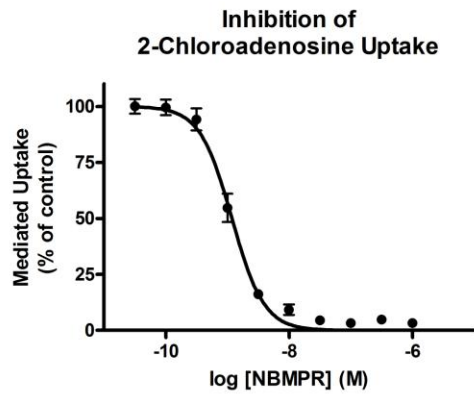
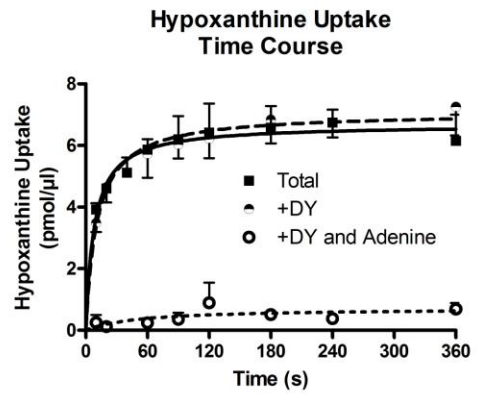
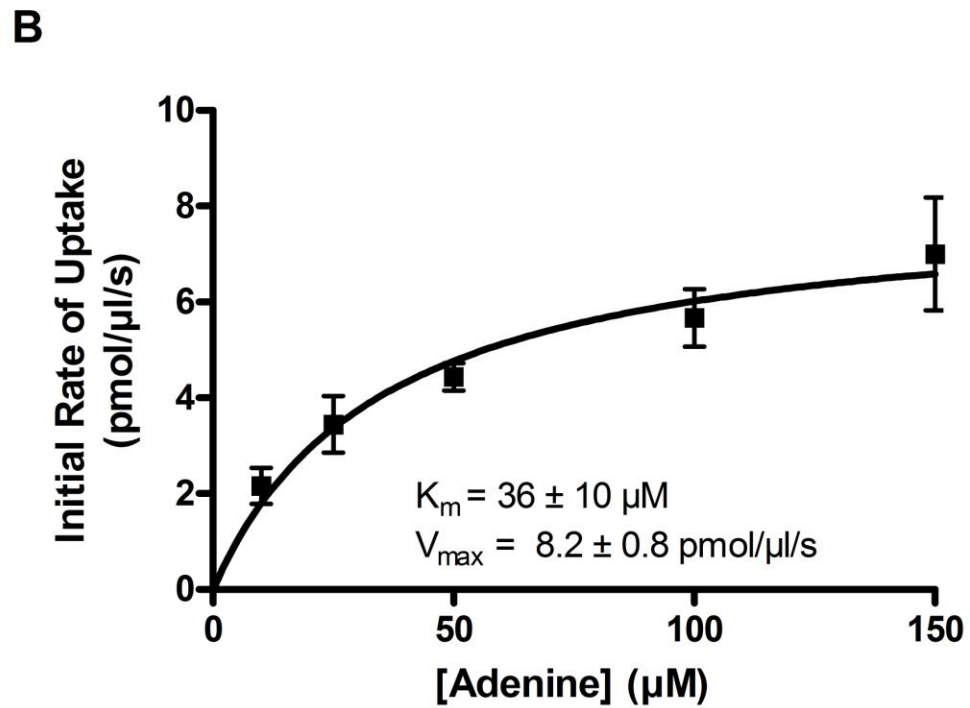
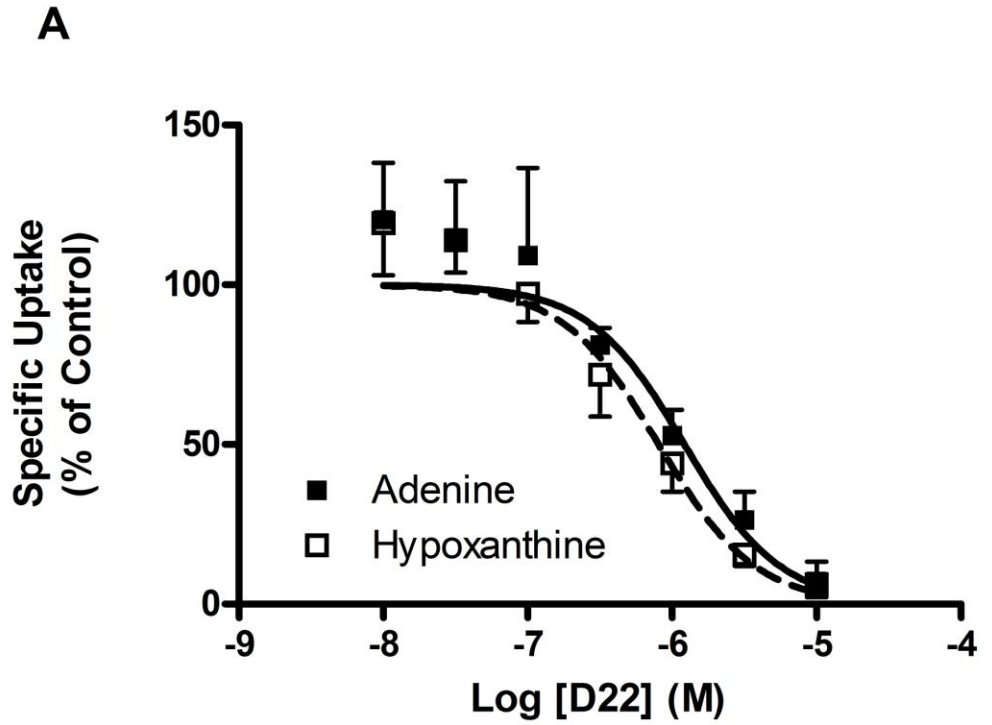
**A****B****C****D**





Figure 3.10. Decynium-22 and [<sup>3</sup>H]adenine  $K_m/V_{max}$ .

A) PK15NTD cells were preincubated with increasing concentrations of decynium-22 (D-22) for 15 min followed by exposure to 5  $\mu$ M [<sup>3</sup>H]adenine (solid squares) or 50  $\mu$ M [<sup>3</sup>H]hypoxanthine (open squares) for 20 s (n = 4). B) PK-15 NTD cells were ATP-depleted as described and preincubated with 10  $\mu$ M D-22 (non-mediated) or DMSO (total) for 15 minutes before exposure to increasing concentrations of [<sup>3</sup>H]adenine for 15 s (n = 5).



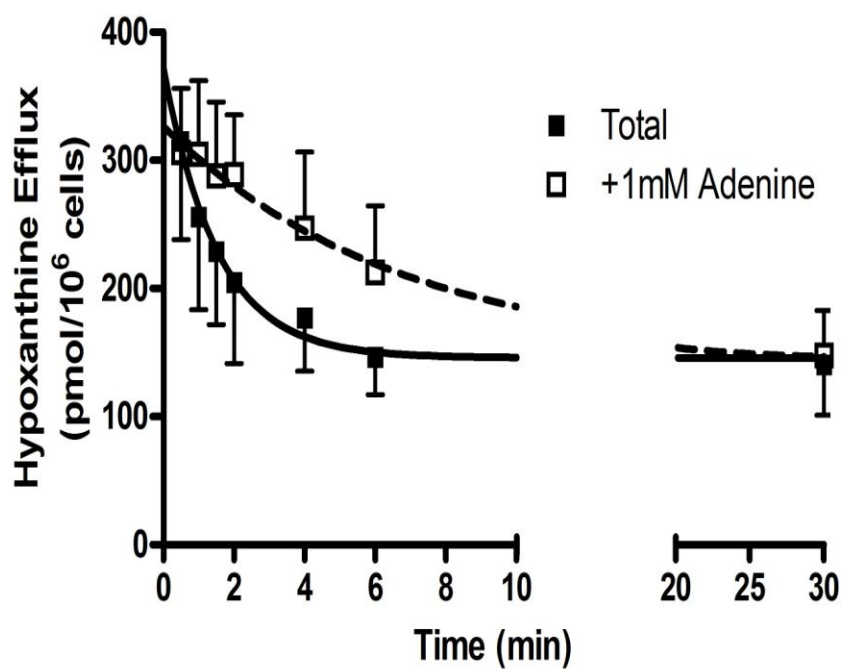
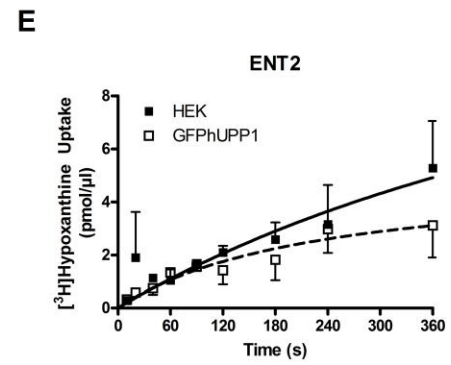
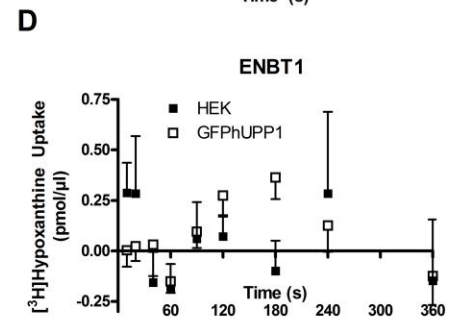
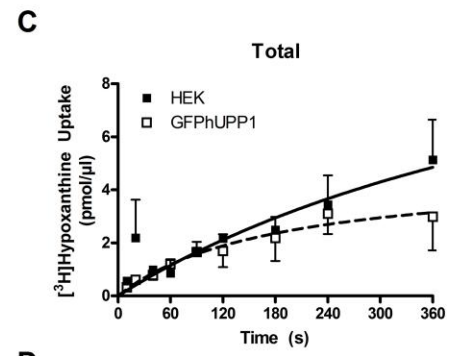
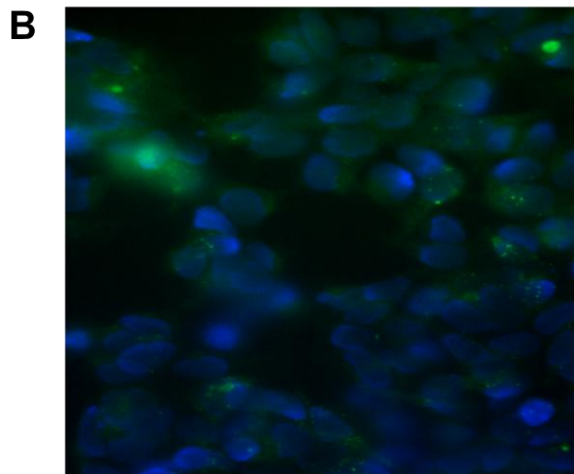
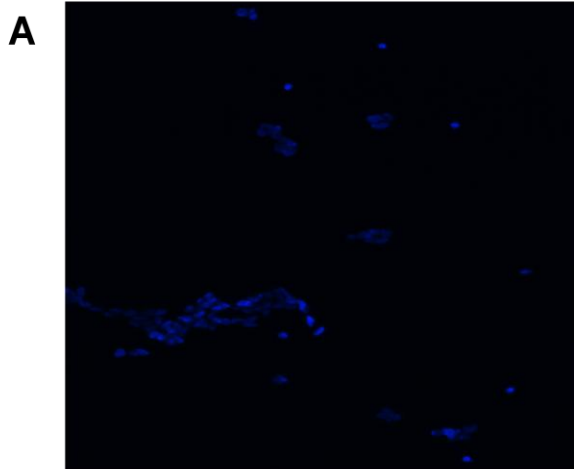


Figure 3.11. [<sup>3</sup>H]hypoxanthine efflux. PK15NTD cells were ATP-depleted and loaded with 100  $\mu$ M [<sup>3</sup>H]hypoxanthine for 10 min. Cells were collected by brief centrifugation and resuspended in buffer  $\pm$  1 mM adenine. Aliquots of cells were taken at the indicated time points and centrifuged through oil as described in the methods section 3.2.3 (n = 3).



Figure 3.12. GFP-hUPP1 does not increase hypoxanthine uptake in HEK cells.

HEK cells (A) or HEK cells stably transfected with GFP-hUPP1 (B) were depleted of ATP and subjected to uptake of 5  $\mu\text{M}$  [ $^3\text{H}$ ]hypoxanthine over time. C) Total uptake of 5  $\mu\text{M}$  [ $^3\text{H}$ ]hypoxanthine of HEK cells (solid squares) and GFP-hUPP1 cells (open squares, dotted line). D) Uptake of 5  $\mu\text{M}$  [ $^3\text{H}$ ]hypoxanthine in the presence of 10  $\mu\text{M}$  dipyridamole, representing any uptake that is mediated by ENBT1. No significant uptake was observed in HEK cells or GFP-hUPP1 cells. E) ENT2 mediated [ $^3\text{H}$ ]hypoxanthine uptake as determined by subtracting uptake in the presence of dipyridamole from total uptake. Uptake data is mean  $\pm$  SEM of 4 independent experiments.



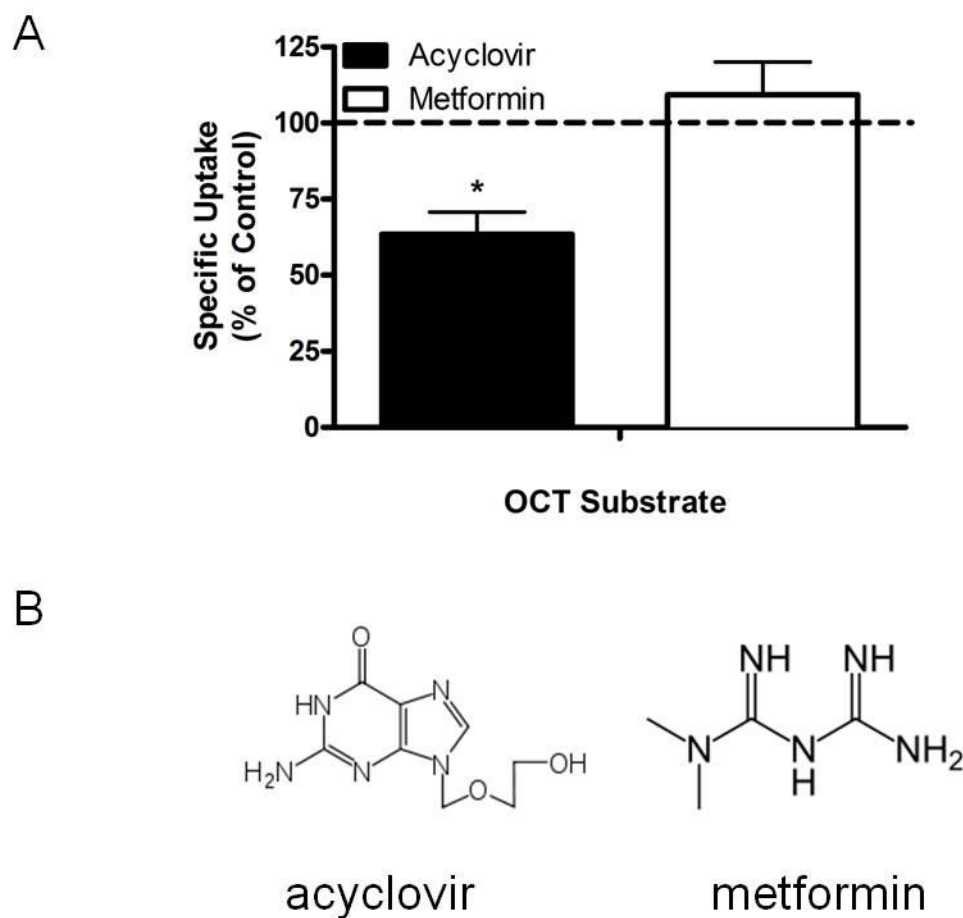


Figure 3.13. OCT substrate acyclovir but not metformin can inhibit hypoxanthine uptake.

A) 1 mM acyclovir (solid bar) or metformin (open bar) was co-incubated with 5  $\mu$ M [ $^3$ H]hypoxanthine for 60 s. Control (or 100%) was defined as accumulation of 5  $\mu$ M [ $^3$ H]hypoxanthine after 60 s incubation in the absence of any inhibitor. \* $P < 0.05$  compared to 100%. Data are mean  $\pm$  SEM of 4 independent experiments performed in duplicate.

B) Chemical structures of acyclovir (nucleobase analogue) and metformin (non-nucleobase).

### 3.4 DISCUSSION

The microvasculature forms a barrier between the circulation and peripheral tissues and is responsible for mediating nutrient exchange between these two compartments. MVEC regulation of nucleosides via NTs can have profound effects on the cardiovascular actions of adenosine, warranting further investigation of NTs as potential therapeutic targets (23).

#### *3.4.1 Characterization of Nucleoside Transport in Human Cardiac Microvascular Endothelial Cells.*

Human cardiac MVECs have both high- and low-affinity binding sites for the ENT1-selective probe NBMPR. The  $K_d$  of the high-affinity site is consistent with reported values for ENT1 (19). Our group, in rat skeletal muscle MVECs (3), and others (7) have reported the presence of the low-affinity population of NBMPR binding sites, which may be a result of [<sup>3</sup>H]NBMPR binding to intracellular ENT1 proteins. The high-affinity maximum binding capacity of ~53,000 ENT1 sites/cell likely represents the transporters associated with the plasma membrane.

2-Chloroadenosine is an established substrate of NTs and was chosen to limit the effects of intracellular metabolism on the measurement of transport kinetics (6; 20). Na<sup>+</sup>-independent uptake of 2-chloroadenosine in the presence or absence of a low concentration of NBMPR (50 nM) to inhibit ENT1 revealed no significant contribution of the NBMPR-insensitive ENT2 to the overall uptake. In addition, NBMPR, dilazep, drafazine, and dipyridamole all produced monophasic inhibition curves for inhibiting 2-chloroadenosine uptake (pseudo Hill coefficients were approximately -1) with  $K_i$  values



typical of ENT1 inhibition (36). Numerous endothelial cell models express a combination of ENT1 and ENT2, including primary rat MVECs (3), human umbilical vein endothelial cells (2), primary mouse MVECs (see Chapter 5), and EVC 304 cells (26). In this regard, human MVECs, which demonstrate only ENT1 function, appear to be an exception.

### *3.4.2 Identification of a Novel Nucleobase Transporter in Human Cardiac Microvascular Endothelial Cells.*

Although human cardiac MVECs had no functional ENT2, they were still able to accumulate hypoxanthine under  $\text{Na}^+$ -free conditions. Uptake was insensitive to dipyridamole; however, other purine nucleobases were capable of blocking influx. There was no significant change in uptake in the presence of  $\text{Na}^+$ , thus ruling out the ascorbic acid transport system. An increase in  $\text{H}^+$  had no effect, and uptake was not inhibited by monoamines; thus this hypoxanthine transporter is not the recently identified ENT4 (14). The apparent  $K_m$  of hypoxanthine uptake ( $96 \pm 37 \mu\text{M}$ ) was threefold lower, and the  $K_i$  of adenine inhibition of hypoxanthine uptake ( $19 \pm 7 \mu\text{M}$ ) reported in this study was  $\sim 140$  times lower than previously reported for human ENT2 (26). Together, these data support that hypoxanthine uptake in human cardiac MVECs was mediated by a transport system distinct from ENT2. Further characterization showed that the transport system as purine nucleobase selective. The only pyrimidine tested that could inhibit hypoxanthine uptake was thymidine at nonphysiological concentrations ( $>1 \text{ mM}$ ). The nucleoside adenosine also inhibited uptake at high concentrations ( $\text{IC}_{50} > 1 \text{ mM}$ ), but this may be the result of adenosine metabolism releasing adenine.

The chemotherapeutic purine nucleobase analogs 6-MP and 6-TG demonstrated an affinity for the nucleobase transport system, whereas the pyrimidine analog 5-FU did not. The  $K_i$  determined for 6-MP and 6-TG inhibition of hypoxanthine uptake ( $\sim 20\text{--}30\ \mu\text{M}$ ) were similar to reported values of therapeutic concentrations found within cells (13). This has relevance in the role that the vasculature plays in delivering chemotherapeutic agents to the intended target such that if this nucleobase transport system is blocked or down-regulated the chemotherapeutic purine nucleobase analogs would be less able to gain access to their intracellular site of cytotoxic action.

#### *3.4.3 Physiological Importance of Nucleobase Transport*

The ability of a cell to mediate the transmembrane flux of nucleobases is important, as evidenced by the existence of at least two distinct transport systems for nucleobases in many cell types. Regulation of intracellular levels of nucleobases, such as hypoxanthine, may be critical during periods of physiological stress, including hypoxia or ischemia. During hypoxia or ischemia in the heart, the breakdown of ATP in cardiomyocytes results in an increase in adenosine, which is released to the interstitial space via NTs (16). The surrounding endothelium then accumulates this extracellular adenosine. Adenosine kinase becomes saturated with the excess adenosine therefore shifting the metabolism to inosine via adenosine deaminase. Subsequent metabolism by purine nucleoside phosphorylase produces hypoxanthine as an intermediate to the final product of uric acid (33). It is in the production of hypoxanthine that the role of MVEC nucleobase transporters may hold importance. Because hypoxanthine is metabolized to xanthine by xanthine oxidase, reactive oxygen species (ROS) are produced (25). Links have been

established between xanthine oxidase-derived ROS and endothelial dysfunction (5; 29). Therefore, having a system capable of regulating hypoxanthine levels, before xanthine oxidase-mediated metabolism of hypoxanthine were to occur, may prevent or reduce ROS-induced endothelial dysfunction.

The molecular identity of this distinctive dipyridamole-insensitive, purine-selective nucleobase transporter is presently not known. Despite this lack of identity, we have named the transporter equilibrative nucleobase transporter 1 (ENBT1). There is some evidence in the literature that similar transporters may exist (28; 32), and we have been able to identify its presence through function in several cell types from various species. Preliminary data from our laboratory have suggested that mouse MVECs are more similar to human cardiac MVECs than rat MVECs with respect to their nucleoside and nucleobase transport properties. However, rat MVECs appear to have less of the dipyridamole-insensitive [<sup>3</sup>H]hypoxanthine transporter and instead use ENT2 as the primary nucleobase transport system. This needs to be considered when using rat as a model for human extrapolation studies.

Of the cells tested, only HEK-293 cells appeared to be deficient in ENBT1. Thus HEK-293 cells may prove useful to the heterologous expression of candidate genes for ENBT1. In contrast, PK15NTD cells, which lack ENTs, have very high levels of ENBT1. Thus PK15NTD cells may provide a useful model to study dipyridamole-insensitive hypoxanthine transport. The lack of ENTs in these cells allows for the transfection of a NT of interest for the study of interactions between nucleoside and nucleobase transporters, as we have shown with the PK15NTD-human ENT2 cell line. HMEC-1 are an immortalized cell

line created from human dermal microvascular endothelial cells that were transfected with the simian virus 40 large T antigen, that are generally accepted to be a suitable model for the study of microvascular endothelial cells (1). Given that HMEC-1 cells appear to have identical transport characteristics as the primary human MVECs, we conclude that at the general level of nucleoside and nucleobase transport that these cells are a suitable substitute for primary human cells. However, it remains to be seen if HMEC-1 cells will respond in a similar manner when exposed to stimuli that elicit physiological responses.

The 4.5-fold enhancement of hypoxanthine accumulation in the presence of dipyridamole in PK15NTD-human ENT2 cells (see Fig. 3.8) may be the result of intracellular trapping of hypoxanthine metabolites, or perhaps hypoxanthine itself, that normally are substrates for ENT2. It is possible for ENT2-preferring nucleosides, like inosine (36), to be formed from hypoxanthine by purine nucleoside phosphorylase when normal physiological conditions are changed to allow the enzyme to catalyze the preferred reaction of nucleoside synthesis (8). Thus nucleobases can be used to replenish depleted nucleoside and nucleotide stores, using ENBT1 as a salvage pathway. Cells that lack ENT2, like human MVECs, or ones that have their existing ENT2 transporters blocked will see an enhancement of this salvage pathway, possibly leading to improved cellular function during periods of physiological stress.

Decynium-22 is a known inhibitor of organic cation transporters and has been shown to inhibit the purine nucleobase uptake in PK15NTD cells by others (18; 31). We too have shown that D-22 works as an inhibitor in our hands. Before this discovery, the only

inhibitor of ENBT1 was adenine, which was not suitable for determining the uptake kinetics of adenine itself. The use of D-22 allowed a  $K_m/V_{max}$  profile for adenine to be generated, however the reason that transport rates returned to zero at high concentrations remains unresolved (Figure 3.10B). Since PK15NTD cells lack nucleoside transporters, it was unlikely that a nucleoside metabolite was being transported out of the cells. A more likely explanation would be an inability of D-22 to completely inhibit the transporter at very high concentrations of substrate.

Despite the overlap of D-22 and nucleobase analogues with ENBT1 and OCTs, the non-nucleobase OCT substrate metformin was unable to inhibit hypoxanthine mediated uptake. Like the ENT family, there are multiple OCTs and metformin is transported by OCT1 and OCT3 (9; 24; 34; 37). The lack of inhibition in this study lowers the likelihood that ENBT1 is actually an OCT, however there is still the possibility that ENBT1 resembles an OCT in some genetic or structural manner.

The ability to move substrates bi-directionally across the plasma membrane is a defining feature of equilibrative transporters. ENBT1 is truly equilibrative, as hypoxanthine was transported out of PK15NTD cells in an adenine sensitive manner (Figure 3.11). This evidence supports the hypothesis that ENBT1 is capable of regulating intracellular nucleobase concentrations that may impact on ROS production. In an ischemic event, as hypoxanthine accumulates in the endothelial cell as a result of adenosine metabolism through the deaminase pathway, the concentration gradient of hypoxanthine would be from the intracellular compartment out. Transport of hypoxanthine out of the cell

through ENBT1 would reduce the amount of substrate available for xanthine oxidase and ROS production when oxygen returns.

In summary, we have characterized the nucleoside and nucleobase transporters of primary human cardiac MVECs. Human cardiac MVECs rely solely on ENT1 for nucleoside transport, and we have identified a novel nucleobase transport system, which we have named ENBT1. ENBT1 is present in a variety of different cell types in combination with ENT2; however, this combination varies between species and cell types. We recommend that future studies involving nucleoside or nucleobase regulation in the microvasculature be conducted in mouse models if human models are unavailable. The role of nucleoside and nucleobase transporters in the vasculature is important and complex. Regulation of extracellular adenosine levels, either through ENT expression or pharmacological intervention, will impact cardiovascular function. Considering the vasodilatory effects of adenosine, ENT regulation of purine levels can impact perfusion and thus nutrient exchange between the microvasculature and surrounding tissues (23). Control of nucleobase levels by ENT2 or ENBT1 will have implications in nutrient salvage, chemotherapy, and ROS production during hypoxia or ischemia.

### 3.5 REFERENCES

1. **Ades EW, Candal FJ, Swerlick RA, George VG, Summers S, Bosse DC and Lawley TJ.** HMEC-1: establishment of an immortalized human microvascular endothelial cell line. *J Invest Dermatol* 99: 683-690, 1992.
2. **Aguayo C, Casado J, Gonzalez M, Pearson JD, Martin RS, Casanello P, Pastor-Anglada M and Sobrevia L.** Equilibrative nucleoside transporter 2 is expressed in human umbilical vein endothelium, but is not involved in the inhibition of adenosine transport induced by hyperglycaemia. *Placenta* 26: 641-653, 2005.
3. **Archer RG, Pitelka V and Hammond JR.** Nucleoside transporter subtype expression and function in rat skeletal muscle microvascular endothelial cells. *Br J Pharmacol* 143: 202-214, 2004.
4. **Baldwin SA, Beal PR, Yao SY, King AE, Cass CE and Young JD.** The equilibrative nucleoside transporter family, SLC29. *Pflugers Arch* 447: 735-743, 2004.
5. **Berry CE and Hare JM.** Xanthine oxidoreductase and cardiovascular disease: molecular mechanisms and pathophysiological implications. *J Physiol* 555: 589-606, 2004.
6. **Bone DB, Robillard KR, Stolk M and Hammond JR.** Differential regulation of mouse equilibrative nucleoside transporter 1 (mENT1) splice variants by protein kinase CK2. *Mol Membr Biol* 24: 294-303, 2007.
7. **Boumah CE, Hogue DL and Cass CE.** Expression of high levels of nitrobenzylthioinosine-sensitive nucleoside transport in cultured human choriocarcinoma (BeWo) cells. *Biochem J* 288: 987-996, 1992.
8. **Bzowska A, Kulikowska E and Shugar D.** Purine nucleoside phosphorylases: properties, functions, and clinical aspects. *Pharmacol Ther* 88: 349-425, 2000.
9. **Chen L, Pawlikowski B, Schlessinger A, More SS, Stryke D, Johns SJ, Portman MA, Chen E, Ferrin TE, Sali A and Giacomini KM.** Role of organic cation transporter 3 (SLC22A3) and its missense variants in the pharmacologic action of metformin. *Pharmacogenet Genomics* 20: 687-699, 2010.

10. **Cheng Y and Prusoff WH.** Relationship between the inhibition constant (K<sub>1</sub>) and the concentration of inhibitor which causes 50 per cent inhibition (I<sub>50</sub>) of an enzymatic reaction. *Biochem Pharmacol* 22: 3099-3108, 1973.
11. **Ciarimboli G.** Organic cation transporters. *Xenobiotica* 38: 936-971, 2008.
12. **Deussen A, Stappert M, Schafer S and Kelm M.** Quantification of extracellular and intracellular adenosine production: understanding the transmembranous concentration gradient. *Circulation* 99: 2041-2047, 1999.
13. **Duley JA and Florin TH.** Thiopurine therapies: problems, complexities, and progress with monitoring thioguanine nucleotides. *Ther Drug Monit* 27: 647-654, 2005.
14. **Engel K and Wang J.** Interaction of organic cations with a newly identified plasma membrane monoamine transporter. *Mol Pharmacol* 68: 1397-1407, 2005.
15. **Engel K, Zhou M and Wang J.** Identification and characterization of a novel monoamine transporter in the human brain. *J Biol Chem* 279: 50042-50049, 2004.
16. **Gorlach A.** Control of adenosine transport by hypoxia. *Circ Res* 97: 1-3, 2005.
17. **Gray JH, Owen RP and Giacomini KM.** The concentrative nucleoside transporter family, SLC28. *Pflugers Arch* 447: 728-734, 2004.
18. **Hoque KM, Chen L, Leung GP and Tse CM.** A purine-selective nucleobase/nucleoside transporter in PK15NTD cells. *Am J Physiol Regul Integr Comp Physiol* 294: R1988-R1995, 2008.
19. **Hyde RJ, Cass CE, Young JD and Baldwin SA.** The ENT family of eukaryote nucleoside and nucleobase transporters: recent advances in the investigation of structure/function relationships and the identification of novel isoforms. *Mol Membr Biol* 18: 53-63, 2001.
20. **Jarvis SM, Martin BW and Ng AS.** 2-Chloroadenosine, a permeant for the nucleoside transporter. *Biochem Pharmacol* 34: 3237-3241, 1985.



21. **King AE, Ackley MA, Cass CE, Young JD and Baldwin SA.** Nucleoside transporters: from scavengers to novel therapeutic targets. *Trends Pharmacol Sci* 27: 416-425, 2006.
22. **Lin W and Buolamwini JK.** Synthesis, flow cytometric evaluation, and identification of highly potent dipyridamole analogues as equilibrative nucleoside transporter 1 inhibitors. *J Med Chem* 50: 3906-3920, 2007.
23. **Loffler M, Morote-Garcia JC, Eltzschig SA, Coe IR and Eltzschig HK.** Physiological roles of vascular nucleoside transporters. *Arterioscler Thromb Vasc Biol* 27: 1004-1013, 2007.
24. **Moreno-Navarrete JM, Ortega FJ, Rodriguez-Hermosa JI, Sabater M, Pardo G, Ricart W and Fernandez-Real JM.** OCT1 Expression in adipocytes could contribute to increased metformin action in obese subjects. *Diabetes* 60: 168-176, 2011.
25. **Nemeth I, Talosi G, Papp A and Boda D.** Xanthine oxidase activation in mild gestational hypertension. *Hypertens Pregnancy* 21: 1-11, 2002.
26. **Osses N, Pearson JD, Yudilevich DL and Jarvis SM.** Hypoxanthine enters human vascular endothelial cells (ECV 304) via the nitrobenzylthioinosine-insensitive equilibrative nucleoside transporter. *Biochem J* 317: 843-848, 1996.
27. **Podgorska M, Kocbuch K and Pawelczyk T.** Recent advances in studies on biochemical and structural properties of equilibrative and concentrative nucleoside transporters. *Acta Biochim Pol* 52: 749-758, 2005.
28. **Redzic ZB, Gasic JM, Segal MB, Markovic ID, Isakovic AJ, Rakic ML, Thomas SA and Rakic LM.** The kinetics of hypoxanthine transport across the perfused choroid plexus of the sheep. *Brain Res* 925: 169-175, 2002.
29. **Rieger JM, Shah AR and Gidday JM.** Ischemia-reperfusion injury of retinal endothelium by cyclooxygenase- and xanthine oxidase-derived superoxide. *Exp Eye Res* 74: 493-501, 2002.
30. **Schaper W.** Dipyridamole, an underestimated vascular protective drug. *Cardiovasc Drugs Ther* 19: 357-363, 2005.

31. **Schomig E, Babin-Ebell J and Russ H.** 1,1'-diethyl-2,2'-cyanine (decynium22) potently inhibits the renal transport of organic cations. *Naunyn Schmiedeberg's Arch Pharmacol* 347: 379-383, 1993.
32. **Shayeghi M, Akerman R and Jarvis SM.** Nucleobase transport in opossum kidney epithelial cells and *Xenopus laevis* oocytes: the characterisation, structure-activity relationship of uracil analogues and oocyte expression studies of sodium-dependent and -independent hypoxanthine uptake. *Biochim Biophys Acta* 1416: 109-118, 1999.
33. **Shryock JC and Belardinelli L.** Adenosine and adenosine receptors in the cardiovascular system: biochemistry, physiology, and pharmacology. *Am J Cardiol* 79: 2-10, 1997.
34. **Solbach TF, Grube M, Fromm MF and Zolk O.** Organic cation transporter 3: Expression in failing and nonfailing human heart and functional characterization. *J Cardiovasc Pharmacol* 2011.
35. **Takeda M, Khamdang S, Narikawa S, Kimura H, Kobayashi Y, Yamamoto T, Cha SH, Sekine T and Endou H.** Human organic anion transporters and human organic cation transporters mediate renal antiviral transport. *J Pharmacol Exp Ther* 300: 918-924, 2002.
36. **Ward JL, Sherali A, Mo ZP and Tse CM.** Kinetic and pharmacological properties of cloned human equilibrative nucleoside transporters, ENT1 and ENT2, stably expressed in nucleoside transporter-deficient PK15 cells. Ent2 exhibits a low affinity for guanosine and cytidine but a high affinity for inosine. *J Biol Chem* 275: 8375-8381, 2000.
37. **Zhou K, Donnelly LA, Kimber CH, Donnan PT, Doney AS, Leese G, Hattersley AT, McCarthy MI, Morris AD, Palmer CN and Pearson ER.** Reduced-function SLC22A1 polymorphisms encoding organic cation transporter 1 and glycemic response to metformin: a GoDARTS study. *Diabetes* 58: 1434-1439, 2009.
38. **Zhu Z, Hofmann PA and Buolamwini JK.** Cardioprotective effects of novel tetrahydroisoquinoline analogs of nitrobenzylmercaptapurine riboside in an isolated perfused rat heart model of acute myocardial infarction. *Am J Physiol Heart Circ Physiol* 292: H2921-H2926, 2007.

## CHAPTER FOUR

REGULATION OF HUMAN MICROVASCULAR ENDOTHELIAL CELL PURINE TRANSPORTERS.

#### 4.1 Introduction

In human microvascular endothelial cells, transmembrane flux of nucleosides and nucleobases is controlled by equilibrative nucleoside transporter 1 (ENT1) and equilibrative nucleobase transporter 1 (ENBT1) respectively (4). In mice, there is an additional small, but measurable, contribution to both nucleoside and nucleobase transport by equilibrative nucleoside transporter 2 (ENT2) (4). These transporters act as important regulators of intracellular concentrations of their substrates, and influence the interaction of these compounds with receptors on the plasma membrane. Thus, alteration of the expression and/or function of purine transporters can have far reaching consequences for the microvascular endothelium.

Regulation of nucleoside and nucleobase transporters in the context of hypoxia and ischemia is an under-appreciated field. As described in Chapter One, hypoxia/ischemia results in increased extracellular adenosine, a substrate of ENT1 (and ENT2). Extracellular adenosine is known to promote protection of surrounding tissue during hypoxia/ischemia. Intracellular adenosine metabolism produces hypoxanthine, a substrate of ENBT1 (and ENT2), and reactive oxygen species (ROS). Therefore, understanding the function of transporters during hypoxia/ischemia may contribute to the understanding of pathologies such as ischemia-reperfusion injury.

It has been shown previously that ENT1 can be transcriptionally regulated by hypoxia inducible factor 1 alpha (HIF-1 $\alpha$ ) in human, mouse, and rat cell lines representing epithelial, endothelial, cardiomyocyte, and carcinoma cells (9; 15; 25), but not in primary microvascular endothelial cells (MVECs). One gene target of HIF-1 $\alpha$  is vascular

endothelial growth factor (VEGF). Interestingly, adenosine is also capable of promoting VEGF production. However, the potential interaction between VEGF and nucleoside/nucleobase transporters has not yet been investigated.

Surprisingly, the effect of adenosine receptor activation/inhibition on nucleoside transport is poorly understood. Some attempts have been made to study the interaction, however the results are not readily interpretable (16; 33). Instead, there has been more success on studying downstream effector proteins including protein kinase A (PKA) (13; 27) and protein kinase C (PKC) (10; 12; 14; 18; 21). An additional kinase, protein kinase CKII (CKII), has also been implicated in nucleoside transport regulation (Figure 4.1) (6; 14; 41). The factors linking these studies together are 1) most are in immortalized cell lines, 2) several are from rodent cell lines, and 3) nucleobase transport was not addressed.

The effects of ROS on nucleoside and nucleobase transport function have not been directly addressed. Endothelial cells produce nitric oxide (NO), which can react with the free radical superoxide to produce the reactive nitrogen species (RNS) peroxynitrite (ONOO<sup>-</sup>). Peroxynitrite, a very powerful oxidant, has been shown to reduce the function of other transport proteins, as well as prevent adenosine accumulation in rat astrocytes (42). However, ENT1 mediated transport of adenosine following peroxynitrite exposure was not properly addressed in that study.

While the effect of ROS and RNS on transporter function is not well studied, there have been efforts to understand the effects of hypoxia on ENT1. It has been previously shown that ENT1 was transcriptionally regulated by HIF-1 $\alpha$  in a number of cell lines following

chronic hypoxia (9; 15; 25). Short term hypoxia (2 hr or less) had no effect on ENT1 expression. The impact of ischemia, however, has not been addressed, nor has the model of primary MVECs been reported.

## 4.2 Materials and Methods

### 4.2.1 Materials

2-[<sup>3</sup>H]Chloroadenosine, [2,8-<sup>3</sup>H]hypoxanthine (28.7 Ci/mmol), [<sup>3</sup>H]NBMPR (23.8 Ci/mmol), and [<sup>3</sup>H]water (1mCi/ml) were purchased from Moravek Biochemicals (Brea, CA). Non-radiolabeled, 2-chloroadenosine, hypoxanthine, NBMPR, nitrobenzylthioguanine riboside (NBTGR), and adenine were from Sigma-Aldrich. Human recombinant VEGF-165 was purchased from Cell Signaling Technology (Danvers, MA). Sunitinib malate (*N*-[2-(Diethylamino)ethyl]-5-[(*Z*)-(5-fluoro-1,2-dihydro-2-oxo-3*H*-indol-3-ylidene)methyl]-2,4-dimethyl-1*H*-pyrrole-3-carboxamide (2*S*)-2-hydroxybutanedioate salt), ZM323881 (5-((7-Benzyloxyquinazolin-4-yl)amino)-4-fluoro-2-methylphenol hydrochloride), CGS21680 (4-[2-[[6-Amino-9-(*N*-ethyl-β-D-ribofuranuronamidoyl)-9*H*-purin-2-yl]amino]ethyl]benzene propanoic acid hydrochloride), NECA (1-(6-Amino-9*H*-purin-9-yl)-1-deoxy-*N*-ethyl-β-D-ribofuranuronamide), forskolin, sp-cAMP, KT5270 ((9*R*,10*S*,12*S*)-2,3,9,10,11,12-Hexahydro-10-hydroxy-9-methyl-1-oxo-9,12-epoxy-1*H*-diindolo[1,2,3-*fg*:3',2',1'-*kl*]pyrrolo[3,4-][1,6]benzodiazocine-10-carboxylic acid, hexyl ester), 8-CPT-2Me-cAMP(8-(4-Chlorophenylthio)-2'-*O*-methyladenosine-3',5'-cyclic monophosphate sodium salt), PMA (phorbol 12-myristate 13-acetate), Gö6983 (3-[1-[3-(Dimethylamino)propyl]-5-methoxy-1*H*-indol-3-yl]-4-(1*H*-indol-3-yl)-1*H*-pyrrole-2,5-

dione), Gö6976 (5,6,7,13-Tetrahydro-13-methyl-5-oxo-12*H*-indolo[2,3-*a*]pyrrolo[3,4-*c*]carbazole-12-propanenitrile), and TBB (4,5,6,7-tetrabromobenzotriazole) were obtained from Tocris Bioscience (Ellisville, MO). 4 $\alpha$ -PMA and BFA ( $\gamma$ ,4-Dihydroxy-2-(6-hydroxy-1-heptenyl)-4-cyclopentanecrotonic acid  $\lambda$ -lactone) were from Sigma. Tert-butyl hydroperoxide (TBHP), menadione, and cobalt chloride (CoCl<sub>2</sub>) were from Sigma-Aldrich. 3-Morpholinopyrrolidine hydrochloride (SIN-1) was from BIOMOL Research Laboratories (Plymouth Meeting, PA) and manganese(III) tetrakis(1-methyl-4-pyridyl)porphyrin (MnTMPyP) was from Calbiochem (Mississauga, ON). One percent oxygen gas was from Praxair (London, ON).

#### *4.2.2 Vascular Endothelial Growth Factor Treatment*

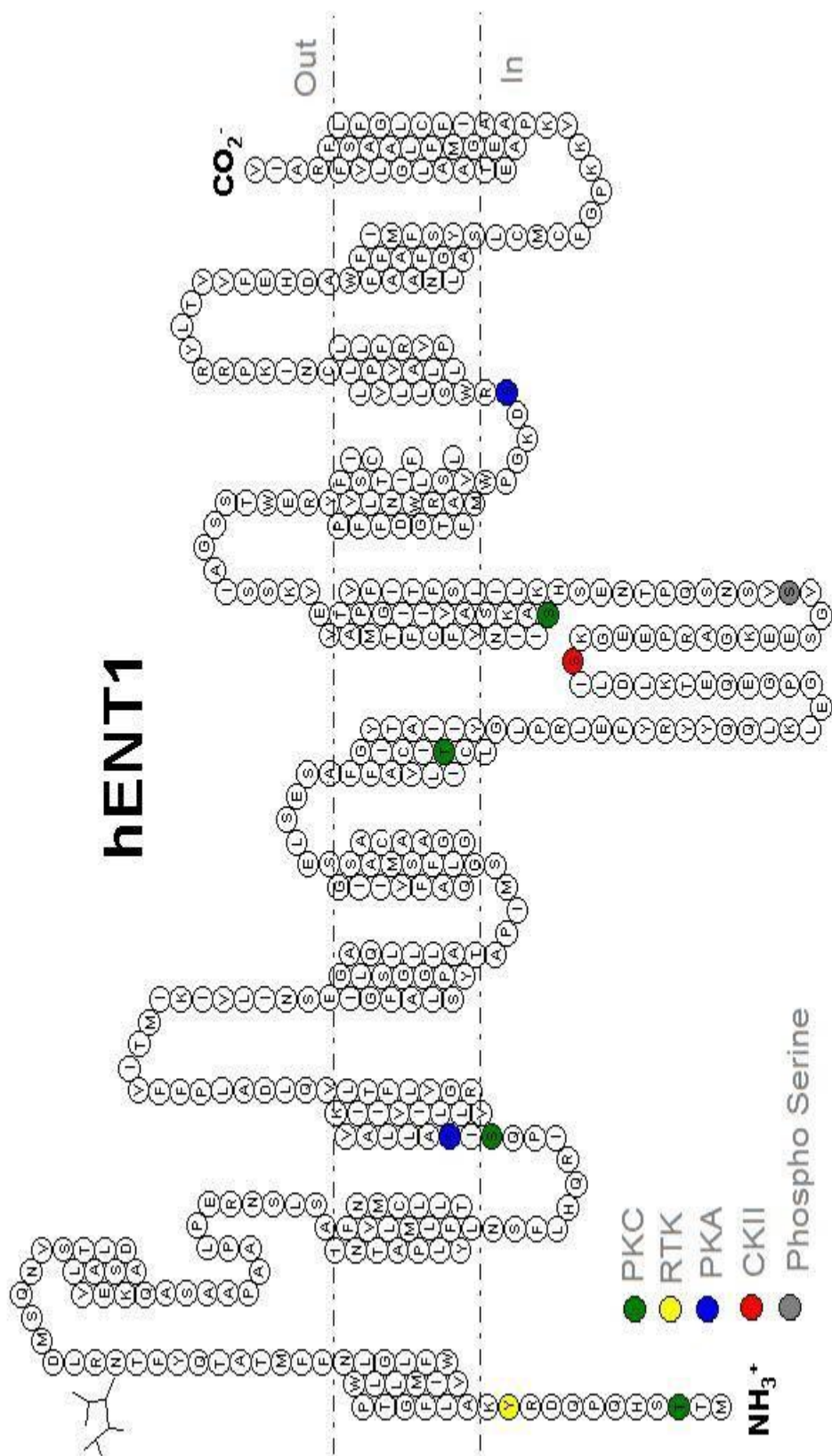
Confluent cells were washed with PBS and fed with EBM-2 medium or MCDB 131 medium for MVECs and HMEC-1 cells respectively, without serum or other growth factors plus the indicated concentration of human recombinant VEGF or PBS and cultured for 24 hr. In cases where treatment time was less than 24 hr, cells were cultured in basal medium without serum until VEGF was added. The total time in serum free medium was always 24 hr. When required, cells were pretreated with 1  $\mu$ M sunitinib (non-selective VEGF receptor inhibitor) or 1  $\mu$ M ZM323881 (VEGFR2 selective inhibitor) for 1 hr before the addition of VEGF.





Figure 4.1. Putative intracellular phosphorylation sites on human ENT1.

Amino acid sequence and predicted topology of human ENT1 with highlighted residues predicted to be phosphorylated by receptor tyrosine kinases (RTK), protein kinase C (PKC), protein kinase CKII (CKII), or protein kinase A (PKA). Residues were predicted using NetPhos 2.0 web based software (<http://www.cbs.dtu.dk/services/NetPhos/>) (3).



#### *4.2.3 Protein Kinase Modulation*

Serum starved cells were harvested and resuspended in HBSS. Cells were then treated with 100  $\mu$ M forskolin or 1  $\mu$ M of the direct PKA activator sp-cAMP and incubated at 37°C for 15 min. When used, inhibitors were added to the cells 15 min at 37°C before the addition of forskolin or sp-cAMP. Treated cells were then used for substrate uptake assays as described in Chapter 2. Alternatively, cells were then treated with the PKC activator PMA for 15 min at 37°C. Inhibitors were added to the cells 15 min at 37°C before the addition of PMA.

To test the contribution of CKII to transporter regulation, cells were washed and fed with medium containing 10  $\mu$ M TBB or DMSO and incubated at 37°C for 24 to 48 hr prior to uptake assays.

#### *4.2.4 Adenosine Receptor Agonists*

For uptake assays, cells were harvested, resuspended in buffer and treated with the indicated concentration of agonist or antagonist for the time mentioned at 37°C. Following incubation, cells were harvested and subjected to substrate uptake assays.

#### *4.2.5 Treatment with a Reactive Oxygen Species Generator*

Menadione, an intracellular superoxide generator, was dissolved in 100% ethanol and prepared fresh each day. Cells were washed with warm HBSS and fed with warmed HBSS containing vehicle (control) or 100  $\mu$ M menadione. In some cases, 100  $\mu$ M MnTMPyP, a superoxide dismutase mimetic dissolved in ddH<sub>2</sub>O, was also added to cells at the same time as menadione, or to cells alone. Cells were incubated at 37°C for 30 min before harvesting and subsequent uptake studies (as described in Chapter 2).

#### *4.2.6 Simulated Hypoxia and Ischemia*

##### *4.2.6.1 Cobalt Chloride Treatment*

Cobalt chloride ( $\text{CoCl}_2$ ) is an established stabilizer of HIF-1 $\alpha$  (35). Confluent cells were washed with PBS and fed with medium containing 100  $\mu\text{M}$   $\text{CoCl}_2$  and incubated at 37°C for the time indicated before harvesting for substrate uptake assays.

##### *4.2.6.2 Simulated Ischemia*

Based on a method developed by Meldrum and colleagues(29), primary mouse cells were harvested and resuspended in fresh complete medium. Cell suspensions were placed in a 37°C 5% $\text{CO}_2$ -95% air humidified atmosphere for 1 hr to equilibrate. Following equilibration, a cell lot was centrifuged briefly and all medium was aspirated off with the exception of enough to keep the pellet covered. The pellet was resuspended by flicking the tube. Simulated ischemia was initiated by the layering of mineral oil over the concentrated cell suspension, creating a gas exchange barrier. Mineral oil overlayed cells were placed back in the atmosphere described above for 2 hr. Control cells were left in the complete medium with no overlay. Cells were gently mixed every 30 min. Following treatment, cells were washed with PBS, centrifuged, and supernatant was aspirated. This procedure was repeated three times to ensure no mineral oil was remaining. Cells were then resuspended in a final volume appropriate for substrate uptake assays.

## 4.3 RESULTS

### 4.3.1 Regulation of transport by VEGF

4.3.1.1 VEGF protects against serum starvation cell death in primary but not immortalized microvascular endothelial cells.

Primary human cardiac microvascular endothelial cells (MVEC) and immortalized cell line HMEC-1 were treated with human recombinant VEGF<sub>165</sub> for 24 hr at concentrations ranging from 0.1 to 25 ng/ml. A dose-dependent increase in cell concentration, as determined by cell counting, was observed with MVECs cells but not HMEC-1 cells (Figure 4.2).

4.3.1.2 VEGF reduces [<sup>3</sup>H]NBMPR binding sites in microvascular endothelial cells.

Treatment with VEGF for 24 hr in serum free medium resulted in a dose-dependent decrease in the number of [<sup>3</sup>H]NBMPR binding sites, representative of ENT1 protein, to a maximum of  $66 \pm 4$  % of control at a concentration of 25 ng/ml in MVECs (Figure 4.3A). HMEC-1 cells also had reduced [<sup>3</sup>H]NBMPR binding sites after VEGF treatment, however this effect was achieved at a lower concentration of 1 ng/ml. The magnitude of drop was similar to MVECs at  $65 \pm 9$  % of control (Figure 4.3B).

4.3.1.3 The reduction in [<sup>3</sup>H]NBMPR binding is temporally different between MVEC and HMEC-1 cells.

Primary MVECs and immortalized HMEC-1 cells were treated with 25 ng/ml and 1 ng/ml VEGF, respectively, over a range of different times. The number of [<sup>3</sup>H]NBMPR binding sites in MVECs was unaffected up to 2 hr of treatment. However, after 4 hr of treatment, [<sup>3</sup>H]NBMPR binding was reduced to  $69 \pm 9$  % of control and remained

depressed at the same level at both 6 and 24 hr (Figure 4.4A). In contrast, the number of [<sup>3</sup>H]NBMPR sites in HMEC-1 remained at control levels until 24 hr (Figure 4.4B).

4.3.1.4 VEGF reduction in [<sup>3</sup>H]NBMPR binding sites in MVECs may be mediated by VEGFR2.

Primary MVECs were pretreated with the non-selective VEGF receptor antagonist sunitinib malate or the VEGFR2 selective antagonist ZM323881 at a concentration 1  $\mu$ M for 15 min. Following pretreatment, 25 ng/ml VEGF was added to culture medium and cells were incubated for an additional 24 hr. The VEGFR2 inhibitor ZM323881 was able to prevent a VEGF mediated reduction in [<sup>3</sup>H]NBMPR  $B_{max}$ . Sunitinib malate failed to prevent a VEGF induced reduction in [<sup>3</sup>H]NBMPR binding sites, however sunitinib alone also significantly reduced [<sup>3</sup>H]NBMPR  $B_{max}$  (Figure 4.5). Both ZM323881 and sunitinib were able to directly inhibit [<sup>3</sup>H]NBMPR binding at high concentrations (10 $\mu$ M), however there was no significant inhibition of [<sup>3</sup>H]NBMPR binding at the 1 $\mu$ M concentration used for both compounds in the [<sup>3</sup>H]NBMPR binding assay (Figure 4.6).

4.3.1.5 Nucleobase, but not nucleoside transport is increased by VEGF.

In contrast to the findings that VEGF was capable of reducing the number of [<sup>3</sup>H]NBMPR binding sites in both primary MVECs and HMEC-1 cells, the transport of 2-[<sup>3</sup>H]chloroadenosine by ENT1 was not affected by 24 hr VEGF treatment of either cell type. Interestingly, the  $V_{max}$  of [<sup>3</sup>H]hypoxanthine uptake indicating an increase in the activity of the purine selective nucleobase transporter ENBT1 was significantly increased in HMEC-1 cells to from  $4.3 \pm 0.3$  to  $6.0 \pm 0.6$  pmol/ $\mu$ l/s ( $n = 4$ ). The primary MVEC

[<sup>3</sup>H]hypoxanthine uptake  $V_{max}$  was also increased from,  $7.8 \pm 1.7$  to  $11.8 \pm 2.5$  pmol/ $\mu$ l/s, however this did not reach statistical significance in this data set (Figure 4.7).

#### 4.3.2 Regulation by PKC

Treatment of serum starved hMVECs with 100 nM PMA for 15 min resulted in a  $35 \pm 6$  % decrease in ENT1 mediated uptake of 10  $\mu$ M 2-[<sup>3</sup>H]chloroadenosine compared to control. In contrast PMA had no effect on ENBT1 mediated uptake of 50  $\mu$ M [<sup>3</sup>H]hypoxanthine (Figure 4.8A). The effect of PMA on ENT1 was inhibited by the compound Go6983 which is a non-specific PKC inhibitor, but was not affected by Go6976 which is selective for the alpha and beta isoforms of PKC. The inactive PMA analogue 4 $\alpha$ -PMA had no effect on ENT1 mediated transport (Figure 4.8B)

Kinetic analysis of ENT1 transport of 2-[<sup>3</sup>H]chloroadenosine after 100 nM PMA treatment revealed a  $74 \pm 11$  % decrease in  $V_{max}$  and an  $81 \pm 9$  % decrease in  $K_m$  compared to control (Figure 4.8C).

Treatment with 100 nM PMA in serum free medium for 24 hr was also performed. Uptake of 10  $\mu$ M 2-[<sup>3</sup>H]chloroadenosine by ENT1 was increased to  $180 \pm 33$  % of control (n=4). Additionally, uptake of 50  $\mu$ M [<sup>3</sup>H]hypoxanthine by ENBT1 dramatically increased to  $279 \pm 39$  % of control (Figure 4.8D).

#### 4.3.3 Regulation by CKII

Treatment with 10  $\mu$ M TBB in serum free medium for 24 hr, resulted in a substantial decrease in 10  $\mu$ M 2-[<sup>3</sup>H]chloroadenosine uptake to  $21 \pm 6$  % of control. Additionally, there was a significant decrease in 50  $\mu$ M [<sup>3</sup>H]hypoxanthine uptake to  $52 \pm 11$  % of control (Figure 4.9).

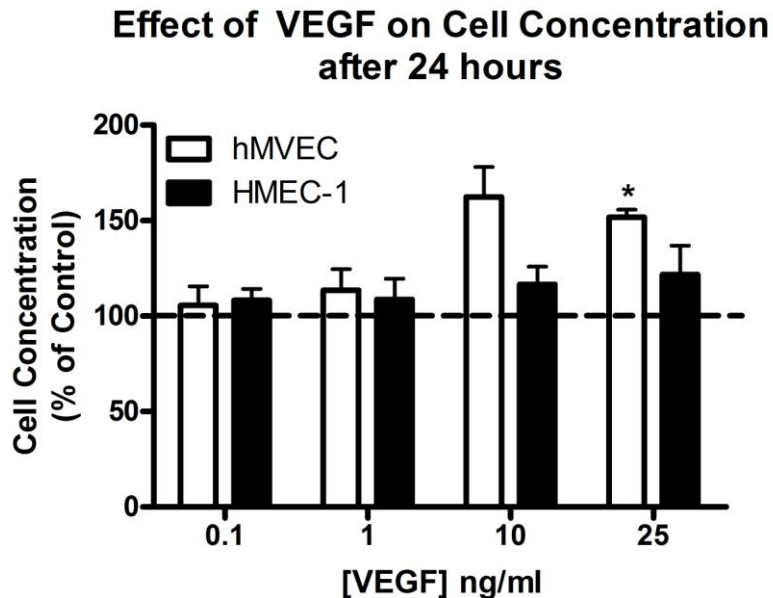


Figure 4.2 VEGF enhances cell concentration in primary MVECs but not immortalized HMEC-1 cells.

Primary hMVECs or immortalized HMEC-1 cells were washed with PBS and then cultured with serum free medium containing vehicle or the indicated concentration of VEGF for 24 h (shaded boxes). Cells were harvested and resuspended in buffer and counted by using either a hemocytometer or TC-10 automated cell counter. Cell concentration in cells/ml of VEGF treated cells was taken as a percentage of control cells. \* $P < 0.05$  one sample t-test compared to 100%,  $n \geq 3$ . Data are means  $\pm$  SEM.





Figure 4.3. VEGF decreased [<sup>3</sup>H]NBMPR binding B<sub>max</sub> in both hMVECs and HMEC-1 cells.

Confluent primary hMVECs or immortalized HMEC-1 cells were washed with PBS and then fed with serum free medium containing vehicle or the indicated concentration of VEGF for 24 h. Cells were harvested and resuspended in PBS and subjected to [<sup>3</sup>H]NBMPR binding as described in the methods. A) Primary MVECs had a significant decrease in [<sup>3</sup>H]NBMPR binding B<sub>max</sub> compared to 66 ± 4 % of control at 25 ng/ml (\*P<0.05, one sample t-test vs 100%, n = 3). B) HMEC-1 cells had a significant decrease in [<sup>3</sup>H]NBMPR binding sites to 65 ± 9 % of control at 1 ng/ml VEGF (n ≥ 4).

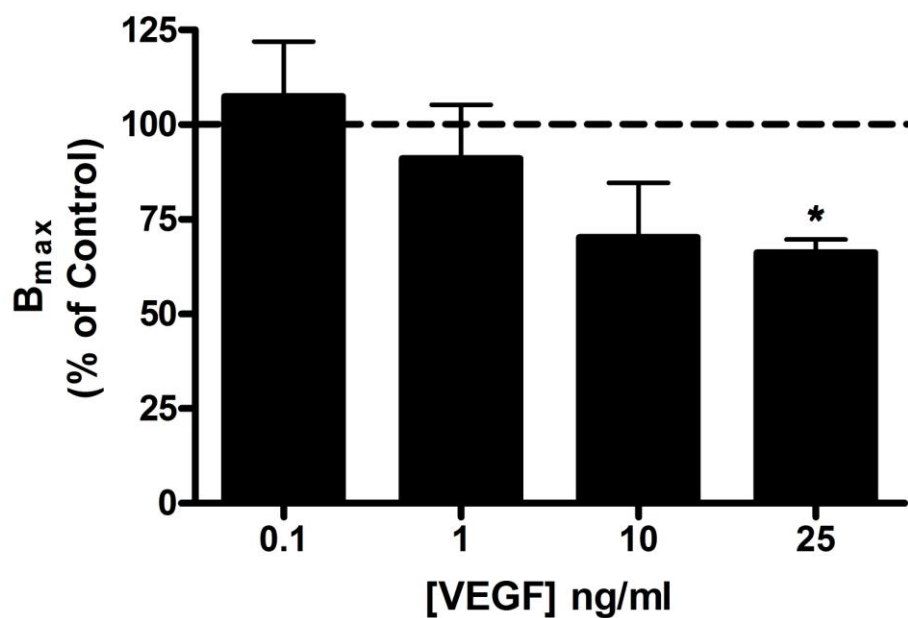
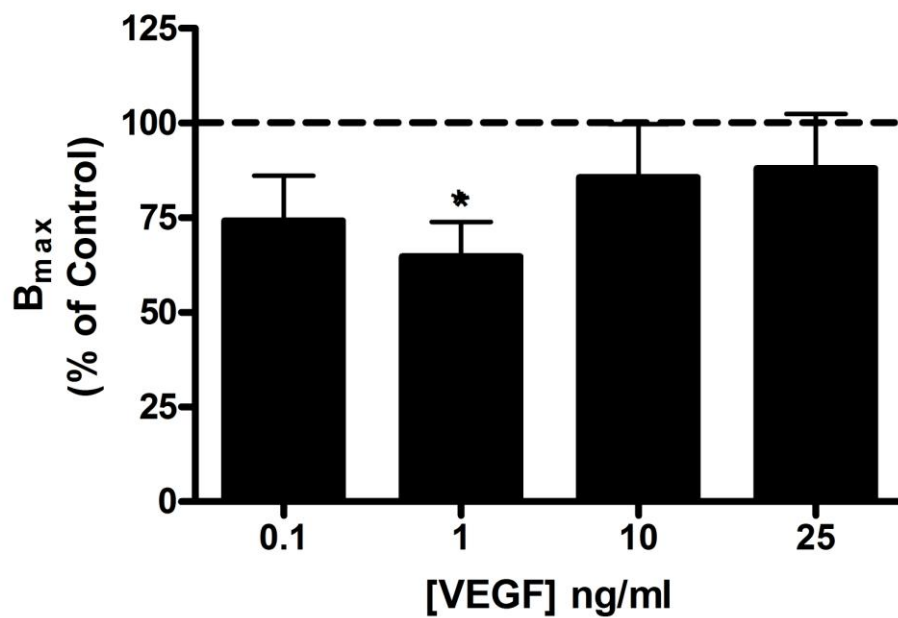
**A****Effect of VEGF on  
ENT1  $B_{max}$  in hMVEC****B****Effect of VEGF on  
ENT1  $B_{max}$  in HMEC-1**



Figure 4.4. The reduction in [<sup>3</sup>H]NBMPR binding was temporally different between MVEC and HMEC-1 cells.

A) Primary MVECs were incubated with 25 ng/ml VEGF for the times indicated and [<sup>3</sup>H]NBMPR binding was measured. A significant decrease to  $69 \pm 9$  % of control was obtained after 4 hr and did not change at 6 or 24 hr of treatment (\* $P < 0.05$  one sample, two-tailed t-test vs 100%,  $n \geq 3$ ).

B) HMEC-1 cells were incubated with 1 ng/ml VEGF for the times indicated and [<sup>3</sup>H]NBMPR binding was measured. A significant decrease to 65 % of control was seen at 24 hr of treatment (\* $P < 0.05$  one sample, two-tailed t-test vs 100%,  $n \geq 3$ ).

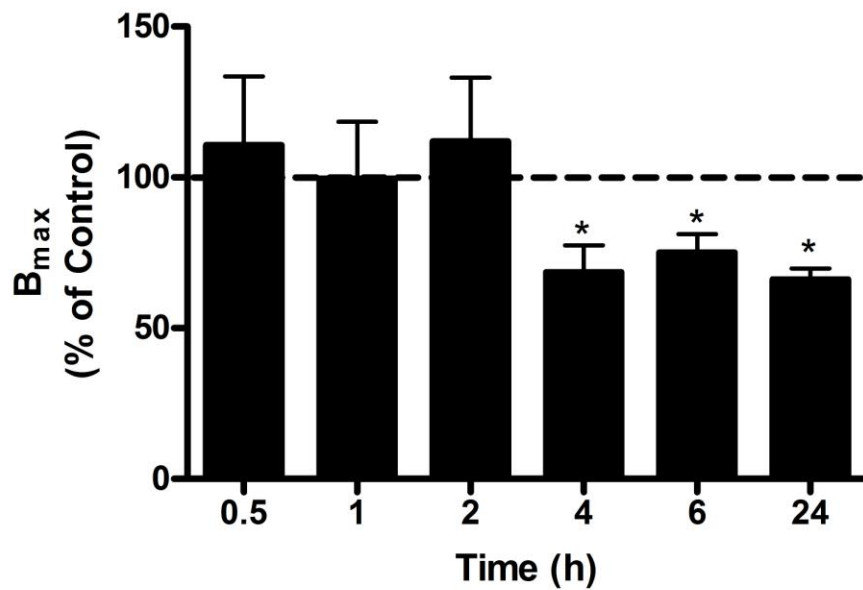
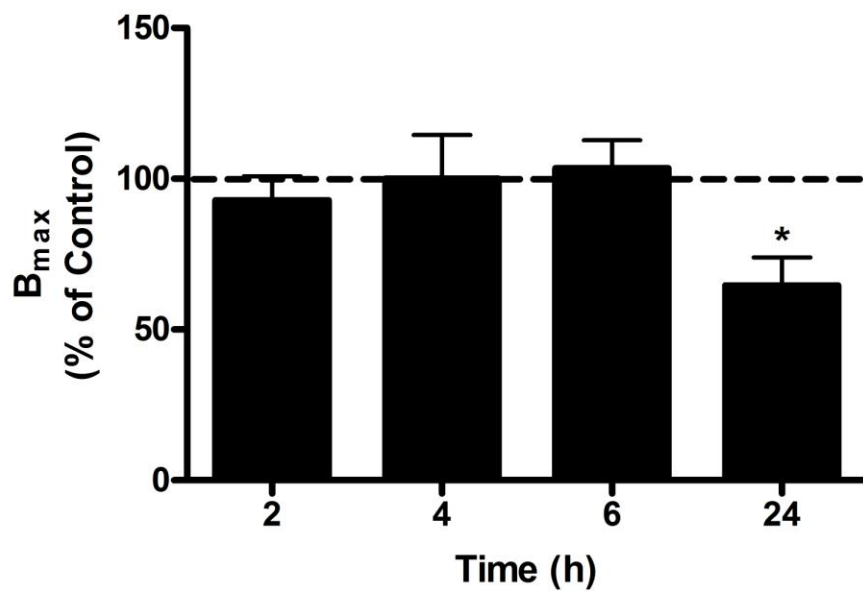
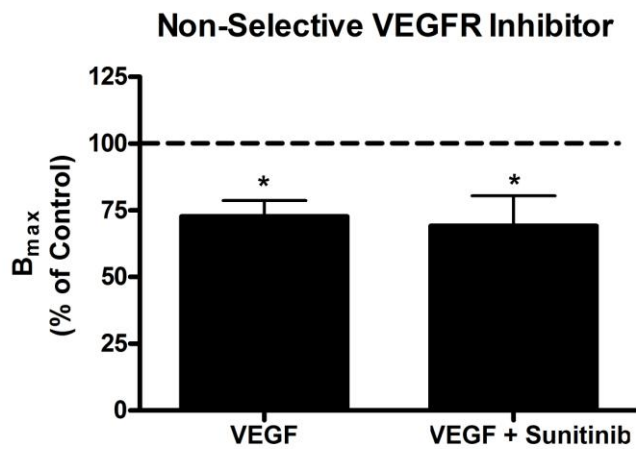
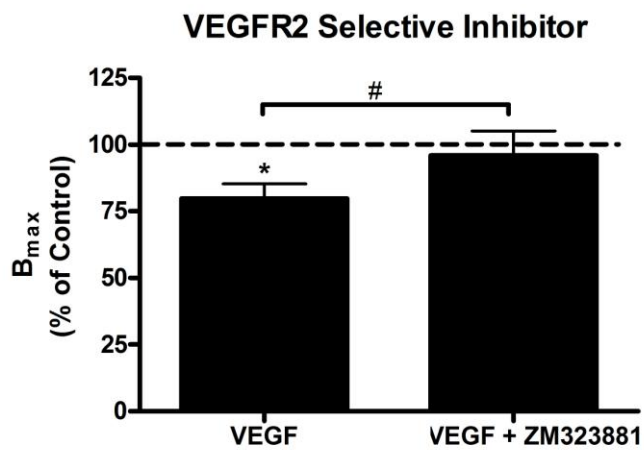
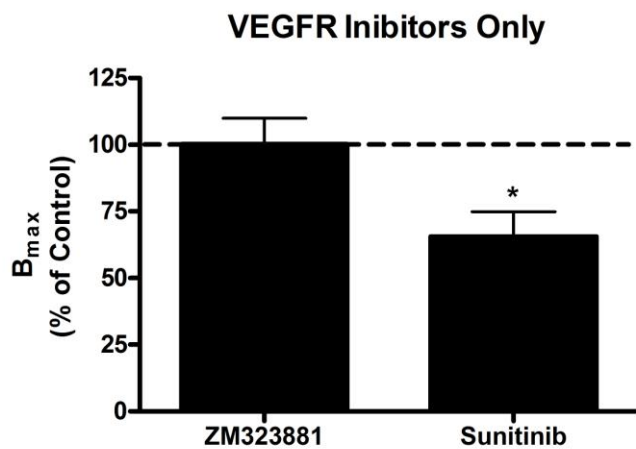
**A****Time Course of 25ng/ml VEGF  
Effects in hMEVC****B****Time Course of 1ng/ml VEGF  
Effects in HMEC-1**



Figure 4.5. VEGF reduction in [<sup>3</sup>H]NBMPR B<sub>max</sub> was mediated by VEGF receptor VEGFR2. Primary MVECs were pretreated with or without 1 μM of the non-selective VEGFR inhibitor sunitinib (A) or the VEGFR2 selective inhibitor ZM323881 (B) for 15 min prior to the addition of 25 ng/ml VEGF in serum free medium. In parallel, cells were treated with inhibitors only (C). Cells were incubated for 24 hr followed by the determination of [<sup>3</sup>H]NBMPR B<sub>max</sub>. Changes in B<sub>max</sub> were compared to serum free control in the absence of VEGF or inhibitors. Data is mean ± SEM of 9 experiments performed in duplicate. \*P<0.05 two-tailed, one sample t-test vs 100%. #P<0.05 two-tailed t-test.



**A****B****C**

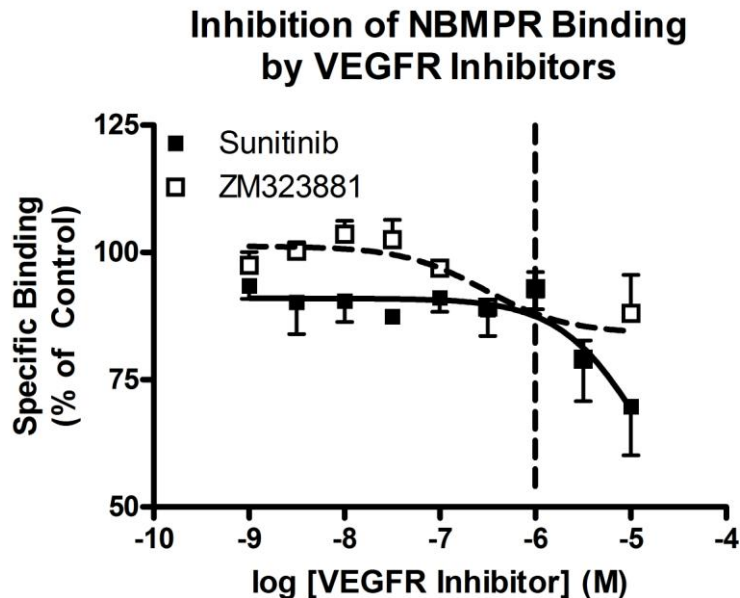


Figure 4.6. Sunitinib inhibition of [ $^3\text{H}$ ]NBMPR binding does not correspond to  $B_{\text{max}}$  decreases.

Primary hMVECs were co-incubated with 0.15 nM [ $^3\text{H}$ ]NBMPR and increasing concentrations of sunitinib (closed squares) or ZM323881 (open squares) for 45 min at room temperature. Specific bound [ $^3\text{H}$ ]NBMPR in the presence of a VEGFR inhibitor was taken as a percentage of specific bound [ $^3\text{H}$ ]NBMPR in the absence of any inhibitor.

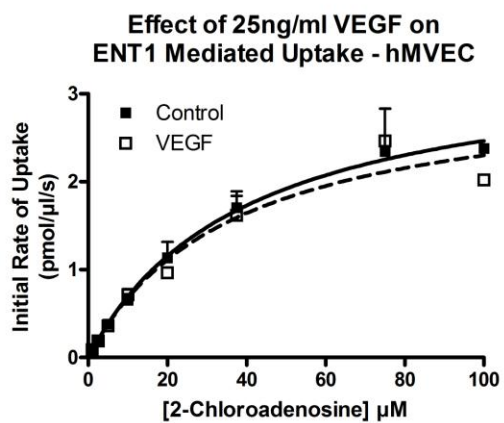
The vertical dotted line represents the concentration of sunitinib and ZM323881 that were used to inhibit the effects of 24 hr treatment with 25 ng/ml VEGF as described by Figure 4.5.



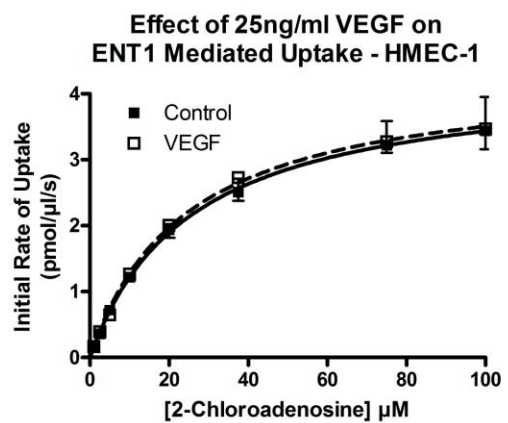
Figure 4.7. Nucleobase transport, but not nucleoside transport, is increased by VEGF.

Primary MVECs and immortalized HMEC-1 cells were treated with 25 ng/ml VEGF for 24 hr. ENT1 mediated transport of 2-[<sup>3</sup>H]chloroadenosine was unchanged in MVECs (A) or HMEC-1 cells (B). The  $V_{max}$  of ENBT1 mediated transport of [<sup>3</sup>H]hypoxanthine was increased in both MVECs (C) and HMEC-1 cells (D) The increase in  $V_{max}$  in HMEC-1 cells reached statistical significance. ( $P < 0.05$  two-tailed t-test,  $n = 4$ ).

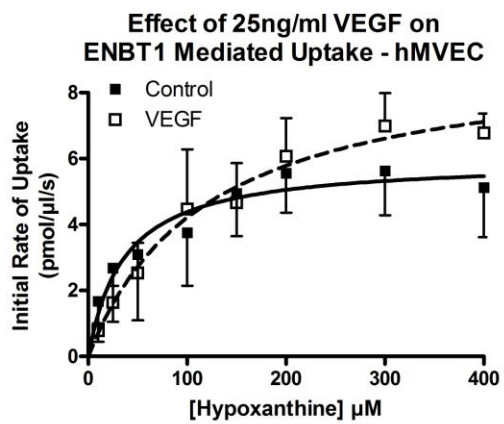
A



B



C



D

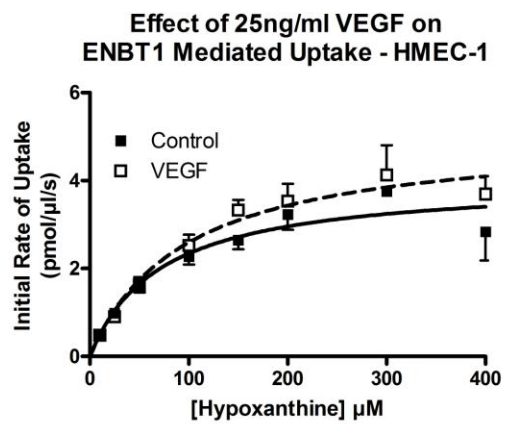




Figure 4.8. Nucleoside and nucleobase transport are differentially regulated by PKC.

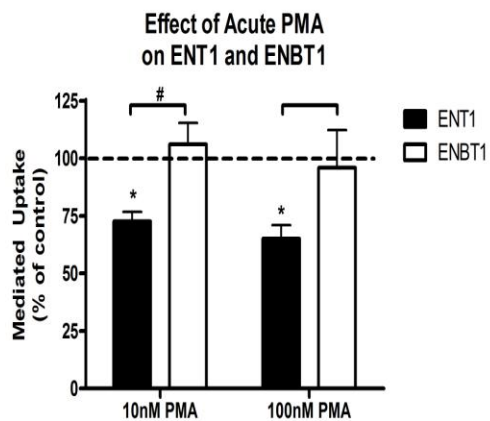
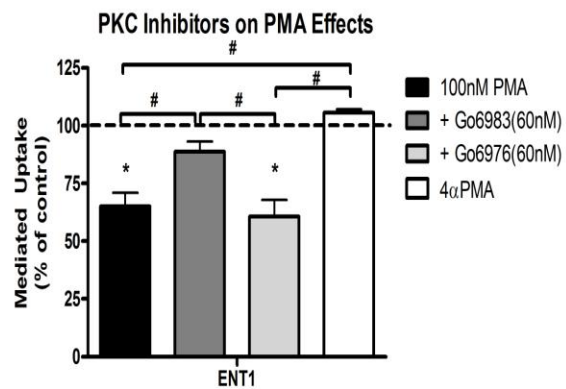
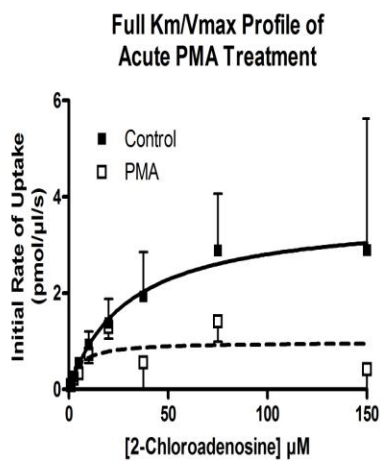
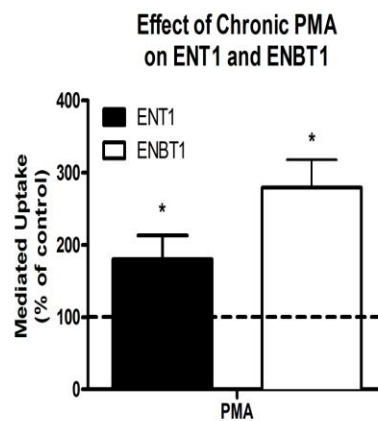
A) Serum starved cells were harvested and treated with PMA for 15 min at 37°C in HBSS prior to analysis of 10  $\mu\text{M}$  2-[ $^3\text{H}$ ]chloroadenosine(ENT1) and 50  $\mu\text{M}$  [ $^3\text{H}$ ]hypoxanthine (ENBT1) uptake. \* $P < 0.05$  two-tailed, one sample t-test vs 100%. # $P < 0.05$  two-tailed t-test. Data are means  $\pm$  SEM of four independent experiments performed in duplicate.

B) Serum starved cells were harvested and pretreated with the broad spectrum PKC inhibitor Go6983 or the PKC- $\alpha/\beta$  selective inhibitor Go6976 for 15 min prior to the addition of PMA. Some cells were treated with 100 nM 4 $\alpha$ -PMA, an inactive analogue of PMA. Mediated uptake of 10 $\mu\text{M}$  2-[ $^3\text{H}$ ]chloroadenosine after 5 sec was then determined. \* $P < 0.05$  two-tailed, one sample t-test vs 100%. # $P < 0.05$  two-tailed t-test.

Data are means  $\pm$  SEM of at least 4 independent experiments performed in duplicate. C)

Serum starved cells were treated with 100 nM PMA (open squares, dotted line) for 15 min prior to 2-[ $^3\text{H}$ ]chloroadenosine uptake. PKC activation resulted in a  $74 \pm 11$  % decrease in  $V_{\text{max}}$  and an  $81 \pm 9$  % decrease in  $K_m$  compared to control ( $P < 0.05$  two-tailed, one sample t-test vs 100%,  $n = 3$ ).

D) Cells were treated with 100 nM PMA for 24 hr in serum free medium. Cells were then harvested and subjected to 10  $\mu\text{M}$  2-[ $^3\text{H}$ ]chloroadenosine uptake (ENT1) and 50  $\mu\text{M}$  [ $^3\text{H}$ ]hypoxanthine uptake (ENBT1). Data are means  $\pm$  SEM of three independent experiments performed in duplicate. \* $P < 0.05$  two-tailed, one sample t-test vs 100%.

**A****B****C****D**



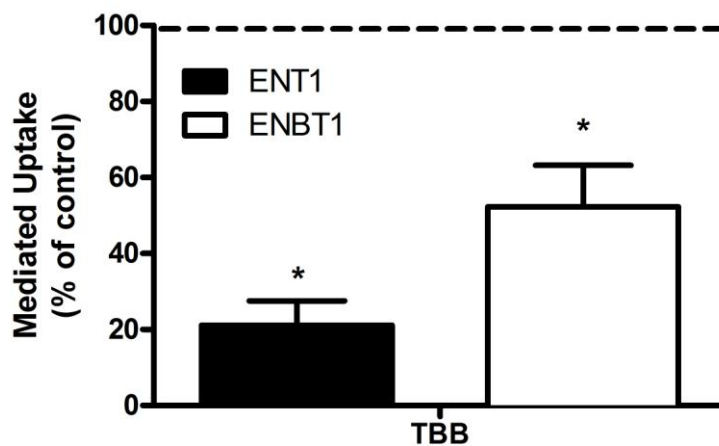


Figure 4.9. Inhibition of CKII decreases nucleoside and nucleobase uptake.

Primary hMVECs were treated with or without 10  $\mu$ M TBB in serum free medium for 24 hrs. Treated cells were then harvested and subjected to uptake assay of 10  $\mu$ M 2- $^3$ H]chloradenosine (ENT1) or 50  $\mu$ M  $^3$ H]hypoxanthine. Data is mean  $\pm$  SEM of three independent experiments performed in duplicate. \*P<0.05 two-tailed, one sample t-test vs 100%.

#### 4.3.4 Regulation by PKA

ENT1 mediated transport of 10  $\mu$ M 2- $^3$ H]chloroadenosine was decreased by both forskolin and sp-cAMP, whereas ENBT1 mediated transport of  $^3$ H]hypoxanthine was unaffected. The adenylate cyclase activator forskolin decreased ENT1 function by  $40 \pm 11$  % of control, and the cAMP analogue sp-cAMP reduced ENT1 by  $56 \pm 13$  % of control (Figure 4.10A)

The PKA inhibitor KT5720 was unable to inhibit the decrease in ENT1 function caused by forskolin or sp-cAMP. In fact, KT5720 caused a concentration-dependent enhancement of the effects of both forskolin and sp-cAMP (Figure 4.10B). When tested against  $^3$ H]NBMMPR binding, KT5720 inhibited specific binding with a  $K_i$  of  $70 \pm 17$  nM (Figure 4.10C).

Both adenosine  $A_{2A}$  and  $A_{2B}$  receptors are known to couple to  $G_s$  proteins which stimulate the production of cAMP through the activation of adenylate cyclase. However, treatment with the  $A_{2A}$  selective agonist CGS21680 or the non selective agonist NECA did not have any effect on ENT1 (Figure 4.11)

#### 4.3.5 Effect of ROS on nucleoside and nucleobase transporter function.

HMEC-1 cells were treated with the intracellular superoxide generator menadione as described in section 4.2.5. Both ENT1 and ENBT1  $V_{max}$  was significantly reduced by menadione to  $46 \pm 3$  and  $28 \pm 9$  percent of control respectively. The superoxide dismutase mimetic MnTMPyP could not prevent the reduction in ENT1  $V_{max}$ , however MnTMPyP significantly diminished the effect of menadione on the reduced  $V_{max}$  of  $^3$ H]hypoxanthine uptake by ENBT1 (Figure 4.12).

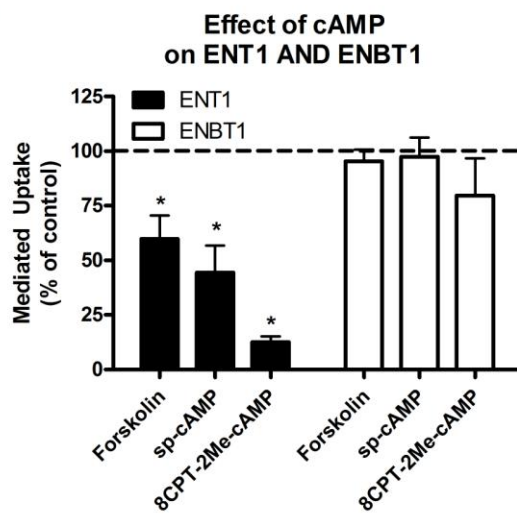
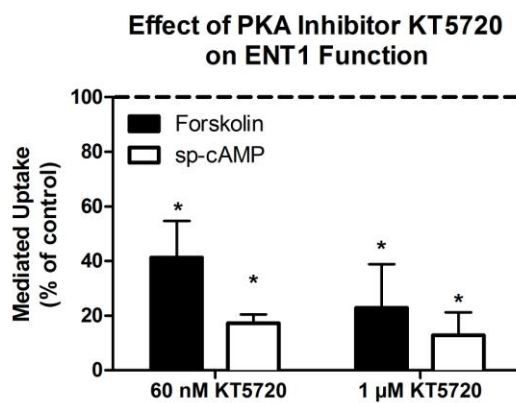
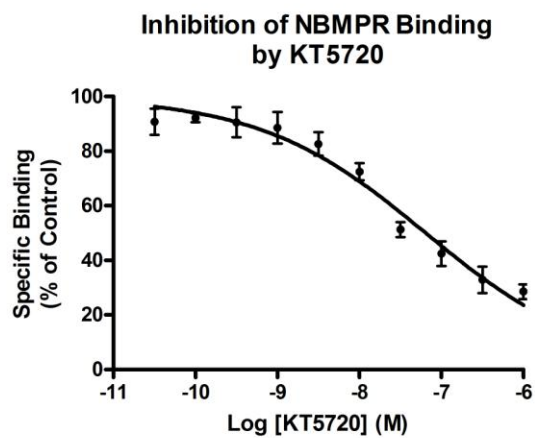


Figure 4.10. Effect of cAMP on nucleoside and nucleobase transporter function.

A) Cells were serum starved for 24 hrs, harvested and treated with 100  $\mu$ M forskolin, 1  $\mu$ M sp-cAMP, or 10 mM 8CPT-2Me-cAMP for 15 min at 37°C in HBSS followed by analysis uptake of 10  $\mu$ M 2-[ $^3$ H]chloroadenosine(ENT1) and 50  $\mu$ M [ $^3$ H]hypoxanthine (ENBT1). Data are mean  $\pm$  SEM of at least 3 experiments performed in duplicate. \*P<0.05 two-tailed, one sample t-test vs 100%, n  $\geq$  3. #P<0.05 two-tailed t-test compared to ENT1.

B) Cells were pretreated with the PKA inhibitor KT5720 for 15 min at 37°C in HBSS prior to the addition of 100  $\mu$ M forskolin (solid bars) or 1  $\mu$ M sp-cAMP (open bars) for an additional 15 min at 37°C. Data are mean  $\pm$  SEM of three experiments performed in duplicate. \*P<0.05 two-tailed, one sample t-test vs 100%.

C) Primary human MVECs were harvested and incubated with 0.15 nM [ $^3$ H]NBMPPR and increasing concentrations of KT5720 for 45 min at room temperature. Using the Cheng-Prusoff equation, KT5720 was found to have a  $K_i$  of  $70 \pm 17$  nM. Data are means  $\pm$  SEM of three independent experiments performed in duplicate.

**A****B****C**

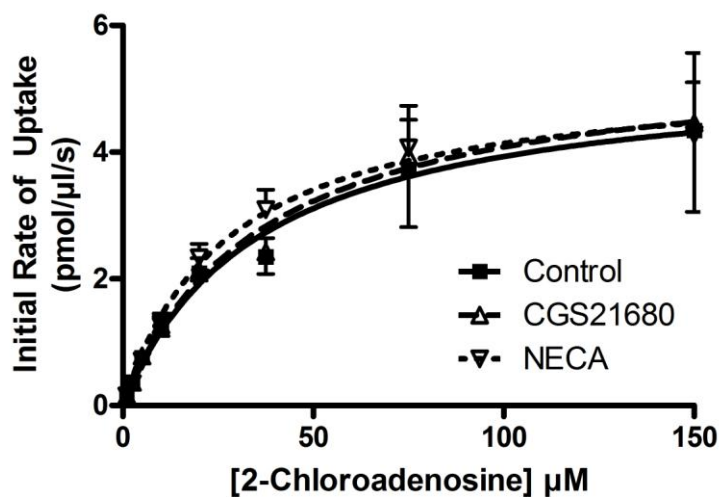


Figure 4.11. Adenosine A<sub>2</sub> receptor agonism does not alter ENT1 function.

Primary MEVCs were treated with 300 nM of the A<sub>2A</sub> selective agonist CGS21680 or 10 μM of the non-selective A<sub>2</sub> agonist NECA for 2 hrs in HBSS at 37°C. Cells were then harvested and subjected to analysis of 2-[<sup>3</sup>H]chloroadenosine uptake. Data are mean ± SEM of six independent experiments.



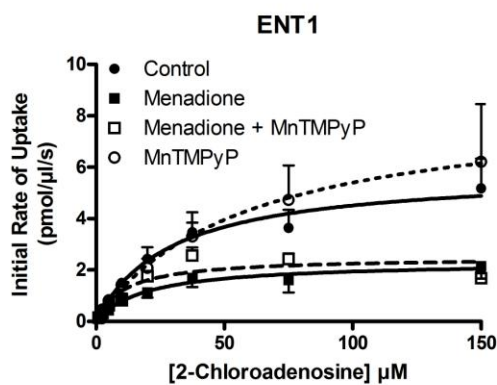
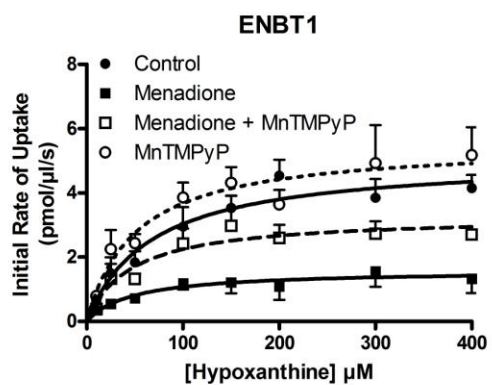
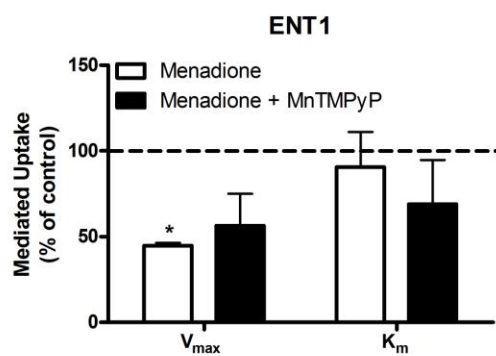
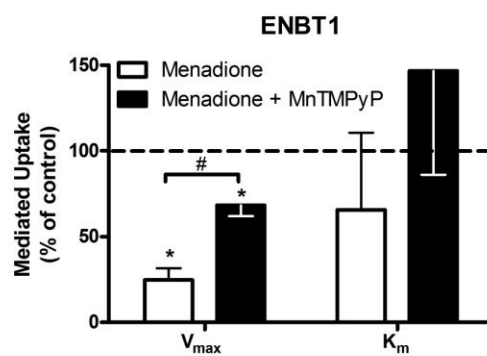
Figure 4.12. Intracellular superoxide production by menadione reduced ENBT1 but not ENT1 function.

HMEC-1 cells were treated with 100  $\mu$ M menadione in HBSS at 37°C for 30 min  $\pm$  100  $\mu$ M MnTMPyP. A) The  $V_{\max}$  of 2-[ $^3$ H]chloroadenosine uptake by ENT1 was significantly reduced to  $45 \pm 2$  % of control. MnTMPyP had no effect on menadione treated cells or on its own.

B) The  $V_{\max}$  of [ $^3$ H]hypoxanthine uptake by ENBT1 was significantly reduced to  $25 \pm 7$  % of control. Co-treatment with MnTMPyP was able to limit the reduction in  $V_{\max}$  to  $68 \pm 6$  % of control. As with ENT1, MnTMPyP had no effect on ENBT1 transport alone.

Panels C) and D) show the effects of menadione  $\pm$  MnTMPyP on  $V_{\max}$  and  $K_m$  parameters as percent of control. Effects of MnTMPyP alone are excluded for clarity. \* $P < 0.05$ , two-tailed one sample t-test vs 100%,  $n \geq 3$ . # $P < 0.05$  one way ANOVA with a Tukey-Kramer post hoc test,  $n \geq 4$ .



**A****B****C****D**

#### 4.3.6. Simulated Ischemia

Treatment with the HIF-1 $\alpha$  stabilizer CoCl<sub>2</sub> had no effect on ENT1 or ENBT1 in primary hMVECs (Figure 4.13 A-B). The mineral oil overlay to simulate ischemia had no significant effect on 2-[<sup>3</sup>H]chloroadenosine transport with V<sub>max</sub> of 2.0  $\pm$  0.4 pmol/ $\mu$ l/s and 2.0  $\pm$  0.2 pmol/ $\mu$ l/s for control and ischemia respectively. However, mineral oil overlay dramatically reduced [<sup>3</sup>H]hypoxanthine uptake by ENBT1 to levels that resembled non-mediated uptake (Figure 4.13 C-D).

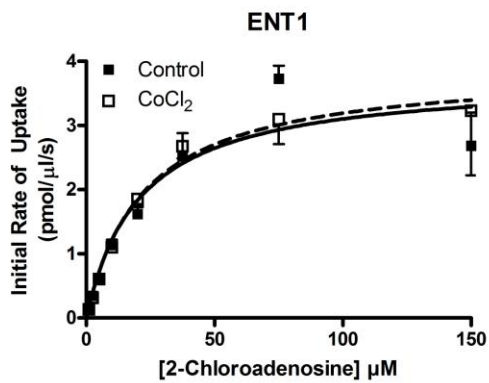
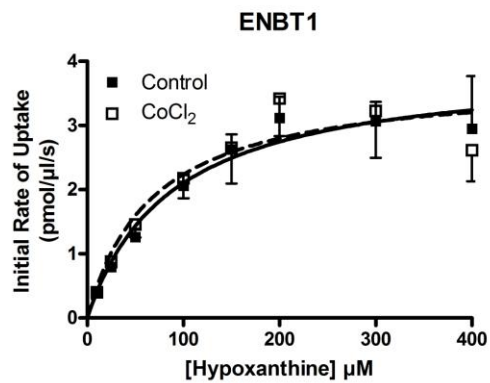
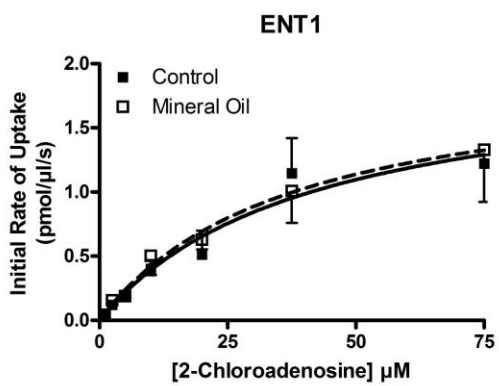
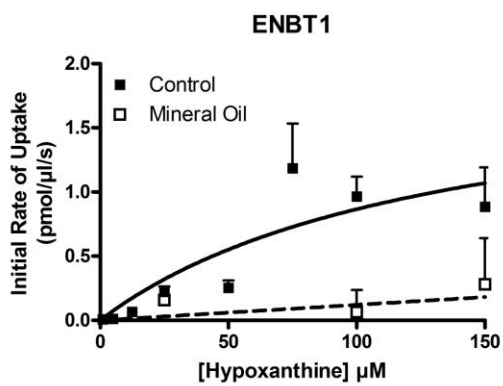


Figure 4.13 Effects of hypoxia and ischemia on nucleoside and nucleobase transport.

A & B) Primary MVECs were treated with 100  $\mu\text{M}$   $\text{CoCl}_2$  for 2 hrs at 37°C in complete medium. 2- $^3\text{H}$ chloroadenosine (A) and  $^3\text{H}$ hypoxanthine (B) uptake assays were performed. Data are mean  $\pm$  SEM of four experiments.

C&D) Cells were subjected to mineral oil overlay as described in Section 4.2.3.2.

2- $^3\text{H}$ chloroadenosine uptake by ENT1 was not significantly affected (C) however,  $^3\text{H}$ hypoxanthine uptake by ENBT1 (D) was abolished following 2 hrs of mineral-oil overlay ischemia. Data are mean  $\pm$  SEM of four experiments.

**A****B****C****D**

## 4.4 Discussion

This chapter addressed the regulation of purine transporters in the context of hypoxia/ischemia. This included the generation and effects of ROS as well as physiological molecules, receptors, and kinases that have been shown to be important in both the normal vasculature, as well as during times of vascular stress.

### 4.4.1 Regulation of Transport by VEGF

This is the first study to demonstrate that VEGF is a regulator of purine transporters in microvascular endothelial cells. VEGF acts through a family of transmembrane receptor tyrosine kinases (RTKs). A recent study by Vega et al., demonstrated that transforming growth factor beta 1, another molecule that signals through a family of RTKs, limits the expression of ENT1 in human umbilical vein endothelial cells (44). While the model is different, the overlap in signaling pathways between TGF- $\beta$  and VEGF receptors supports our finding that VEGF has the potential to regulate ENT1. *In silico* analysis of the ENT1 protein revealed a potential RTK phosphorylation consensus sequence at Tyr-2 of intracellular N-terminal, suggesting a possible direct link between RTK activation and ENT1 post-translational regulation.

It is widely accepted that changes in [ $^3\text{H}$ ]NBMPR binding are mirrored by similar changes in substrate transport, i.e. a decrease in [ $^3\text{H}$ ]NBMPR binding would result in decreased transport. However, in the current study, we found that there was no decrease in nucleoside transport despite a decrease in [ $^3\text{H}$ ]NBMPR binding of about 35%. The decrease in [ $^3\text{H}$ ]NBMPR binding could be a result of a conformational change elicited by phosphorylation of the transporter by VEGFR2 that alters the [ $^3\text{H}$ ]NBMPR binding site

that does not impact the substrate translocation site. The physiological relevance of this effect remains to be elucidated.

We observed a difference between the primary hMVECs and the immortalized HMEC-1 cells in the response to VEGF-165 treatment. This was despite the fact that HMEC-1 cells have a comparable number of ENT1 sites per cell to hMVECs and show a complete lack of functional ENT2 (5). The HMEC-1 cell line is a well established endothelial cell model created from human dermal microvascular endothelial cells that were transfected with the simian virus 40 large T antigen (1). This cell line is reported to maintain many of the characteristics of the original microvascular endothelial cells, and is capable of producing VEGF (17).

The observation that the nucleoside transporter ENT1, as measured by [<sup>3</sup>H]NBMPR binding, is reduced by VEGF while cell numbers increased is counter-intuitive. In fact, ENT1 expression has been shown to increase during cell proliferation (7). This finding suggests that the VEGF cell proliferation and ENT1 regulation pathways are divergent. This also suggests, therefore, that ENT1 regulation by VEGF signaling is of greater importance than regulation via normal cell cycle progression. The VEGFR2 selective antagonist ZM323881 was able to prevent a VEGF-mediated decrease in ENT1, suggesting that it is the VEGFR2 receptor responsible for this effect. These data are consistent with VEGF pharmacology as the VEGF-165 used in this study is the most common form of the protein produced and the VEGFR2 receptor is believed to be the receptor subtype that mediates the biological effect of VEGF-165 (49). However, VEGFR2 may not be the only RTK capable of regulating ENT1 expression. The drug

sunitinib is capable of inhibiting a wide variety of RTKs including platelet derived growth factor receptor (PDGFR), stem cell grown factor receptor (KIT), and fms-like tyrosine kinase receptor-3 (FLT3) (30; 31). Given that inhibition [<sup>3</sup>H]NBMPR binding and reduction of [<sup>3</sup>H]NBMPR binding sites after 24 hr treatment of sunitinib do not co-relate (Figures 4.5,4.6), it is possible that the sunitinib effect is receptor mediated.

When viewed in a physiological context, VEGF release and signaling is most likely to occur during periods of hypoxia/ischemia. During hypoxia, adenosine levels increase as a result of increased ATP breakdown. Adenosine is a known stimulator of VEGF production (11). Additionally, the VEGF gene contains a hypoxia response element, and therefore is directly regulated by oxygen tension (19). Thus, a VEGF signal in endothelial cells causing a decrease in ENT1 protein may be acting to potentiate the protective actions of adenosine by reducing the amount taken up into the endothelium. Reduced intracellular adenosine accumulation in the endothelium could also be a protective mechanism against ischemia-reperfusion injury. Adenosine metabolism to hypoxanthine provides substrate for xanthine oxidase to produce reactive oxygen species upon re-oxygenation. Less adenosine in the cell means less hypoxanthine and therefore less ROS. The other main observation of this study is the VEGF mediated increase in the function of the hypoxanthine transporter ENBT1 in HMEC-1 cells, with a trending towards a similar increase in MVECs. This increase would compliment an endothelial protective function for VEGF, as more ENBT1 would result in enhanced removal of hypoxanthine from the cells and thus another way to limit ROS production.



There is also potential application of the presented results to cancer treatment. It is well known that solid tumours are hypoxic and rely on VEGF to generate new blood vessels to supply the tumour with blood (22; 26; 48). Given that VEGF increases ENBT1 function, therapies involving nucleobase analogues that are potential substrates for ENBT1, like 6-mercaptopurine or 6-thioguanine (5), may more effectively cross the endothelial barrier and reach the tumour cells.

#### *4.4.2 Regulation by Protein Kinase C*

Regulation of ENT1 by PKC is a widely studied phenomenon. However, the effect on ENT1 function, and by which PKC isoform, is still disputed. In human MCF7 and HeLa cancer cell lines, short term PMA treatment (10 min) caused an increase in uptake that was mediated through PKC- $\delta$  or - $\epsilon$ , whereas chronic treatment (24 hr) caused a decrease in uptake (12). In mouse HL-1 cardiomyocytes acute PMA (10 min) also caused an increase in ENT1 mediated transport (10). However, in human umbilical vein endothelial cells, PMA treatment (30 min) resulted in decreased ENT1 activity (34). In rat cardiac fibroblasts, PKC- $\zeta$  has been implicated in the down-regulation of ENT1 in response to elevated glucose (21), and PKC- $\epsilon$  down-regulation by chronic hypoxia (18 hr) has also been linked to decreased ENT1 activity (9). In Figure 4.8, activation and inhibition of PKC with PMA and Go6983, respectively, supports a role for PKC- $\delta/\epsilon$ , however the effects on ENT1 are the opposite of that observed in MCF7 and HeLa cells as well as the mouse HL-1 cardiomyocyte cell line.

The role of PKC in the regulation of ENBT1 is much more complex. Acute PMA treatment of serum starved cells had no effect on ENBT1 function; however chronic PMA exposure

resulted in a significant increase in the uptake of 50  $\mu\text{M}$  hypoxanthine. These data suggest that PKC has no direct effect on ENBT1 function, rather that ENBT1 is regulated by another protein that is the target of PKC phosphorylation. Alternatively, ENBT1 may be constitutively phosphorylated and the decrease in PKC activity caused by chronic PMA treatment leads to a decreased ENBT1 phosphorylation state. Recent evidence in human umbilical vein endothelial cells showed that PKC inhibition led to increased nitric oxide (NO) production (40), perhaps a similar mechanism occurs in MVECs and is responsible for the [ $^3\text{H}$ ]hypoxanthine uptake increase. However, since the uptake assay was performed in ATP-replete conditions to allow cellular regulation events to function properly, the increase in [ $^3\text{H}$ ]hypoxanthine uptake could be an artifact of altered metabolism. That is, with ATP present, nucleobase scavaging enzymes, such as hypoxanthine-guanine phosphoribotransferase are capable of producing [ $^3\text{H}$ ]nucleotides from [ $^3\text{H}$ ]hypoxanthine, trapping the [ $^3\text{H}$ ]label inside the cell, and thus artificially increasing the apparent rate of [ $^3\text{H}$ ]hypoxanthine uptake.

#### *4.4.3 Regulation by CKII*

In agreement with the study by Bone *et al.*,(6) CKII inhibition by TBB resulted in decreased ENT1 transport activity. However, this was not achieved under the same conditions as that study, instead, the decrease was observed after 24 hr in serum free medium, compared to 48 hr in complete medium as described by Bone (6). Differences in cell model and culture medium could contribute to the temporal differences observed between the two studies. The cells used by Bone were nucleoside transporter deficient

cells stably expressing recombinant human ENT1 (6) compared to the primary MVECs used presently.

#### 4.4.4 Regulation by Protein Kinase A

The *in silico* analysis of ENT1 predicted potential PKA phosphorylation sites (Figure 4.1), therefore the effects of PKA activators were investigated on nucleoside and nucleobase transport. Forskolin, an adenylate cyclase activator and therefore an indirect PKA activator, and the cAMP analogue sp-cAMP, a direct PKA activator, both led to a decrease in ENT1 mediated uptake but had no effect on ENBT1 mediated nucleobase uptake. The decrease in ENT1 mediated uptake is in agreement with a study by Sen *et al.*, who showed that forskolin was able to decrease ENT1 uptake by 30% in mouse Neuro-2a cells (39). It has also been shown that active PKA is required for ethanol mediated inhibition of adenosine uptake in neuronal cells (13). However a difficulty arose when trying to confirm PKA as the protein responsible for the ENT1 down-regulation. The cAMP analogue 8-CPT-2Me-cAMP, a direct activator of another cAMP binding protein Epac-1, is a direct inhibitor of ENT1 (46). Additionally, the commonly used PKA inhibitor H89 is a direct ENT1 inhibitor as well (23). Thus a different PKA inhibitor, KT5720 was used, however it also turned out to be a direct, high affinity inhibitor of ENT1 as shown by the ability to inhibit [<sup>3</sup>H]NBMPR binding with a K<sub>i</sub> of 70 nM.

Adenosine A<sub>2</sub> receptors stimulate adenylate cyclase activity and thus activate PKA when presented with an agonist. Therefore, it was expected that the adenosine A<sub>2A</sub> agonist CGS21680 or the non-selective A<sub>2</sub> agonist NECA would produce the same effect as

forskolin and sp-cAMP. However, this was not the case as adenosine receptor agonism had no effect on 2-[<sup>3</sup>H]chloroadenosine uptake (Figure 4.11). Primary human MVECs are expected to express the adenosine A<sub>2A</sub> receptor (38) therefore the lack of response could be a lack of sufficient cAMP production to effectively activate PKA. Another possibility could be that cAMP, forskolin, or sp-cAMP directly interact with ENT1 to prevent [<sup>3</sup>H]NBMPR binding. The presence of potential PKA phosphorylation sites on ENT1 suggests that PKA is responsible for the decrease in ENT1 function, but without a PKA inhibitor that does not directly interfere with ENT1 function this phenomenon could not be properly addressed.

#### *4.4.5 Effects of ROS on Purine Transporters*

The superoxide generator menadione had differential effects on ENT1 and ENBT1 transport of nucleosides and nucleobases, respectively. Menadione reduced the V<sub>max</sub> of both ENT1 and ENBT1 mediated uptake (Figure 4.12). The superoxide dismutase mimetic, MnTMPyP reduced the effect of menadione on ENBT1 uptake but not ENT1. Therefore, ENBT1 transport function is sensitive to the presence of superoxide, and thus most likely selectively oxidized on a residue important to transport function. Oxidation of sulphhydryl groups, especially those found on cysteine residues, is typically the cause of modifications that lead to protein dysfunction (2; 8; 36). Modification of cysteine residues has been shown to inhibit function of a number of different transporter types (24; 43; 45).

Unfortunately, it cannot be determined using menadione if ENT1 is also sensitive to superoxide modification. Since MnTMPyP could not reverse the effects of menadione,

direct inhibition of ENT1 by menadione is the probable outcome. Direct inhibition of ENT1 by menadione is supported by the fact that antibiotics containing quinone, the same class of chemical as menadione, reduced nucleoside uptake via ENT1 (32).

#### *4.4.6 Effects of Simulated Hypoxia and Ischemia on Purine Transporters*

CoCl<sub>2</sub> stabilizes HIF-1 $\alpha$  in the presence of normal oxygen concentrations, thus making it an easier tool to study the impact of HIF-1 $\alpha$  (and by extension hypoxia) on your gene of interest (35). The mineral-oil overlay model has been shown to reduce oxygen concentrations to which the cells are exposed (28; 29). The lack of effect of CoCl<sub>2</sub> after 2 hr indicates that stabilization of HIF-1 $\alpha$  does not impact ENT1 or ENBT1 in the short term (Figure 4.13). It was previously shown that ENT1 responds to actual hypoxia after 8 hr in HUVEC cells (15), and thus these data are not totally unexpected. The loss of ENBT1 function, with no effect on ENT1 after 2 hr of ischemia, suggests that another mechanism other than low oxygen is mediating this effect. *In vivo*, ischemia-reperfusion is known to produce ROS (20; 37; 47), and may be produced in culture leading to oxidation of ENBT1. However, another possibility could be an increase in intracellular hypoxanthine, as a result of increase adenosine metabolism, that establishes a concentration gradient favouring efflux. However, in this model of ischemia, it could be argued that the resuspension of cells in buffer and washing away of the mineral oil is the reperfusion step. This would allow both efflux and metabolism of any endogenous hypoxanthine, generating superoxide and establishing the proper conditions for uptake. Thus, taken with the data generated with menadione treatment, these data suggest that

ENBT1 is indeed sensitive to the presence of ROS, to the point of complete loss of function.

#### *4.4.7 Conclusions*

Primary human MVECs were used to study the roles of VEGF, intracellular kinases, adenosine receptors, reactive oxygen species, and ischemia on purine transport. These studies were successful in identifying VEGF as a novel regulator of purine transporters through VEGFR2. Additionally, intracellular kinases PKC and CKII are capable of altering transport function. The intracellular kinase PKA may also play a role in the regulation of ENT1, however more work is needed to confirm a PKA interaction and rule out a direct cAMP interaction with the transporter.

These data suggest that the microvascular purine transporters ENT1 and ENBT1 may be altered in the pathophysiology of hypoxia/ischemia and oxidative stress. Intracellular superoxide, generated by menadione, produced dramatic decreases in transporter  $V_{max}$ . ROS may also be a contributing factor to the down-regulation of ENBT1 during ischemia, with ENT1 being less sensitive to oxidative insult. Further ROS dose response studies are needed to clarify the mechanism of regulation.

These alterations may contribute to endothelial dysfunction, especially the down-regulation of ENBT1, which would trap the superoxide producing hypoxanthine inside endothelial cells. Fortunately, these transporters are also regulated by proteins that are targets of pharmacological manipulation and thus interventions could be devised to prevent or reduce the impact they have on endothelial cell oxidative stress.

#### 4.5 References

1. **Ades EW, Candal FJ, Swerlick RA, George VG, Summers S, Bosse DC and Lawley TJ.** HMEC-1: establishment of an immortalized human microvascular endothelial cell line. *J Invest Dermatol* 99: 683-690, 1992.
2. **Avery SV.** Molecular targets of oxidative stress. *Biochem J* 434: 201-210, 2011.
3. **Blom N, Gammeltoft S and Brunak S.** Sequence and structure-based prediction of eukaryotic protein phosphorylation sites. *J Mol Biol* 294: 1351-1362, 1999.
4. **Bone DB and Hammond JR.** Nucleoside and nucleobase transporters of primary human cardiac microvascular endothelial cells: characterization of a novel nucleobase transporter. *Am J Physiol Heart Circ Physiol* 293: H3325-H3332, 2007.
5. **Bone DB and Hammond JR.** Nucleoside and nucleobase transporters of primary human cardiac microvascular endothelial cells: characterization of a novel nucleobase transporter. *Am J Physiol Heart Circ Physiol* 293: H3325-H3332, 2007.
6. **Bone DB, Robillard KR, Stolk M and Hammond JR.** Differential regulation of mouse equilibrative nucleoside transporter 1 (mENT1) splice variants by protein kinase CK2. *Mol Membr Biol* 24: 294-303, 2007.
7. **Cass CE, Dahlig E, Lau EY, Lynch TP and Paterson AR.** Fluctuations in nucleoside uptake and binding of the inhibitor of nucleoside transport, nitrobenzylthioinosine, during the replication cycle of HeLa cells. *Cancer Res* 39: 1245-1252, 1979.
8. **Cecarini V, Gee J, Fioretti E, Amici M, Angeletti M, Eleuteri AM and Keller JN.** Protein oxidation and cellular homeostasis: Emphasis on metabolism. *Biochim Biophys Acta* 1773: 93-104, 2007.
9. **Chaudary N, Naydenova Z, Shuralyova I and Coe IR.** Hypoxia regulates the adenosine transporter, mENT1, in the murine cardiomyocyte cell line, HL-1. *Cardiovasc Res* 61: 780-788, 2004.
10. **Chaudary N, Naydenova Z, Shuralyova I and Coe IR.** The adenosine transporter, mENT1, is a target for adenosine receptor signaling and protein kinase Cepsilon in

hypoxic and pharmacological preconditioning in the mouse cardiomyocyte cell line, HL-1. *J Pharmacol Exp Ther* 310: 1190-1198, 2004.

11. **Clark AN, Youkey R, Liu X, Jia L, Blatt R, Day YJ, Sullivan GW, Linden J and Tucker AL.** A1 adenosine receptor activation promotes angiogenesis and release of VEGF from monocytes. *Circ Res* 101: 1130-1138, 2007.
12. **Coe I, Zhang Y, McKenzie T and Naydenova Z.** PKC regulation of the human equilibrative nucleoside transporter, hENT1. *FEBS Lett* 517: 201-205, 2002.
13. **Coe IR, Dohrman DP, Constantinescu A, Diamond I and Gordon AS.** Activation of cyclic AMP-dependent protein kinase reverses tolerance of a nucleoside transporter to ethanol. *J Pharmacol Exp Ther* 276: 365-369, 1996.
14. **Coe IR, Yao L, Diamond I and Gordon AS.** The role of protein kinase C in cellular tolerance to ethanol. *J Biol Chem* 271: 29468-29472, 1996.
15. **Eltzschig HK, Abdulla P, Hoffman E, Hamilton KE, Daniels D, Schonfeld C, Loffler M, Reyes G, Duszenko M, Karhausen J, Robinson A, Westerman KA, Coe IR and Colgan SP.** HIF-1-dependent repression of equilibrative nucleoside transporter (ENT) in hypoxia. *J Exp Med* 202: 1493-1505, 2005.
16. **Escudero C, Casanello P and Sobrevia L.** Human equilibrative nucleoside transporters 1 and 2 may be differentially modulated by A2B adenosine receptors in placenta microvascular endothelial cells from pre-eclampsia. *Placenta* 29: 816-825, 2008.
17. **Feoktistov I, Goldstein AE, Ryzhov S, Zeng D, Belardinelli L, Voyno-Yasenetskaya T and Biaggioni I.** Differential expression of adenosine receptors in human endothelial cells: role of A2B receptors in angiogenic factor regulation. *Circ Res* 90: 531-538, 2002.
18. **Fernandez CP, Galmarini CM, Canones C, Gamberale R, Saenz D, Avalos JS, Chianelli M, Rosenstein R and Giordano M.** Modulation of the human equilibrative nucleoside transporter1 (hENT1) activity by IL-4 and PMA in B cells from chronic lymphocytic leukemia. *Biochem Pharmacol* 75: 857-865, 2008.



19. **Forsythe JA, Jiang BH, Iyer NV, Agani F, Leung SW, Koos RD and Semenza GL.** Activation of vascular endothelial growth factor gene transcription by hypoxia-inducible factor 1. *Mol Cell Biol* 16: 4604-4613, 1996.
20. **Granger DN.** Ischemia-reperfusion: mechanisms of microvascular dysfunction and the influence of risk factors for cardiovascular disease. *Microcirculation* 6: 167-178, 1999.
21. **Grden M, Podgorska M, Kocbuch K, Rzepko R, Szutowicz A and Pawelczyk T.** High glucose suppresses expression of equilibrative nucleoside transporter 1 (ENT1) in rat cardiac fibroblasts through a mechanism dependent on PKC-zeta and MAP kinases. *J Cell Physiol* 215: 151-160, 2008.
22. **Guo S, Colbert LS, Fuller M, Zhang Y and Gonzalez-Perez RR.** Vascular endothelial growth factor receptor-2 in breast cancer. *Biochim Biophys Acta* 1806: 108-121, 2010.
23. **Huang M, Wang Y, Cogut SB, Mitchell BS and Graves LM.** Inhibition of nucleoside transport by protein kinase inhibitors. *J Pharmacol Exp Ther* 304: 753-760, 2003.
24. **Jimenez-Vidal M, Gasol E, Zorzano A, Nunes V, Palacin M and Chillaron J.** Thiol modification of cysteine 327 in the eighth transmembrane domain of the light subunit xCT of the heteromeric cystine/glutamate antiporter suggests close proximity to the substrate binding site/permeation pathway. *J Biol Chem* %19;279: 11214-11221, 2004.
25. **Kobayashi S, Zimmermann H and Millhorn DE.** Chronic hypoxia enhances adenosine release in rat PC12 cells by altering adenosine metabolism and membrane transport. *J Neurochem* 74: 621-632, 2000.
26. **Korpanty G, Smyth E, Sullivan LA, Brekken RA and Carney DN.** Antiangiogenic therapy in lung cancer: focus on vascular endothelial growth factor pathway. *Exp Biol Med (Maywood )* 235: 3-9, 2010.
27. **Leung GP, Tse CM and Man RY.** Characterization of adenosine transport in H9c2 cardiomyoblasts. *Int J Cardiol* %20;116: 186-193, 2007.

28. **Meldrum KK, Hile K, Meldrum DR, Crone JA, Gearhart JP and Burnett AL.** Simulated ischemia induces renal tubular cell apoptosis through a nuclear factor-kappaB dependent mechanism. *J Urol* 168: 248-252, 2002.
29. **Meldrum KK, Meldrum DR, Hile KL, Burnett AL and Harken AH.** A novel model of ischemia in renal tubular cells which closely parallels in vivo injury. *J Surg Res* 99: 288-293, 2001.
30. **Mendel DB, Laird AD, Xin X, Louie SG, Christensen JG, Li G, Schreck RE, Abrams TJ, Ngai TJ, Lee LB, Murray LJ, Carver J, Chan E, Moss KG, Haznedar JO, Sukbuntherng J, Blake RA, Sun L, Tang C, Miller T, Shirazian S, McMahon G and Cherrington JM.** In vivo antitumor activity of SU11248, a novel tyrosine kinase inhibitor targeting vascular endothelial growth factor and platelet-derived growth factor receptors: determination of a pharmacokinetic/pharmacodynamic relationship. *Clin Cancer Res* 9: 327-337, 2003.
31. **O'Farrell AM, Abrams TJ, Yuen HA, Ngai TJ, Louie SG, Yee KW, Wong LM, Hong W, Lee LB, Town A, Smolich BD, Manning WC, Murray LJ, Heinrich MC and Cherrington JM.** SU11248 is a novel FLT3 tyrosine kinase inhibitor with potent activity in vitro and in vivo. *Blood* 101: 3597-3605, 2003.
32. **Perchellet EM, Sperflage BJ, Qabaja G, Jones GB and Perchellet JP.** Quinone isomers of the WS-5995 antibiotics: synthetic antitumor agents that inhibit macromolecule synthesis, block nucleoside transport, induce DNA fragmentation, and decrease the growth and viability of L1210 leukemic cells more effectively than ellagic acid and genistein in vitro. *Anticancer Drugs* 12: 401-417, 2001.
33. **Pinto-Duarte A, Coelho JE, Cunha RA, Ribeiro JA and Sebastiao AM.** Adenosine A2A receptors control the extracellular levels of adenosine through modulation of nucleoside transporters activity in the rat hippocampus. *J Neurochem* 93: 595-604, 2005.
34. **Puebla C, Farias M, Gonzalez M, Vecchiola A, Aguayo C, Krause B, Pastor-Anglada M, Casanello P and Sobrevia L.** High D-glucose reduces SLC29A1 promoter activity and adenosine transport involving specific protein 1 in human umbilical vein endothelium. *J Cell Physiol* 215: 645-656, 2008.
35. **Ran R, Xu H, Lu A, Bernaudin M and Sharp FR.** Hypoxia preconditioning in the brain. *Dev Neurosci* 27: 87-92, 2005.

36. **Rasmussen HH, Hamilton EJ, Liu CC and Figtree GA.** Reversible oxidative modification: implications for cardiovascular physiology and pathophysiology. *Trends Cardiovasc Med* 20: 85-90, 2010.
37. **Rieger JM, Shah AR and Gidday JM.** Ischemia-reperfusion injury of retinal endothelium by cyclooxygenase- and xanthine oxidase-derived superoxide. *Exp Eye Res* 74: 493-501, 2002.
38. **Ryzhov S, Solenkova NV, Goldstein AE, Lamparter M, Fleenor T, Young PP, Greelish JP, Byrne JG, Vaughan DE, Biaggioni I, Hatzopoulos AK and Feoktistov I.** Adenosine receptor-mediated adhesion of endothelial progenitors to cardiac microvascular endothelial cells. *Circ Res* 102: 356-363, 2008.
39. **Sen RP, Delicado EG and Miras-Portugal MT.** Differential modulation of nucleoside transport types in neuroblastoma cells by protein kinase activation. *Neuropharmacology* 38: 1009-1015, 1999.
40. **Spyridopoulos I, Luedemann C, Chen D, Kearney M, Chen D, Murohara T, Principe N, Isner JM and Losordo DW.** Divergence of angiogenic and vascular permeability signaling by VEGF: inhibition of protein kinase C suppresses VEGF-induced angiogenesis, but promotes VEGF-induced, NO-dependent vascular permeability. *Arterioscler Thromb Vasc Biol* 22: 901-906, 2002.
41. **Stolk M, Cooper E, Vilk G, Litchfield DW and Hammond JR.** Subtype-specific regulation of equilibrative nucleoside transporters by protein kinase CK2. *Biochem J* 386: 281-289, 2005.
42. **Tanaka A, Nishida K, Okuda H, Nishiura T, Higashi Y, Fujimoto S and Nagasawa K.** Peroxynitrite treatment reduces adenosine uptake via the equilibrative nucleoside transporter in rat astrocytes. *Neurosci Lett* 498: 52-56, 2011.
43. **Tanaka K, Zhou F, Kuze K and You G.** Cysteine residues in the organic anion transporter mOAT1. *Biochem J* 380: 283-287, 2004.
44. **Vega JL, Puebla C, Vasquez R, Farias M, Alarcon J, Pastor-Anglada M, Krause B, Casanella P and Sobrevia L.** TGF-beta1 inhibits expression and activity of hENT1 in a nitric oxide-dependent manner in human umbilical vein endothelium. *Cardiovasc Res* 82: 458-467, 2009.

45. **Vyas S, Ahmadi B and Hammond JR.** Complex effects of sulfhydryl reagents on ligand interactions with nucleoside transporters: evidence for multiple populations of ENT1 transporters with differential sensitivities to N-ethylmaleimide. *Arch Biochem Biophys* 403: 92-102, 2002.
46. **Waidmann O, Pleli T, Dvorak K, Baehr C, Mondorf U, Plotz G, Biondi RM, Zeuzem S and Piiper A.** Inhibition of the equilibrative nucleoside transporter 1 and activation of A2A adenosine receptors by 8-(4-chlorophenylthio)-modified cAMP analogs and their hydrolytic products. *J Biol Chem* %20;284: 32256-32263, 2009.
47. **Weseler AR and Bast A.** Oxidative stress and vascular function: implications for pharmacologic treatments. *Curr Hypertens Rep* 12: 154-161, 2010.
48. **Winder T and Lenz HJ.** Vascular endothelial growth factor and epidermal growth factor signaling pathways as therapeutic targets for colorectal cancer. *Gastroenterology* 138: 2163-2176, 2010.
49. **Zachary I and Glikli G.** Signaling transduction mechanisms mediating biological actions of the vascular endothelial growth factor family. *Cardiovasc Res* 49: 568-581, 2001.

CHAPTER FIVE

MICROVASCULAR ENDOTHELIAL CELLS ISOLATED FROM MICE: TRANSPORTER  
CHARACTERIZATION AND REGULATION, SUBSTRATE METABOLISM, AND  
CONSEQUENCES OF ENT1 KNOCKOUT<sup>1</sup>

<sup>1</sup>A version of this chapter has been published:

Bone, DBJ, Choi, DS, Coe, IR, and Hammond, JR. Nucleoside/nucleobase transport and metabolism by microvascular endothelial cells isolated from ENT1 *-/-* mice. *Am J Physiol Heart Circ Physiol.* 2010 Sep;299(3):H847-56. Epub 2010 Jun 11. doi:10.1152/ajpheart.00018.2010

## 5.1 INTRODUCTION

All mammalian cells express at least one form of equilibrative transporter responsible for the cellular uptake and release of endogenous nucleosides such as adenosine. The predominant transporters are equilibrative nucleoside transporter subtypes 1 (ENT1; SLC29A1) and 2 (ENT2; SLC29A2) (4). The inhibition of ENTs has been shown to enhance the cardioprotective (28) and neuroprotective (17) actions of adenosine. These transporters are also responsible for the cellular uptake of cytotoxic nucleoside analogs used to treat cancer and viral infections (35).

An ENT1-null ( $ENT1^{-/-}$ ) mouse model has been generated by Choi and colleagues (12). The  $ENT1^{-/-}$  mice are phenotypically normal with the only difference from wild-type (WT) littermates being a slight (<10%) decrease in body weight and some differences in their behavioral characteristics. The ENT1-null mice are less sensitive to the intoxicating effects of ethanol compared with their WT littermates (12), and they also display less anxiety-like behavior (11). It has been noted that there is less tonic  $A_1$  adenosine receptor signaling in the brains of  $ENT1^{-/-}$  mice (12), reflecting either reduced extracellular adenosine levels or a decreased sensitivity of the receptor to adenosine, suggesting that ENT1 plays an important role in modulating the interaction of adenosine with its concomitant receptors in the central nervous system.

In addition to its regulatory activities in the nervous system, adenosine is well established as an endogenous cardioprotective agent via interactions with cardiomyocytes and is also a potent vasodilator through actions on vascular smooth muscle and endothelial cells (23). The availability of  $ENT1^{-/-}$  mice will now allow an in-

depth examination of the role of ENT1 (and the effects of its absence) in adenosine metabolism and bioactivity in the various cell types that constitute the cardiovascular system under both normal and pathophysiological conditions. We have recently published the results of a study based on cardiomyocytes isolated from WT and ENT1<sup>-/-</sup> mice (31). The present study extends this work to an examination of the impact of ENT1 loss on the nucleoside flux and metabolism in microvascular endothelial cells (MVECs). Previous studies from our laboratory have established that rat MVECs express high levels of both ENT1 and ENT2 (3), whereas human MVECs express predominantly the ENT1 subtype of nucleoside transporter (7). MVECs are considered to be the major site of accumulation and metabolism of the adenosine released into the interstitial space by myocytes during periods of high energy demand in heart and skeletal muscle (15); therefore, in the absence of biological compensation, one might expect the loss of ENT1 to have dramatic effects on the vascular actions of adenosine.

In this communication, we describe the nucleoside and nucleobase transport profile of MVECs derived from skeletal muscle of ENT1<sup>-/-</sup> mice and their WT littermate controls.

## **5.2 MATERIALS AND METHODS**

### *5.2.1 Materials*

8-2-[<sup>3</sup>H]chloroadenosine(4–7 Ci/mmol), 2,8-[<sup>3</sup>H]hypoxanthine (24–35 Ci/mmol), [<sup>3</sup>H]nitrobenzylmercaptapurine riboside (NBMPR) (5.5 Ci/mmol), and [<sup>3</sup>H]water (1 mCi/g) were purchased from Moravek Biochemicals (Brea, CA). Nonradiolabeled 2-chloroadenosine, hypoxanthine, NBMPR, nitrobenzylthioguanine riboside, dipyridamole

{2,6-bis(diethanolamino)-4,8-dipiperidinopyrimido-[5,4-d]pyrimidine}, collagenase, trypsin, BSA, tert-butyl hydroperoxide (TBHP), menadione, and cobalt chloride ( $\text{CoCl}_2$ ) were obtained from Sigma-Aldrich (St. Louis, MO). All cell culture media, fetal bovine serum (FBS), culture grade Dulbecco's PBS, trypsin-EDTA, antibiotic/antimycotic (penicillin, streptomycin, and amphotericin B), and heparin were purchased from GIBCO/BRL (Burlington, ON, Canada). Endothelial cell growth supplement (ECGS) was supplied by Beckton Dickinson (Oakville, ON, Canada). Rabbit polyclonal anti-adenosine deaminase (ADA), goat polyclonal anti-ENT3, rabbit polyclonal anti-adenosine receptor  $A_3$ , and donkey anti-goat horseradish peroxidase conjugated antibodies were all from Santa Cruz Biotechnology (Santa Cruz, CA). Mouse monoclonal anti-adenosine receptor  $A_{2a}$  and rabbit-anti mouse horseradish peroxidase-conjugated and mouse anti-rabbit horseradish peroxidase-conjugated antibodies were from Abcam (Cambridge, MA).

### 5.2.2 $ENT1^{-/-}$ mouse model

$ENT1^{-/-}$  mice were generated in the laboratory of Dr. Doo-Sup Choi as described previously (12);  $ENT1^{-/-}$  mice were backcrossed with outbred WT C57BL/6 mice to generate  $ENT1^{-/+}$  mice. Only  $ENT1^{-/+}$  mice were crossed (producing  $ENT1^{+/+}$ ,  $ENT1^{+/-}$ , and  $ENT1^{-/-}$  offspring) to establish a breeding colony at the University of Western Ontario. Genotyping was done using isolated genomic DNA and standard PCR as previously described (11). All aspects of this study were conducted in accordance with the policies and guidelines set forth by the Canadian Council on Animal Care and were approved by the Animal Use Committee of the University of Western Ontario.



### 5.2.3 MVEC isolation/culture

MVECs were isolated as described previously for rats (3), based on the affinity of their  $\alpha$ -d-(+)galactosyl residues for isolectin B<sub>4</sub> from *Bandeiraea simplicifolia* (BSI-B4; Sigma) bound to magnetic microbeads (Dynabeads, M-450 Epoxy, Dynal, Lake Success, NY). The extensor digitorum longus muscles of female mice were removed from the hindlimbs under anesthesia by pentobarbital sodium (42 mg/kg ip). After careful removal and disposal of tissue containing larger blood vessels, the isolated muscle was sliced into ~0.5-mm pieces and digested for 30–45 min in 0.84 mg/ml collagenase, 0.12 mg/ml trypsin and dispase, and 1.62 mg/ml BSA in 50 ml Krebs-Ringer solution containing (in mM) 127 NaCl, 4.6 KCl, 1.1 MgSO<sub>4</sub>, 1.2 KH<sub>2</sub>PO<sub>4</sub>, 8.3 d-glucose, 24.8 NaHCO<sub>3</sub>, 2 pyruvate, 11.4 creatinine, 20 taurine, 5 d-ribose, 2 l-asparagine, 2 l-glutamine, 1 l-arginine, and 0.5 uric acid in a 37°C water-jacketed organ bath bubbled with 95% O<sub>2</sub>-5% CO<sub>2</sub>. The enzymatic digest was filtered through 100- $\mu$ m nylon mesh to remove undigested fragments, and the dissociated cells were collected by centrifugation and washed in 37°C DMEM-F12 media. Cells were then resuspended with  $\sim 1 \times 10^6$  BSI-B4 coated Dynabeads (in DMEM-F12 media) and rotated on a spindle for 10–15 min. Endothelial cells bound to the magnetic beads were collected using a magnetic particle collector (MPC-1, Dynal), washed twice, and transferred to six-well plates in DMEM-F12 media supplemented with 20% FBS, 100 U/ml penicillin G, 100  $\mu$ g/ml streptomycin sulfate, 0.25  $\mu$ g/ml amphotericin B, 2 mM l-glutamine, 0.025 IU/ml heparin, and 125  $\mu$ g/ml ECGS and cultured at 37°C in a 5% CO<sub>2</sub>-95% room air humidified atmosphere. The media was changed routinely every 3 to 4 days, and the cells were passaged using 0.05% trypsin in

0.53 mM EDTA upon reaching confluence. After *passage 3*, the FBS and ECGS levels were reduced to 10% and 75  $\mu\text{g/ml}$ , respectively. The endothelial cell phenotype was confirmed by the presence of von Willebrand factor VIII and BSI-B4 antigens as described previously (3). The cultures were typically found to contain >95% endothelial cells. In general, five passages were required to obtain sufficient cells to undertake the transport assays described herein.

In preparation for experimental assays, MVECs (*passage 5–15*) were trypsinized for 5 min at 37°C and then diluted with DMEM-F12 media + 10% FBS and collected by centrifugation. The cells were washed once by resuspension/centrifugation in PBS containing (in mM) 137 NaCl, 6.3 Na<sub>2</sub>HPO<sub>4</sub>, 2.7 KCl, 1.5 KH<sub>2</sub>PO<sub>4</sub>, 0.9 CaCl<sub>2</sub>·2H<sub>2</sub>O, and 0.5 MgCl<sub>2</sub>·6H<sub>2</sub>O (pH 7.4) or a modified Na<sup>+</sup>-free PBS containing *N*-methyl-d-glucamine (NMG) buffer consisting of (in mM) 140 NMG, 10 HEPES, 5 KCl, 4.2 KHCO<sub>3</sub>, 0.44 KH<sub>2</sub>PO<sub>4</sub>, 0.36 K<sub>2</sub>HPO<sub>4</sub>, 1.3 CaCl<sub>2</sub>·2H<sub>2</sub>O, and 0.5 MgCl<sub>2</sub>·6H<sub>2</sub>O (pH 7.4) as appropriate to the assay and then resuspended in the same buffer for immediate use as described in [<sup>3</sup>H]NBMPR binding and [<sup>3</sup>H]substrate uptake. In some cases, the cells were depleted of ATP by sequential incubation at 37°C with rotenone and 2-deoxyglucose as described previously (3).

#### 5.2.4 Analysis of [<sup>3</sup>H]hypoxanthine metabolites in MVECs

[<sup>3</sup>H]Hypoxanthine can be phosphorylated to inosine 5'-monophosphate by hypoxanthine-guanine phosphoribosyltransferase (HGPRT) or oxidized to xanthine via xanthine oxidase. To determine whether the ENT1<sup>-/-</sup> MVECs metabolized hypoxanthine differently than WT cells, we assessed the [<sup>3</sup>H]metabolites arising from incubating cells

for 20 min with 100  $\mu\text{M}$  [ $^3\text{H}$ ]hypoxanthine. The cells were harvested as described in *MVEC isolation/culture*, ATP depleted, and then incubated for 15 min in the presence and absence of 5  $\mu\text{M}$  dipyridamole before exposure to [ $^3\text{H}$ ]hypoxanthine for 20 min at room temperature. After incubation with [ $^3\text{H}$ ]hypoxanthine, the cells were centrifuged through oil as described in [ $^3\text{H}$ ]substrate uptake, and the cell pellet was digested with 7% perchloric acid for  $\sim$ 16 h. The acid soluble extract was removed and neutralized with an equal volume of 1 M potassium hydroxide and then centrifuged (10,000  $g$  for 10 min) to remove insoluble precipitate. Extracts were stored at  $-20^\circ\text{C}$  until required.

The separation of purine nucleobases, nucleosides, and nucleotides was performed using two one-dimensional thin-layer chromatography methods modified from Metz et al. (25) (6 min 0.5 M LiCl, 10 min 1.0 M LiCl, and remainder in 1.5 M LiCl, all at pH 4.0 and included 0.1 M EDTA; *condition 1*) and Shimizu et al. (33) (*n*-butanol:ethyl acetate:methanol:ammonium hydroxide; 7:4:3:4, vol:vol; *condition 2*). Plastic-backed PEI-cellulose F TLC plates (EMD Chemicals or Merck) were loaded with 10- $\mu\text{l}$  aliquots of neutralized extract and developed using the two solvent conditions in parallel. Purine metabolite locations were determined under UV light, and the  $R_f$  values were calculated and compared with standards for identification. The plates were then cut into 5-mm strips for liquid scintillation analysis of [ $^3\text{H}$ ] content using Beckman Ready Protein<sup>+</sup> scintillation fluid.

Neither solvent system on its own was capable of separating all the purine metabolites of interest. The organic solvent (*condition 2*) was able to retard all nucleotides at the loading point on the plate and could clearly isolate adenosine and xanthine. However,

the hypoxanthine and inosine spots overlapped. The LiCl gradient (*condition 1*), on the other hand, could isolate inosine effectively but produced a blended hypoxanthine-adenosine spot. Thus the amount of hypoxanthine was determined from the equation:  $\text{dpm hypoxanthine} = \text{dpm hypoxanthine/adenosine (condition 1)} - \text{dpm adenosine (condition 2)}$ . Since xanthine oxidase removes the tritium at the two position of 2,8- $[\text{}^3\text{H}]$ hypoxanthine to give 8- $[\text{}^3\text{H}]$ xanthine, the dpm values associated with xanthine were doubled to compensate for this.

#### *5.2.5 Reverse-transcriptase polymerase chain reaction*

Total RNA was isolated from the WT and ENT1<sup>-/-</sup> MVECs using the phenol-chloroform extraction. First-strand DNA template was generated using 5  $\mu\text{g}$  (MVECs) of DNaseI (Invitrogen, Carlsbad, CA)-treated total RNA and the Superscript First Strand Synthesis System for RT-PCR using oligo d(T) primers (Invitrogen).

RT-PCR amplifications were performed using Platinum Taq DNA polymerase (Invitrogen) in a Thermocycler PE 480 (Perkin Elmer, Norwalk, CT) using an oil-overlaid 50- $\mu\text{l}$  reaction mixture in 500- $\mu\text{l}$  thin-walled reaction tubes. Reaction conditions included a 2-min 94°C initial activation, followed by 25, 30, or 35 cycles of 30 s at 94°C, 30 s at 55°C, and 30 s at 72°C. Preliminary experiments determined the number of cycles of PCR that were required to obtain a visible product on agarose gels for each of the transcripts while remaining on the log-linear portion of the cycle number versus product formation curves. PCR products were resolved by electrophoresis on 2% agarose gels against the O'GeneRuler 50-bp DNA ladder mix (Fermentas, Burlington, ON, Canada). Based on qualitative PCR, ENT1, ENT3, ADA, and the adenosine receptor A<sub>2a</sub> and A<sub>3</sub> genes were

chosen for quantitative real-time PCR analysis using a Roche LightCycler (Roche Applied Sciences, Mississauga, ON, Canada).  $\beta$ -Actin was chosen as a reference control. All primers used were the same as those for qualitative PCR. Standard curves for all transcripts were generated using the same cDNA preparation at concentrations ranging from  $10^{-7}$  to  $10^{-12}$  M. The PCR was conducted using 1  $\mu$ l of WT or knockout (KO) cDNA and SYBR Green Jumpstart Taq ReadyMix capillary formulation (Sigma). PCR conditions were as follows: initial denaturing at 94°C for 30 s, followed by 40 cycles of 94°C for 0 s, 55°C for 5 s, 72°C for 17 s, and 78°C for 1 s. The melting curve analysis of products at the end of the reaction revealed single products from each primer pair. At least three individual reactions were performed using two different cDNA preparations.

Primer sequences and expected sizes are summarized in Table 5.1 for ENT1; ENT2; ENT3; ENT4; concentrative nucleoside transporter subtypes 1 (CNT1), 2 (CNT2), and 3 (CNT3); adenosine kinase; ADA; adenine phosphoribotransferase; hypoxanthine-guanine phosphoribotransferase; purine nucleoside phosphorylase; xanthine oxidase; A<sub>1</sub>, A<sub>2a</sub>, A<sub>2b</sub>, and A<sub>3</sub> adenosine receptors; and  $\beta$ -actin.

### *5.2.6 Immunoblots*

Extensor digitorum longus muscles were isolated from age- and sex-matched mice and quickly placed in ice-cold lysis buffer containing 20 mM Tris·HCl, 150 mM NaCl, 1 mM Na<sub>2</sub>EDTA, 1 mM EGTA, 1% Triton, 2.5 mM sodium pyrophosphate, 1 mM  $\beta$ -glycerophosphate, 1 mM Na<sub>3</sub>VO<sub>4</sub>, and 1  $\mu$ g/ml leupeptin (pH 7.5), supplemented with 1 mM phenylmethylsulfonyl fluoride just before use (Cell Signaling Technology, Pickering, ON, Canada). Total protein from tissue lysates (100  $\mu$ g for ADA and ENT3; and 200  $\mu$ g for

adenosine receptor A<sub>2a</sub> and A<sub>3</sub>) was subjected to SDS-PAGE and transferred to polyvinylidene difluoride membranes. Membranes were incubated overnight ( $\geq 12$  h) at 4°C with one of the following primary antibody dilutions: ADA, 1:1,000; ENT3, 1:400; adenosine receptor A<sub>2a</sub>, 1:1,000; or adenosine receptor A<sub>3</sub>, 1:200. Secondary antibodies were used at dilutions of 1:10,000, 1:1,000, 1:4,000, and 1:1,000 for ADA, ENT3, A<sub>2a</sub>, and A<sub>3</sub>, respectively, and incubated with membranes for 1 h at room temperature. Detection was performed using LumiGLO chemiluminescent substrate (Cell Signaling Technology) and the VersaDoc Imaging System (Bio-Rad). After exposure, the membranes were stripped (200 mM glycine, 1% Tween-20, and 0.1% SDS; pH 2.2) and then probed for GAPDH using a 1:1,000 dilution of primary antibody for 2 h at room temperature. The secondary antibody was used at dilutions of 1:2,000 for ADA and ENT3 and 1:4,000 for adenosine receptor A<sub>2a</sub> to account for the double amount of protein used. Densitometry was performed using ImageJ software (<http://rsbweb.nih.gov/ij/index.html>). In all cases, the major protein detected by each antibody reflected the expected size of the product based on manufacturers' specifications and previously published data using these antibodies (10; 27).

#### *5.2.7 Treatment with Reactive Oxygen Species Generators*

Reactive oxygen species (ROS) generators were made fresh each day. TBHP was diluted in ddH<sub>2</sub>O from a concentrated stock. Menadione was dissolved in 100% ethanol. In all cases, confluent cells were washed with warm PBS and fed with warmed complete medium containing vehicle (control) or the indicated concentration of ROS generator.

Cells were placed back into the 37°C CO<sub>2</sub> incubator for the desired time before harvesting and subsequent uptake studies (as described in Chapter 2).

### *5.2.8 Simulated Ischemia and Hypoxia*

#### 5.2.8.1 Cobalt Chloride Treatment

Cobalt chloride (CoCl<sub>2</sub>) is an established stabilizer of HIF-1 $\alpha$  (30). Confluent cells were washed with PBS and covered with medium containing 100  $\mu$ M CoCl<sub>2</sub> and incubated at 37°C for the time indicated before harvesting for uptake.

#### 5.2.8.2 Simulated Ischemia

Based on a method developed by Meldrum and colleagues (24), primary mouse cells were harvested and resuspended in fresh complete medium. Cell suspensions were placed in a 37°C 5%CO<sub>2</sub>-95% air humidified atmosphere for 1 hour to equilibrate. Following equilibration, a cell lot was centrifuged briefly and all medium was aspirated off with the exception of enough to keep the pellet covered. The pellet was resuspended by flicking the tube. Simulated ischemia was initiated by the layering of mineral oil over the medium, creating a gas exchange barrier. Mineral oil overlaid cells were placed back in the atmosphere described above for 2 hr. Control cells were left in the complete medium with no overlay. Cells were gently mixed every 30 minutes. Following treatment, cells were washed with PBS, centrifuged, and supernatant was aspirated. This procedure was repeated three times to ensure no mineral oil was remaining. Cells were then resuspended in a final volume appropriate for substrate uptake assay.

### 5.2.8.3 Hypoxia

For true low oxygen exposure, culture flasks were placed in Hypoxia Chambers (Billips-Rothenberg, Del Mar, CA). Chambers were flushed with 1% O<sub>2</sub> for 5 min and expelled air was measured with an O<sub>2</sub> detector to confirm low oxygen levels. Chambers were then sealed and placed in a 37°C incubator for the desired time. Following hypoxia, flasks were removed from the chambers and harvested for uptake.

## 5.3 RESULTS

### 5.3.1 MVECs from *ENT1*<sup>-/-</sup> Lack [<sup>3</sup>H]NBMPR Binding

The gross phenotype of the *ENT1*<sup>-/-</sup> mice was similar to that reported previously by Choi and colleagues (12). The *ENT1*<sup>-/-</sup> mice had a consistently lower body weight. They were also notably easier to handle than WT mice (less distress because of handling), likely reflecting the anxiolytic phenotype reported previously (11). Quantitative RT-PCR confirmed the loss of the full-length *ENT1* transcript in the *ENT1*<sup>-/-</sup> mice (Figure 5.2). MVECs from the *ENT1*<sup>-/-</sup> mice had no detectable high-affinity binding sites for the *ENT1*-selective radioligand probe [<sup>3</sup>H]NBMPR (Figure 5.1), confirming the specificity of this radioligand for the *ENT1* protein. WT mouse MVECs had 150,000 ± 27,000 [<sup>3</sup>H]NBMPR sites/cell with an affinity of 0.09 ± 0.02 nM, which is typical of NBMPR binding to *ENT1*.

### 5.3.2 Compensatory Changes in Purinergic Genes in *ENT1*<sup>-/-</sup> MVECs

We found no evidence for Na<sup>+</sup>-dependent CNT1, CNT2, and CNT3, and we confirmed that MVECs do not express the A<sub>1</sub> adenosine receptor subtype (19). No changes were observed in the expression of the *ENT2* subtype of plasma membrane-located



nucleoside transporters in ENT1<sup>-/-</sup> mice compared with littermate controls (Figure 5.2A), nor was the ENT4 transcript detected in either the WT or ENT1<sup>-/-</sup> cells. Furthermore, no significant differences were noted in the expression of adenosine kinase, xanthine oxidase, HGPRT, adenine phosphoribotransferase, purine nucleoside phosphorylase, or A<sub>2B</sub> adenosine receptors in the ENT1<sup>-/-</sup> MVECs compared with WT controls (Figure 5.2A). However, MVECs from ENT1<sup>-/-</sup> mice showed significant increases of 15 ± 3- and 11 ± 2-fold, respectively, in the expression of mRNA transcripts for ADA and A<sub>2a</sub> adenosine receptors, relative to WT littermate controls (Figure 5.2B). There was a trend toward a decrease in adenosine A<sub>3</sub> receptor transcript in the ENT1<sup>-/-</sup> mice, but this did not reach statistical significance and there was no corresponding change in A<sub>3</sub> receptor protein levels (Figure 5.3). Likewise, there was a small but significant increase in ENT3 transcript (Figure 5.2B), which was also not paralleled by an increase in ENT3 protein in skeletal muscle (Figure 5.3). Attempts to measure ADA and A<sub>2a</sub> adenosine receptor protein levels in the MVECs proved to be problematic. However, significant increases in ADA (2.1-fold) and adenosine A<sub>2a</sub> receptor (2.4-fold) protein was evident by immunoblotting using the skeletal muscle tissue of ENT1<sup>-/-</sup> mice from which the MVECs were derived, relative to WT mice (Figure 5.3).

### 5.3.3 Nucleoside and Nucleobase Transport Function in WT and ENT1<sup>-/-</sup> MVECs

In terms of the ability to accumulate [<sup>3</sup>H]substrates associated with ENT activity, the WT MVECs accumulated both [<sup>3</sup>H]formycin B (Figure 5.4) and 2-[<sup>3</sup>H]chloroadenosine (Figure 5.5) via two distinct Na<sup>+</sup>-independent dipyridamole-sensitive processes (Table 5.2). The majority (~90%) of the substrate uptake in WT MVECs was inhibited by 50 nM NBMPR

and hence was mediated by ENT1. The remainder of the uptake was inhibited by dipyridamole, but not NBMPR, and hence was mediated by ENT2. The uptake of [<sup>3</sup>H]formycin B (Figure 5.4) and 2-[<sup>3</sup>H]chloroadenosine (Figure 5.5) by MVECs was reduced dramatically in the cells derived from the ENT1<sup>-/-</sup> mice (Table 5.2). The initial rate of uptake of 10 μM [<sup>3</sup>H]formycin B in the ENT1<sup>-/-</sup> MVECs was 0.07 ± 0.01 pmol/μl/s, which is not significantly different from the rate of ENT2-mediated formycin B uptake by WT mMVECs (0.06 ± 0.01 pmol/μl/s) (Figure 5.4). When 2-[<sup>3</sup>H]chloroadenosine was used as a substrate, it was evident that in WT MVECs, ENT1 accounted for the majority of nucleoside transport, with ENT2 providing a very small component of the total. In ENT1<sup>-/-</sup> MVECs, only ENT2 mediated transport was present. Interestingly, the V<sub>max</sub> of 2-chloroadenosine uptake in the ENT1<sup>-/-</sup> mice (0.19 ± 0.07 pmol/μl/s) was actually significantly lower than the V<sub>max</sub> of ENT2-mediated 2-chloroadenosine uptake in the WT mice (1.2 ± 0.5 pmol/μl/s) (Figure 5.5).

To further assess the ENT2-mediated component in the MVECs, the uptake of [<sup>3</sup>H]hypoxanthine was examined after depleting the cells of ATP to reduce trapping of [<sup>3</sup>H]hypoxanthine metabolites. ENT2 differs from ENT1 in that it accepts nucleobases, such as hypoxanthine, as substrates in addition to purine and pyrimidine nucleosides. It was apparent from the initial time course studies using 10 μM hypoxanthine that mouse MVECs readily accumulated hypoxanthine via a saturable system that was relatively insensitive to dipyridamole but that was inhibited by adenine (Figure 5.6). These data suggest that hypoxanthine was being accumulated via an ENT-independent transport process. When adenine (1 mM) is used to define the nonmediated uptake component,

the WT mouse MVECs accumulated hypoxanthine with  $K_m$  and  $V_{max}$  estimates of  $125 \pm 29 \mu\text{M}$  and  $16.5 \pm 3.8 \text{ pmol}/\mu\text{l}/\text{s}$ , respectively, while  $\text{ENT1}^{-/-}$  cells had similar  $K_m$  and  $V_{max}$  values of  $123 \pm 28 \mu\text{M}$  and  $11.6 \pm 2.1 \text{ pmol}/\mu\text{l}/\text{s}$ , respectively (Figure 5.7).

Interestingly, the apparent rate of [ $^3\text{H}$ ]hypoxanthine influx tended to increase when cells from WT mice were incubated with the ENT blocker dipyridamole before the uptake measurements, particularly at higher ( $>100 \mu\text{M}$ ) concentrations of hypoxanthine (Figure 5.7). In contrast, dipyridamole had no effect on hypoxanthine uptake by  $\text{ENT1}^{-/-}$  MVECs.

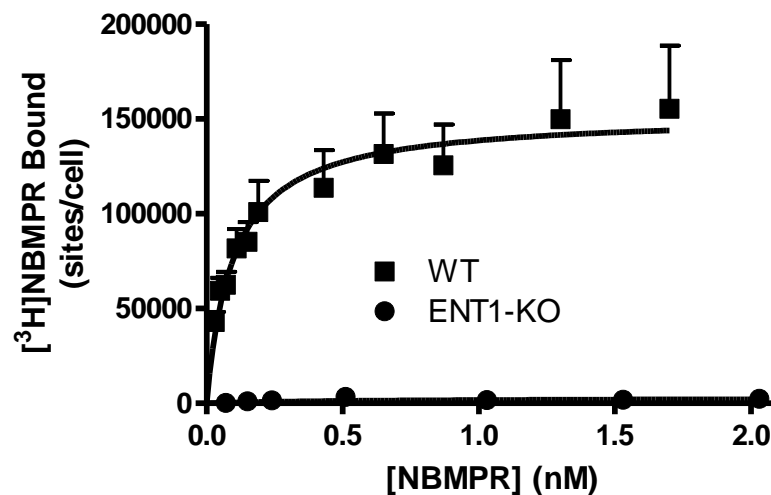


Figure 5.1. MVECs from  $ENT1^{-/-}$  lack  $[^3H]NBMPR$  binding.

MVECs isolated from either wild-type (WT) or equilibrative nucleoside transporter subtype-1 (ENT1) knockout (KO) ( $ENT1^{-/-}$ ) littermates were exposed to a range of concentrations of  $[^3H]$ nitrobenzylmercaptopyrine riboside (NBMPR) (abscissa) in the absence (total binding) or presence (nonspecific binding) of  $10 \mu M$  nitrobenzylthioguanine riboside. Specific binding (ordinate) was calculated as the difference between total and nonspecific binding. Each point is the mean  $\pm$  SEM of 5 experiments performed in duplicate.

Gene	Primer 5'-3'	Product Size (bp)	# of cycles
ENT1	CAAGTATTTCAAAACCGCTGGAC GAAACGAGTTGAGGCAGGTGAAGAC	196	25
ENT2	GACCTCTGCTCTTGGATACTTCAT GACAACAAAGACTGAAGGTTTTCC	288	35
ENT3	CCCTCCCTGCTGTTCTGGT CATGGGAAGGAGCCTGTGA	245	30
ENT4	ATTGGCGGCTGTGCTCCTAAA TGCCGTGCTCTCTCCAGTCAT	279	35
CNT1	GCAGCTGTTTGAGTGATCA ACCACACAGGTGATGACGAA	120	35
CNT2	ATTTGTGGCCTACCAGCAAC GCCTCCAGTGTGATTCTA	169	35
CNT3	TGTGCGATAAGCTCCACAG CAAGTTTTGTTGGCCAGTT	243	35
Adenosine Kinase	TGGAGCGGAAGTGGTGGTGG GGAAGAGCCTGCGCTTTTTGG	300	30
Adenosine Deaminase	GAAGGCAAAGGAGGGCGTGGTCTA GATGTCCACAGCCTCACGCACAAC	423	25
Adenine Phosphoribosyltransferase	CAAGATCGACTACATCGAGGTCT GCTCACACTCCACCACTCAG	297	25
Hypoxanthine-Guanine Phosphoribosyltransferase	CATTGTGGCCTCTGTGTGCTCAA CGAGAGGTCTTTTACCAGCAAGC	326	25
Purine nucleoside phosphorylase	GCCGACTGGTGTGGATTGCTG TCGTTGCTCCCCATTTGTTCC	358	25
Xanthine Oxidase	TGCCTGCTTGACCCCATCTG CCTCCACAGCACCCACCATCC	299	30
A <sub>1</sub> adenosine receptor	ATCCCTCTCCGGTACAAGACAGT ACTCAGTTGTTCCAGCCAAAC	119	35
A <sub>2A</sub> adenosine receptor	CCGAATTCCTCCGGTACA CAGTTGTTCCAGCCAGCAT	119	35
A <sub>2B</sub> adenosine receptor	TCTTCTCGCCTGCTTCGT CCAGTGACCAAACCTTTATACCTGA	120	35
A <sub>3</sub> adenosine receptor	ACTTCTATGCTGCCTTTTCATGT AACCCTTCTATATCTGACTGTCAGCTT	128	35
β-actin	GTGACGTTGACATCCGTA CTCAGGAGGCAATGATCT	148	25

Table 5.1 RT-PCR primers

Primers used for the amplification of each of the indicated genes are shown along with the expected product size and the number of cycles used in the PCR reactions. The cycle number was selected based on the lowest number that revealed a product up to a maximum of 35 cycles in the qualitative reverse-transcriptase PCR reactions. ENT, equilibrative nucleoside transporter; CNT, concentrative nucleoside transporter.



Figure 5.2. Analysis of purine transporter/metabolic enzyme gene expression in MVECs. *A*: qualitative reverse-transcriptase PCR: PCR reactions were conducted using the primers shown in Table 5.1, and the products were resolved on 2% agarose gels. The same PCR conditions were used for each primer pair in both the WT and ENT1<sup>-/-</sup> samples, and all amplifications shown on each gel set were done in parallel using the same WT and KO cDNA preparations. The first lane on each gel set represents the DNA ladder (bp sizes as labeled). *Set 1*: ENT1, ENT2, ENT3, and β-actin (the vertical bar indicates where a blank section of the gel image was removed between the ENT3 and β-actin lanes); *set 2*: adenosine A<sub>2A</sub> receptor, adenosine A<sub>2B</sub> receptor, A<sub>3</sub> receptor, and β-actin; and *set 3*: adenosine kinase (ADK), adenosine deaminase (ADA), adenine phosphoribosyltransferase (APRT), hypoxanthine-guanine phosphoribosyltransferase (HGPRT), purine nucleoside phosphorylase (PNP), xanthine oxidase (XO), and β-actin. All products were of the expected size. *B*: quantitative real-time PCR: apparent differences in gene expression between the WT and ENT1<sup>-/-</sup> MVECs, as noted in the studies shown in *A*, were confirmed by real-time PCR. Crossing point (CP) values, obtained from SYBR green I fluorescence signals, were used to compute the concentrations of ENT3, ADA, and adenosine A<sub>2A</sub> and A<sub>3</sub> receptor transcripts, relative to β-actin. β-Actin CP values were 19.3 ± 0.6 and 18.8 ± 0.7 for the WT and ENT1<sup>-/-</sup> samples, respectively. The gene-to-β-actin ratios derived from each independent experiment were then averaged to obtain the data shown. Each bar is the mean ± SEM of 3 separate amplification runs from 2 independent mRNA isolations (*n* = 6). \**P*<0.05, significant difference in expression between the WT and ENT1<sup>-/-</sup> cells (Student's *t*-test). *C*: data from *B* plotted as the relative change between the WT and ENT1<sup>-/-</sup> mice.

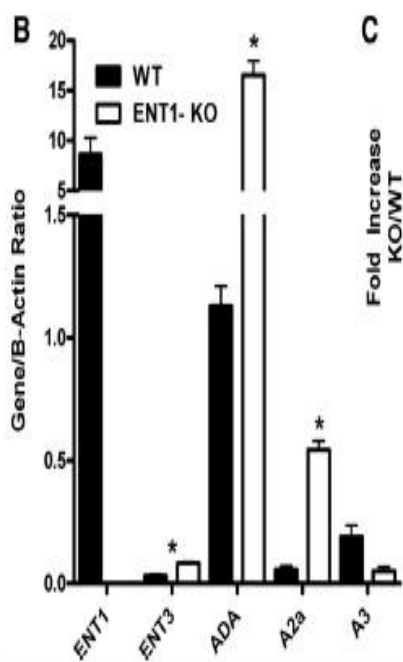
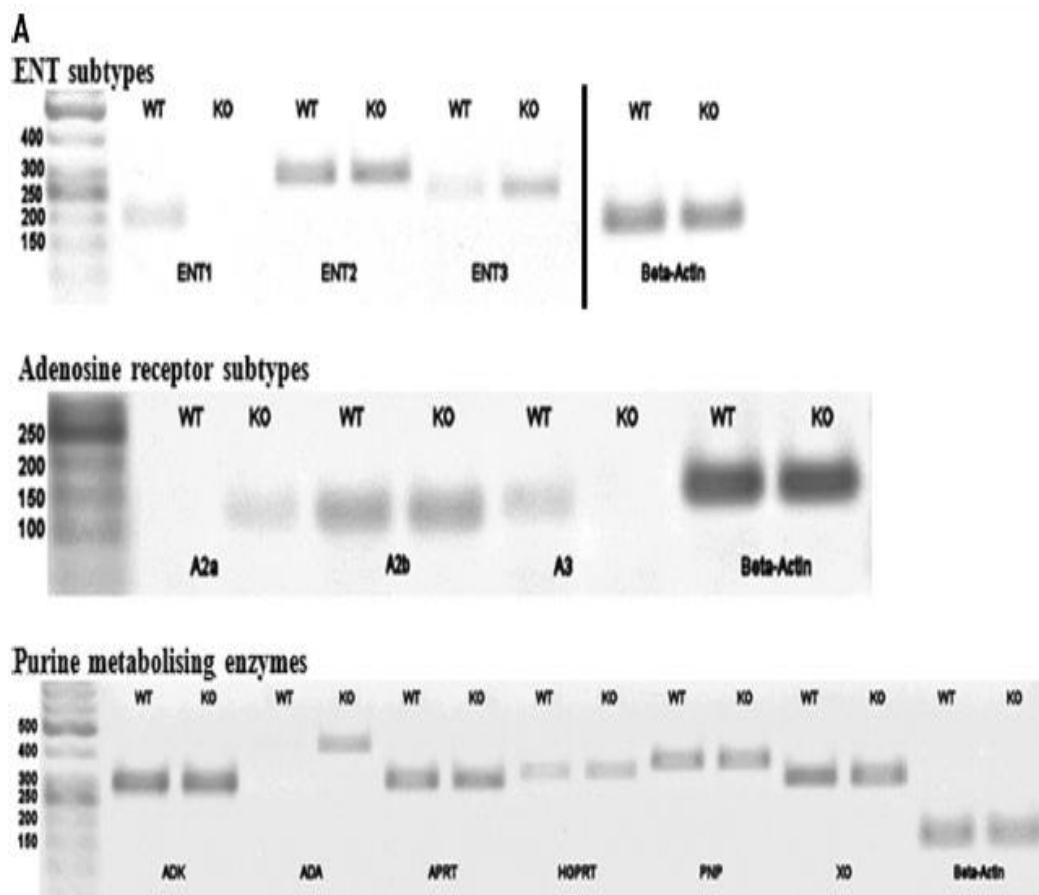






Figure 5.3. ADA and A<sub>2A</sub> are upregulated at the protein level.

Proteins extracted from the extensor digitorum longus muscles of WT and ENT1<sup>-/-</sup> mice were separated by electrophoresis and immunoblotted, in parallel, with antibodies to GAPDH (37 kDa), ADA (50 kDa), adenosine A<sub>2A</sub> receptor (45 kDa), adenosine A<sub>3</sub> receptor (43 kDa), and ENT3 (52 kDa). Representative immunoblots are shown in A. The results (mean ± SEM) of densitometry analysis of 3 independent experiments with adenosine receptor A<sub>2A</sub> and ADA are shown in B as a ratio relative to GAPDH. \**P*<0.05, significant difference in expression between the WT and ENT1<sup>-/-</sup> muscle (Student's *t*-test).

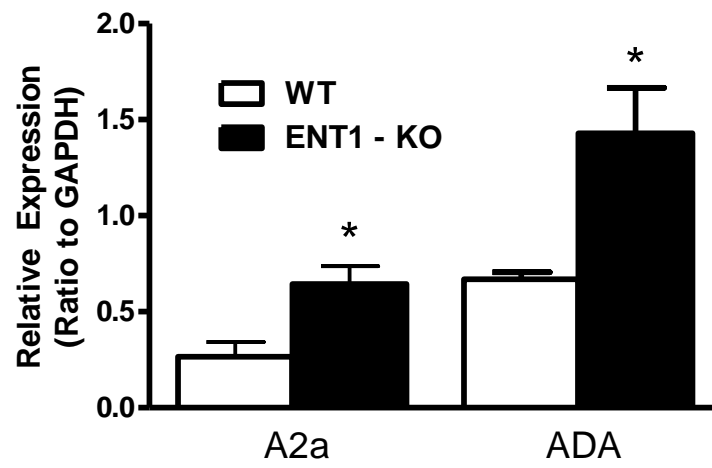
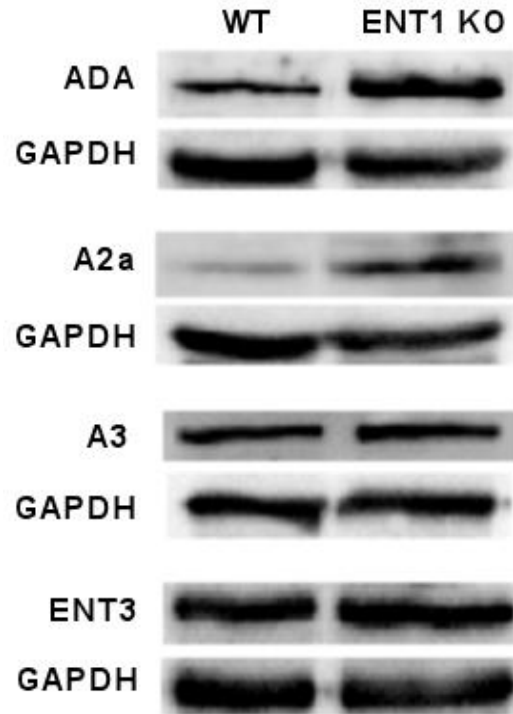




Figure 5.4. Formycin B uptake by ENT2 is unchanged in MVECs from ENT1<sup>-/-</sup> mice.

MVECs isolated from either WT (A) or ENT1<sup>-/-</sup> (B) mice were incubated with 10  $\mu$ M [<sup>3</sup>H]formycin B (FB) in the absence (Total,  $\blacksquare$ ) or presence of 50 nM NBMPR (+NBMPR; selective inhibition of ENT1-mediated uptake,  $\square$ ) or 10  $\mu$ M dipyridamole/NBMPR (+DY; complete inhibition of transporter-mediated uptake,  $\bullet$ ) for the times indicated. Uptake is represented as picomoles of [<sup>3</sup>H]FB accumulated per microliters of intracellular water. Each point is the mean  $\pm$  SEM from 4 experiments.

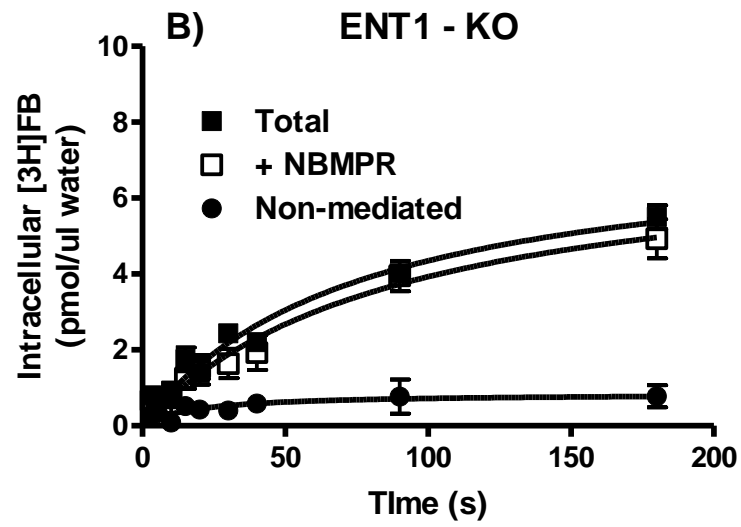
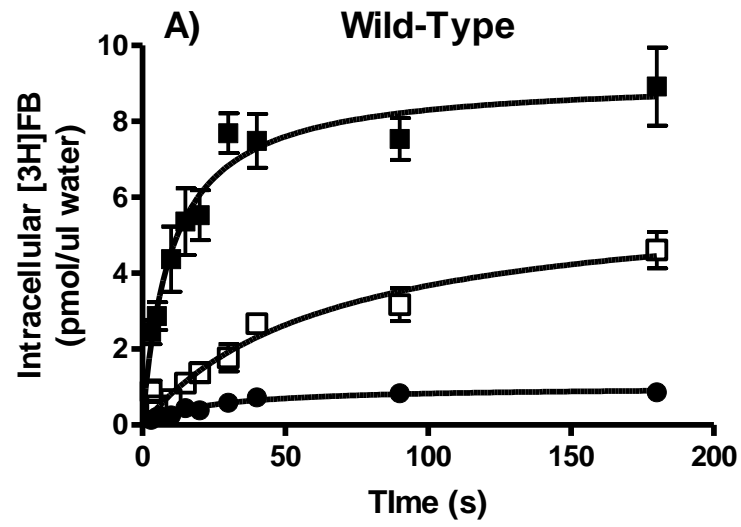




Figure 5.5. Uptake of 2-[<sup>3</sup>H]chloroadenosine by ENT2 is reduced in MVECS from ENT1<sup>-/-</sup> mice.

MVECs isolated from either WT (A) or ENT1<sup>-/-</sup> (B) mice were incubated for 5 or 15 s, respectively, with the indicated concentrations of 2-[<sup>3</sup>H]chloroadenosine. Parallel assays were conducted in the absence (total influx) and presence of either 50 nM NBMPR (NBMPR-resistant influx) or 10 μM DY/NBMPR (nonmediated uptake) as described in Figure 5.4 for [<sup>3</sup>H]FB uptake. The total transporter-mediated uptake of substrate was calculated as the total influx minus the nonmediated component. The ENT2-mediated uptake was calculated as the NBMPR-resistant uptake minus the nonmediated component, and the ENT1-mediated uptake was estimated as the difference between the total uptake and that seen in the presence of NBMPR. Results are plotted as picomoles of 2-[<sup>3</sup>H]chloroadenosine accumulated per microliter of cell water per second ( $V_i$ , ordinate) against the concentration of 2-[<sup>3</sup>H]chloroadenosine used (abscissa). Each point is the mean ± SEM from 5 experiments. The transporter kinetic constants derived from these data are shown in Table 5.2.



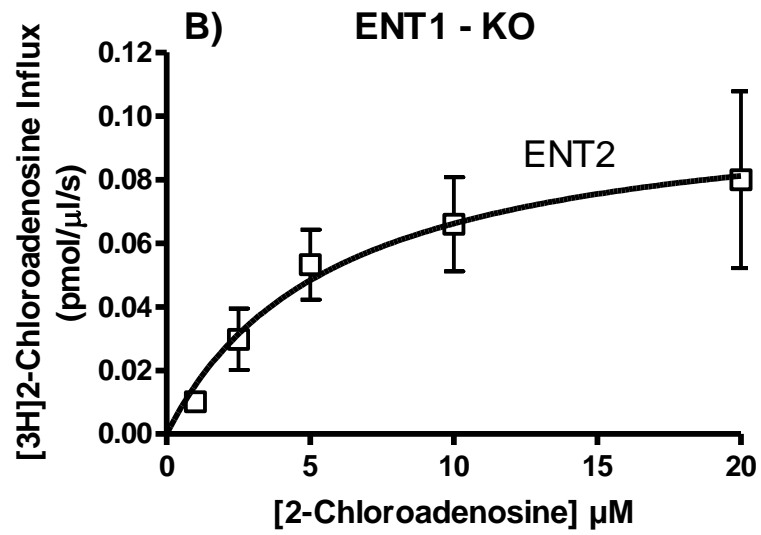
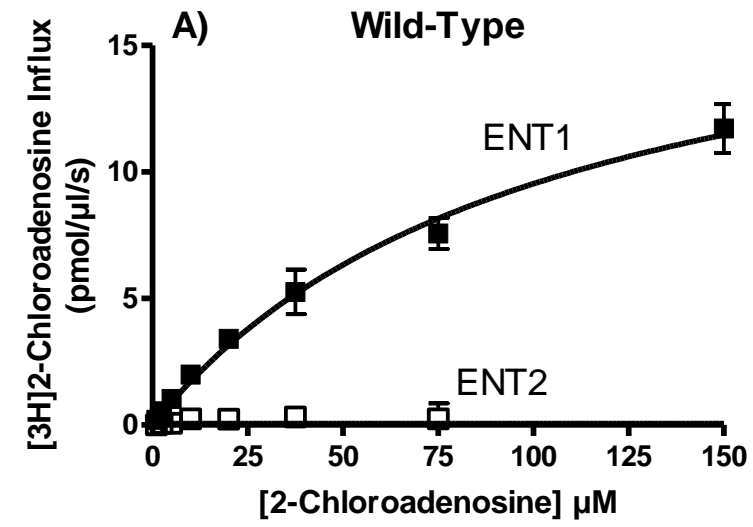




Figure 5.6. Uptake of [<sup>3</sup>H]hypoxanthine was mediated by a dipyridamole-insensitive transporter.

MVECs isolated from either WT (A) or ENT1<sup>-/-</sup> (B) mice were incubated with 5 μM [<sup>3</sup>H]hypoxanthine in the absence (Total) or presence of 10 μM DY (inhibition of ENT2-mediated uptake) or 1 mM adenine for the times indicated. Uptake is represented as picomoles of [<sup>3</sup>H]hypoxanthine accumulated per microliter of intracellular water (in μM). Each point is the mean ± SEM from 4 experiments.

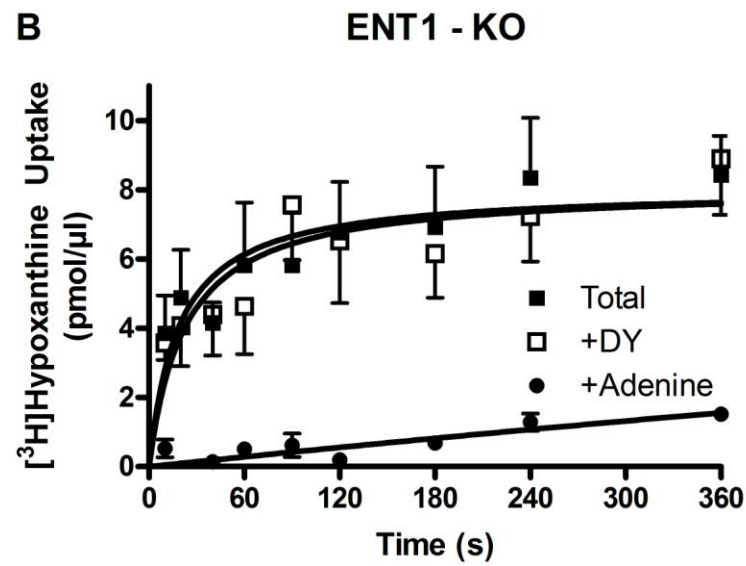
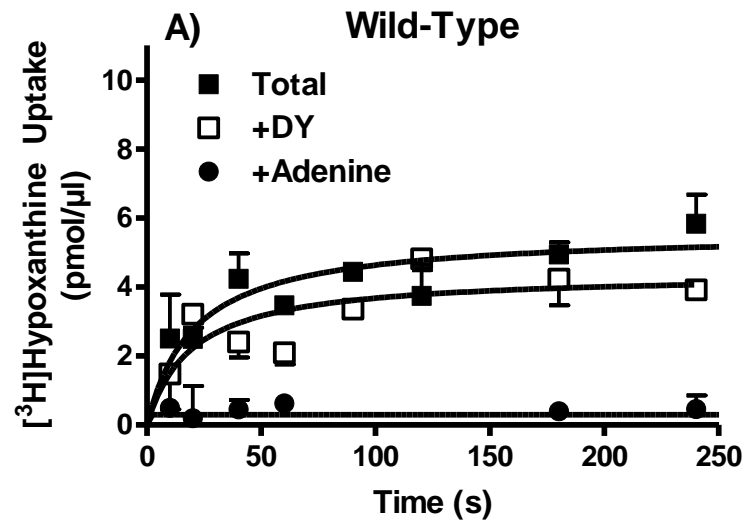
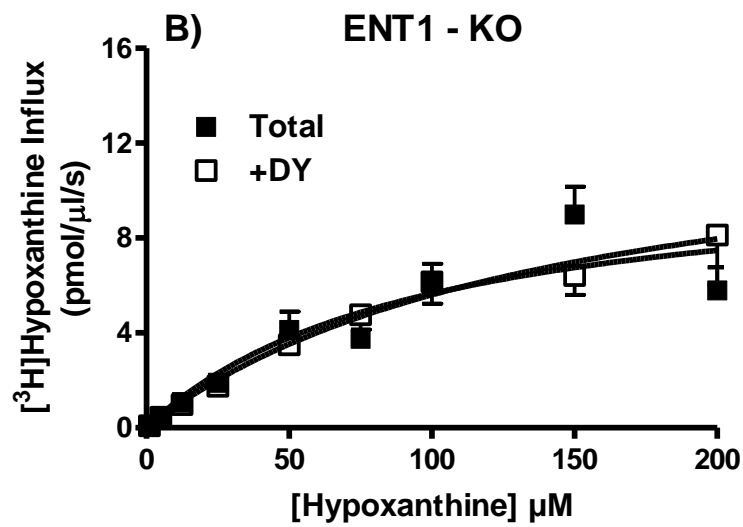
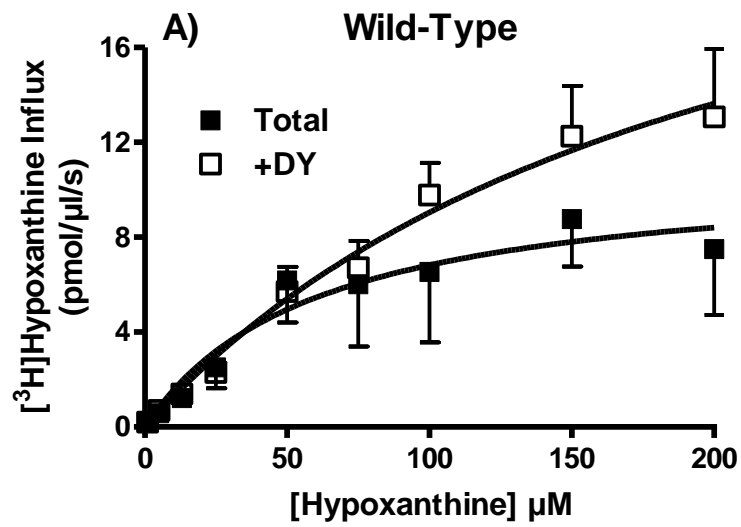




Figure 5.7. Dipyridamole enhanced  $[^3\text{H}]$ hypoxanthine uptake in WT, but not ENT1<sup>-/-</sup> MVECS.

MVECs isolated from either WT (A) or ENT1<sup>-/-</sup> (B) mice were incubated for 10 s with the indicated concentrations of  $[^3\text{H}]$ hypoxanthine (abscissa). Parallel assays were conducted in the absence and presence of 1 mM adenine with or without the inclusion of 10  $\mu\text{M}$  DY as described in Figure 5.6. Results are plotted as the transporter-mediated uptake of substrate (in pmol per  $\mu\text{l}$  of cell water accumulated per s;  $V_i$ , ordinate) after subtraction of the adenine-insensitive component. Each point is the mean  $\pm$  SEM from 5 experiments. The transporter kinetic constants derived from these data are shown in Table 5.2.



#### 5.3.4 Purine Metabolism in *ENT1*<sup>-/-</sup> MVECs

We examined the [<sup>3</sup>H]metabolite profile of WT and *ENT1*<sup>-/-</sup> MVECs after exposure to [<sup>3</sup>H]hypoxanthine under the conditions that we used for the uptake assays (Figure 5.8). *ENT1*<sup>-/-</sup> MVECs had significantly higher intracellular levels of [<sup>3</sup>H]hypoxanthine than did the WT MVECs after exposure to 100 μM [<sup>3</sup>H]hypoxanthine for 20 min. [<sup>3</sup>H]inosine levels showed a trend toward being increased in *ENT1*<sup>-/-</sup> MVECs; however, this difference was not significant unless dipyridamole was present to block the remaining ENT2-mediated efflux. The difference between the WT and *ENT1*<sup>-/-</sup> MVECs was also attenuated in the presence of the ENT blocker dipyridamole.

#### 5.3.5 Effects of Free Radical Generators on Purine Transport in Mouse MVECs

The hydroxy radical producing TBHP had no effect on ENT1, ENT2 or ENBT1 in primary mouse MVECs following 100 μM treatment for 30 minutes (Figure 5.9). Following treatment with the intracellular ROS generator menadione, the V<sub>max</sub> of ENT1 mediated 2-[<sup>3</sup>H]chloroadenosine uptake dropped significantly from 15.6 ± 2.7 pmol/μl/s to 4.9 ± 2.1 pmol/μl/s. The V<sub>max</sub> of ENT2 also appeared to drop, however the small amount of ENT2 present in mMVECs resulted in high background that prevented statistical analysis. [<sup>3</sup>H]Hypoxanthine mediated uptake via ENBT1 was not affected by menadione treatment, however the small amount of ENT2 mediated [<sup>3</sup>H]hypoxanthine uptake that was present in control cells appeared to be abolished in menadione treated cells (Figure 5.10).



Table 5.2 Kinetic parameters for the transporter-mediated uptake of 2-chloroadenosine and hypoxanthine by MVECs isolated from WT and ENT1<sup>-/-</sup> mice.

	WT			ENT1 <sup>-/-</sup>		
	Total	ENT1	ENT2	Total	ENT1	ENT2
<b>2-Chloroadenosine</b>						
V <sub>max</sub> (pmol/μl/s)	18 ± 3	24 ± 5	1.2 ± 0.5	-	nd *	0.19 ± 0.06 *
K <sub>m</sub> (μM)	84 ± 17	147 ± 44	9 ± 3	-	nd *	13 ± 6
	Total	DY -insensitive	ENT2	Total	DY -insensitive	ENT2
<b>Hypoxanthine</b>						
V <sub>max</sub> (pmol/μl/s)	12 ± 2	17 ± 4	nd	10 ± 2	12 ± 2	nd
K <sub>m</sub> (μM)	84 ± 20	126 ± 29	nd	96 ± 29	131 ± 32	nd

Values are means ± SEM; *n* = 5 WT and 5 ENT1<sup>-/-</sup> mice. MVECs, microvascular endothelial cells; WT, wild-type; ENT1<sup>-/-</sup>, ENT knockout; DY, dipyridamole; ND, no transport activity detected. \**P*<0.05, significant difference between WT and ENT1<sup>-/-</sup> (Student's *t*-test).

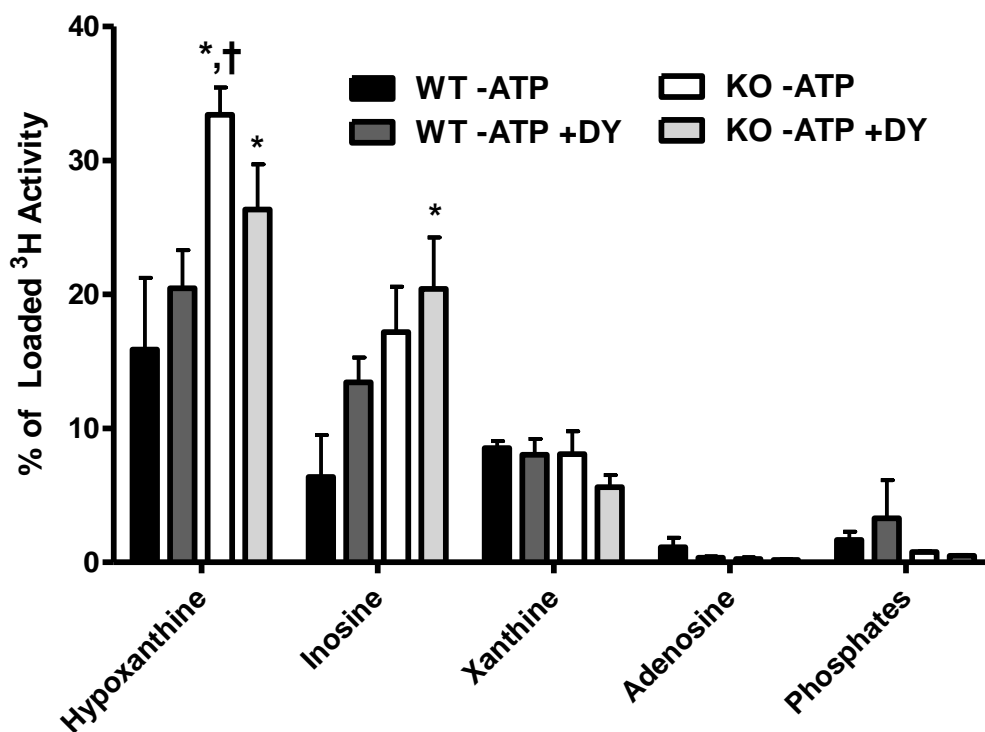


Figure 5.8. [<sup>3</sup>H]Metabolite profile in WT and ENT1<sup>-/-</sup> MVECs.

MVECs isolated from WT and ENT1<sup>-/-</sup> mice were depleted of ATP and incubated with 100 μM [<sup>3</sup>H]hypoxanthine in the absence and presence of 10 μM DY for 20 min. Acid extracts of cell pellets were neutralized with 1 M KOH, and aliquots were subjected to thin-layer chromatography as described in section 5.2.4. A repeated-measures ANOVA was performed within each metabolite group. \**P*<0.05 compared with WT -ATP condition; †*P*<0.05 compared with WT -ATP +DY condition.

### 5.3.6 Effects of Ischemia and Hypoxia on Purine Transporters

Treatment with the HIF-1 $\alpha$  stabilizer CoCl<sub>2</sub> resulted in a significant decrease in mENBT1 V<sub>max</sub> of [<sup>3</sup>H]hypoxanthine uptake to 21  $\pm$  10% of control. 2-[<sup>3</sup>H]Chloroadenosine uptake by mENT1 was not affected (Figure 5.11A-B). Exposure of cells to a simulated ischemic environment by mineral oil overlay caused significant reduction in ENBT1 V<sub>max</sub> in primary mouse MVECs. (Figure 5.11C). When cells were exposed to true hypoxia of 1% O<sub>2</sub> ENBT1 V<sub>max</sub> of [<sup>3</sup>H]hypoxanthine uptake increased significantly from 9.5  $\pm$  2.2 pmol/ $\mu$ l/s to 31.4  $\pm$  5.1 pmol/ $\mu$ l/s in MVECs (Figure 5.11D).



Figure 5.9. TBHP had no effect on purine transport.

Primary mouse MVECs were treated with 100  $\mu$ M TBHP for 30 minutes at 37°C. Uptake of 2- $^3$ H]chloroadenosine(A and B) and  $^3$ H]hypoxanthine (C and D) was determined as described in Chapter 2. Data are means  $\pm$  SEM of 6 (A and B) or 5 independent experiments (C and D).

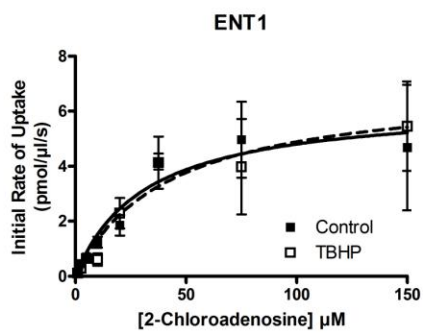
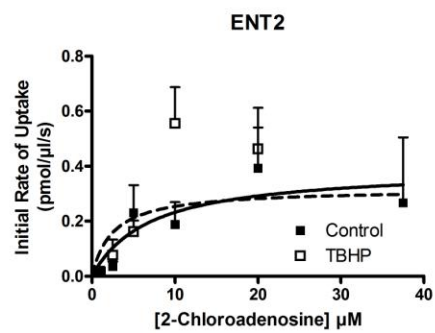
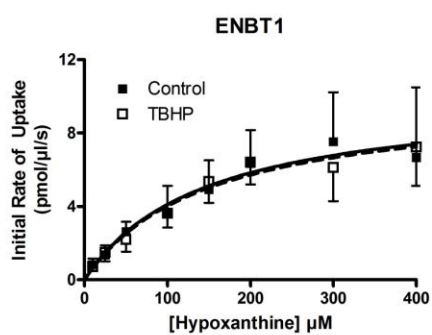
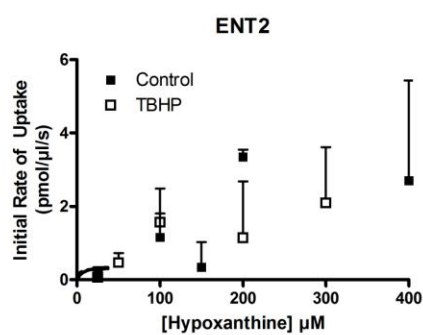
**A****B****C****D**



Figure 5.10. Menadione reduced the  $V_{\max}$  of ENT1 mediated 2-chloroadenosine uptake. Primary mouse MVECs were treated with 100  $\mu\text{M}$  menadione for 30 minutes at 37°C prior to uptake of 2- $^3\text{H}$ chloroadenosine (A and B) and  $^3\text{H}$ hypoxanthine (C and D). A) Uptake of 2- $^3\text{H}$ chloroadenosine by ENT1 following menadione treatment (open squares, dotted line) had a  $V_{\max}$  of  $4.9 \pm 2.1$  pmol/ $\mu\text{l/s}$  compared to the  $V_{\max}$  of control cells (solid squares, solid line) of  $15.6 \pm 2.7$  pmol/ $\mu\text{l/s}$ . Data are mean  $\pm$  SEM of three independent experiments,  $P < 0.05$  by two-tailed t-test. B) ENT2 mediated uptake of 2- $^3\text{H}$ chloroadenosine also appeared to decrease following menadione treatment but high variability prevented statistical analysis ( $n=3$ ). C) ENT1 mediated uptake of  $^3\text{H}$ hypoxanthine was not affected by menadione treatment ( $n=3$ ). D) ENT2 mediated uptake of  $^3\text{H}$ hypoxanthine was abolished ( $n=3$ ).



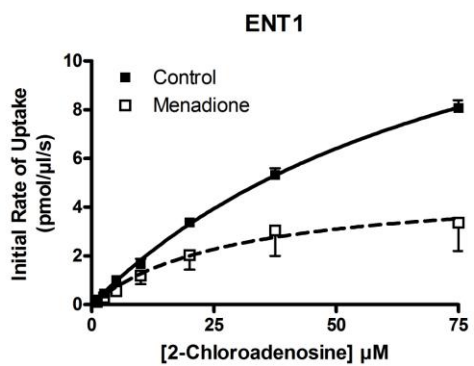
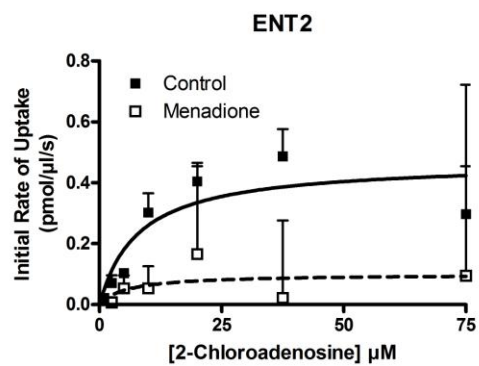
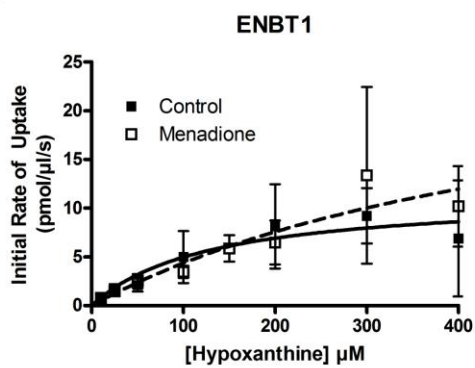
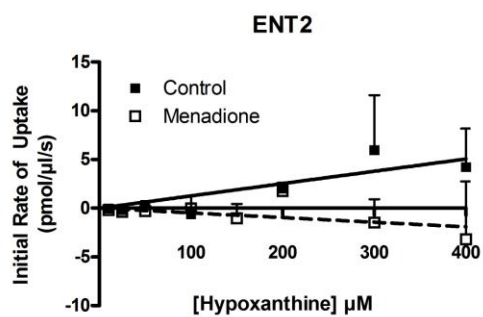
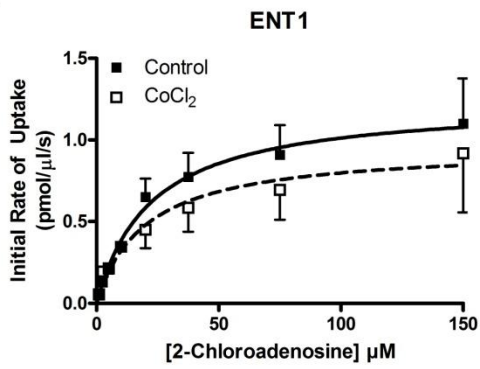
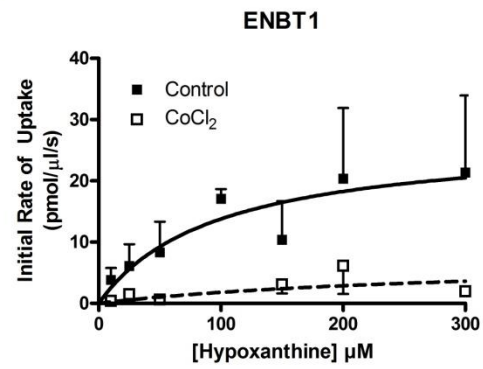
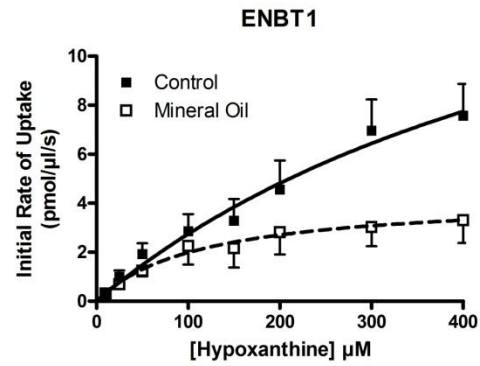
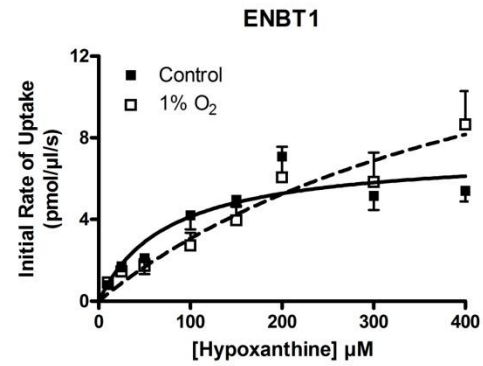
**A****B****C****D**



Figure 5.11. Hypoxanthine uptake can be altered by both ischemia and hypoxia in mouse MVECs.

Primary mouse MVECs were treated with 100  $\mu\text{M}$   $\text{CoCl}_2$  for 2 hr at 37°C. ENT1 and ENBT1 uptake of 2- $^3\text{H}$ chloroadenosine and  $^3\text{H}$ hypoxanthine, respectively, (A and B) was determined. Only ENBT1 function was altered. The  $V_{\text{max}}$  of  $\text{CoCl}_2$  treated cells (open squares, dotted line) decreased to  $21 \pm 10\%$  of control (solid squares, solid line). Data are means  $\pm$  SEM of 4 independent experiments for each substrate. C) MVECs were subjected to simulated ischemia by mineral oil overlay. The  $V_{\text{max}}$  of ENBT1 mediated uptake of  $^3\text{H}$ hypoxanthine dropped from  $23 \pm 6$  pmol/ $\mu\text{l/s}$  to  $5 \pm 1$  pmol/ $\mu\text{l/s}$  after 2 hr of simulated ischemia.  $P < 0.05$  two-tailed t-test,  $n = 4$ . D) Following exposure to 1%  $\text{O}_2$  for 2 hr, uptake of  $^3\text{H}$ hypoxanthine increased in primary mouse MVECs following hypoxia, with ENBT1  $V_{\text{max}}$  increasing from  $9.5 \pm 2.2$  pmol/ $\mu\text{l/s}$  to  $31.4 \pm 5.1$  pmol/ $\mu\text{l/s}$ ,  $P < 0.05$  two-tailed t-test,  $n = 3$ .

**A****B****C****D**

## 5.4. DISCUSSION

### 5.4.1 *Compensatory Changes in ENT1<sup>-/-</sup> MVECs*

We performed both semi-quantitative and quantitative real-time PCR to determine which purinergic genes, if any, had altered transcript expression as a result of the genetic loss of ENT1. Statistical differences in PCR were followed up by western blotting. While there were significant changes in adenosine receptor A<sub>3</sub> and ENT3 at the transcript level, the lack of correlation between changes in mRNA versus protein levels for these relatively low abundance transcripts may reflect posttranscriptional regulation of translation efficiency and protein processing. The significant increases in ADA and A<sub>2A</sub> transcripts were confirmed at the protein level as well. These adaptive changes can be rationalized, from a cell homeostasis perspective, if one assumes that the loss of ENT1 is leading to a reduced efflux of adenosine (arising from ATP metabolism) from the MVECs. This would result in an increased cytoplasmic adenosine and a decreased extracellular adenosine in the ENT1<sup>-/-</sup> compared with WT mice. The increase in ADA would lead to more adenosine metabolism to inosine, which may then be converted to either hypoxanthine or inosine monophosphate (2), thereby reducing intracellular adenosine. Adenosine has well-established vasodilatory (5) and anti-inflammatory activities (21), mediated in part via extracellular adenosine A<sub>2A</sub> receptors on vascular endothelial cells. Thus the increase in adenosine A<sub>2A</sub> receptor expression may be compensating for the lower levels of adenosine-mediated signaling in the ENT1<sup>-/-</sup> mice as a consequence of reduced extracellular adenosine concentrations. A previous study has also invoked lower extracellular adenosine levels as an explanation for the reduced A<sub>1</sub> adenosine

receptor signaling observed in the brains of ENT1<sup>-/-</sup> mice (12). In contrast to our findings in MVECs, there does not appear to be a compensatory upregulation of adenosine A<sub>2a</sub> receptors in cardiomyocytes isolated from the ENT1<sup>-/-</sup> mice (31), suggesting that different cell types respond differently to changes in adenosine bioavailability. With the consideration that adenosine receptor expression varies between different tissues and therefore adenosine has differing physiological effects in each tissue, the compensatory changes that would result from altered adenosine levels might be expected to differ in different tissues and cell types.

#### *5.4.2 Alterations in Purine Transport Capacity*

The WT MVECs accumulated both [<sup>3</sup>H]formycin B (Figure 5.4) and 2-[<sup>3</sup>H]chloroadenosine (Figure 5.5) via two distinct Na<sup>+</sup>-independent dipyriddyamole-sensitive processes (Table 5.2). The majority (~90%) of the substrate uptake in WT MVECs was inhibited by 50 nM NBMPR and hence was mediated by ENT1. The remainder of the uptake was inhibited by dipyriddyamole, but not NBMPR, and hence was mediated by ENT2. It is noteworthy that mouse MVECs are very different from rat MVECs where ENT2 mediates ~50% of the total nucleoside uptake (3). Thus one would expect an ENT1-selective inhibitor such as NBMPR to have a much greater effect on nucleoside levels in the cardiovascular system of mouse compared with its effects in rat. The lack of change in ENT2 mediated [<sup>3</sup>H]formycin B uptake corresponds to the lack of change in ENT2 transcript levels. The interesting observation that the 2-[<sup>3</sup>H]chloroadenosine V<sub>max</sub> for ENT2 was significantly decreased in ENT1<sup>-/-</sup> knockout cells may be an artifact of the uptake procedure, as ENT2 mediated uptake is defined as

2-[<sup>3</sup>H]chloroadenosine uptake in the presence of 50 nM NBMPR, to inhibit ENT1 transport function.

Mouse MVECs appear to have a dipyridamole-insensitive nucleobase transporter very similar to the ENBT1 transporter described in detail in Chapter 3, and therefore quite possibly was the mouse ortholog of the human transporter. As such, ENBT1 was used to refer to the dipyridamole-insensitive hypoxanthine transporter in mMVECs. Hypoxanthine is a metabolite of adenosine metabolism and would be produced in the endothelial cells under conditions of high adenosine release from surrounding cells, such as would occur during tissue ischemia (2; 15; 16). This hypoxanthine is metabolized intracellularly by xanthine oxidase with the consequent production of reactive oxygen species. Reactive oxygen species are believed to play a role in mediating the endothelial dysfunction observed in various pathological conditions including diabetes and ischemia-reperfusion injury (6; 20; 32). Therefore, understanding how MVECs handle hypoxanthine is important in the overall evaluation of purine metabolism in the vasculature. It appears that both mouse and human MVECs, which have low or no ENT2, respectively, rely heavily on this nucleobase transporter for the transfer of nucleobases across the cell membrane. Rat MVECs, on the other hand, which express high levels of ENT2 (which can transport nucleobases), do not appear to express functional ENBT1. Further studies on this novel nucleobase transport system are needed.

When studying ENBT1 transport kinetics in mouse MVECs, it was found that the ENT2 blocker dipyridamole caused an apparent increase in  $V_{max}$  in WT cells but had no effect in ENT1<sup>-/-</sup> cells (Figure 5.7). Given that part of the hypoxanthine uptake in the MVECs

would be due to the activity of ENT2, one should actually expect to see a small decrease in hypoxanthine uptake in the presence of dipyridamole. One interpretation of these data is that dipyridamole was blocking the efflux of a metabolite of hypoxanthine via ENT1. In normal cell metabolism, hypoxanthine is typically formed as a metabolite of inosine and is efficiently metabolized by xanthine oxidase to xanthine or by HGPRT to inosine monophosphate such that there is little free hypoxanthine in cells. However, under the experimental conditions used in this study, where cells are exposed to high concentrations of hypoxanthine, it is possible that the [<sup>3</sup>H]hypoxanthine is being metabolized to [<sup>3</sup>H]inosine via purine nucleoside phosphorylase (9). As noted above, inosine is a substrate for ENT2 and ENT1, both of which are blocked by dipyridamole. The WT MVECs, with their high level of expression of ENT1, would release the [<sup>3</sup>H]inosine formed in this way much more rapidly than would the ENT1-deficient cells and would thus be more sensitive to the effects of dipyridamole. To test this hypothesis, a [<sup>3</sup>H]metabolite profile was produced using a 1-D TLC method. The profile generated (Figure 5.8) supported the idea that [<sup>3</sup>H]hypoxanthine is being metabolized to [<sup>3</sup>H]inosine by nucleoside phosphorylase under these assay conditions and that this [<sup>3</sup>H]inosine is not released from ENT1<sup>-/-</sup> cells as effectively as it is from WT MVECs. These data also show that the ATP-depletion protocol used led to the expected reduction in the conversion of hypoxanthine to its phosphorylated metabolites.

#### *5.4.3 Impact of Ischemia and Hypoxia on Purine Transport in WT MVECs*

The oxidation of proteins is known to result in altered function. To determine how nucleoside and nucleobase transporters respond to the presence of increased ROS,



cultured primary cells were treated with extracellular (TBHP) or intracellular (menadione) ROS generators. Only menadione affected transport, and resulted in decreased transport capacity. This effect was similar to that observed in primary human MVECs in Chapter 4. Menadione (2-methyl-1,4-naphthoquinone) produces ROS intracellularly via metabolism by NAD(P)H:quinone oxidoreductase 1 in a redox cycling manner, directly generating superoxide anions(14). This is in contrast to TBHP, a peroxide, which forms hydroxyl radicals in the presence of iron via the Fenton reaction, or in the presence of superoxide anions by the Haber-Wells reaction. Peroxides are also detoxified to water and oxygen enzymatically by glutathione peroxidase (26). Thus, it is possible that the lack of effect of TBHP on purine transport could be at least three fold: 1) the conditions were not suitable for hydroxyl radicals to be formed, 2) glutathione peroxidase removed all TBHP prior to radical formation, or 3) ENT1 and ENBT1 transporters are not sensitive to oxidation by hydroxyl radicals.

The superoxide anions produced by menadione are usually short lived and are converted into hydrogen peroxide by superoxide dismutase. However, in the presence of nitric oxide (NO) which is produced by endothelial nitric oxide synthase, the two radicals combine to form peroxynitrite ( $\text{ONOO}^-$ ), a much more potent oxidizing agent (34). Peroxynitrite has been shown to decrease the function of other transport proteins including the high affinity choline transporter, the human serotonin transporter(8), and the human dopamine transporter (29). Therefore it is possible that that the decrease in ENT1 and ENT2 function observed following mMVEC exposure to menadione was the result of peroxynitrite formation.

It has been previously established that ENT1 is a target of the HIF-1 $\alpha$  transcription factor(1; 18). However the time required for a down-regulation was upwards of 8 hr (18). It was unknown if the nucleobase transporter ENBT1 was also a target. Initial experiments were conducted with the known HIF-1 $\alpha$  stabilizer, CoCl<sub>2</sub> (30). Treatment with 100  $\mu$ M CoCl<sub>2</sub> for 2 hr was only capable of reducing transport function of ENBT1, not ENT1. The treatment time used was much less than that known to cause HIF mediated ENT1 down-regulation but was chosen to reflect an acute ischemic event in the vasculature. In Chapter 4, it was shown that CoCl<sub>2</sub> has no effect on human transporters. CoCl<sub>2</sub> has also been shown to generate ROS in addition to HIF-1 $\alpha$  stabilization, and the effects of CoCl<sub>2</sub> are selectively blocked by the antioxidant ascorbic acid (vitamin C)(13). A major difference between the mouse and human MVEC medium was that the CoCl<sub>2</sub> added to the human medium contained an additional supplementation of ascorbic acid (concentration unknown; proprietary information). Therefore, the lack of similar ENBT1 down-regulation in hMVECs may have been due to the protective presence of ascorbic acid.

The nucleobase transporter ENBT1 was extremely sensitive to 2 hr of simulated ischemia with hypoxanthine uptake function being reduced by approximately 80%, similar to that of the human ENBT1 as shown in Chapter 4. The increase in  $V_{\max}$  of ENBT1 mediated [<sup>3</sup>H]hypoxanthine uptake after 2 hr of hypoxia (1% O<sub>2</sub>) suggests that ischemia and hypoxia cause differential effects in mouse MVECs. Since these assays were conducted in ATP-replete conditions as not to interfere with any regulatory processes, the most likely explanation for the apparent increased  $V_{\max}$  is due to increases in

[<sup>3</sup>H]hypoxanthine metabolism. Hypoxia is known to convert xanthine dehydrogenase to the hypoxanthine metabolizing xanthine oxidase.

#### *5.4.4 Conclusions*

The loss of ENT1 in the ENT1<sup>-/-</sup> mice leads to a dramatic reduction in the ability of MVECs to accumulate and release nucleosides such as adenosine. Despite this loss of nucleoside transport capacity, the ENT1<sup>-/-</sup> mice appear phenotypically normal under baseline conditions. There did not appear to be any compensatory upregulation of the other major plasma membrane nucleoside transporter ENT2 in the ENT1<sup>-/-</sup> mice, but there were increases in both ADA and A<sub>2A</sub> adenosine receptor expression in MVECs and the skeletal muscle tissue from which the cells were isolated. The consequent changes in adenosine metabolism and adenosine-mediated signaling via the A<sub>2A</sub> receptor likely compensate for decreased extracellular adenosine levels in the ENT1<sup>-/-</sup> mice and allow them to function normally under baseline conditions. However, given the widely acknowledged role of adenosine as a cardioprotectant in conditions of cardiovascular stress, it might be anticipated that the ENT1<sup>-/-</sup> mice will be less able to respond to cardiovascular stresses associated with conditions such as diabetes and ischemia-reperfusion injury. Alternatively, a reduced uptake of extracellular adenosine might potentiate adenosine-receptor activation and subsequent cardioprotection, suggesting that ENT1<sup>-/-</sup> mice might be permanently preconditioned (22; 23) and thus protected from ischemic or hypoxic challenge.

The studies in this chapter have provided the ground work for studying the role of purine transporters in oxidative stress in the microvasculature. Observations that the

hypoxanthine transporter, ENBT1 is affected by both intracellular ROS and ischemia point to ENBT1 being a contributing factor to endothelial dysfunction following an ischemic insult. Using the ENT1<sup>-/-</sup> MVECs will establish how ENT1 and thus adenosine transport contribute to the generation of ROS and the impact on ENBT1 function.

## 5.5 REFERENCES

1. **Abdulla P and Coe IR.** Characterization and functional analysis of the promoter for the human equilibrative nucleoside transporter gene, hENT1. *Nucleosides Nucleotides Nucleic Acids* 26: 99-110, 2007.
2. **Arch JR and Newsholme EA.** The control of the metabolism and the hormonal role of adenosine. *Essays Biochem* 14:82-123.: 82-123, 1978.
3. **Archer RG, Pitelka V and Hammond JR.** Nucleoside transporter subtype expression and function in rat skeletal muscle microvascular endothelial cells. *Br J Pharmacol* 143: 202-214, 2004.
4. **Baldwin SA, Beal PR, Yao SY, King AE, Cass CE and Young JD.** The equilibrative nucleoside transporter family, SLC29. *Pflugers Arch* 447: 735-743, 2004.
5. **Belardinelli L, Shryock JC, Snowdy S, Zhang Y, Monopoli A, Lozza G, Ongini E, Olsson RA and Dennis DM.** The A2A adenosine receptor mediates coronary vasodilation. *J Pharmacol Exp Ther* 284: 1066-1073, 1998.
6. **Berry CE and Hare JM.** Xanthine oxidoreductase and cardiovascular disease: molecular mechanisms and pathophysiological implications. *J Physiol* 555: 589-606, 2004.
7. **Bone DB and Hammond JR.** Nucleoside and nucleobase transporters of primary human cardiac microvascular endothelial cells: characterization of a novel nucleobase transporter. *Am J Physiol Heart Circ Physiol* 293: H3325-H3332, 2007.
8. **Bryan-Lluka LJ, Papacostas MH, Paczkowski FA and Wanstall JC.** Nitric oxide donors inhibit 5-hydroxytryptamine (5-HT) uptake by the human 5-HT transporter (SERT). *Br J Pharmacol* 143: 63-70, 2004.
9. **Bzowska A, Kulikowska E and Shugar D.** Purine nucleoside phosphorylases: properties, functions, and clinical aspects. *Pharmacol Ther* 88: 349-425, 2000.

10. **Carreira MC, Camina JP, Diaz-Rodriguez E, Alvear-Perez R, Llorens-Cortes C and Casanueva FF.** Adenosine does not bind to the growth hormone secretagogue receptor type-1a (GHS-R1a). *J Endocrinol* 191: 147-157, 2006.
11. **Chen J, Rinaldo L, Lim SJ, Young H, Messing RO and Choi DS.** The type 1 equilibrative nucleoside transporter regulates anxiety-like behavior in mice. *Genes Brain Behav* 6: 776-783, 2007.
12. **Choi DS, Cascini MG, Mailliard W, Young H, Paredes P, McMahon T, Diamond I, Bonci A and Messing RO.** The type 1 equilibrative nucleoside transporter regulates ethanol intoxication and preference. *Nat Neurosci* 7: 855-861, 2004.
13. **Ciafre SA, Niola F, Giorda E, Farace MG and Caporossi D.** CoCl<sub>2</sub>-simulated hypoxia in skeletal muscle cell lines: Role of free radicals in gene up-regulation and induction of apoptosis. *Free Radic Res* 41: 391-401, 2007.
14. **Criddle DN, Gillies S, Baumgartner-Wilson HK, Jaffar M, Chinje EC, Passmore S, Chvanov M, Barrow S, Gerasimenko OV, Tepikin AV, Sutton R and Petersen OH.** Menadione-induced reactive oxygen species generation via redox cycling promotes apoptosis of murine pancreatic acinar cells. *J Biol Chem* 281: 40485-40492, 2006.
15. **Deussen A.** Metabolic flux rates of adenosine in the heart. *Naunyn Schmiedebergs Arch Pharmacol* 362: 351-363, 2000.
16. **Deussen A.** Quantitative integration of different sites of adenosine metabolism in the heart. *Ann Biomed Eng* 28: 877-883, 2000.
17. **Dunwiddie TV and Masino SA.** The role and regulation of adenosine in the central nervous system. *Annu Rev Neurosci* 24:31-55.: 31-55, 2001.
18. **Eltzschig HK, Abdulla P, Hoffman E, Hamilton KE, Daniels D, Schonfeld C, Loffler M, Reyes G, Duszenko M, Karhausen J, Robinson A, Westerman KA, Coe IR and Colgan SP.** HIF-1-dependent repression of equilibrative nucleoside transporter (ENT) in hypoxia. *J Exp Med* 202: 1493-1505, 2005.
19. **Feoktistov I, Goldstein AE, Ryzhov S, Zeng D, Belardinelli L, Voyno-Yasenetskaya T and Biaggioni I.** Differential expression of adenosine receptors in

human endothelial cells: role of A2B receptors in angiogenic factor regulation. *Circ Res* 90: 531-538, 2002.

20. **Hack B, Witting PK, Rayner BS, Stocker R and Headrick JP.** Oxidant stress and damage in post-ischemic mouse hearts: effects of adenosine. *Mol Cell Biochem* 287: 165-175, 2006.
21. **Hasko G and Pacher P.** A2A receptors in inflammation and injury: lessons learned from transgenic animals. *J Leukoc Biol* 83: 447-455, 2008.
22. **Linden J.** Adenosine in tissue protection and tissue regeneration. *Mol Pharmacol* 67: 1385-1387, 2005.
23. **Loffler M, Morote-Garcia JC, Eltzschig SA, Coe IR and Eltzschig HK.** Physiological roles of vascular nucleoside transporters. *Arterioscler Thromb Vasc Biol* 27: 1004-1013, 2007.
24. **Meldrum KK, Meldrum DR, Hile KL, Burnett AL and Harken AH.** A novel model of ischemia in renal tubular cells which closely parallels in vivo injury. *J Surg Res* 99: 288-293, 2001.
25. **Metz S, Holland S, Johnson L, Espling E, Rabaglia M, Segu V, Brockenbrough JS and Tran PO.** Inosine-5'-monophosphate dehydrogenase is required for mitogenic competence of transformed pancreatic beta cells. *Endocrinology* 142: 193-204, 2001.
26. **Misra MK, Sarwat M, Bhakuni P, Tuteja R and Tuteja N.** Oxidative stress and ischemic myocardial syndromes. *Med Sci Monit* 15: RA209-RA219, 2009.
27. **Mortellaro A, Hernandez RJ, Guerrini MM, Carlucci F, Tabucchi A, Ponzoni M, Sanvito F, Doglioni C, Di SC, Biasco L, Follenzi A, Naldini L, Bordignon C, Roncarolo MG and Aiuti A.** Ex vivo gene therapy with lentiviral vectors rescues adenosine deaminase (ADA)-deficient mice and corrects their immune and metabolic defects. *Blood* 108: 2979-2988, 2006.
28. **Mubagwa K and Flameng W.** Adenosine, adenosine receptors and myocardial protection: an updated overview. *Cardiovasc Res* 52: 25-39, 2001.

29. **Park SU, Ferrer JV, Javitch JA and Kuhn DM.** Peroxynitrite inactivates the human dopamine transporter by modification of cysteine 342: potential mechanism of neurotoxicity in dopamine neurons. *J Neurosci* 22: 4399-4405, 2002.
30. **Ran R, Xu H, Lu A, Bernaudin M and Sharp FR.** Hypoxia preconditioning in the brain. *Dev Neurosci* 27: 87-92, 2005.
31. **Rose JB, Naydenova Z, Bang A, Eguchi M, Sweeney G, Choi DS, Hammond JR and Coe IR.** Equilibrative nucleoside transporter 1 plays an essential role in cardioprotection. *Am J Physiol Heart Circ Physiol* 298: H771-H777, 2010.
32. **Salas A, Panes J, Elizalde JI, Granger DN and Pique JM.** Reperfusion-induced oxidative stress in diabetes: cellular and enzymatic sources. *J Leukoc Biol* 66: 59-66, 1999.
33. **Shimizu H, Daly JW and Creveling CR.** A radioisotopic method for measuring the formation of adenosine 3',5'-cyclic monophosphate in incubated slices of brain. *J Neurochem* 16: 1609-1619, 1969.
34. **Weseler AR and Bast A.** Oxidative stress and vascular function: implications for pharmacologic treatments. *Curr Hypertens Rep* 12: 154-161, 2010.
35. **Zhang J, Visser F, King KM, Baldwin SA, Young JD and Cass CE.** The role of nucleoside transporters in cancer chemotherapy with nucleoside drugs. *Cancer Metastasis Rev* 26: 85-110, 2007.



## CHAPTER SIX

ADDITIONAL PHENOTYPES OF THE ENT1<sup>-/-</sup> MOUSE: FROM HYPOTENSION TO  
SPINAL HYPEROSTOSIS.

## 6.1 Introduction

The equilibrative nucleoside transporter 1 (ENT1; SLC29A1) is the predominant nucleoside transporter expressed in mammalian cells. ENT1 is a sodium-independent, facilitative diffusion transporter that is responsible for the movement of hydrophilic nucleosides, like the purine adenosine, across biological membranes in a concentration dependent manner. Pharmacological inhibition of ENT1 has been shown to increase local adenosine levels and promote the cardio- and neuro-protective actions of the nucleoside.

An ENT1<sup>-/-</sup> mouse has been generated by Choi and his collaborators (4). ENT1<sup>-/-</sup> mice were viable but had a slightly lower body weight upon reaching maturity. The behaviour of the ENT1<sup>-/-</sup> mice is altered compared to their wild-type (WT) counterparts, especially in respect to increased ethanol consumption (4) and decreased anxiety (3).

Work in our lab has explored changes at the cellular level in the microvascular endothelium (MVEC) and in cardiomyocytes. In MVECs, ENT1 loss results in an increase in both adenosine receptor A<sub>2A</sub> and adenosine deaminase transcript and protein(1). Cardiomyocytes from ENT1<sup>-/-</sup> mice are more resistant to ischemic insult(23).

Despite the work that has already been done, a complete phenotype of the ENT1<sup>-/-</sup> mouse has not been described. In particular it is unknown what phenotypes manifest as the mouse ages. Here we report for the first time novel cardiovascular and skeletal phenotypes of the ENT1<sup>-/-</sup> mouse.

## 6.2 Materials and Methods

### 6.2.1 Animals

ENT1<sup>-/-</sup> mice were generated in the laboratory of Dr. Doo-Sup Choi as described previously(4); ENT1<sup>-/-</sup> mice were backcrossed with outbred WT C57BL/6 mice to generate ENT1<sup>-/+</sup> mice. ENT1<sup>-/-</sup> had reduced reproductive viability, therefore only ENT1<sup>-/+</sup> mice were crossed (producing ENT1<sup>+/+</sup>, ENT1<sup>+/-</sup>, and ENT1<sup>-/-</sup> offspring) to establish a breeding colony at the University of Western Ontario. Genotyping was done using isolated genomic DNA and standard PCR as previously described(1). All aspects of this study were conducted in accordance with the policies and guidelines set forth by the Canadian Council on Animal Care and were approved by the Animal Use Committee of the University of Western Ontario.

### 6.2.2 Quantitative Real-Time PCR

Female ENT1<sup>-/-</sup> and wild type mice were sacrificed simultaneously at 4 to 6 weeks of age. Whole heart, brain and kidney samples were extracted and placed in 10 ml guanidine thiocyanate (GTC) buffer (4.2M GTC, 25mM sodium citrate, 1mM EDTA, 0.7% (v/v) 2-mercapto-ethanol, in distilled water; pH adjusted to 7.0) per gram of tissue. Tissue was homogenized using a Polytron® benchtop homogenizer. First-strand DNA template was generated using 5 µg (MVECs) of DNaseI (Invitrogen, Carlsbad, CA)-treated total RNA and the Superscript First Strand Synthesis System for RT-PCR using oligo d(T) primers (Invitrogen). Quantitative real-time PCR analysis was performed using a Roche LightCycler (Roche Applied Sciences, Mississauga, ON, Canada) as described in Chapter 5, section 5.2.5.

### 6.2.3 Haemodynamics

Heart rate and blood pressure were determined using the CODA-6 non-invasive tail-cuff machine (Kent Scientific) (8). Where needed, anaesthesia was induced using ketamine/xylazine at 80% of a 100/10 mg/kg dose. Anaesthetized animals were kept on a heated pad to prevent loss of body temperature. Animals were subjected to five acclimatization rounds (no data collection) followed by two separate acquisition cycles of 15 measurements each. There was a 60 second rest between acquisition cycles. The tail cuff deflated over a period of 20 seconds during data acquisition.

### 6.2.4 High Performance Liquid Chromatography

Three month old mice were anaesthetized with pentobarbital and blood was collected by cardiac puncture into a syringe containing 118 mM NaCl, 5mM KCl, 13.2mM EDTA, 10 $\mu$ M 5-iodotubercidin, 100 $\mu$ M *erythro*-9-(2-Hydroxy-3-nonyl)adenine hydrochloride (EHNA), and 10 $\mu$ M dilazep (21). Serum was isolated by centrifugation at 3000 x g for 10 minutes at 4°C. Serum was applied to a 10 kDa cutoff ultra-filtration column and centrifuged at 14 000 x g for 15 minutes at 4°C. Filtrate was used for HPLC analysis(5). Filtered serum was analyzed on an Onyx monolithic C18 column with a slightly modified protocol established by Farthing D *et al* (5) in which adenosine was detected with a UV-detector at 260nm and adenosine metabolites were detected at 250nm, instead of all compounds being detected at 250nm.

### 6.2.5 Micro Computed Tomography ( $\mu$ CT) Imaging

Formalin fixed or snap frozen whole mice and spines were imaged in collaboration with Dr. David Holdsworth at the Preclinical Imaging Research Centre at Robarts Research

Institute (London, ON) using the *explore speCZT* scanner (GE Healthcare Biosciences, London, Ontario, Canada). Data were acquired with an x-ray tube voltage of 90 kV and a current of 40 mA. In one continuous rotation, 900 views were obtained at an angular increment of  $0.4^\circ$ . The scan time was 5 minutes. A calibrating phantom, consisting of a vial of water, air and a synthetic bone (SB3), was imaged together with the specimens. Images were acquired at isotropic voxel size of 50  $\mu\text{m}$  and reconstructed into 3D images, at the same voxel size, using a modified conebeam algorithm (6). The reconstructed data were expressed in Hounsfield units by calibrating the grey level values against those of water and air.

#### *6.2.6 Histology*

Spines and joints were dissected from WT and  $\text{ENT1}^{-/-}$  mice of various ages and fixed in 10% neutral buffered formalin. Samples were processed by The Molecular Pathology Laboratory at Robarts Research Institute (London, ON) and were decalcified before being embedded in paraffin, sectioned, and stained with hematoxylin and eosin (H&E).

#### *6.2.7 Scanning Electron Microscopy*

A small section of spine isolated from an  $\text{ENT1}^{-/-}$  mouse that included two vertebrae and their corresponding intervertebral space was sent to The Nanofabrication Facility at the University of Western Ontario. The sample was analyzed with a Leo (Zeiss) 1540XB scanning electron microscope (SEM).

## 6.3 Results

### 6.3.1 Changes in Purinergic Genes in Organs

Organs were chosen with respect to known adenosine physiology. ENT2 transcript levels were found to be significantly increased in the kidney and significantly decreased in the heart of ENT1<sup>-/-</sup> mice as compared to their wild type litter mates. CNT2 expression was found to be significantly elevated in both kidney and brain tissue from ENT1<sup>-/-</sup> mice. Adenosine receptor A<sub>2A</sub> transcript levels were significantly higher in brain tissue of ENT1<sup>-/-</sup> mice and significantly lower in the heart as compared to the wild type. There was no difference in A<sub>2A</sub> expression between wild type and ENT1<sup>-/-</sup> kidney samples. Expression of adenosine deaminase (ADA), purine nucleoside phosphorylase (PNP) and xanthine oxidase (XO) was compared between wild type and ENT1<sup>-/-</sup> kidney, brain and heart samples. ADA transcript was present at a significantly higher level in kidney samples of ENT1<sup>-/-</sup> mice as compared to the wild type. No significant differences in ADA expression were observed in brain or heart. PNP expression was also significantly elevated in ENT1<sup>-/-</sup> kidneys compared to the wild type with no differences in expression of this gene in the brain or heart. XO expression was shown to be significantly lower in ENT1<sup>-/-</sup> mouse brain tissue than in wild type brain tissue. No significant differences in XO expression were found in kidney or heart samples (Figure 6.1).

### 6.3.2 Haemodynamics

The heart rate of awake WT mice was 680 ± 20 beats/minute and was significantly higher than the 590 ± 20 beats/minute heart rate of ENT1<sup>-/-</sup> mice (n=7; P<0.05 Student's t-test) (Figure 6.2). There was no strain-related difference in blood pressure between

awake animals. However, when the animals were anaesthetized, the heart rate for both WT and ENT1<sup>-/-</sup> mice was the same, 440 ± 20 and 430 ± 20 beats/minute respectively. To ensure animals were on an equal baseline, all subsequent measurements were performed on anaesthetized mice. In mice aged 2-3 months, WT mice had significantly higher blood pressure than their ENT1<sup>-/-</sup> counterparts, systolic: 131 ± 12 mm/Hg, 115 ± 5 mm/Hg; diastolic: 99 ± 9 mm/Hg, 80 ± 6 mm/Hg; mean arterial pressure: 110 ± 10 mm/Hg, 91 ± 5 mm/Hg respectively. Interestingly, mice aged >6 months did not. In fact there was a trend towards the reverse with older ENT1<sup>-/-</sup> mice having elevated blood pressure compared to their WT counterparts (Figure 6.2).

### 6.3.3 Plasma Purines

Free plasma adenosine in WT animals was 600 ± 100 ng/ml where as ENT1<sup>-/-</sup> animals had 2.75 fold higher levels at 1650 ± 370 ng/ml (Figure 6.3).

### 6.3.4 Unexpected Paresis and Paralysis

During the studies leading to the publication by Bone *et al.* (2), a number of ENT1<sup>-/-</sup> mice were left to age without any intervention, simply for the sake of not wanting to sacrifice the poorly breeding genotype. When ENT1<sup>-/-</sup> mice reached an age of around 8 months it was noted that they had decreased mobility in their hind limbs. Mice would live from anywhere between 12 and 16 months of age before their condition required euthanasia. Some mice requiring euthanasia had complete paralysis of their hind limbs. All mice had abnormal curved spines that were extremely rigid; freshly euthanized ENT1<sup>-/-</sup> mice were unable to be laid out flat on their backs. Any ENT1<sup>-/-</sup> mouse to reach this age





Figure 6.1. Purinergic gene changes in other organs.

Purinergic genes of interest were examined by quantitative real-time PCR. Solid bars represent wild-type (WT) mRNA levels while open bars represent ENT1<sup>-/-</sup> (KO) mRNA levels, normalized to  $\beta$ -actin. Statistical comparisons were made between WT and KO per gene per organ. No comparisons were made between genes or between organs. ENT2, equilibrative nucleoside transporter 2; CNT2, concentrative nucleoside transporter 2; ADA, adenosine deaminase; PNP, purine nucleoside phosphorylase; XO, xanthine oxidase; A<sub>2a</sub>, adenosine receptor 2A. \*P<0.05 two-tailed t-test, n  $\geq$  3.

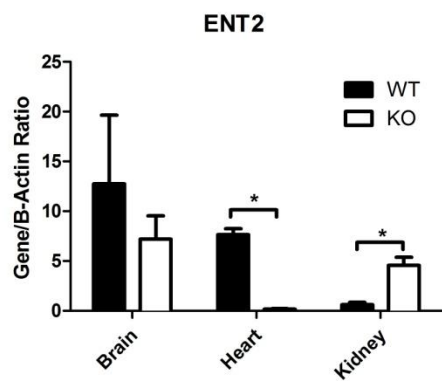
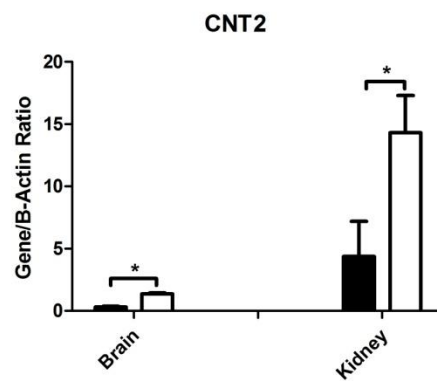
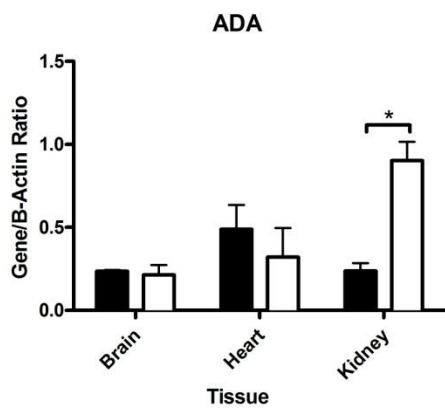
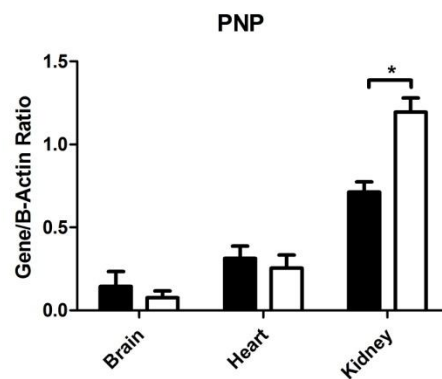
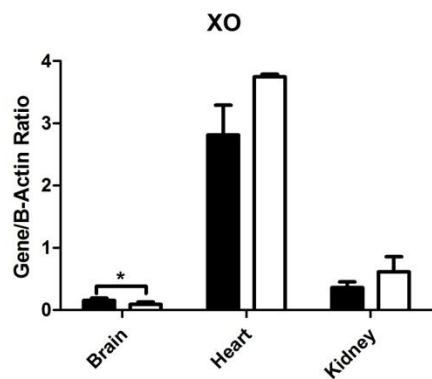
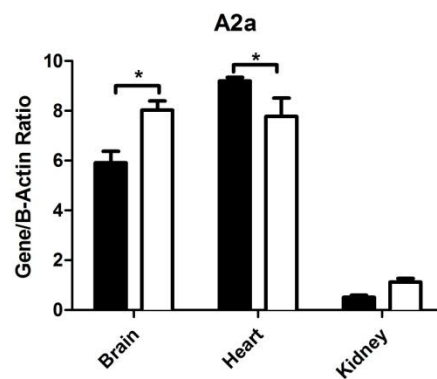
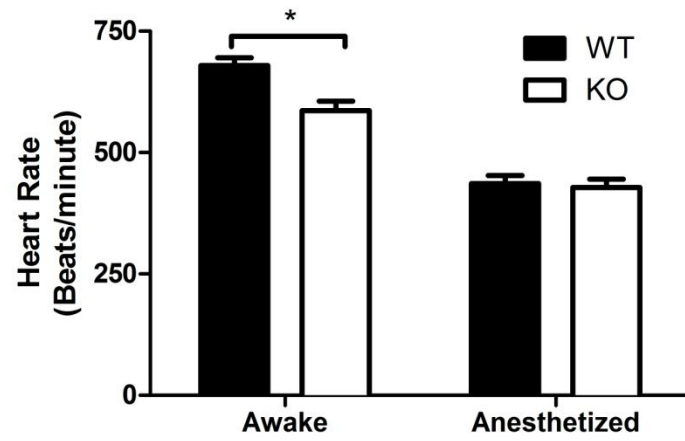
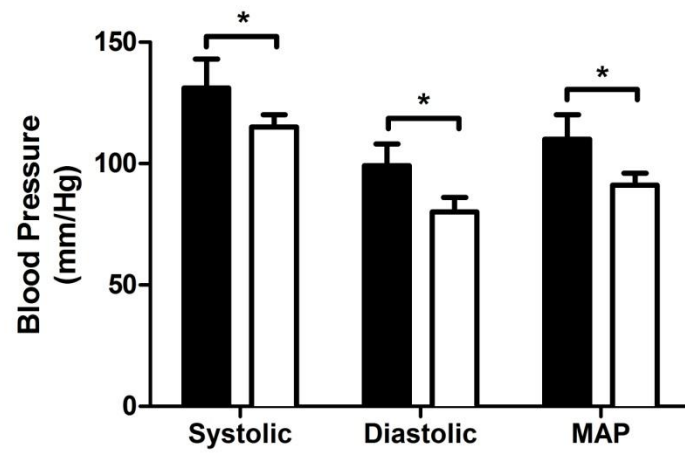
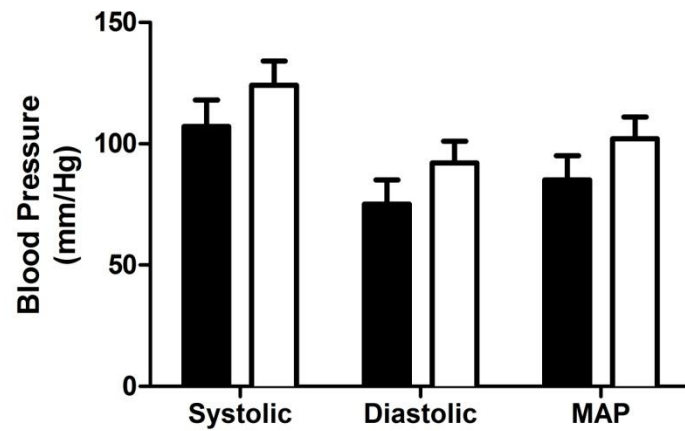
**A****B****C****D****E****F**



Figure 6.2. ENT1<sup>-/-</sup> mice have lower blood pressure than WT mice.

Aged matched male mice were analyzed with a CODA-6 non-invasive tail-cuff machine as described in the methods. A) Heart rates of awake WT and ENT1<sup>-/-</sup> mice were determined. WT mice had an elevated mean heart rate of  $680 \pm 20$  beats/minute compared to  $590 \pm 20$  beats/minute heart rate of ENT1<sup>-/-</sup> mice ( $n=7$ ;  $P<0.05$  Student's t-test). There was no difference between the heart rate of anaesthetized animals at  $440 \pm 20$  and  $430 \pm 20$  beats/minute for WT and ENT1<sup>-/-</sup> animals respectively. B) Blood pressure of anaesthetized 2-3 month old male mice was determined. C) Blood pressure was determined in anaesthetized WT and ENT1<sup>-/-</sup> mice older than 6 months. No statistical differences were observed however there was a trend towards increased pressure in the ENT1<sup>-/-</sup> mice.

**A****B****C**

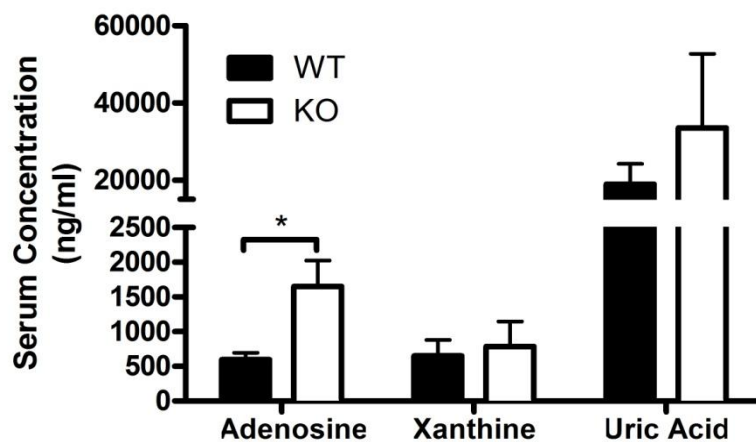


Figure 6.3. Circulating plasma adenosine is elevated in  $ENT1^{-/-}$  mice.

Blood was obtained from age matched WT and  $ENT1^{-/-}$  mice via cardiac puncture and processed for HPLC analysis as described in the methods. Adenosine levels were significantly elevated in  $ENT1^{-/-}$  mice at  $1650 \pm 370$  ng/ml compared to  $600 \pm 100$  ng/ml in WT mice. There were no differences in xanthine or uric acid concentrations.

developed these symptoms. A post-mortem analysis conducted on one male  $ENT1^{-/-}$  mouse revealed the presence of hard, white deposits on the ventral side of the spine. These deposits were most numerous in the thoracic region however, they did extend into the lumbar spine. In the lumbar region, the lesions were much more organized and appeared to be localized in the intervertebral space (Figure 6.4).

#### *6.3.5 Histology*

Histological examination of formalin-fixed, decalcified, paraffin-embedded sections of spine confirmed the lesions were associated with the intervertebral spaces and were large, irregular accumulations of eosinophilic, amorphous material. In fact, the lesions appeared to have replaced the intervertebral discs in their entirety in the thoracic region. Some lesions were so large they would protrude into the spinal column and impinge on the spinal cord, leading to compression that most likely was the source of the paresis and paralysis observed. Lesions appeared to be specific to the ventral spine (Figure 6.5)

Joints, including knees and shoulders were examined histologically for evidence of abnormal mineralization or mineral deposits between opposing bones. Interestingly, there was no indication of abnormal mineral being present in these areas (Appendix 4).

#### *6.3.6 $\mu$ CT Scanning*

Since the lesions forming on the spine contained minerals similar to bone,  $\mu$ CT scanning was used to examine both whole mice and isolated spines preserved at fixed ages. Scans of a one year old  $ENT1^{-/-}$  mouse confirmed the extensive mineral deposits were





Figure 6.4. ENT1<sup>-/-</sup> mice develop mineralized lesions on the spine.

Spines from WT and ENT1<sup>-/-</sup> mice (KO) were removed and examined with a Nikon SMZ1500 microscope with digital camera. A) WT and KO thoracic spinal sections (as labelled) were compared side by side ventrally. Abnormal mineralization is highlighted by arrows. 1: vertebrae, 2: intervertebral disc, 3: rib. B) Ventral view of lumbar spines from WT and KO mice. Abnormal mineral is highlighted by arrow. 4: vertebrae, 5: intervertebral disc.

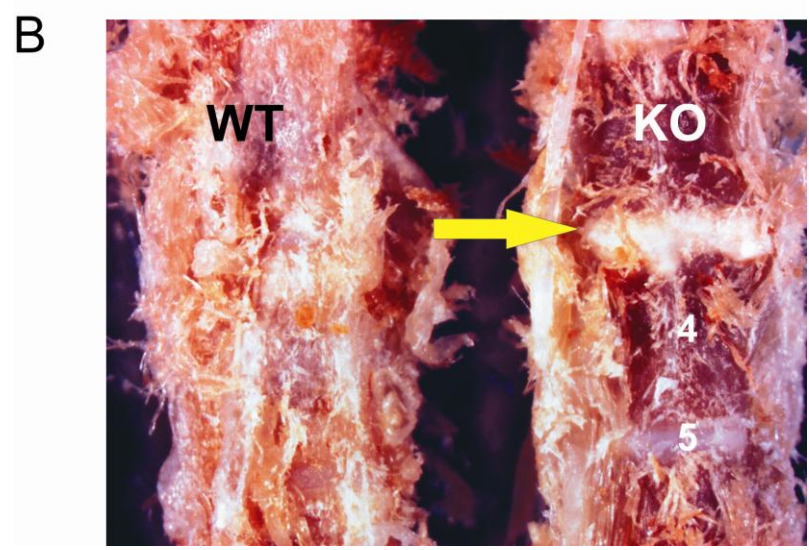
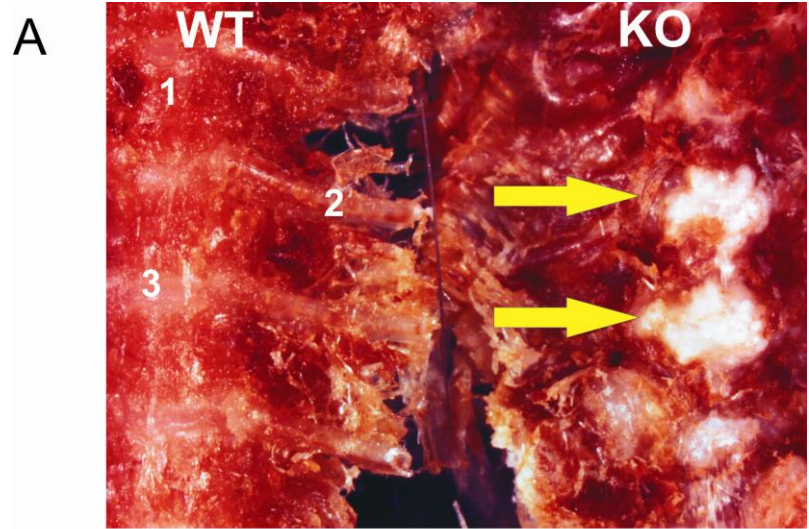
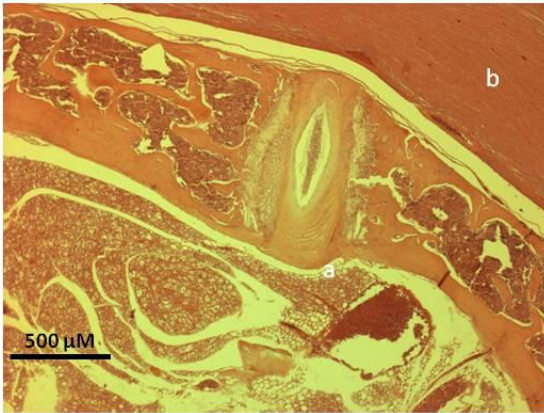




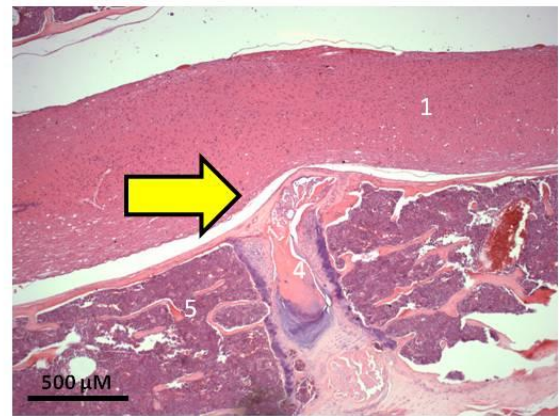
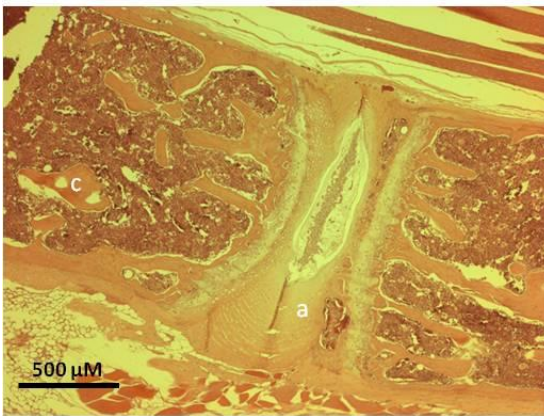
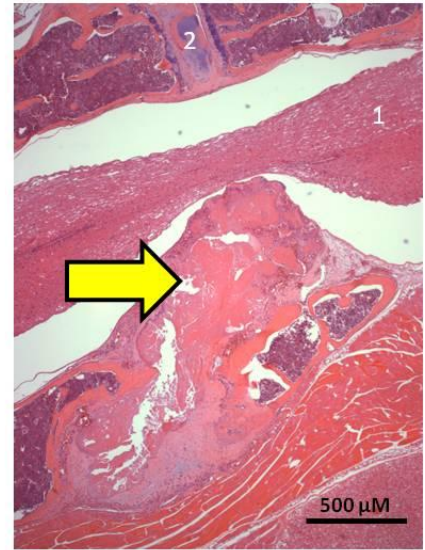
Figure 6.5. Histology of ENT1<sup>-/-</sup> spines reveals spinal cord impingement.

Formalin fixed, decalcified spines were sectioned longitudinally and stained with H&E. Images were captured at 4x magnification, with dorsal orientation at the top of the image. Top images are sections of thoracic spine, bottom images are sections of lumbar spine. Images on the left are from a wild-type (WT) mouse and images on the right are from an ENT1<sup>-/-</sup> (KO) mouse. Yellow arrow identifies abnormal mineralization protruding into spinal column and resultant spinal cord compression. a: normal intervertebral disc, b: normal spinal cord, c: normal vertebra, 1: compressed spinal cord, 2: dorsal intervertebral disc, 4: ventral intervertebral disc, 5: vertebra.

WT



KO



localized to the spine and confined to the intervertebral spaces in a ventral specific manner (Figures 6.6A&C). A rostral to caudal view through the spinal column showed that some lesions did indeed intrude into the spinal column as first seen in histological sections (Figures 6.6B&D). A time course of lesion development and progression was also developed using  $\mu$ CT scanning. Spines from 2, 4, 5, and 6 month old WT and ENT1<sup>-/-</sup> mice were scanned and compared. Mineralized lesions could be seen in the 2 month old ENT1<sup>-/-</sup> mice (Figure 6.7A). A very distinct pattern of lesion development was observed, with the cervical spine being affected first. At the age of five months, lesions can be observed in the thoracic spine (Figure 6.7C). Very specific lesion formation was also observed at the first false rib (Figures 6.7C&D).

In contrast to the histology and  $\mu$ CT performed on spines of 12 month old mice, these time course data suggest the abnormal mineralization begins to form on the outside of the spine and slowly progresses into the intervertebral space.

#### *6.3.7 Scanning Electron Microscopy*

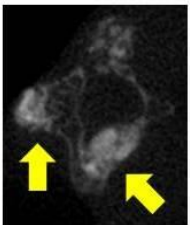
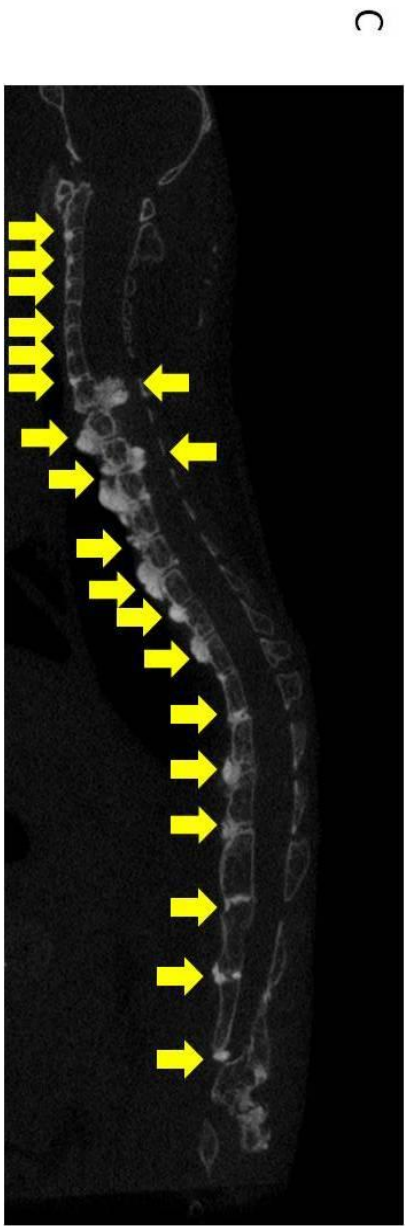
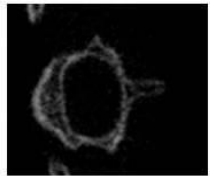
High resolution, high magnification images of the mineral deposit found in the intervertebral space supported descriptions of the lesion from histological sections. The lesion appeared devoid of any biological material. Organization resembled that of angular crystals (Figure 6.8).



Figure 6.6. Micro computed tomography of ENT1<sup>-/-</sup> spines.

Micro CT scans were performed and maximum intensity projections (MIP) images were made. A) Spine from a WT mouse age 12 months. a: anterior, d: dorsal, p: posterior, v:ventral. B) Rostral to caudal view showing individual vertebra and spinal column. C) Spine from age matched ENT1<sup>-/-</sup> mouse. Arrows highlight areas of abnormal mineralization. Orientation is the same as A). D) Rostral to caudal view of ENT1<sup>-/-</sup> spine. Arrow highlights mineral protrusion into spinal column.





C

D

A

B



Figure 6.7. Time course of lesion development in ENT1<sup>-/-</sup> mice.

Spines from age matched WT and ENT1<sup>-/-</sup> mice (KO) were isolated and fixed in formalin.

Micro CT scans were performed and MIP images were rendered at 100 μm resolution.

A) WT (left) and KO (right) spines from 2 month old mice. B) 4 months old. C) 5 months old. D) 6 months old. In all cases arrows highlight areas of abnormal mineralization.

These images are representative of μCT scans performed on at least three mice at each age point.

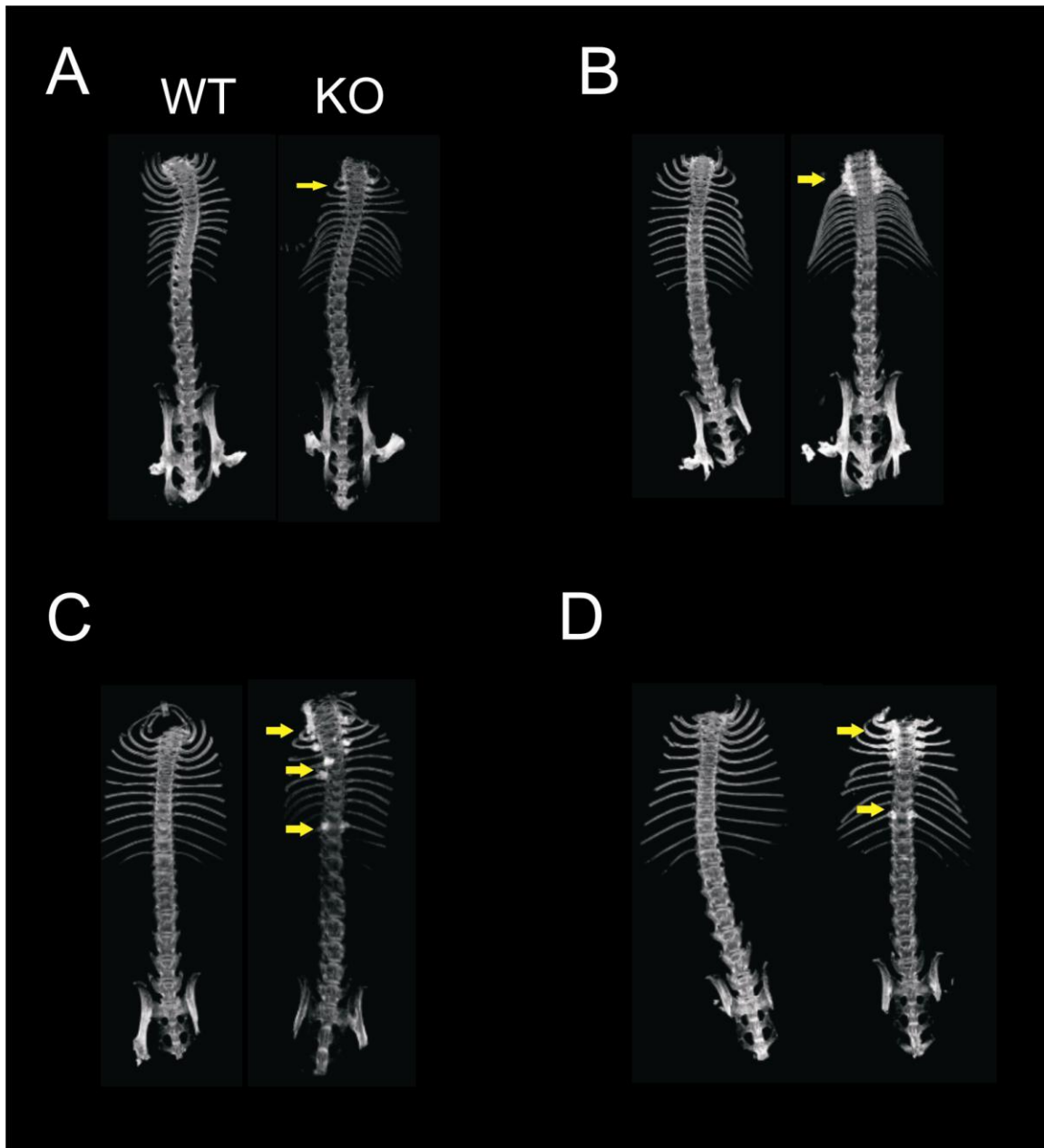
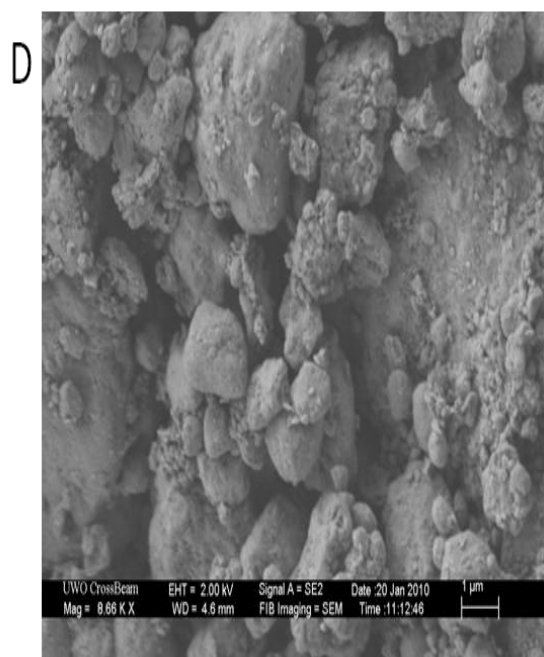
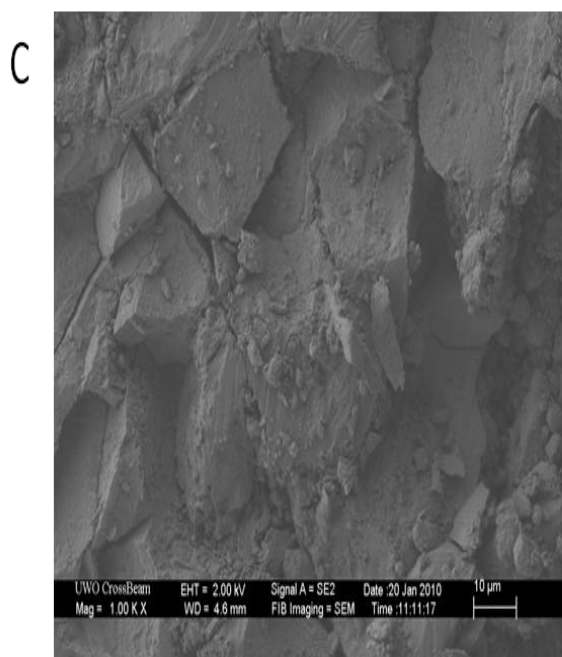
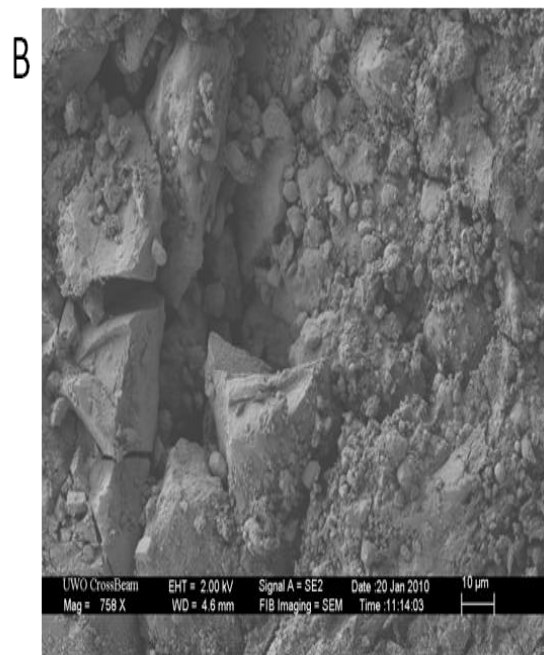
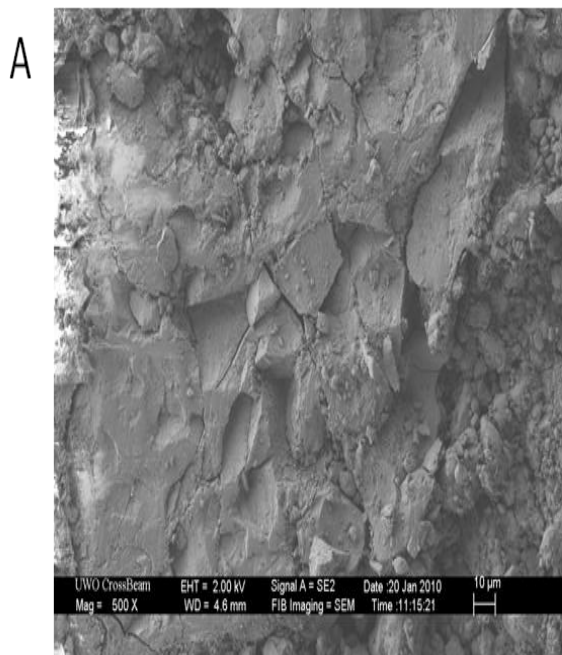




Figure 6.8 Scanning electron microscopy (SEM) images of mineral deposits in ENT1<sup>-/-</sup> intervertebral spaces.

A sample of ENT1<sup>-/-</sup> spine that had a mineralized lesion in the intervertebral space was imaged by SEM. A representative area was chosen and images were captured at 4 different magnifications: A) 500x, B) 758x, C) 1000x, D) 8660x.

Note the lack of any cellular or other biological presence. Since the mineral deposits do not occur in WT mice, there are no images for comparison between the two strains.



## 6.4 Discussion

We have characterized previously unreported age-related phenotypes of the ENT1<sup>-/-</sup> mouse. This study furthers our understanding of the physiological roles of ENT1 and adenosine, with particular focus on the local control of mineralization of paraspinal tissue.

### 6.4.1 Altered gene expression

Changes in gene expression in microvascular endothelial cells isolated from mouse skeletal muscle of ENT1<sup>-/-</sup> were presented in Chapter 5. Organs were chosen based on the overall cardiovascular aspect of this thesis (heart) and organs in which adenosine plays key physiological roles (brain, kidney, and heart). Of particular note are genes that differentially change depending on the organ. ENT2 drops significantly in KO hearts but rises significantly in KO kidneys. Adenosine receptor A<sub>2A</sub> rises significantly in the KO brain but drops significantly in the KO heart. Rose and colleagues also examined gene expression changes in the heart of ENT1<sup>-/-</sup> mice and found no statistical differences, however there was a trend towards decreased A<sub>2A</sub> mRNA as well (23). The only other reported gene change in the ENT1<sup>-/-</sup> mouse is an increase in adenosine receptor A<sub>1</sub> protein in the striatum (4). In other model, where human ENT1 was over-expressed in mouse neurons, there were no reported changes in gene expression (19). Clinically based work examining the lack of human ENT1 expression in cancer, have linked ENT1 to response to nucleoside analogue chemotherapy (18; 25). Given that there are known polymorphisms in the ENT1 gene (14; 17), and that the lack of ENT1 affects the



expression of other genes that regulate adenosine bioactivity, more research is needed to study the role of ENT1 in human diseases of the heart, brain, and kidney.

#### *6.4.2 Altered cardiovascular function*

ENT1<sup>-/-</sup> mice had a lower awake heart rate than their WT counterparts. The CODA-6 system has holding tubes for awake mice that limits mobility to obtain accurate readings. This environment would lead to stress and anxiety in the WT mouse, whereas the ENT1<sup>-/-</sup> mouse is known to be less anxious in stressful situations(3). The normal heart rate for C57BL/6 mice that are trained for the tail-cuff apparatus ranges between 600 and 620 bpm (11; 24), which is lower than the 680 bpm reported for the WT mice in this study and higher than the 590 bpm of the ENT1<sup>-/-</sup> mice (Figure 6.2). Therefore, it is proposed that anxiety in the WT mouse translated into a higher heart rate. This was supported by the equal heart rates in anaesthetized mice, and evidence that anxiety in mice results in elevated heart rates (7).

To avoid the differences in anxiety between WT and ENT1<sup>-/-</sup> mice, blood pressure was measured in anaesthetized animals. ENT1<sup>-/-</sup> male mice aged 2-3 months had lower blood pressure than aged matched WT mice (Figure 6.2). Our group has previously reported that ENT1<sup>-/-</sup> mice have elevated adenosine receptor A<sub>2A</sub> protein expression in microvascular endothelial cells isolated from skeletal muscle(1). A<sub>2A</sub> receptor signaling is known to mediate vasodilation. In fact, the A<sub>2A</sub><sup>-/-</sup> mouse is hypertensive (16). Adding to the increased A<sub>2A</sub> expression previously reported, the current study showed that ENT1<sup>-/-</sup> had an elevated adenosine concentration in plasma from whole blood collected by cardiac puncture (Figure 6.3). An increase in both the vasodilatory receptor and the

ligand could result in consistently decreased peripheral resistance, resulting in lower blood pressure in young mice. However, as these mice age, additional unknown factors contribute to a normalization of blood pressure. While it is known that blood pressure in mice increases as they age (8), the differential change between WT and ENT1<sup>-/-</sup> suggests an altered condition in the ENT1<sup>-/-</sup> animal. It could be possible that there is a progressive hardening of vessel walls, due to ectopic mineralization as seen with the soft tissue found around the intervertebral spaces of the ENT1<sup>-/-</sup> mice. There are links between adenosine, adenine nucleotides, and the calcification of arteries (12; 26). However, since there is no  $\mu$ CT evidence, either the calcification is extremely diffuse to be undetectable, or alternatively perhaps there is a gradual overcompensation of vasoconstrictor production that eventually takes over the initial vasodilatory signal.

#### *6.4.3 Abnormal mineral deposits in the spine*

The role of adenosine in the formation of abnormal mineral deposits is poorly understood. Abnormal calcification of vascular smooth muscle cells isolated from rat aorta is enhanced by a cAMP dependent mechanism that aids in the reduction of extracellular inorganic pyrophosphate (PPi) accumulation (20). Adenosine is capable of increasing cAMP levels via the adenosine A<sub>2A</sub> and A<sub>2B</sub> receptor subtypes. However, a very recent report by St. Hilarie *et al.*, (26) suggests that adenosine is an inhibitor of calcification. In that study, human patients with a non-function mutation in the CD73 enzyme that forms adenosine from AMP presented with abnormal vascular mineralization. Fibroblasts isolated from one patient spontaneously formed calcium

deposits in culture that was reversed by the addition of adenosine to the culture medium (26).

A similar phenotype to our identified hypermineralization has been reported in mice lacking nucleotide pyrophosphatase phosphodiesterase-1 (NPP1; *Enpp1*<sup>-/-</sup>). NPP1 is responsible for the production of PPi via the metabolism of triphosphate nucleotides, like ATP, to monophosphate nucleotides. These *Enpp1*<sup>-/-</sup> mice, also known as tip-toe walking mice, spontaneously develop progressive ankylosing intervertebral and peripheral joint hyperostosis and articular cartilage calcification (10). However, our *ENT1*<sup>-/-</sup> mice do not appear to have any abnormal mineralization in other joints, suggesting a different mechanism.

Interestingly, our spinal mineralization phenotype most closely resembles the human condition diffuse idiopathic skeletal hyperostosis (DISH). DISH affects about 25% of the male population over the age of 65, with a slightly lower occurrence in women (27). Resnick and Niwayama state that a diagnosis of DISH must meet the following criteria: 1) the involvement of at least 4 contiguous vertebrae of the thoracic spine, 2) preservation of the intervertebral disc space (distinct from ankylosing spondylitis), and 3) absence of apophyseal joints or sacroiliac inflammatory changes (22). Our phenotype clearly agrees with conditions 1 and 3. If examined solely on 12 months of age or older mice, then it would appear that condition 2 is not met. However, the  $\mu$ CT images of younger mice (Figure 6) would suggest that as the mineralization develops the intervertebral disc is intact. In reality, the severity of the mineral deposits in older mice is much more likely an extreme that would not be found in human patients because

humans will report their discomfort much sooner and more effectively than mice. Much like the phenotype of our ENT1<sup>-/-</sup> mice, DISH is asymptomatic until there is compression of surrounding tissues including the glottis resulting in dysphagia, or compression of the spinal cord producing neurological complications (28). The etiology of DISH is unknown. However in attempts to aid in the understanding of DISH, the Boxer dog has been identified as having an unusually high prevalence (41% compared to an average of 4% in other breeds) of DISH (15). Our lab had previously cloned the dog ENT1 gene (9), and given the DISH like phenotype in the ENT1<sup>-/-</sup> mouse there was interest in the ENT1 gene of the Boxer dog. *In silico* analysis of the ENT1 gene from mouse, human, Boxer dog, and Alsatian dog, revealed that the Boxer dog has an altered ENT1 gene resulting in a mutated protein missing 7 amino acids in a highly conserved region (Figure 6.9A). When mapped to the proposed structure of ENT1, this deletion is predicted to be in the second extracellular loop (Figure 6.9B), a region identified to be important in transport function (13). Given the similarities between this condition and the hypermineralization phenotype of our ENT1<sup>-/-</sup> mice, we are currently pursuing the hypothesis that alterations in local adenosine concentrations as a result of the loss of ENT1 function contributes to the development of DISH.

#### 6.4.4 Conclusions

In conclusion, the ENT1<sup>-/-</sup> mouse is a valuable model for the study of adenosine mediated regulation of vascular tone and is a possible novel model for the study of a common but poorly understood human disease.

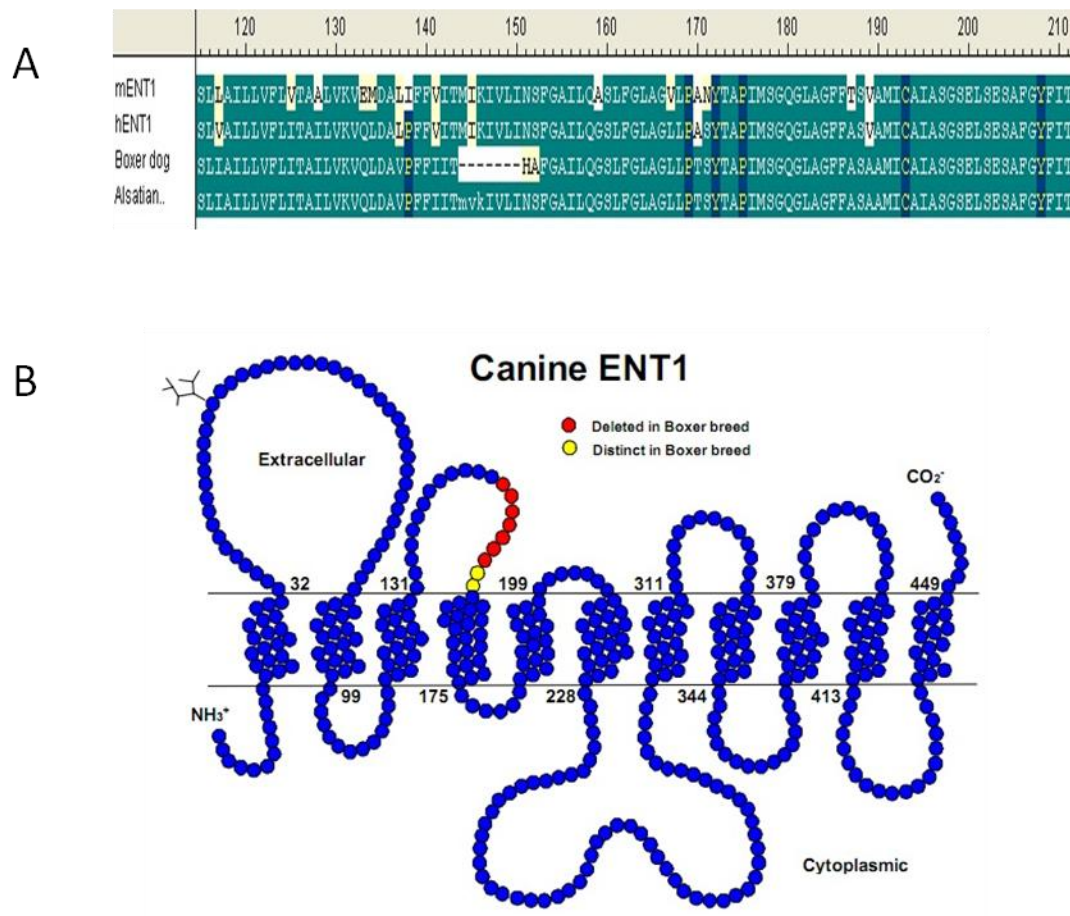


Figure 6.9. Alterations in Boxer dog ENT1 protein.

A) Alignment of ENT1 sequences (from Genbank). Letters are single character amino acid codes. Green colour indicates conserved, yellow indicated a unique residue, dashed line represents missing residues.

B) Schematic of the proposed topology of dog ENT1 with missing amino acids identified in red and unique amino acids in yellow. Additional species specific differences are not shown.

## 6.5 References

1. **Bone DB, Choi DS, Coe IR and Hammond JR.** Nucleoside/nucleobase transport and metabolism by microvascular endothelial cells isolated from ENT1<sup>-/-</sup> mice. *Am J Physiol Heart Circ Physiol* 299: H847-H856, 2010.
2. **Bone DB, Choi DS, Coe IR and Hammond JR.** Nucleoside/nucleobase transport and metabolism by microvascular endothelial cells isolated from ENT1<sup>-/-</sup> mice. *Am J Physiol Heart Circ Physiol* 299: H847-H856, 2010.
3. **Chen J, Rinaldo L, Lim SJ, Young H, Messing RO and Choi DS.** The type 1 equilibrative nucleoside transporter regulates anxiety-like behavior in mice. *Genes Brain Behav* 6: 776-783, 2007.
4. **Choi DS, Cascini MG, Mailliard W, Young H, Paredes P, McMahon T, Diamond I, Bonci A and Messing RO.** The type 1 equilibrative nucleoside transporter regulates ethanol intoxication and preference. *Nat Neurosci* 7: 855-861, 2004.
5. **Farthing D, Sica D, Gehr T, Wilson B, Fakhry I, Larus T, Farthing C and Karnes HT.** An HPLC method for determination of inosine and hypoxanthine in human plasma from healthy volunteers and patients presenting with potential acute cardiac ischemia. *J Chromatogr B Analyt Technol Biomed Life Sci* 854: 158-164, 2007.
6. **Feldkamp LA, Davis LC and Kress JW.** Practical cone-beam algorithm. *J Opt Soc Am A* 1: 612-619, 1984.
7. **Gaburro S, Stiedl O, Giusti P, Sartori SB, Landgraf R and Singewald N.** A mouse model of high trait anxiety shows reduced heart rate variability that can be reversed by anxiolytic drug treatment. *Int J Neuropsychopharmacol* 1-15, 2011.
8. **Gros R, Van WR, You X, Thorin E and Husain M.** Effects of age, gender, and blood pressure on myogenic responses of mesenteric arteries from C57BL/6 mice. *Am J Physiol Heart Circ Physiol* 282: H380-H388, 2002.

9. **Hammond JR, Stolk M, Archer RG and McConnell K.** Pharmacological analysis and molecular cloning of the canine equilibrative nucleoside transporter 1. *Eur J Pharmacol* 491: 9-19, 2004.
10. **Harmey D, Hesse L, Narisawa S, Johnson KA, Terkeltaub R and Millan JL.** Concerted regulation of inorganic pyrophosphate and osteopontin by akp2, enpp1, and ank: an integrated model of the pathogenesis of mineralization disorders. *Am J Pathol* 164: 1199-1209, 2004.
11. **Hoit BD, Kiatchosakun S, Restivo J, Kirkpatrick D, Olszens K, Shao H, Pao YH and Nadeau JH.** Naturally occurring variation in cardiovascular traits among inbred mouse strains. *Genomics* 79: 679-685, 2002.
12. **Hsu HH and Camacho NP.** Isolation of calcifiable vesicles from human atherosclerotic aortas. *Atherosclerosis* 143: 353-362, 1999.
13. **Hyde RJ, Cass CE, Young JD and Baldwin SA.** The ENT family of eukaryote nucleoside and nucleobase transporters: recent advances in the investigation of structure/function relationships and the identification of novel isoforms. *Mol Membr Biol* 18: 53-63, 2001.
14. **Kim SR, Saito Y, Maekawa K, Sugiyama E, Kaniwa N, Ueno H, Okusaka T, Morizane C, Yamamoto N, Ikeda M, Yoshida T, Minami H, Furuse J, Ishii H, Saijo N, Kamatani N, Ozawa S and Sawada J.** Thirty novel genetic variations in the SLC29A1 gene encoding human equilibrative nucleoside transporter 1 (hENT1). *Drug Metab Pharmacokinet* 21: 248-256, 2006.
15. **Kranenburg HC, Westerveld LA, Verlaan JJ, Oner FC, Dhert WJ, Voorhout G, Hazewinkel HA and Meij BP.** The dog as an animal model for DISH? *Eur Spine J* 19: 1325-1329, 2010.
16. **Ledent C, Vaugeois JM, Schiffmann SN, Pedrazzini T, El YM, Vanderhaeghen JJ, Costentin J, Heath JK, Vassart G and Parmentier M.** Aggressiveness, hypoalgesia and high blood pressure in mice lacking the adenosine A2a receptor. *Nature* 388: 674-678, 1997.
17. **Myers SN, Goyal RK, Roy JD, Fairfull LD, Wilson JW and Ferrell RE.** Functional single nucleotide polymorphism haplotypes in the human equilibrative nucleoside transporter 1. *Pharmacogenet Genomics* 16: 315-320, 2006.

18. **Oguri T, Achiwa H, Muramatsu H, Ozasa H, Sato S, Shimizu S, Yamazaki H, Eimoto T and Ueda R.** The absence of human equilibrative nucleoside transporter 1 expression predicts nonresponse to gemcitabine-containing chemotherapy in non-small cell lung cancer. *Cancer Lett* 256: 112-119, 2007.
19. **Parkinson FE, Xiong W, Zamzow CR, Chestley T, Mizuno T and Duckworth ML.** Transgenic expression of human equilibrative nucleoside transporter 1 in mouse neurons. *J Neurochem* 109: 562-572, 2009.
20. **Prosdocimo DA, Wyler SC, Romani AM, O'Neill WC and Dubyak GR.** Regulation of vascular smooth muscle cell calcification by extracellular pyrophosphate homeostasis: synergistic modulation by cyclic AMP and hyperphosphatemia. *Am J Physiol Cell Physiol* 298: C702-C713, 2010.
21. **Ramakers BP, Pickkers P, Deussen A, Rongen GA, van den Broek P, van der Hoeven JG, Smits P and Riksen NP.** Measurement of the endogenous adenosine concentration in humans in vivo: methodological considerations. *Curr Drug Metab* 9: 679-685, 2008.
22. **Resnick D and Niwayama G.** Radiographic and pathologic features of spinal involvement in diffuse idiopathic skeletal hyperostosis (DISH). *Radiology* 119: 559-568, 1976.
23. **Rose JB, Naydenova Z, Bang A, Eguchi M, Sweeney G, Choi DS, Hammond JR and Coe IR.** Equilibrative nucleoside transporter 1 plays an essential role in cardioprotection. *Am J Physiol Heart Circ Physiol* 298: H771-H777, 2010.
24. **Shah AP, Siedlecka U, Gandhi A, Navaratnarajah M, Al-Saud SA, Yacoub MH and Terracciano CM.** Genetic background affects function and intracellular calcium regulation of mouse hearts. *Cardiovasc Res* 87: 683-693, 2010.
25. **Spratlin J, Sangha R, Glubrecht D, Dabbagh L, Young JD, Dumontet C, Cass C, Lai R and Mackey JR.** The absence of human equilibrative nucleoside transporter 1 is associated with reduced survival in patients with gemcitabine-treated pancreas adenocarcinoma. *Clin Cancer Res* 10: 6956-6961, 2004.
26. **St HC, Ziegler SG, Markello TC, Brusco A, Groden C, Gill F, Carlson-Donohoe H, Lederman RJ, Chen MY, Yang D, Siegenthaler MP, Arduino C, Mancini C, Freudenthal B, Stanescu HC, Zdebik AA, Chaganti RK, Nussbaum RL, Kleta R,**



**Gahl WA and Boehm M.** NT5E mutations and arterial calcifications. *N Engl J Med* 364: 432-442, 2011.

27. **Weinfeld RM, Olson PN, Maki DD and Griffiths HJ.** The prevalence of diffuse idiopathic skeletal hyperostosis (DISH) in two large American Midwest metropolitan hospital populations. *Skeletal Radiol* 26: 222-225, 1997.
28. **Wilson FM and Jaspan T.** Thoracic spinal cord compression caused by diffuse idiopathic skeletal hyperostosis (DISH). *Clin Radiol* 42: 133-135, 1990.

CHAPTER SEVEN  
GENERAL DISCUSSION

## 7.1 Review of Research Questions

In Chapter 2 research questions were identified that would be addressed in this thesis. Study of nucleoside transporters in the microvasculature had been neglected, with the majority of studies using the macrovascular HUVECs as a model. The understanding of nucleobase transport was even sparser.

Choosing primary human MVECs as a model, questions regarding the expression and function of nucleoside and nucleobase transporters were addressed. This work included identifying what transporters existed in this cell type to mediated nucleoside and nucleobase transport, as well as the molecular mechanisms in place that regulated the function of these transporters.

An ENT1<sup>-/-</sup> mouse was also studied to understand how ENT1 contributes to purine handling in the microvasculature. Through culturing primary mouse MVECs, it was possible to address questions about compensatory mechanisms that exist to respond to the missing nucleoside transporter ENT1. The whole animal was also studied to determine the impact of the loss of ENT1 on cardiovascular physiology.

## 7.2 Picking an Appropriate Model: Differences in species and cell type

The idea that differences exist between species and cell types is not new. In fact there are already several examples in the nucleoside transporter field that highlight this. It has long been known that the pharmacology of ENT1 is species-dependent with inhibitor affinities displaying a rank order of human being the most sensitive, rat being least sensitive, and mouse falling in the middle (8). Additionally, the mouse ENT1 gene has

multiple splice variants that affect transporter regulation and expression that do not appear to exist in humans (9; 17).

### *7.2.1 Differences in expression of nucleoside and nucleobase between species.*

It has been previously shown that primary MVECs isolated from rat skeletal muscle express ENT1 and ENT2 in approximately equal amounts (1). In these cells ENT2 was the nucleobase transporter of note and mediated both the uptake and release of hypoxanthine (16). However, as shown in Chapter 3, primary human cardiac MVECs did not display any functional ENT2. Additionally, it was discovered that a novel purine-selective nucleobase transporter, ENBT1, was the transporter responsible for the uptake and release of hypoxanthine. In Chapter 5, primary mouse skeletal muscle MVECs were found to be different from both human cardiac and rat skeletal muscle. Mouse MVECs expressed both ENT1 and ENT2, however the contribution of ENT2 to nucleoside uptake was minimal. A mouse orthologue of ENBT1 was also discovered and was the predominant nucleobase transporter. The relative expression of ENT1, ENT2, and ENBT1 with respect to species is highlighted in Table 7.1.

### *7.2.2 Impact of cell type.*

In Chapter 4 regulation of ENT1 and ENBT1 was examined in primary human MVECs and in some cases the immortalized endothelial cell line HMEC-1.

The effect of PKC activation and down-regulation in MVECs on ENT1 (Figure 4.8) was the opposite of reported effects in cancer cells (4), but similar to HUVECs (13). The effect of the CKII inhibitor TBB was similar to a recombinant expression model (3), but different from a dominant negative model (18). Adenosine A<sub>2</sub> receptor agonists had no effect on

ENT1 in MVECs whereas it has been shown previously that both receptors can affect ENT1 and ENT2 in HUVECs (6). There was even temporal and concentration differences in the response to VEGF between MVECs and HMEC-1 cells within this work (Figures 4.3 and 4.4).

### *7.2.3 Species differences and cell types: conclusions.*

It is clear that the choice of species and cell type is critical to the proper interpretation of data. Based on rat MVECs it was predicted that human MVECs would express ENT2 as both a nucleoside and nucleobase transporter. If human or mouse MVECs were not actually studied, then the discovery of ENBT1 would not have occurred and the realization that rat is not an appropriate model of nucleoside/nucleobase transport would not have been made. Mouse, although closer to human MVECs than rat, is still not an ideal model; however, mice have the advantage of providing genetically modified models to study gene function.

The variation seen in response in different cell types when studying transporter regulation reinforces the importance of proper model selection and highlights the need to be careful when extrapolating results to another model.

Table 7.1. Relative expression of nucleoside and nucleobase transporters in primary MVECs from different species

Species	Tissue	ENT1	ENT2	ENBT1
Human	Cardiac	+	-	*
Mouse	Skeletal muscle	+++	+	***
Rat	Skeletal muscle	+	+	n.d.

In human primary MVECs only ENT1 and ENBT1 are expressed for nucleoside and nucleobase transport respectively. In mouse, there is some detectable ENT2 expression, however the contribution to either nucleoside or nucleobase transport is minimal, hence the 3:1 ratio of symbols (this ratio is representative and not meant to be an absolute measure of expression levels). In rat MVECs there is approximately equal ENT1 and ENT2 distribution.

-: no expression

n.d.: not determined (1; 16)

## 7.3 Physiological Relevance

### 7.3.1 *Discovery of a novel purine nucleobase transporter: A change in dogma.*

Following the cloning and molecular characterization of ENT1 and ENT2, it was generally accepted that ENT1 was the primary sodium-independent nucleoside transporter and ENT2 was the sole sodium-independent nucleobase transporter (23). However, it is clear from the data presented in this thesis that this dogma is in need of revision.

The existence of ENBT1, the dipyridamole-insensitive purine selective nucleobase transporter changes the understanding of purine transport in mammalian cells. Understanding that ENT2 most likely is not the transporter mediating uptake or release of nucleobases and nucleobase analogues will change our views on cardiovascular physiology, chemotherapy in cancer and other conditions, and possibly other areas of physiology and pharmacology that are not yet appreciated. Figure 7.1 contrasts the old and new understanding of nucleoside and nucleobase transport in mammalian cells.

#### 7.3.1.1 Future Directions: The Genetic Identity of ENBT1

Characterization of ENBT1, as presented in Chapter 3, has laid the ground work for understanding how the transporter functions. However, without knowing the genetic, and therefore, molecular identity of ENBT1, these studies are limited in progression. Expression studies using PCR and western blotting techniques are impossible without this knowledge. Additionally, structure-function studies that would provide better understanding of substrate recognition and inhibitor sensitivities, and even allow for the rational design of nucleobase analogues that could be used in chemotherapies, are not possible without knowing the genetic identity of ENBT1.

With the sequencing of the human genome complete, the gene that encodes ENBT1 is known, it just needs to be found. A group in Japan has ruled out that ENBT1 is a member of the SLC23 family, or sodium-dependent ascorbate transporters (see Chapter 1). Since ENT2 has a similar substrate profile to ENBT1, and the amino acids in ENT2 that help confer the ability to transport nucleobases is known, genome searches for similar regions may prove to be a good starting point.

In an alternative approach, further examination of the OCT family of transporters can be performed. Chapter 3 tested a potential candidate, hUPP1, without success. As well, substrates of OCT1 and OCT3 were tested as potential inhibitors of [<sup>3</sup>H]hypoxanthine uptake, with mixed results. Despite these outcomes, there is still enough potential in an OCT to justify a different approach. Expression of recombinant OCTs in HEK cells (which lack functional ENBT1) can be used in gain of function experiments to better test the possibility that an OCT is ENBT1.

### *7.3.2 ENBT1 and Ischemia-Reperfusion injury of MVECs*

The generation of ROS from purine metabolism in endothelial cells during reperfusion after ischemia is an established phenomenon (12). There is also evidence that ROS generated in this manner contributes to endothelial dysfunction (7; 15; 22). The sensitivity of the hypoxanthine transporter ENBT1 to superoxide produced intracellularly by menadione may contribute to increased ROS production and overall endothelial dysfunction through oxidative stress. Figure 7.2 proposes a model of how ENBT1 contributes to ROS production and endothelial dysfunction.





Figure 7.1. Changes in nucleoside and nucleobase transporter dogma.

Following the cloning of ENT1 and ENT2 it was generally accepted that ENT1 was the primary Na-independent nucleoside transporter and ENT2 was the sole nucleobase transporter that could also contribute to nucleoside transport. The top panel depicts that view. Inhibitors of transport, NBMPR and dipyridamole, are connected to their targets with red arrows.

The bottom panel depicts the current view of nucleoside and nucleobase transport in primary human MVECs based on discoveries presented in this thesis. In place of ENT2, ENBT1 is the sole nucleobase transporter, and is selective for purine nucleobases. ENBT1 is also insensitive to dipyridamole inhibition.

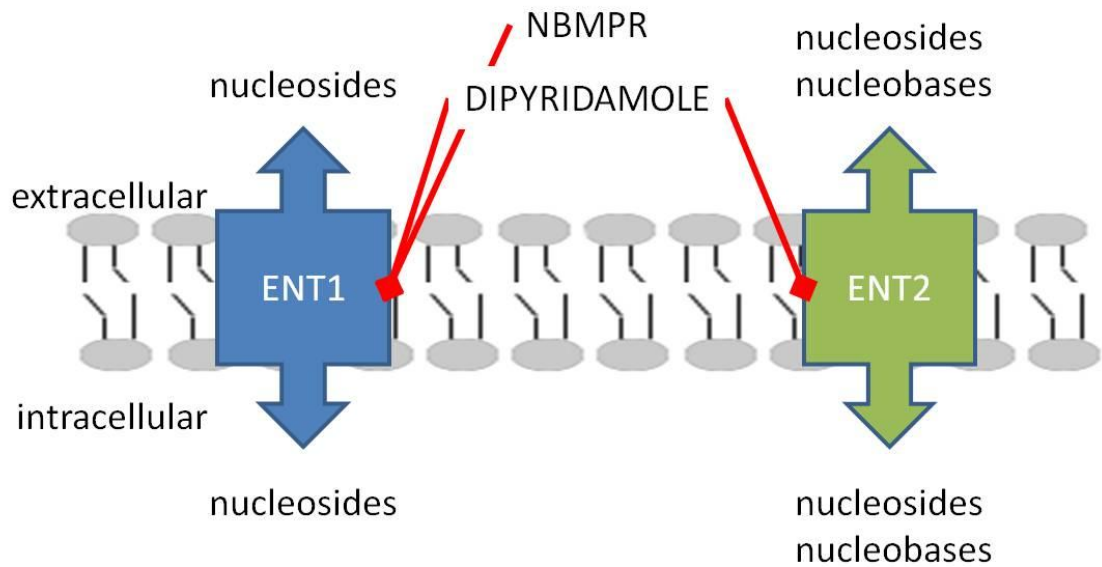
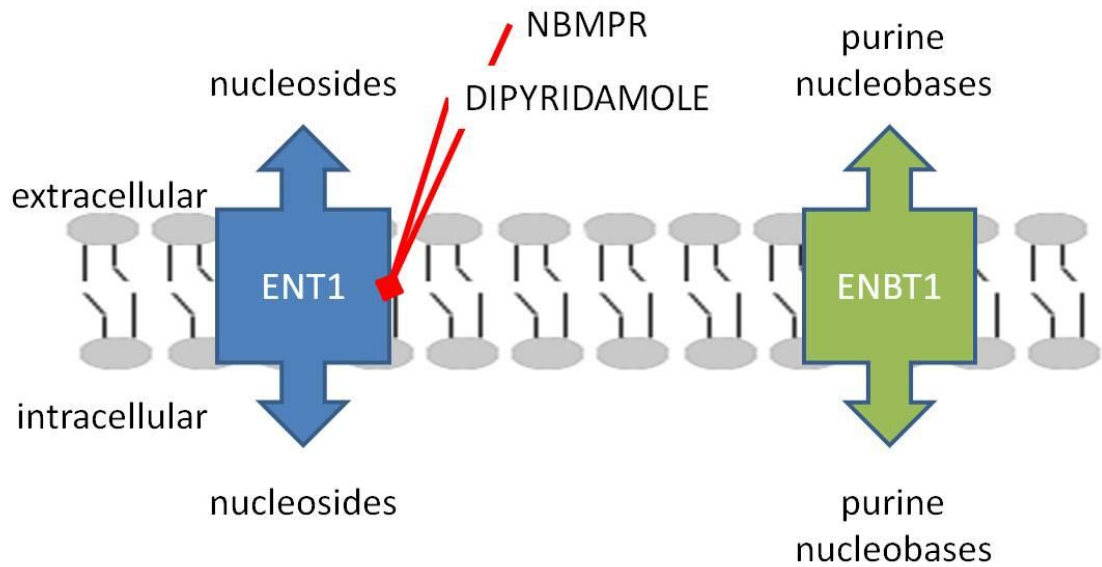
**PREVIOUS****CURRENT**



Figure 7.2. ENBT1 and ischemia-reperfusion injury of the microvascular endothelium.

The following schematic is a proposed model of how ENBT1 may contribute to injury of the endothelium following ischemia-reperfusion.

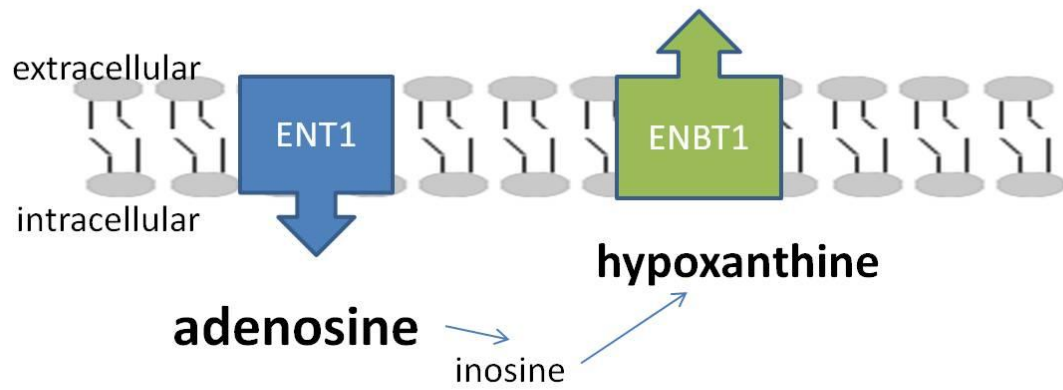
During ischemia, adenosine released by surrounding cardiomyocytes accumulates in the MVECs, via uptake by ENT1. Adenosine kinase is inactivated by ATP depletion and thus the excess adenosine is metabolized to hypoxanthine. Without oxygen, the metabolism of hypoxanthine cannot continue. ENBT1 mediates the efflux of hypoxanthine.

Upon reperfusion, the return of oxygen allows xanthine oxidase to metabolize hypoxanthine to xanthine and xanthine to uric acid, producing ROS in the process. The ROS produced attacks ENBT1, leading to decreased hypoxanthine efflux.

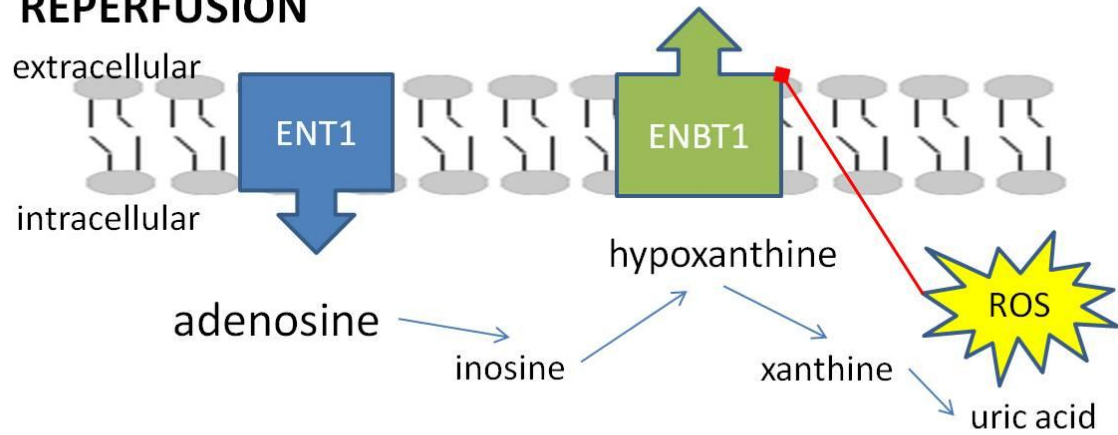
The resulting lack of ENBT1 function promotes increased hypoxanthine metabolism and an increase in ROS, contributing to increased cellular oxidative stress, injury, and possible endothelial dysfunction.

Notes: Inhibitory effect of ROS on ENBT1 is depicted by red arrow with diamond tip. The non-functional or reduced function ENBT1 is depicted with as a red arrowless box with a yellow starburst to suggest oxidative modification by ROS.

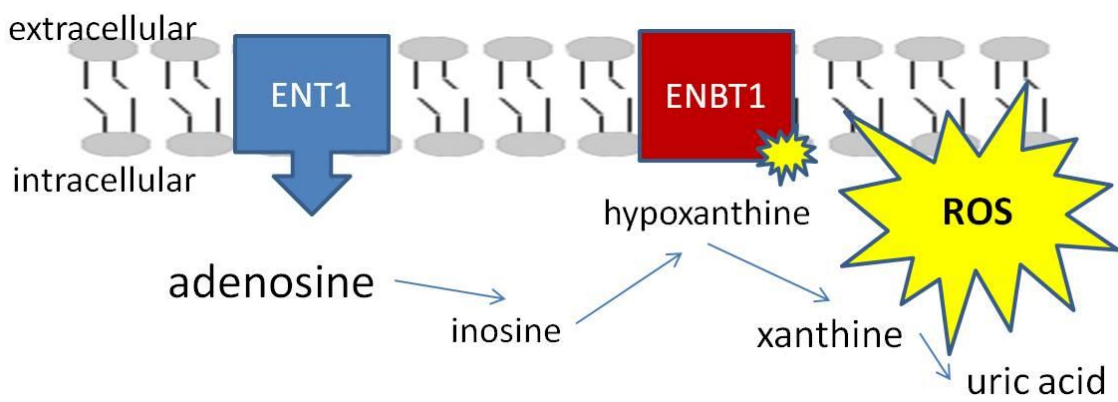
## ISCHEMIA



## REPERFUSION



## INJURY



### 7.3.2.1 Future Directions: ENT1, ENBT1, and ROS production

In Chapter 4, it was found that the intracellular superoxide generator menadione reduced hypoxanthine uptake by a process that could be blocked by a superoxide dismutase mimetic (Figure 4.12). While it would seem that this effect was mediated by superoxide, no measurement of ROS was made.

Measuring ROS production, by use of fluorescent dyes, would strengthen the proposed mechanism of reduced hypoxanthine uptake by menadione. As well, measurement of ROS would allow the investigation of the role of ENBT1 and hypoxanthine transport on the intracellular production of superoxide by hypoxanthine metabolism.

ROS measurement would also be useful after the mineral oil-overlay ischemia treatment to determine a possible mechanism of action as the effects of ischemia are similar to that of menadione treatment (Figure 4.13).

Other oxidants should also be tested on the ability to affect ENT1 and ENBT1 function. As superoxide is rapidly converted to hydrogen peroxide or can react with NO to form peroxynitrite, there is potential that there are additional mechanisms of oxidative stress that could affect transport function (5; 11; 15). In fact, one recent study claimed that the peroxynitrite donor SIN-1 reduced adenosine uptake in rat astrocytes (19). However, the conditions of that study resulted in total adenosine accumulation rather than ENT1 mediated transport and the effects of SIN-1 on adenosine metabolism were not addressed. Treatment of cells with stable peroxides, like tert-butyl hydroperoxide, or with the peroxynitrite donor SIN-1 is needed to complete the profile of oxidative stress on transporter function.

### 7.3.3 New roles of ENT1 in disease

The ENT1<sup>-/-</sup> mouse has identified the contribution of ENT1 to the regulation of blood pressure (Figure 6.2) and control of mineralization of tissues in the spine (Figures 6.4-6.6).

The link between ENT1 and blood pressure is not surprising, given that the ENT1 substrate adenosine is a potent vasodilator (2). However, the hypotension phenotype raises the possibility that ENT1 may be a suitable target for the treatment of hypertension. It may also be possible that enhanced ENT1 function contributes to the development of hypertension, by limiting the exposure of adenosine to the vascular lumen (10).

The hind limb paralysis and abnormal spinal mineralization observed in ENT1<sup>-/-</sup> mice was a serendipitous discovery. The connection between ENT1 and mineralization, especially in such a specific manner, is not immediately clear. However, the resemblance of the ENT1<sup>-/-</sup> mice to human patients with the condition DISH is exciting (14; 21). The cause of DISH is currently unknown and there is no treatment option besides surgery. DISH is the second most common form of arthritis, and the ENT1<sup>-/-</sup> mouse may prove to be an excellent model to better understand this disease (20; 21).

#### 7.3.3.1 Future Directions: The Role of ENT1 in Disease

Chapters 5 and 6 examined the role of ENT1 in MVECs and whole animals using ENT1<sup>-/-</sup> mice. While some changes in gene expression in MVECs were found, the impact of ENT1 to hypoxia, ischemia-reperfusion, and oxidative stress could not be completely addressed due to difficulty in culturing ENT1<sup>-/-</sup> MVECs. Once the culturing process has



been properly adjusted, data can be generated to complement the wild-type responses observed in Chapter 5.

The ENT1<sup>-/-</sup> mouse had two interesting phenotypes, hypotension in young mice, and abnormal mineralization in the spine, as discussed in Chapter 6.

The hypotension phenotype was determined with a tail-cuff system. Confirmation of the phenotype should be performed using telemetry to obtain more natural measurements of the course of a day. The potential of ENT1 in the treatment of hypertension can be studied using isolated blood vessels and myograph systems.

The abnormal mineralization observed in the spine resembles the human condition DISH. The mechanism behind the lack of ENT1 and abnormal mineralization has yet to be determined. Altered gene expression that may contribute to the formation or deposit of mineral in the ENT1<sup>-/-</sup> will be determined using quantitative PCR. Blood chemistry analysis will be performed to identify possible changes in calcium or phosphorous levels. Additionally, the specific tissue affected is currently unknown. More in depth histological analyses need to be performed using mice at a variety of age points. Samples from boxer dogs, who display a high rate of DISH, as well as from diagnosed humans, for the study of ENT1 function will also help form a link between the nucleoside transporter and the disease.

#### **7.4 Closing Remarks**

The discoveries presented in this thesis strengthen the need to understand nucleoside and nucleobase transporters, their expression, function, and regulation. It is evident that these transporters are important in the microvasculature as well as overall cardiovascular function, and even long term health.

Better understanding of ENT1 and ENBT1 at the molecular level will improve the effectiveness of using these transporters as pharmacological targets in cardiovascular disease, cancer, and surprisingly, pathological mineralization in the spine.

## 7.5 References

1. **Archer RG, Pitelka V and Hammond JR.** Nucleoside transporter subtype expression and function in rat skeletal muscle microvascular endothelial cells. *Br J Pharmacol* 143: 202-214, 2004.
2. **Belardinelli L, Shryock JC, Snowdy S, Zhang Y, Monopoli A, Lozza G, Ongini E, Olsson RA and Dennis DM.** The A2A adenosine receptor mediates coronary vasodilation. *J Pharmacol Exp Ther* 284: 1066-1073, 1998.
3. **Bone DB, Robillard KR, Stolk M and Hammond JR.** Differential regulation of mouse equilibrative nucleoside transporter 1 (mENT1) splice variants by protein kinase CK2. *Mol Membr Biol* 24: 294-303, 2007.
4. **Coe I, Zhang Y, McKenzie T and Naydenova Z.** PKC regulation of the human equilibrative nucleoside transporter, hENT1. *FEBS Lett* 517: 201-205, 2002.
5. **Elahi MM, Kong YX and Matata BM.** Oxidative stress as a mediator of cardiovascular disease. *Oxid Med Cell Longev* 2: 259-269, 2009.
6. **Escudero C, Casanello P and Sobrevia L.** Human equilibrative nucleoside transporters 1 and 2 may be differentially modulated by A2B adenosine receptors in placenta microvascular endothelial cells from pre-eclampsia. *Placenta* 29: 816-825, 2008.
7. **Fatehi-Hassanabad Z, Chan CB and Furman BL.** Reactive oxygen species and endothelial function in diabetes. *Eur J Pharmacol* 636: 8-17, 2010.
8. **Hammond JR.** Interaction of a series of draflazine analogues with equilibrative nucleoside transporters: species differences and transporter subtype selectivity. *Naunyn Schmiedebergs Arch Pharmacol* 361: 373-382, 2000.
9. **Kiss A, Farah K, Kim J, Garriock RJ, Drysdale TA and Hammond JR.** Molecular cloning and functional characterization of inhibitor-sensitive (mENT1) and inhibitor-resistant (mENT2) equilibrative nucleoside transporters from mouse brain. *Biochem J* 352 Pt 2:363-72.: 363-372, 2000.

10. **Ledent C, Vaugeois JM, Schiffmann SN, Pedrazzini T, El YM, Vanderhaeghen JJ, Costentin J, Heath JK, Vassart G and Parmentier M.** Aggressiveness, hypoalgesia and high blood pressure in mice lacking the adenosine A2a receptor. *Nature* 388: 674-678, 1997.
11. **Meneshian A and Bulkley GB.** The physiology of endothelial xanthine oxidase: from urate catabolism to reperfusion injury to inflammatory signal transduction. *Microcirculation* 9: 161-175, 2002.
12. **Nemeth I, Talosi G, Papp A and Boda D.** Xanthine oxidase activation in mild gestational hypertension. *Hypertens Pregnancy* 21: 1-11, 2002.
13. **Puebla C, Farias M, Gonzalez M, Vecchiola A, Aguayo C, Krause B, Pastor-Anglada M, Casanello P and Sobrevia L.** High D-glucose reduces SLC29A1 promoter activity and adenosine transport involving specific protein 1 in human umbilical vein endothelium. *J Cell Physiol* 215: 645-656, 2008.
14. **Resnick D and Niwayama G.** Radiographic and pathologic features of spinal involvement in diffuse idiopathic skeletal hyperostosis (DISH). *Radiology* 119: 559-568, 1976.
15. **Rieger JM, Shah AR and Gidday JM.** Ischemia-reperfusion injury of retinal endothelium by cyclooxygenase- and xanthine oxidase-derived superoxide. *Exp Eye Res* 74: 493-501, 2002.
16. **Robillard KR, Bone DB and Hammond JR.** Hypoxanthine uptake and release by equilibrative nucleoside transporter 2 (ENT2) of rat microvascular endothelial cells. *Microvasc Res* 75: 351-357, 2008.
17. **Robillard KR, Bone DB, Park JS and Hammond JR.** Characterization of mENT1Delta11, a novel alternative splice variant of the mouse equilibrative nucleoside transporter 1. *Mol Pharmacol* 74: 264-273, 2008.
18. **Stolk M, Cooper E, Vilk G, Litchfield DW and Hammond JR.** Subtype-specific regulation of equilibrative nucleoside transporters by protein kinase CK2. *Biochem J* 386: 281-289, 2005.

19. **Tanaka A, Nishida K, Okuda H, Nishiura T, Higashi Y, Fujimoto S and Nagasawa K.** Peroxynitrite treatment reduces adenosine uptake via the equilibrative nucleoside transporter in rat astrocytes. *Neurosci Lett* 498: 52-56, 2011.
20. **Verdone F.** Diffuse idiopathic skeletal hyperostosis in the third millennium: is there (yet) cause for concern? *J Rheumatol* 37: 1356-1357, 2010.
21. **Weinfeld RM, Olson PN, Maki DD and Griffiths HJ.** The prevalence of diffuse idiopathic skeletal hyperostosis (DISH) in two large American Midwest metropolitan hospital populations. *Skeletal Radiol* 26: 222-225, 1997.
22. **Weseler AR and Bast A.** Oxidative stress and vascular function: implications for pharmacologic treatments. *Curr Hypertens Rep* 12: 154-161, 2010.
23. **Young JD, Yao SY, Sun L, Cass CE and Baldwin SA.** Human equilibrative nucleoside transporter (ENT) family of nucleoside and nucleobase transporter proteins. *Xenobiotica* 38: 995-1021, 2008.

APPENDICES

## Appendix 1: Copyright permission for Chapter 3

### Request for Permission to Reproduce Previously Published Material

(please save this file to your desktop, fill out, save again, and e-mail to [permissions@the-aps.org](mailto:permissions@the-aps.org))

Your Name: Derek Bone E-mail: dbone2@uwo.ca

Affiliation: Department of Physiology and Pharmacology, The University of Western Ontario

University Address (for PhD students): M270 Medical Science Building, The University of Western Ontario  
London, ON Canada N6A 5C1

Description of APS material to be reproduced (check all that apply):

Figure  Partial Article  Abstract  
 Table  Full Article  Book Chapter  
 Other (please describe): \_\_\_\_\_

Are you an author of the APS material to be reproduced?  Yes  No

Please provide all applicable information about the APS material you wish to use:

Author(s): Derek B. J. Bone and James E. Hammond

Article or Chapter Title: Nucleoside and nucleobase transporters of primary human cardiac microvascular endot

Journal or Book Title: Am J Physiol Heart Circ Physiol.

Volume: 293 Page No(s): H2125-22 Figure No(s): \_\_\_\_\_ Table No(s): \_\_\_\_\_

Year: 2007 DOI: doi:10.1152/ajpheart.01006.2007.

(If you are reproducing figures or tables from more than one article, please fill out and send a separate form for each citation.)

Please provide all applicable information about where the APS material will be used:

How will the APS material be used? (please select from drop-down list)   
 If "other," please describe: \_\_\_\_\_

Title of publication or meeting where APS material will be used (if used in an article or book chapter, please provide the journal name or book title as well as the article/chapter title):  
Purine Transport and Metabolism in Microvascular Endothelial Cells

Publisher (if journal or book): The University of Western Ontario

URL (if website): \_\_\_\_\_

Date of Meeting or Publication: 2011

Will readers be charged for the material:  Yes  No

Additional Information: \_\_\_\_\_

**APPROVED**  
By prpka at 3:22 pm, Mar 10, 2011

THE AMERICAN PHYSIOLOGICAL SOCIETY  
9650 Rockville Pike, Bethesda, MD 20814-3991

Permission is granted for use of the material specified above, provided the publication is credited as the source, including the words "used with permission."

\_\_\_\_\_  
Publication Manager & Executive Editor

## Appendix 2: Copyright permission for Chapter 5

Request for Permission to Reproduce  
Previously Published Material(please save this file to your desktop, fill out, save again, and e-mail to [permissions@the-aps.org](mailto:permissions@the-aps.org))Your Name: Derek Bone E-mail: dbone@uwo.caAffiliation: Department of Physiology and Pharmacology, The University of Western OntarioUniversity Address (for PhD students): M270 Medical Science Building, The University of Western Ontario  
London, ON Canada N6A 5C1

Description of APS material to be reproduced (check all that apply):

- Figure                       Partial Article                       Abstract  
 Table                          Full Article                          Book Chapter  
 Other (please describe):

Are you an author of the APS material to be reproduced?     Yes     No

Please provide all applicable information about the APS material you wish to use:

Author(s): Derek E. J. Bone, Doo-Rup Choi, Imogen R. Coe, and James R. HammondArticle or Chapter Title: Nucleoside/nucleobase transport and metabolism by microvascular endothelial cellsJournal or Book Title: Am J Physiol Heart Circ PhysiolVolume: 299    Page No(s): H847-54    Figure No(s): \_\_\_\_\_    Table No(s): \_\_\_\_\_Year: 2010    DOI: doi:10.1152/ajpheart.00010.2010

(If you are reproducing figures or tables from more than one article, please fill out and send a separate form for each citation.)

Please provide all applicable information about where the APS material will be used:

How will the APS material be used? (please select from drop-down list) 

If "other," please describe:

Title of publication or meeting where APS material will be used (if used in an article or book chapter, please provide the journal name or book title as well as the article/chapter title):

Purine Transport and Metabolism in Microvascular Endothelial CellsPublisher (if journal or book): The University of Western Ontario

URL (if website): \_\_\_\_\_

Date of Meeting or Publication: 2011Will readers be charged for the material:     Yes     No**APPROVED**  
By *pripka* at 3:26 pm, Mar 10, 2011

Additional Information:

THE AMERICAN PHYSIOLOGICAL SOCIETY  
9650 Rockville Pike, Bethesda, MD 20814-3991

Permission is granted for use of the material specified above, provided the publication is credited as the source, including the words "and with permission."

Publications Manager &amp; Executive Editor



## Appendix 3: Ethics approval for usage of animals



04.24.09

**\*This is the Original Approval for this protocol\***  
 \*A Full Protocol submission will be required in 2013\*

Dear Dr. Hammond:

Your Animal Use Protocol form entitled:

Purine and pyrimidine transport in the cardiovascular

Funding Agency HSFO - Grant#T6376, PWKM

has been approved by the University Council on Animal Care. This approval is valid from **04.24.09 to 05.01.10**.

The protocol number for this project is **2009-030**.

1. This number must be indicated when ordering animals for this project.
2. Animals for other projects may not be ordered under this number.
3. If no number appears please contact this office when grant approval is received.  
 If the application for funding is not successful and you wish to proceed with the project, request that an internal scientific peer review be performed by the Animal Use Subcommittee office.
4. Purchases of animals other than through this system must be cleared through the ACVS office. Health certificates will be required.

#### ANIMALS APPROVED FOR 4 Years

Species	Strain	Other Detail	Pain Level	Animal # Total for 4 Years
Mouse	Various (as outlined in protocol)	Various (as outlined in protocol)	C	1024
Rat	Sprague Dawley	200-250, M	C	24

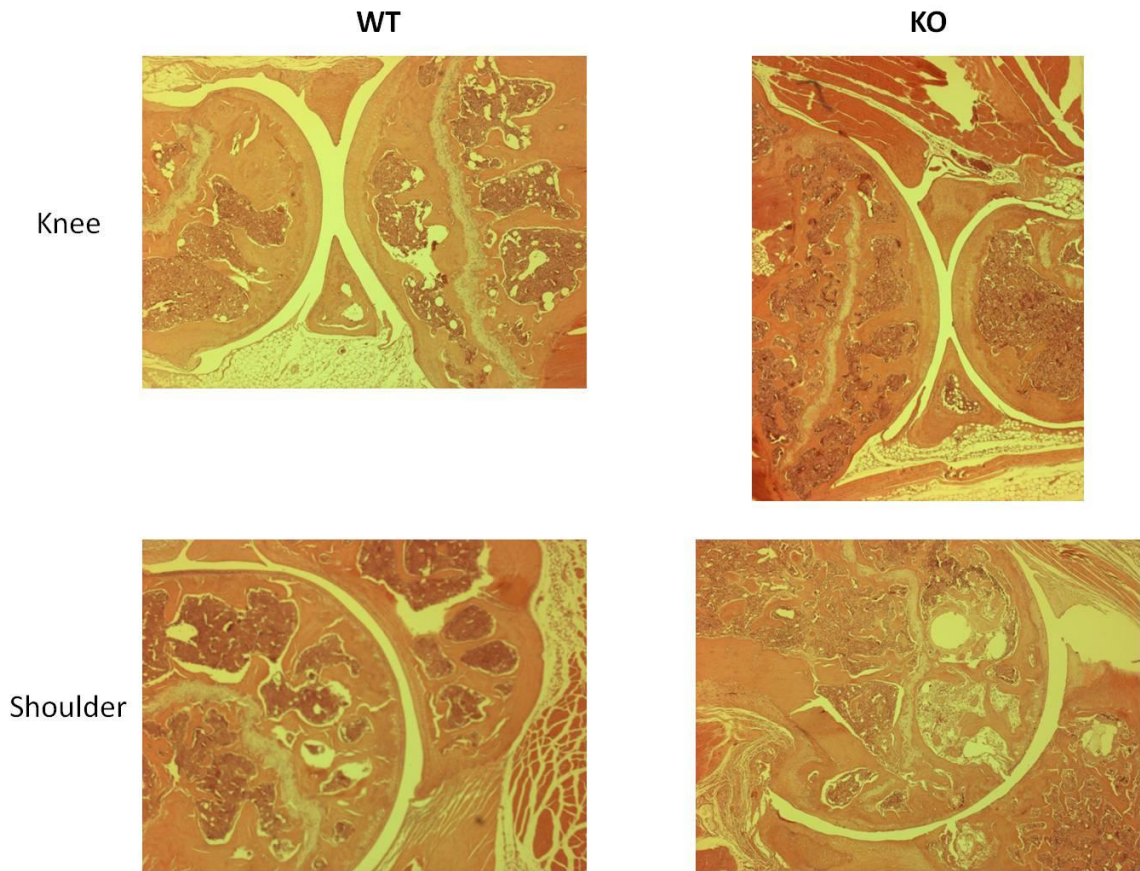
#### REQUIREMENTS/COMMENTS

Please ensure that individual(s) performing procedures on live animals, as described in this protocol, are familiar with the contents of this document.

**The holder of this Animal Use Protocol is responsible to ensure that all associated safety components (biosafety, radiation safety, general laboratory safety) comply with institutional safety standards and have received all necessary approvals. Please consult directly with your institutional safety officers.**

c.c. W Lagerwerf

*The University of Western Ontario*  
 Animal Use Subcommittee / University Council on Animal Care  
 Health Sciences Centre, • London, Ontario • CANADA – N6A 5C1  
 PH: 519-661-2111 ext. 86770 • FL 519-661-2028 • www.uwo.ca / animal

**Appendix 4: Lack of mineralization in other joints**

Unlike the spine from  $ENT1^{-/-}$  animals (KO), joints such as knees and shoulders appear to lack any abnormal mineralization.

## Curriculum Vitae

Derek Benjamin James Bone, B.M.Sc(Hon.)

### Contact Info

Department of Physiology and Pharmacology  
The University of Western Ontario, London, Ontario, Canada

### Education

2007-current: **Ph.D. candidate**, Department of Physiology and Pharmacology, Schulich School of Medicine and Dentistry, The University of Western Ontario (Supervisor: Dr. James R. Hammond)

2005-2007: **M.Sc. candidate**, rolled into Ph.D. program January 2007.

2005: **B.M.Sc. (Hon.) – Pharmacology and Toxicology**, The University of Western Ontario

### Publications

5. **Bone, DBJ**, Choi, DS, Coe, IR, and Hammond, JR. Nucleoside/nucleobase transport and metabolism by microvascular endothelial cells isolated from ENT1<sup>-/-</sup> mice. *Am J Physiol Heart Circ Physiol*. 2010 Sep;299(3):H847-56. Epub 2010 Jun 11.
4. Robillard, KR., **Bone, DBJ.**, Park, JS., and Hammond, JR. Characterization of a novel alternative splice variant of the mouse equilibrative nucleoside transporter 1: mENT1 $\Delta$ 11. *Mol Pharmacol*. 74(1):264-273. Epub: April 15, 2008.
3. Robillard, KR.<sup>1</sup>, **Bone, DBJ.**<sup>1</sup>, and Hammond, JR. Hypoxanthine uptake and release by equilibrative nucleoside transporter 2 (ENT2) of rat microvascular endothelial cells. *Microvasc Res*. 75(3):351-357. Epub: 2007 Oct 18. <sup>1</sup>Equal contribution.
2. **Bone, DBJ** and Hammond JR. Nucleoside and nucleobase transporters of primary human cardiac microvascular endothelial cells: Characterization of a novel nucleobase transporter. *Am J Physiol Heart Circ Physiol*. Dec; 293(6):H3325-32. Epub: 2007 Oct 5.
1. **Bone, DBJ**, Robillard, KR., Stolk, M, and Hammond, JR. Differential regulation of mouse equilibrative nucleoside transporter 1 (mENT1) splice variants by protein kinase CK2. *Mol Membr Biol*. 2007 Jul-Aug; 24(4):294-303

### Conference Abstracts

7. **Bone, DBJ.**, and Hammond JR. Differential regulation of purine transport in primary human cardiac microvascular endothelial cells. IUPHAR XVI, Copenhagen, Denmark, July 2010. *Basic Clin Pharmacol Toxicol*. July 2010; Vol 107 (Supplement s1)
6. **Bone, DBJ.**, Frieburger L, Troup, M., and Hammond JR. Discovery and characterization of a novel purine-selective nucleobase transporter, equilibrative nucleobase transporter 1. Canadian Student Health Research Forum; CIHR National Research Poster Presentation, Winnipeg, Manitoba, Canada. June 2, 2010.
5. Troup, M., **Bone, DBJ.**, and Hammond JR. Hypoxia decreases equilibrative nucleobase transporter 1 (ENBT1) function in microvascular endothelial cells. Innovations in Pharmacology - CSPT 2009, Saskatoon, Saskatchewan, Canada. *Can J Clin Pharmacol* Vol 16 (2) Summer 2009:e298-e321; May 20, 2009.
4. **Bone, DBJ.**, Choi, DS., and Hammond JR. Microvascular endothelial cells from equilibrative nucleoside transporter 1 (ENT1)-knockout mice have altered purine uptake and metabolism profiles. Poster presented at the 9<sup>th</sup> World Conference on Clinical Pharmacology and Therapeutics, Quebec City, Quebec, Canada, July 2008.
3. **Bone, DBJ.**, and Hammond JR. Nucleobase uptake is mediated by multiple facilitative mechanisms in mammalian cells. Banff2007: Pharmacology and Therapeutics Conference, Banff, Alberta, Canada. *Proceedings of the Western Pharmacology Society*. Volume 50, 2007.
2. **Bone, DBJ.**, and Hammond, JR. Nucleoside and nucleobase uptake by human cardiac microvascular endothelial cells (hMVECs): Evidence of a novel transporter. IUPHAR XV, Beijing China, July 2006. *Acta Pharmaca Sinica* July; Supplement 1
1. **Bone, D.**, Stolk, M., and Hammond, J.R. Functional and pharmacological characterization of equilibrative nucleoside transporter splice variants. *Proceedings of the British Pharmacological Society* at <http://www.pa2online.org/abstracts/Vol3Issue2abst008P.pdf>

### Invited Oral Presentations

3. **Bone, DBJ.**, and Hammond JR. Purine transport and metabolism in microvascular endothelial cells. Presented at National Institute of Diabetes and Digestive and Kidney Diseases, National Institutes of Health, Bethesda, USA. February 1, 2011.

2. **Bone, DBJ.,** and Hammond JR. Function and regulation of purine equilibrative transporters in human cardiac microvascular endothelial cells. Presented at Institute of Experimental and Clinical Pharmacology, Friedrich-Alexander University Erlangen-Nürnberg, Erlangen, Germany. July 26, 2010.
1. **Bone, DBJ.,** and Hammond JR. Consequences of equilibrative nucleoside transporter 1 knock-out. Presented at Department of Physiology and Pharmacology Seminar Series, The University of Western Ontario. April 26, 2010.

### **Awards and Scholarships**

- The Hari and Gudrun Sharma Award – Awarded annually to an outstanding pharmacology PhD student, Departmental, 10/2010
- Honourable Mention – CIHR National Research Poster Presentation, Canadian Student Health Research Forum, 06/2010
- Canadian Institutes of Health Research Doctoral Research Award, \$44,000, National, 05/2008-04/2010
- Schulich Graduate Scholarship, \$23,100, Institutional, University of Western Ontario, 01/2007-08/2010
- Ontario Graduate Scholarship in Science and Technology, \$15,000, Institutional, University of Western Ontario, 05/2007-04/2008
- Western Graduate Research Scholarship, \$5,400, Institutional, University of Western Ontario, 09/2005-12/2006
- Mogenson Trust Graduate Student Travel Award, \$500, Institutional, University of Western Ontario, 10/2006

### **Teaching**

- 2005-2010: Teaching Assistant, 3<sup>rd</sup>-year Pharmacology Lab, Department of Physiology and Pharmacology, Schulich School of Medicine and Dentistry, The University of Western Ontario
- 2008: Nominated for Graduate Student Teaching Award
- 2007: Nominated for Graduate Student Teaching Award

**Academic Activities – Committees**

- 2009-2010: Departmental Graduate Students' Council – Founding Member
- 2008-2010: Departmental Graduate Studies Sub Committee – Pharmacology Student Representative
- 2008-2010: Departmental Communications and Outreach Sub Committee – Student Representative

**Supervision and Mentoring**

- 2005-current: 5 fourth year honors thesis students

**Professional Affiliations**

- Canadian Society of Pharmacology and Therapeutics – Student Member